DOCTORAT BIOLOGIE BRETAGNE SANTE LOIRE

UNIVERSITÉ DE NANTES

THESE DE DOCTORAT DE

L'UNIVERSITE DE NANTES

ECOLE DOCTORALE N° 605
Biologie Santé
Spécialité : Biologie, Médecine et Santé

Par

Paul HUMBERT

« Role of the osteoclast in bone regeneration induced by mesenchymal stem cells and calcium phosphate biomaterials »

Thèse présentée et soutenue à Nantes, le 14 décembre 2020

Unité de recherche :
UMR-1238, Phy-OS, Sarcomes Osseux et Remodelage des Tissus Calcifiés

Rapporteurs avant soutenance :

Delphine LOGEART-AVRAMOGLOU
DR, Université de Paris, Ecole Nationale Vétérinaire de Maisons-Alfort, CNRS UMR7052, INSERM U1271, B3OA
Nathalie CHEVALLIER
Maître de Recherche, Université Paris-Est Créteil, EFS, IMRB, INSERM U955

Composition du Jury :

Président :	**Claudine Blin** DR, Université Nice Côte d'Azur, CNRS UMR7370 LP2M
Examinateurs :	**Claudine BLIN** DR, Université Nice Côte d'Azur, CNRS UMR7370 LP2M
Directeur de thèse :	**Pierre LAYROLLE** DR, Université de Nantes, INSERM UMR1238 Phy-OS
Co-directeur de thèse :	**Frédéric BLANCHARD** DR, Université de Nantes, INSERM UMR1238 Phy-OS
Co-encadrant de thèse :	**Meadhbh BRENNAN** Assistante Professeur, National University of Ireland Galway

Publications

For this thesis project:

Humbert, P., Brennan, M.Á., Davison, N., Rosset, P., Trichet, V., Blanchard, F., and Layrolle, P. (2019). Immune Modulation by Transplanted Calcium Phosphate Biomaterials and Human Mesenchymal Stromal Cells in Bone Regeneration. Front. Immunol. *10*, 1–15. (Review)

Humbert, P., De Lima, J., Brion, R., Adrait, A., Couté, Y., Charrier, C., Brulin, B., Trichet, V., Brennan, M.Á., Frédéric Blanchard, B. and Layrolle P. Apoptotic mesenchymal stromal cells support osteoclastogenesis in vitro through secretion of CXCR-1 and CXCR-2 ligands.
Submitted to *Bone Research*

From previous or collaborative work:

Wulf, M.G., Maguire, S., Humbert, P., Dai, N., Bei, Y., Nichols, N.M., Corrêa, I.R., and Guan, S. (2019). Non-templated addition and template switching by Moloney murine leukemia virus (MMLV)-based reverse transcriptases co-occur and compete with each other. J. Biol. Chem. *294*, 18220–18231.

Brennan, M.A., Brulin, B., Gallinetti, S., Humbert, P., Tringides, C., Mooney, D.J., Canal, C., Ginebra, M.P. and Layrolle P. Enhanced bone regeneration and human mesenchymal stromal cell engraftment by biomimetic versus sintered macroporous calcium phosphate scaffolds in calvarial defects.
Submitted to *Acta Biomaterialia*

Summary

Figures & Tables

Introduction

Chapter I

Abbreviations

ATSC = Adipose Tissue-derived Stem Cell

BCP = Biphasic Calcium Phosphate

BMAT = Bone Marrow Adipose Tissue

BMAC = Bone Marrow Aspirate Concentrate

BMP = Bone Morphogenetic Protein

BMU = Bone Multicellular Unit

BSP = Bone SialoProtein

CaP = Calcium Phosphate

CD = Cluster of Differentiation

CM = Conditioned Media

CTSK = Cathepsin K

G/M–CSF = Granulocyte/Macrophage Colony Stimulating Factor

DAMP = Damage-Associated Molecular Pattern

DAPI = 4',6-diamidino-2-phenylindole

DC = Dendritic Cell

DiFMU(P) = 6,8-difluoro-4-methylumbelliferyl (phosphate)

ECM = ExtraCellular Matrix

EPO = Erythropoietin

EV = Extracellular Vesicle

FDA = Food and Drug Administration

FGF = Fibroblast Growth Factor

GFP = Green Fluorescent Protein

HA = HydroxyApatite

HSC = Hematopoietic Stem Cell

IGF = Insulin-like Growth Factor

IL = Interleukine

iPSC = induced Pluripotent Stem Cell

MAMP = Microbe-Associated Molecular Pattern

MCP = Monocyte Chemoattractant Protein

MMP = Matrix MetalloProteinase

MNGC = MultiNucleated Giant Cell

h/rMSC = human/rat Mesenchymal Stem Cell

NHDF = Normal Human Dermal Fibroblast

NK = Natural Killer

OCN = Osteocalcin

OPG = Osteoprotegerin

OPN = Osteopontin

OSM = Oncostatin M

PDGF = Platelet-Derived Growth Factor

PRP = Platelet Rich Plasma

PTH = ParaThyroid Hormone

RANK(-L) = Receptor Activator of NFκB (Ligand)

SCF = Stem Cell Factor

SD = Sprague-Dawley

SDF = Stromal cell-Derived Factor

SEM = Scanning Electron Microscopy

SSC = Skeletal Stem Cell

STS = Staurosporine

T_c / T_h / T_{reg} = cytotoxic / helper / regulatory T cell

TCP = TriCalcium Phosphate

TGF = Transforming Growth Factor

TNAP = Tissue Non-specific Alkaline Phosphatase

TNF = Tumor Necrosis Factor

TPO = Thrombopoietin

TRAP = Tartrate Resistant Acid Phosphatase

VAO = Vessel Associated Osteoclast

VEGF = Vascular Endothelial Growth Factor

Introduction

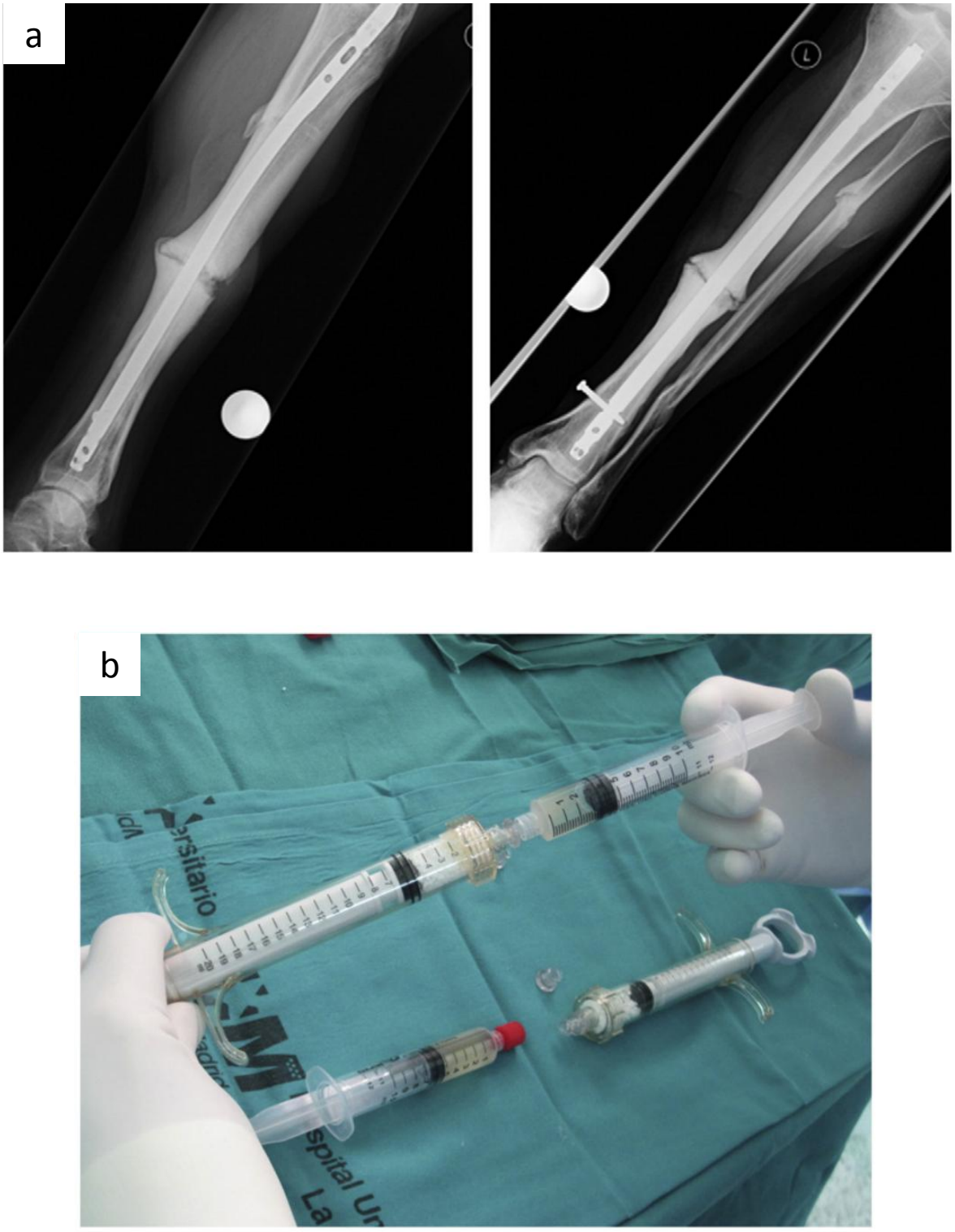

Figure 1: Cell therapy for non-unions. (from Gomez-Barrena et al., 2015)

(a) Radiological images (antero-posterior and lateral views) of a tibial hypertrophic nonunion (b) Syringes of biomaterials (MBCP+ granules) and expanded MSCs mixed before implantation.

A. Context & Significance

The following work is part of the Research and Development arm of the EU-2020-ORTHOUNION project. The core of ORTHOUNION is a phase III clinical trial comparing the efficacy of autologous bone marrow-derived mesenchymal stem cell (MSCs) associated with Biphasic Calcium Phosphate (BCP) granules to autologous bone graft harvested from the iliac crest in the treatment of non-unions following fractures of long bones of the femur, tibia or humerus (Gómez-Barrena et al., 2018). It succeeds to ORTO-1 which demonstrated the safety and feasibility of this type of stem cell therapy (Gómez-Barrena et al., 2019).

Fractures are frequent causes of hospitalization following trauma from sport injury, falls or vehicle accidents for example. A typical treatment for long bone fracture consists of realigning bone segments, with fixation using an external plate or an intra-medullary rod if necessary, followed by immobilization of the limb in a cast. Fracture healing should naturally occur in those stable conditions. A non-union (Figure 1a) is diagnosed if healing is incomplete and the injury site stopped progressing after several months. The overall rate of non-union is often estimated to be between 5% and 10% of fractures. The most recent and methodical study calculated this rate as low as 1.9% (Mills et al., 2017). In any case, the probability of a fracture to progress into a non-union varies drastically depending on the bone impacted, the type and complexity of the fracture and the treatment modalities. Unsurprisingly, complex open-wound fractures from high energy trauma are more at risk. In addition, several patient-related parameters such as smoking, alcohol consumption, medications and diseases, such as osteoporosis, diabetes or obesity, have been identified as risk factors (Zura et al., 2016). Knowing all these parameters, non-unions remain complications that are difficult to predict and impossible to prevent beyond efficient management of the fracture in the first place.

Bone grafts are considered the gold-standard for bone regeneration of non-unions and other skeletal defect due to osteonecrosis or bone tumors. These applications make bone the second most transplanted tissue after blood with around 2 million procedures per year worldwide. The need for bone grafts and the limitations of the technique lead to the development of bone substitute materials (Henkel et al., 2013). Due to their similarities with the mineral fraction of bone, calcium phosphate (CaP) materials are promising substitutes to bone grafts (Habraken et al., 2016). MSCs, in combination with those biocompatible materials, lead to efficient bone formation in both preclinical studies and clinical trials (Figure 1b). Their use was primarily driven by their status of osteoblast progenitors, but it seems that their effectiveness relies on their immunomodulatory properties. Experiments in mice showed that, while inducing bone formation compared to the cell-free control, implanted MSCs are rapidly disappearing and that bone formation is preceded by osteoclast formation on the material (Gamblin et al., 2014). Therefore, the aim of this project is to study the osteoclast as a pivotal cell in bone regeneration induced by CaP-hMSCs therapies.

This first section introduces basic information on bone physiology with a focus on bone cells and their communication during remodeling. The immune system and its interactions with bone cells are explored with a brief description of the major cells types, and the mechanisms of fracture healing and foreign body reaction. Then, bone regeneration treatments are presented, the gold-standard bone graft as well as emerging biomaterial-based approaches. To conclude this introduction, the hypothesis behind this work is detailed in the form of a review article gathering evidences of immunomodulation and osteoclast activation by implanted CaP materials and MSCs.

B. Bone Physiology

Despite its main function as the rigid frame of the body, bone is a cellularized and dynamic tissue in constant renewal. Its strength is given by its organization and its mineral component associated with specific extracellular matrix (ECM) proteins. Osteoblasts and osteoclasts, respectively responsible for the formation and degradation of bone, are the major cell types working in a finely coordinated manner. From the second fetal month to the second decade of life, bones are formed and grow by two major mechanisms; endochondral and intramembranous ossification and are renewed by the remodeling cycle between osteoclasts and osteoblasts.

1. Organization & Composition of Bones

a) Organization of the Skeleton

The skeleton is the structure composed of bones and cartilage supporting all tissues. The axial skeleton regroups the bones of the head, chest and spine while the appendicular skeleton refers to those of the arms and legs. It protects the three main vital functions as the brain is surrounded by the cranium and, the heart and lungs are inside the rib cage. Bones support the attachment of muscles *via* tendons and transmit their force of contraction into movement. They are connected to each other at joints by ligaments and separated by cartilage. Articular cartilage plays an essential role in the posture and motion of the body, bearing compression load and reducing friction.

From the 270 bones present at birth some fuse together, like the bones of the skull roof originally separated by fontanelles, to obtain the 206 bones of the adult skeleton. Bones are often classified based on their shape: long, short, flat and irregular (OpenStax College, 2016). The limbs and their extremities consist mostly of long bones that serve as leverage for motion. The upper arm contains the humerus, the lower arm the radius and ulna, the upper leg the femur and the lower leg the tibia and fibula. The hand and foot have metacarpals and metatarsals respectively followed by phalanges to form the fingers and toes. Short bones are cuboidal bones located only in the wrist (carpals) and ankle (tarsals). The common characteristic of flat bones is their thinness, but they have heterogeneous length, width and curvature. Bones of the skull, the scapulae, the ribs and the sternum are

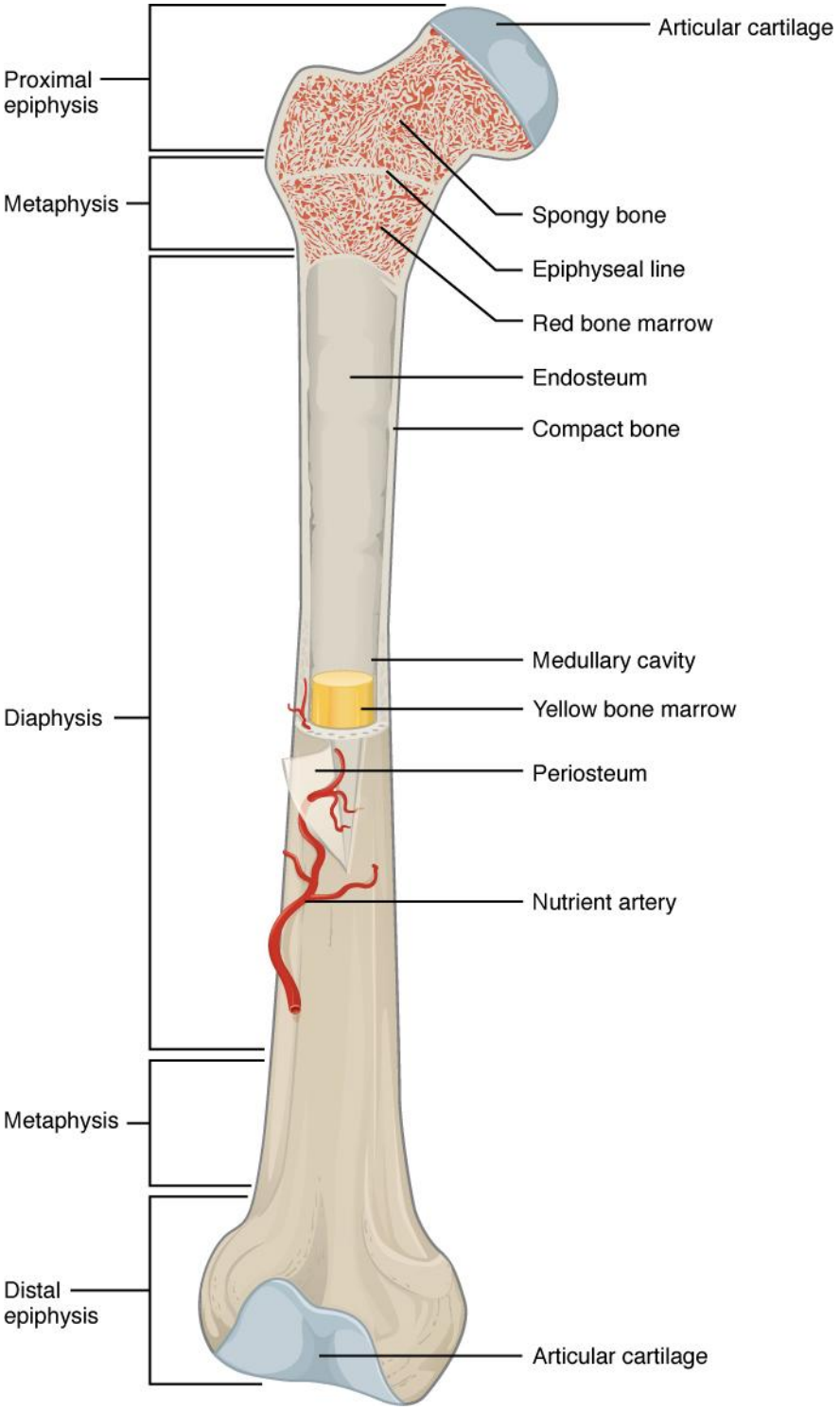

Figure 2: Anatomy of a long bone. (from OpenStax)

all flat bones. Irregular bones form the most diverse category. Their complex shapes are often associated with a specific function such as the vertebrae protecting the spinal cord or the malleus (“hammer”), incus (“anvil”) and stapes (“stirrup”) conduction sound in the middle ear. The patella (or “kneecap”), sometimes classify as a short bone, is an exception to these categories as the only permanent sesamoid bone of the human skeleton. Sesamoid bones are embedded in tendons and help relieving excessive pressures. Their appearance varies from one individual to the other and can be caused by strain on the tendon.

b) Long Bone Structure

Long bones have three major parts; the central diaphysis flanked by the proximal (closest from the axial skeleton) and distal (furthest from the axial skeleton) epiphysis. The diaphysis has a tubular structure of dense cortical (or compact) bone surrounding the yellow bone marrow contained in the medullary cavity. Two membranes lay on the cortical bone, the endosteum on the inside and the periosteum on the outside. The epiphyses are wider and contain trabecular (or cancellous) bone, an interconnected network of plates and rods of thickness around 100 µm. The trabecular space is filled with red bone marrow, in which hematopoiesis takes place. Part of the epiphysis is covered by the articular cartilage forming the joint with the proximate bone and is thus the only part not covered by the periosteum. The epiphyseal plate (or growth plate), at the transition (or metaphysis) between diaphysis and epiphyses, is a hyaline cartilage allowing longitudinal extension of the bone during childhood. It ossifies into the epiphyseal line at the end of growth. (Figure 2)

(1) Cortical & Trabecular Bone

Cortical bone is an assembly of numerous cylindric subunits called osteons or Haversian system (Ascenzi, 2012; Lopes et al., 2018; Tzelepi et al., 2009).The osteon is an assembly of 5 to 15 layers of bone substance, the lamellae, surrounding a vascular (or Haversian) canal. Lamellae average 5 to 10 µm in thickness and the canal between 10 and 70 micrometers width, making the diameter of the osteon in the range of 80 to 300 micrometers. These values vary depending on the anatomical localization of the osteon and, the health and age of the individual. The Haversian canals are connected to each other and to the periosteum by transversal canals passing through lamellae called Volkmann’s canals, permitting nutrients and oxygen supply. The osteons are delimited by cement lines and the spaces between them are occupied by interstitial lamellae. Osteons are also forming large trabeculae in the cancellous bone. Smaller trabeculae do not contain a central vasculature and are therefore irrigated by the bone marrow filling the trabecular space, through the endosteum. The trabecular network orientates itself based on stress lines to improve bone strength while still being lighter than cortical bone due to the bone marrow areas.

(2) Endosteum & Periosteum

The endosteum and periosteum are membranes at the bone surface, essential for vascularization and playing an essential role in fracture repair (Lin et al., 2014). The

endosteum is thinner and covers bone at the interface with bone marrow. It is mostly constituted by bone lining cells, as well as MSCs, osteoblasts and osteoclasts. The periosteum, on the outer surface of bone, is divided in two layers, a fibrous layer on the outside and a cambium layer at the bone surface. The fibrous layer is a matrix of mostly collagen and elastin with embedded fibroblasts while the cambium layer also contains MSCs and osteoblasts.

(3) Red & Yellow Bone Marrow

Based on its composition, bone marrow is generally subdivided into yellow (or fatty) and red (or hematopoietic) marrow. The colors come respectively from the carotenoids in fat droplets and the hemoglobin in erythrocytes. Yellow marrow has few vessels and hardly any role in hematopoiesis. It is constituted for 80% of fat as its cells are almost exclusively adipocytes. Red marrow on the contrary is highly vascularized as it hosts hematopoiesis. The repartition and composition of yellow and red marrow change throughout childhood and teen years. Widespread at birth with almost no fat content, red marrow gets to 40% fat in adults and is restricted to the trabecular space of flat bones and the epiphysis of long bones. This phenomenon can be observed by measuring the cellularity of the bone marrow, the ratio of hematopoietic cells to adipose tissue. It is an interesting medical parameter as it increases with hematopoietic activity, in response to infections for example. (Riley et al., 2009)

The specificities of bone marrow adipose tissue (BMAT) compared to other classical adiposities clusters have been reviewed by Li et al. (2018). Briefly, BMAT within yellow marrow is considered “constitutive” whereas the one in red marrow is “regulated” as it is prone to adapt in response to specific diet, exercise, diseases and more. Expansion of the regulated BMAT will limit the area of hematopoietic tissue and conversely, decreasing or increasing cellularity. Despite this competition for bone marrow space, different studies showed an impact of BMAT derived factors on the regulation of hematopoiesis. In the same way, higher BMAT content has been associated with lower bone mass maybe due to the competition for MSCs, precursor of both osteoblasts and adipocytes, but BMAT could also secrete various factors stimulating either formation or resorption of bone.

c) Extracellular Matrix & Mineral Composition

At the molecular level, bone is a complex composite of mineral and proteins (Boskey, 2013; Stock, 2015). The principal component of bone is its inorganic fraction of hydroxyapatite ($Ca_{10}(PO_4)_6(OH)_2$). For most bones, hydroxyapatite represents 60 to 70% dry weight, with exceptions like the staples of the ear with up to 98%. The mineral fraction also contains carbonate (CO_3^{2-}, approximately 5% of bone weight), citrate ($C_6H_5O_7^{3-}$, 2%) and other ions in smaller amount (Na^+, Mg^{2+}, K^+, F^-, Cl^-). This significant amount of carbonate lead to the term “carbonated apatite” to differentiate this mineral phase from geological hydroxyapatite. The ionic composition has an essential role in cell attachment, metabolism and signaling. It is also suspected to influence bone structure and strength but this area

Family	Protein	Main Function in Bone
Collagens	Type I Collagen	Main structural protein (90% of organic matrix) associated with hydroxyapatite
	Type III Collagen	Regulates type I collagen fibrillogenesis Involved in osteoblastogenesis, endochondral ossification
	Type XII Collagen	Regulates type I collagen fibrillogenesis Involved in osteoblast polarization
RGD-containing proteins	Fibronectin	Cell attachment points
	Vitronectin	Collagen binding
	Thrombospondin (-1, -2, -3, -4)	Collagen matrix organization Cell Attachment
SLRPS	Asporin	Possibly involved in collagen mineralization
	Biglycan	Collagen fibrillogenesis Angiogenesis in fracture healing Osteoblast differentiation
	Decorin	Collagen fibrillogenesis Possible modulator of mineralization
	Osteoadherin	Potential mediator of cell attachment
	Keratocan	
SIBLINGS	Osteopontin (OPN)	Mineralization
	Bone Sialoprotein (BSP)	Osteoblast differentiation Promotes mineralization
	Dentin Matrix Protein 1 (DMP1)	Mineralization (possible promoter)
	Dentin Phosphophoryn (DPP)	Mineralization Suspected role in MSCs differentiation
	Matrix Extracellular Phosphoglycoprotein (MEPE)	Possible inhibitor)mineralization
Carboxylated Proteins	Matrix Gla protein	Potential function in cartilage metabolism Inhibits mineralization
	Osteocalcin (Bone Gla protein)	Regulates mineralization
	Periostin	Cell attachment, especially epithelial cells Function in tissue remodeling
	Protein S	Deficiency results in osteopenia
Matrix Metaloproteinases	MMP-2	Involved in degreadation of ECM
	MMP-14	Regulates osteoblastogenesis and osteoblast-osteocyte transition
Glycoproteins	Osteonectin (ON) / Secreted Protein, Acidic, Cysteine-Rich (SPARC)	Mineralization
	Tetranectin	Possible implication in fracture healing
Serum Proteins	Albumin	Inhibits growth of hydroxyapatite crystals
	α_2HSglycoprotein	Chemoattractant for monocytes Opsonic properties

Table 1: Extracellular matrix proteins.

Major families of proteins found in the ECM of bone and functions of the most common proteins (adapted from de Melo Pereira et al., 2018; Robey, 2008 and Alford et al., 2015)

remains understudied. Roschger et al. (2020) observed differences in calcium to phosphorous ratio, Na and Mg content, crystallinity and particle size between newly formed and remodeled bone, implying differences in the mineralization process of modeling versus remodeling. Costello et al. (2014) observed that the citrate in bone was partially associated with hydroxyapatite (65-80%) but also bound to collagen (20-35%), suggesting a dual structural role.

The organic phase is mostly composed of type I collagen (Stock, 2015), representing around 90% of its dry weight making it the most abundant protein in the body. Type I collagen is an heterotrimer of two α1 and one α2 chains of repeated amino-acid motifs, encoded by the genes COL1A1 and COL1A2, self-assembled in a triple helix of 1.25 nm in diameter and 300 nm length. Several post-translational modifications occur including hydroxylation of specific lysine and proline residues followed by O-glycosylation on hydroxylysines (Terajima et al., 2014). Microfibrils are formed by the cross-linking of five triple-helixes on those glycosylated sites and assembled with separating gaps of 40 nm and a periodicity of 67 nm to form fibrils of 100 to 200 nm. Carbonated hydroxyapatite crystals are present both within the fibrils and on their surface. Collagens of types III and XII are also present in bone, essentially during formation. They are associated with type I collagen fibrils and direct their organization. Knock-out experiments in mice showed that type III collagen seems to be involved in osteoblast differentiation and activity as well as endochondral ossification (Volk et al., 2014) while type XII collagen directs osteoblast polarization (Izu et al., 2011). Fibronectin is another structural protein, guiding collagen fibrils assembly and ensuring the integrity of the matrix.

Other proteins are inferior in abundance but essential for matrix organization, mineralization or bone cells activity and metabolism. Bone ECM includes families of proteins (Table 1) such as small leucine-rich proteoglycans (SLRPS), matrix metalloproteinases (MMP) or small integrin-binding ligand N-linked glycoproteins (SIBLINGS). They sustain numerous functions associated with the organization of the matrix, the mineralization process, the interactions with cells, the regulation of bone remodeling (Alford et al., 2015) and more (Robey, 2008). In addition to proteins, the lipid content of bone, although very low (around 2% of the organic phase), may be important in the metabolism of bone cells. Finally, the water content plays a role in matrix cohesion and protein-mineral bounding.

Cartilage is present at the joint, the epiphyseal plate or as a template during bone development. It is an avascular matrix produced by chondrocytes composed mostly of glycosaminoglycans, proteoglycans, collagens, elastin, and water. The amount of each constituent varies to modulate cartilage properties depending on its function and anatomical localization. In the articular cartilage, aggrecan is the main proteoglycan of and is associated to hyaluronic acid, the main glycosaminoglycan. The aggregates of aggrecan and hyaluronic acids are entrapped in a fibrillar network of type II collagen.

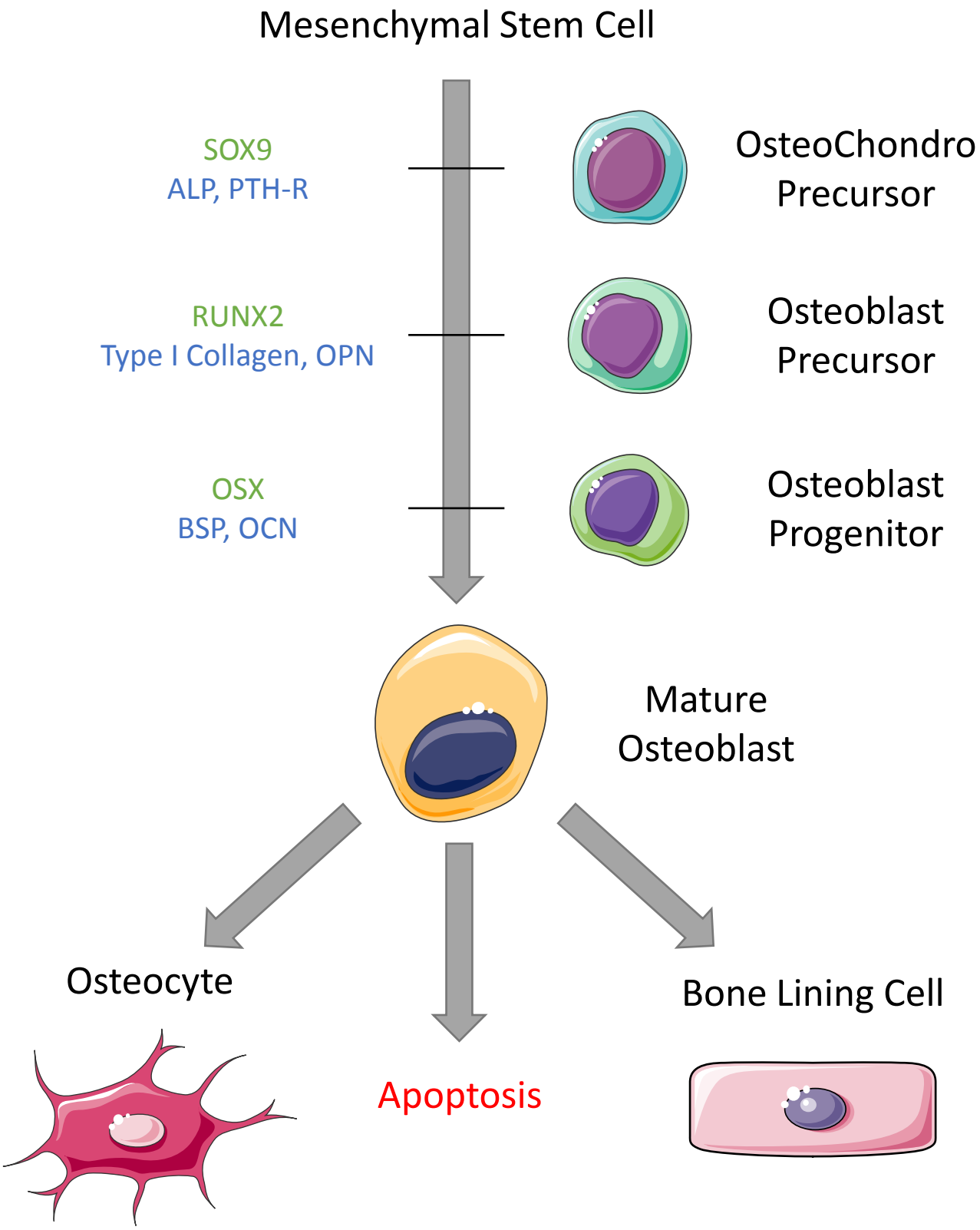

Figure 3: Osteoblastic differentiation. (adapted from Baron, 2001)

Major transcription factors are presented in green and signature proteins in blue.

2. Bone Cells

a) Osteoblasts

Osteoblasts are the cuboidal cells specialized in new bone matrix formation and mineralization during bone formation and remodeling. They differentiate from multipotent mesenchymal precursors from the bone marrow (Figure 3). *In vitro*, osteoblast culture can be performed by differentiation of human MSCs by stimulation with glucocorticoid such as dexamethasone and/or vitamin D, in addition to calcium and phosphate sources allowing mineralization.

Three major criteria were defined to properly identification MSCs for their use in regeneration (Dominici et al., 2006): their ability to attach to plastic, their pluripotency (adipocyte, chondrocyte and osteoblast) and the presence ($CD105^+$, $CD73^+$, $CD90^+$) or absence ($CD45^-$, $CD34^-$, $CD14^-$, $CD79\alpha^-$, $HLA\text{-}DR^-$) of specific surface markers. More recently, a population of skeletal stem cell (SSC, $PDPN^+CD146^-CD73^+CD164^+$) further specialized, not differentiating in adipocyte, was identify in human (Chan et al., 2018). This result suggested a different stem cell niche for marrow adipose tissue than chondrocytes and osteoblasts.

Numerous growth factors direct osteoblasts differentiation, notably the transforming growth factor beta (TGFβ) superfamily including bone morphogenetic proteins (BMPs), Wnt glycoproteins or fibroblast growth factors (FGFs). In early progenitors and in chondrocyte differentiation, the transcription factor SOX9 is present. Commitment to the osteoblastic lineage is guided by the expression of the Runt-related transcription factor 2 (RUNX2 also called Core-Binding Factor subunit alpha 1, CBFα1) initiating differentiation and, later on, osterix (OSX) leading to formation of pre-osteoblasts. They induce the expression of several characteristic proteins implicated in bone matrix production and mineralization. Type I collagen is secreted by osteoblast as the major component of the organic matrix. Osteopontin (OPN) and osteocalcin (OCN or BGLAP for bone gamma-carboxyglutamic acid-containing protein) are, among others, non-collagenic proteins involved in matrix organization and matrix-mineral interaction Bone sialoprotein (BSP) is another component of the osteoid, the unmineralized matrix primarily synthesized by osteoblast. BSP seems to facilitate hydroxyapatite nucleation in the osteoid, allowing mineralization. (Blair et al., 2017; Komori, 2019)

Mineralization is the process of hydroxyapatite deposition in the osteoid (Orimo, 2010). Hydroxyapatite formation begins in matrix vesicles (Figure 4) released by osteoblasts, following the equation:

$$6HPO_4^{2-} + 2H_2O + 10Ca^{2+} \leftrightarrow Ca_{10}(PO_4)_6(OH)_2 + 8H^+$$

Phosphate and calcium ions are respectively brought in by the type III Na/Pi transporter and annexins (A2, A5 and A6). Phosphates are also produced inside vesicles by PHOSPHO1, hydrolyzing the phosphocholine and phosphoethanolamine produce by

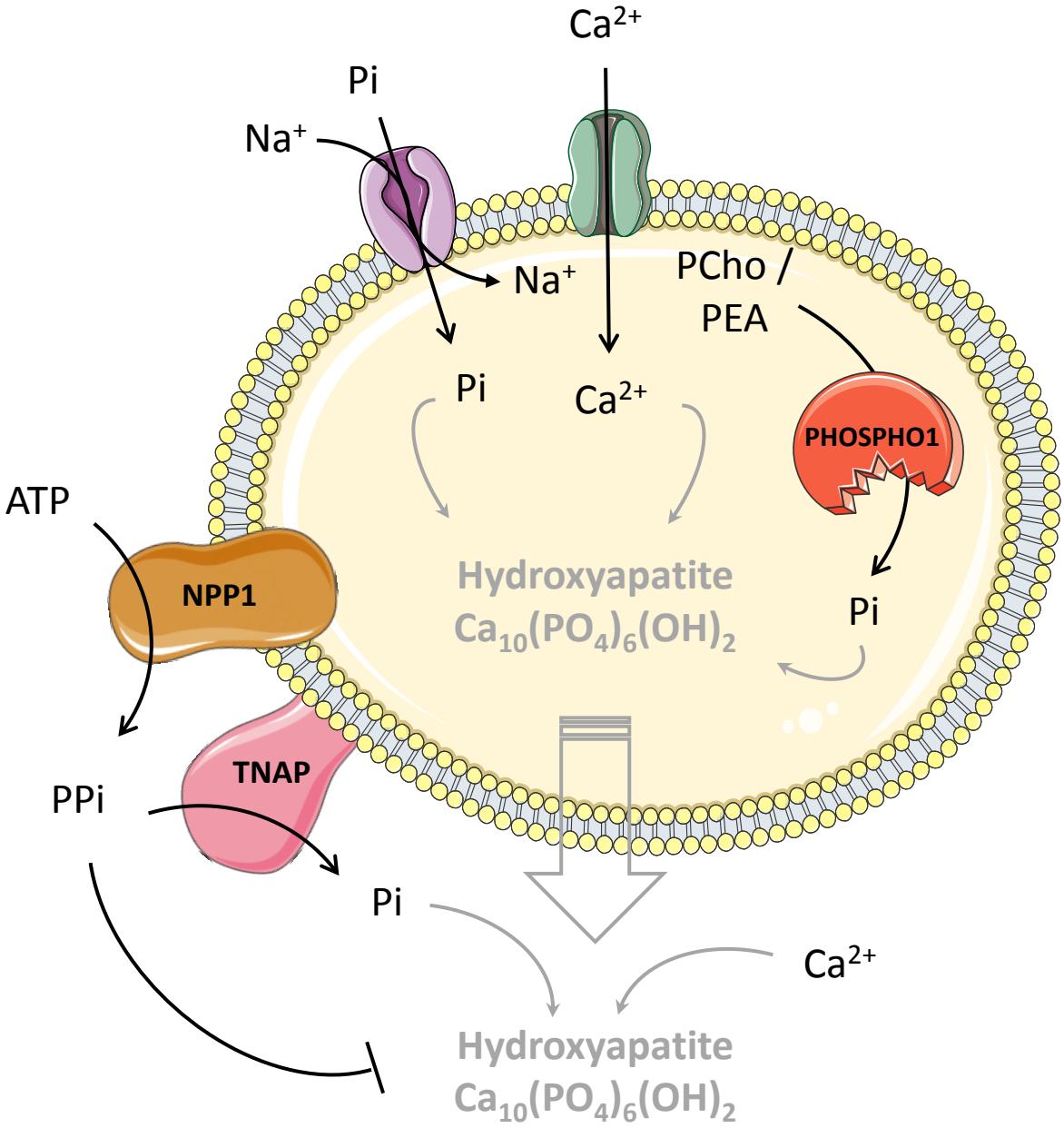

Figure 4: Mineralization from matrix vesicles (adapted from Orimo, 2010).

Pi = Inorganic Phosphate (HPO_4^{2-}); PPi = Inorganic Pyrophosphate ($P_2O_7^{4-}$); Ca^{2+} = Calcium cation; PCho = Phosphocholine; PEA = Phosphoethanolamine; NPP1 = Nucleotide Pyrophosphatase Phosphodiesterase 1; TNAP = Tissue Nonspecific Alkaline Phosphatase; PHOSPHO1 = phosphoethanolamine / phosphocholine phosphatase

phospholipase C from membrane lipids. Hydroxyapatite spontaneously crystallizes once the solubility limit of $CaPO_4$ is reached inside the vesicles. In a second step, hydroxyapatite crystals are further expanded once they get through the vesicle's membrane by the high calcium and phosphate concentration in the extracellular space. One major regulation of mineralization is the phosphate to pyrophosphate ratio, the former contributing to the reaction while the latter inhibits it. The key enzymes influencing this ratio are the nucleotide pyrophosphatase/phosphodiesterase 1 (NPP1) producing pyrophosphate from nucleotide triphosphates and the tissue-nonspecific alkaline phosphatase (TNAP) converting pyrophosphate in phosphates. Given the equation, the acidity produced by hydroxyapatite formation need to be neutralized to drive the reaction to the right. While calcium and phosphate are passively transported as they are consumed in the reaction, protons are actively pumped inside the osteoblast by Cl^-/H^+ exchangers and expelled on the other side by Na^+/H^+ exchangers.

b) Osteocytes and Bone Lining Cells

At the end of their anabolic activity, osteoblasts have three possible fates. Some will undergo apoptosis while others become either bone lining cells at the surface of bone or osteocytes embedded in the matrix.

Osteocytes are the most abundant bone cells, representing 90 to 95% of them. Inside the matrix, osteocytes form an interconnected network, touching each other by their cytoplasmic extensions. These cellular processes extend through canaliculi of around 4 µm in diameter, also reaching lining cells, osteoblasts or osteoclasts on bone surface to deliver signals from the osteocyte network. Osteocytes main function is to sense their environment, i.e. bone quality and mechanical constrain applied on it, and hence regulate modeling and remodeling. They are major modulators of both mineral deposition by osteoblasts, notably as the prime producer of sclerostine, inhibiting bone formation, and matrix resorption by osteoclasts (RANK-L, OPG and various cytokines). As other bone cells, osteocytes are also associated to calcium and phosphate homeostasis through secretion of the parathyroid hormone (PTH) and FGF23, immune cell regulation and energy metabolism. (Atkins and Findlay, 2012)

Bone lining cells (Wein, 2017) are the essential components of the endosteum and periosteum, forming a barrier at the bone surface. They form the canopy during bone remodeling and are therefore very likely involved in the recruitment of cells and the regulation of bone turnover. They are essential for the transition from resorption to bone formation as they remove debris left by the osteoclasts and deposit the first layer of collagen in the resorbed areas on which osteoblasts can attach and continue to produce matrix (Everts et al., 2002). They seem to retain osteogenic potential and be able to differentiate back into bone forming osteoblasts (Matic et al., 2016).

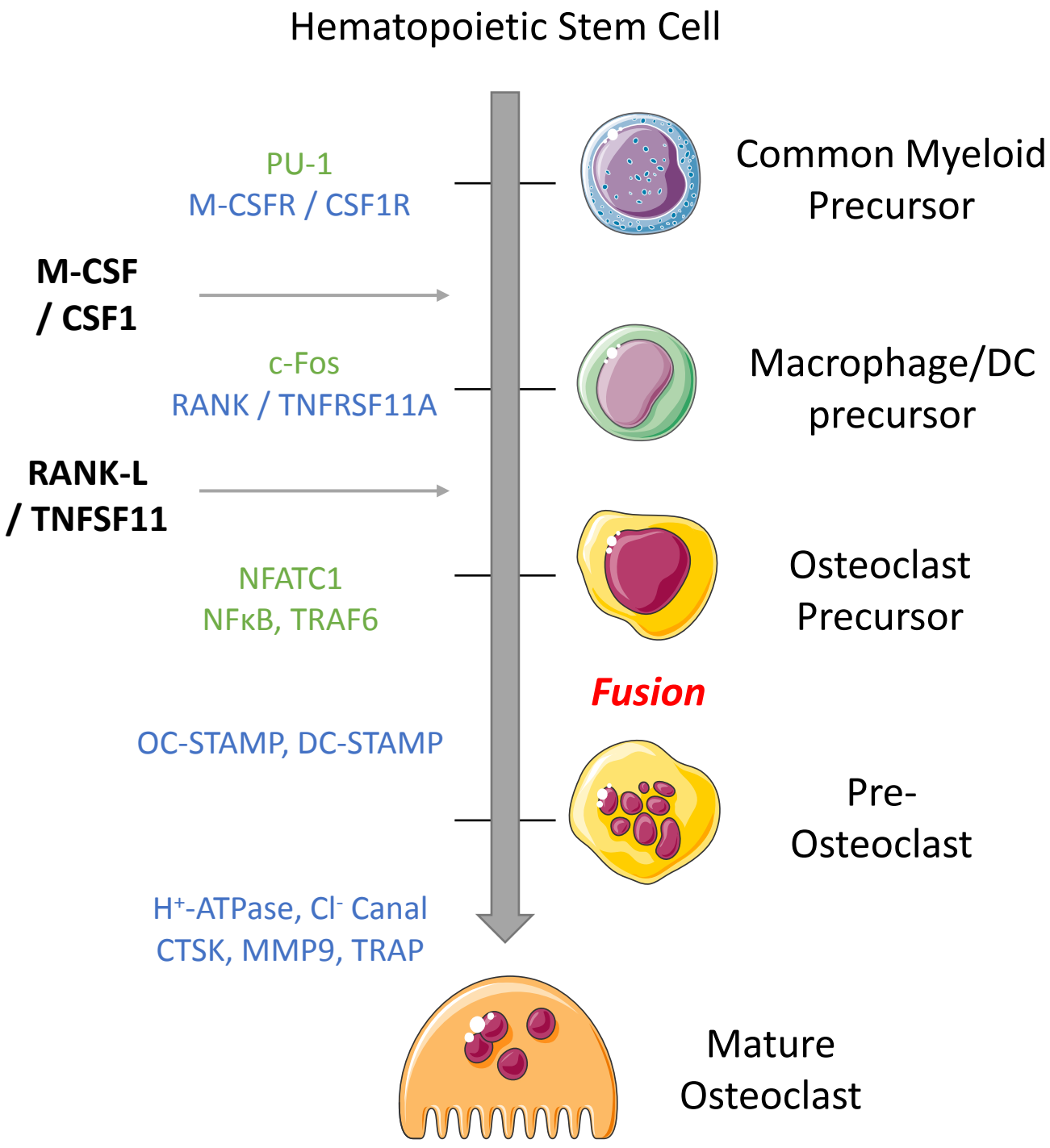

Figure 5: Osteoclastic differentiation. (adapted from Baron, 2001)

Major transcription factors are presented in green and signature proteins in blue.

c) *Osteoclasts*

Osteoblasts counterpart are osteoclasts, whose main function is to resorb bone matrix. They are multinucleated cells formed by the fusion of hematopoietic precursors of the myeloid lineage. *In vitro*, their differentiation is performed from precursors isolated from mice bone marrow or from human peripheral blood with their natural stimulating factors: macrophage colony-stimulating factor (M-CSF or CSF1 for colony stimulating factor 1) and receptor activator of nuclear factor kappa-B ligand (RANK-L or TNFSF11 for tumor necrosis factor ligand superfamily member 11).

It is commonly accepted that adult osteoclasts derive from the hematopoietic stem cell (HSC) through a sequential specialization into a common precursor to the myeloid lineage followed by a precursor of only monocytes, macrophages and dendritic cells (DC). Fusion of those last precursors leads to osteoclast formation (Figure 5). However, it was shown that osteoclasts arising during fetal development originate from embryonic erythro-myeloid precursors rather than HSCs and that mature osteoclasts are maintained by occasional fusion of one HSC-derived cell rather than systematic *de novo* formation from multiple precursors (Jacome-Galarza et al., 2019). M-CSF stimulates survival and proliferation of monocytes while osteoclastogenesis *per se* is induced by a co-stimulation with RANK-L. RANK-L is a member of the tumor necrosis factor (TNF) superfamily, a type II transmembrane protein that can be released in the extracellular compartment by enzymatic cleavage. Its receptor RANK is expressed by monocytic cells, DCs, macrophages and all states of osteoclast differentiation. A decoy receptor, osteoprotegerin (OPG), can prevent RANK-L from interacting with RANK. RANK and OPG are therefore TNF receptors but while RANK is membrane bound, OPG is released as a soluble factor. Osteoclastogenesis is mainly directed by this trio, especially the RANK-L to OPG ratio. (Boyle et al., 2003; Ono et al., 2020) Other factors can replace RANK-L to some extent, at least *in vitro*, to induce the formation of multinucleated cells capable of bone resorption. This "RANK-L-independent" osteoclastogenesis may not be efficient *in vivo* but the factors involved, TNFα, interleukine (IL) 1 or 6 for example, play a critical role in diseases inducing bone resorption (Feng et al., 2019).

To resorb efficiently bone matrix, osteoclasts are highly specialized and have distinctive characteristics linked to their role (Figure 6). They are polarized cells with an apical side on the bone matrix. Tight attachment to the bone surface is made via integrins (heterodimeric receptors of α and β chains) of three types: αvβ3, αvβ5 and α2β1. The major integrin is the vitronectin receptor, αvβ3. On the inside of the cell, a dense actin network defines the area of bonding with the matrix. Podosomes, or focal adhesion points, are punctual cytoskeletal structures that can be observed especially during migration. They contain structural proteins associated with the actin filaments: fimbrin, actinin, cortactin, gelsolin, vinculin or talin. In addition to their role in cell motility, podosomes are also associated with signal transduction and sensing of the surface. During active resorption,

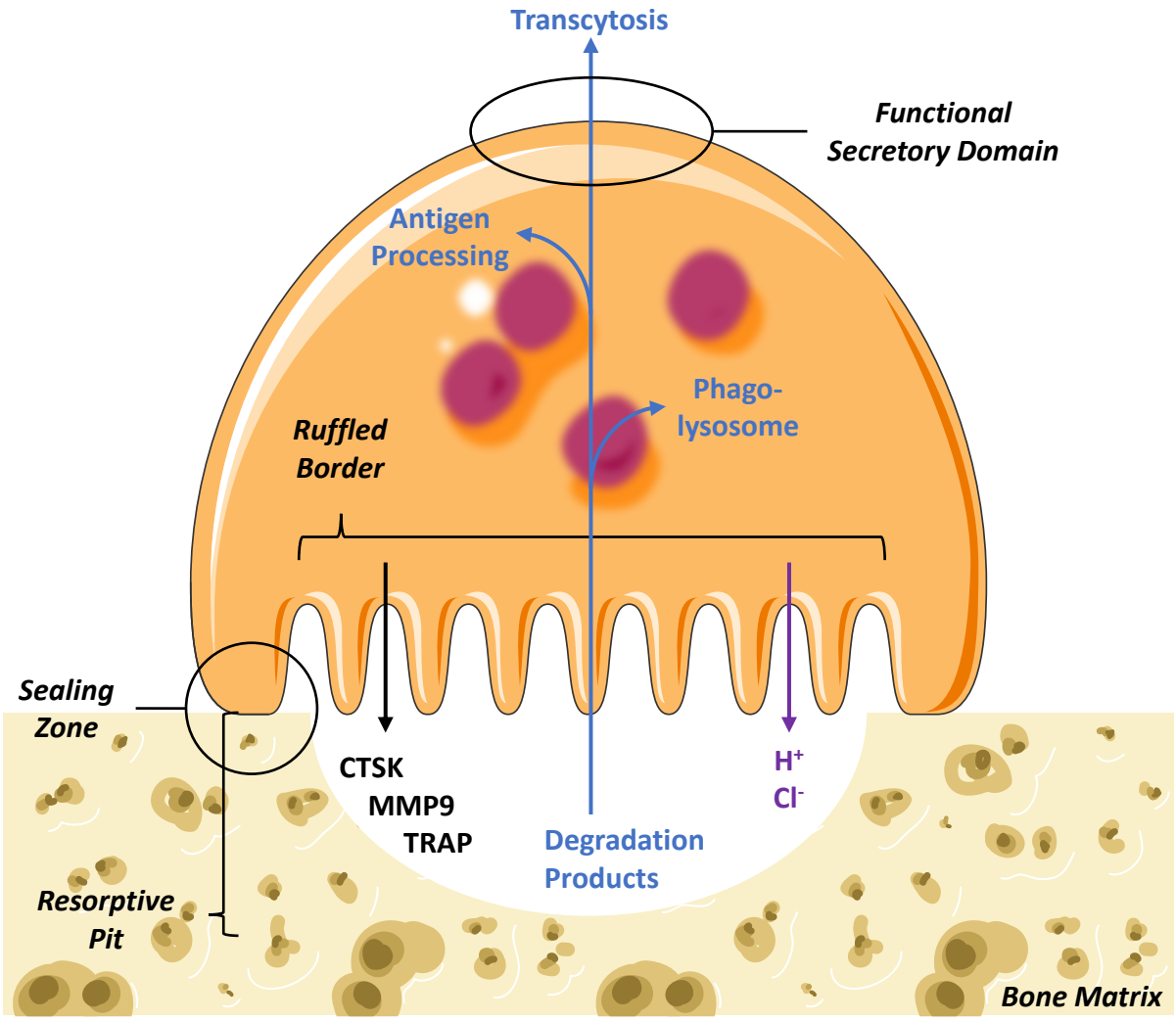

Figure 6: Schematic representation of an osteoclast resorbing bone.

Osteoclasts secrete a variety of factors in the resoprtive pit to degrade the organic fraction of bone or to acidify the environment and dissolve hydroxyapatite. H^+ = proton, Cl^- = chloride, CTSK = cathepsin K, MMP9 = matrix metalloproteinase 9, TRAP = tartrate resistante acid phosphatase

osteoclasts isolate an area of bone beneath them by forming a circular sealing zone. The sealing zone prevents the diffusion of osteoclastic secretions, increasing their local concentration at the interface with bone and thus improving the efficiency of the resorption. Osteoclasts are often described as functioning in cycles where resorption happens in a static state ("pit mode") between two phases of migration but they were also observed resorbing while migrating ("trench mode", Søe and Delaissé, 2017).

The ruffled border is the highly convoluted membrane inside the sealing zone responsible for secretion of resorbing molecules and uptake of degradation products (Mulari et al., 2003). Resorption occurs underneath the ruffle border, creating a resorptive pit (or Howship's lacuna). The dual composition of bone compels the osteoclast to produce both acidic elements to dissolve the mineral fraction and proteases to degrade the organic matrix of bone. Lysosomes from specialized lysosome-related organelles fuse with the plasma membrane in the peripheral region of the ruffle border, conveying ion transporters at the surface and enzymes into the resorptive pit. The acidity is brought by the newly exposed vacuolar H^+-ATPase, pumping out protons produced in the cytoplasm by the carbonic anhydrase II. This process implies several ion exchanges to maintain intracellular pH and membrane polarization. A variety of enzymes active at acidic pH are produced to degrade the demineralized matrix. Cathepsin K (CTSK) and tartrate resistant acid phosphatase (TRAP) are among the well- known and considered to be good markers for osteoclast activity. CTSK is a lysosomal cysteine protease which primary function is to degrade type I collagen. The exact function of TRAP remains unknown but knock-out studies proved that it helps bone degradation (Angel et al., 2000; Hayman et al., 1996). Its suspected roles include the production of reactive oxygen species (ROS) and dephosphorylation of OPN, BSP and mannose-6-phosphate residues on lysosomal proteins (including TRAP itself). Many more enzymes are involved in resorption such as other cathepsins, glycerol-2-phosphatase, β-glucuronidase breaking down glycosylation or matrix metalloproteinases (MMP-2 and -9) degrading various collagens. Endocytosis of degraded matrix components happens in the central area of the ruffle border. Endosomes are trafficking through the osteoclast, from the ruffled border to the functional secretory domain on the basolateral side, to be secreted (Ng et al., 2019).

Additionally, subtypes of osteoclasts and other types of clasts have been described with various degrees of certainty. Chondroclasts are the cartilage equivalent of bone osteoclasts. They seem particularly important in fracture healing, for cartilage callus resorption (Ota et al., 2009). Khan et al. (2020) compared the expression profiles of chondroclasts and osteoclasts isolated by laser capture microdissection, found a distinct signature of the two cell types and predicted potential transcription factor specific to chondroclasts (ATV6, SIRT1 and ATF1). It was also suggested that they participate in cartilage resorption at the epiphyseal plate in concert with endothelial cells (Lewinson and Silbermann, 1992). Few publications evoke another morphologically different cell type having this role, the septoclasts. They were described as Cathepsin-B-expressing

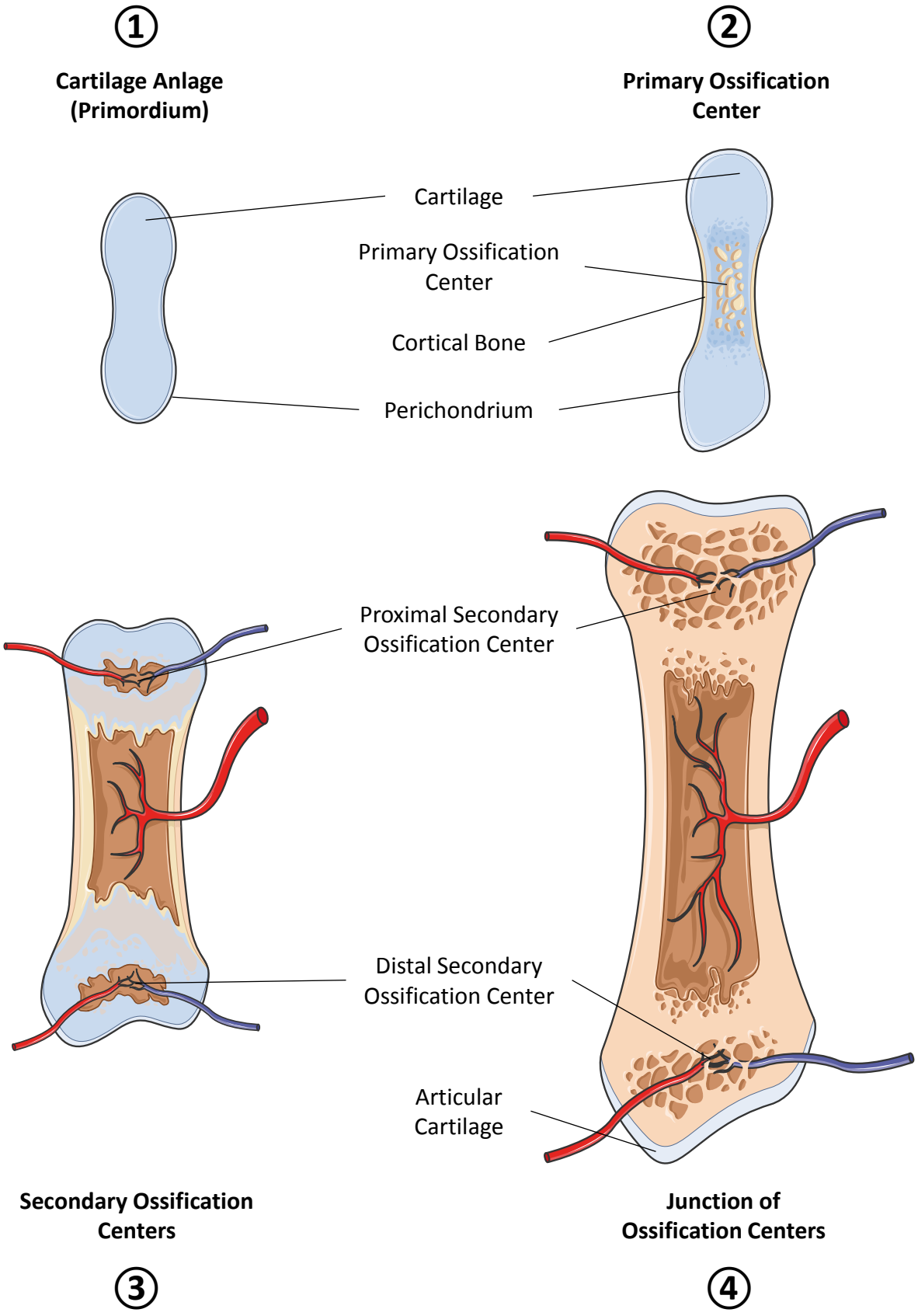

Figure 7: Steps of endochondral ossification (images from Servier Medical Art).

mononuclear cells also associated to the vascular system of the growth plate (Lee et al., 1995). These cells were recently studied in depth, with modern technology such as RNA sequencing and confocal imaging, by Romeo et al. (2019). These authors used the term vessels-associated osteoclasts (VAO) and reported profound differences between those cells and classical bone-associated osteoclasts. Interestingly, the associated endothelial cells were responsible for the production of proteases, particularly MMP-9, while VAOs were not essential for growth plate resorption. Regarding the diversity of osteoclast precursors, trans-differentiation and fusion of macrophages and DCs have been reported, especially under inflammatory condition. The phenotype of subsequent osteoclasts could potentially be more oriented towards communication with immune cells via antigen presentation (Madel et al., 2019). Osteoclasts developing in the synovium during arthritis were shown to fuse from specific circulating macrophages; AtoMs for Arthritis-associated osteoclastogenic Macrophages. Identified in mice with the markers $CX3CR1^{hi}Ly6C^{int}F4/80^{+}I\text{-}A^{+}/I\text{-}E^{+}$, their human counterpart was detect in patients' samples as $CX3CR1^{+}HLA\text{-}DR^{hi}CD11c^{+}CD80^{-}CD86^{+}$ (Hasegawa et al., 2019).

3. Bone Development

a) Formation

The two processes of bone formation are intramembranous and endochondral ossification (Berendsen and Olsen, 2015). Only parts of the cranium, clavicles and patella are formed by intramembranous ossification while endochondral ossification produces the rest of the axial and the entire appendicular skeleton.

During development, MSCs migrate and form dense aggregates at the location of the future bone, defining the shape and size of the skeleton. These MSCs arise from different parts of the mesoderm for most of the skeleton and from the neural crest for teeth and bones of the face and anterior skull. In endochondral ossification (Figure 7), MSCs first differentiate into chondrocytes, producing a cartilage anlage of the future bone. In the center, chondrocytes become hypertrophic and die while the spaces they leave are replaced by blood vessels carrying osteoblast and osteoclast progenitors. The primary ossification center appears as the hypertrophic cartilage is either directly mineralized or resorbed and replaced by bone by osteoblasts, while the bone marrow forms from new vessels and hematopoietic cells. At the same time, the perichondrium, embryonic equivalent of the periosteum, forms around this cartilage template and is the source of vessels and progenitors. Osteoblasts also appear in this perichondrium and start producing cortical bone around the cartilage. As the primary ossification center expand, so does the cartilage and secondary ossification centers appear (at the two extremities in the case of a long bone). At birth, cartilage remains only present at the articulation and at the epiphyseal plate, junction between two ossification centers. This epiphyseal plate will remain active to allow longitudinal growth of the bone.

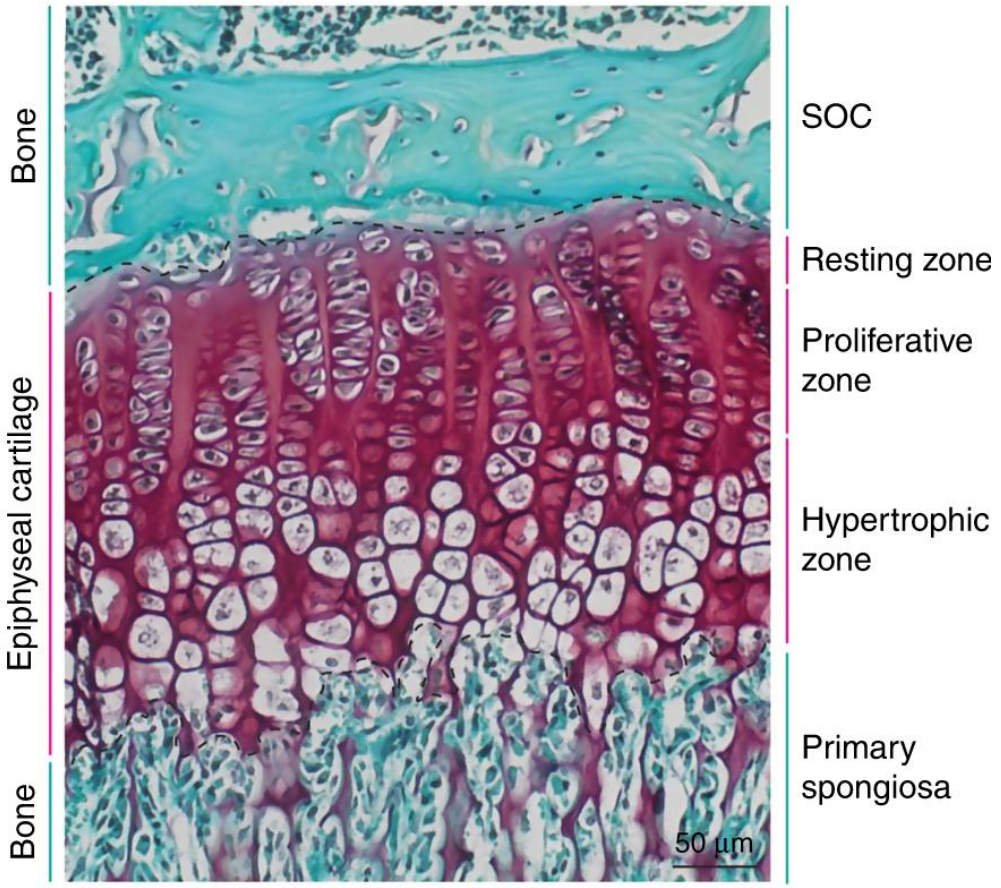

Figure 8: Organization of the growth plate. (from Chagin et al., 2019)

Histological section from 30 days old mouse tibia stained with Safranin O (red for cartilage) and Fast Green (bone and connective tissues). SOC = secondary ossification center

In intramembranous ossification, groups of MSCs within the aggregates directly differentiate in clusters of bone forming osteoblasts. They secrete an osteoid matrix around capillary vessels that mineralized in a few days, forming the trabeculae. On the outside, osteoblast in the periosteum form cortical bone. This type of ossification is continuous from fetal development until bones of the face and cranium reach their adult size.

b) Growth

Bone growth in length is permitted by ossification at the epiphyseal plate (Figure 8). This hyaline cartilage separating the diaphysis from the epiphysis has an activity resembling endochondral ossification but in layered organization. On the epiphyseal side, a layer of undifferentiated chondrocytes entrapped in matrix separate the bone of the epiphysis from the active zones of the plate and is the source of chondroprogenitors. Underneath this resting zone, chondrocytes are in a proliferative state, aligned in columns. Closer to the diaphysis, chondrocytes from the proliferative zone are maturing into hypertrophic chondrocytes. Some transdifferentiate into osteoblasts and calcify the surrounding cartilage while other undergo apoptosis, leaving empty spaces. These lacunae are invaded by new vessels carrying osteoblast progenitors finishing the transformation of the hypertrophic zone into trabecular bone. At the end of growth, chondrocytes stop replicating and are not renewed, leading to the calcification of the plate by the underlying bone. (Chagin and Newton, 2019)

Increase in bone diameter, or appositional growth, rely on bone resorption and formation at different sites. If bone is deposited beneath the periosteum, it increases the diameter of the bone. At the same time, resorption of cortical bone inside the medullary cavity enlarges the bone marrow space. This modeling process is independent of longitudinal growth and continues throughout life to adapt the shape of the skeleton to aging and mechanical constrains.

4. Bone Remodeling

Bone remodeling is essential to repair micro-damages, maintain calcium and phosphate homeostasis and finish the process of fracture healing. While modeling brings major changes to bone shape, remodeling aims at preserving the exact structure. In opposition to modeling, resorption and formation occur sequentially at the same site. To ensure equivalent bone mass, formation needs to precisely counterbalance resorption, implying a precise communication between cells involved. It is estimated that up to 10% of the bone mass is annually remodeled, underlining how important this mechanism is in bone physiology.

a) Phases

The whole process happens at remodeling sites, basic multicellular units (BMUs), of two main shapes depending on if their localization, either on trabecular bone or inside

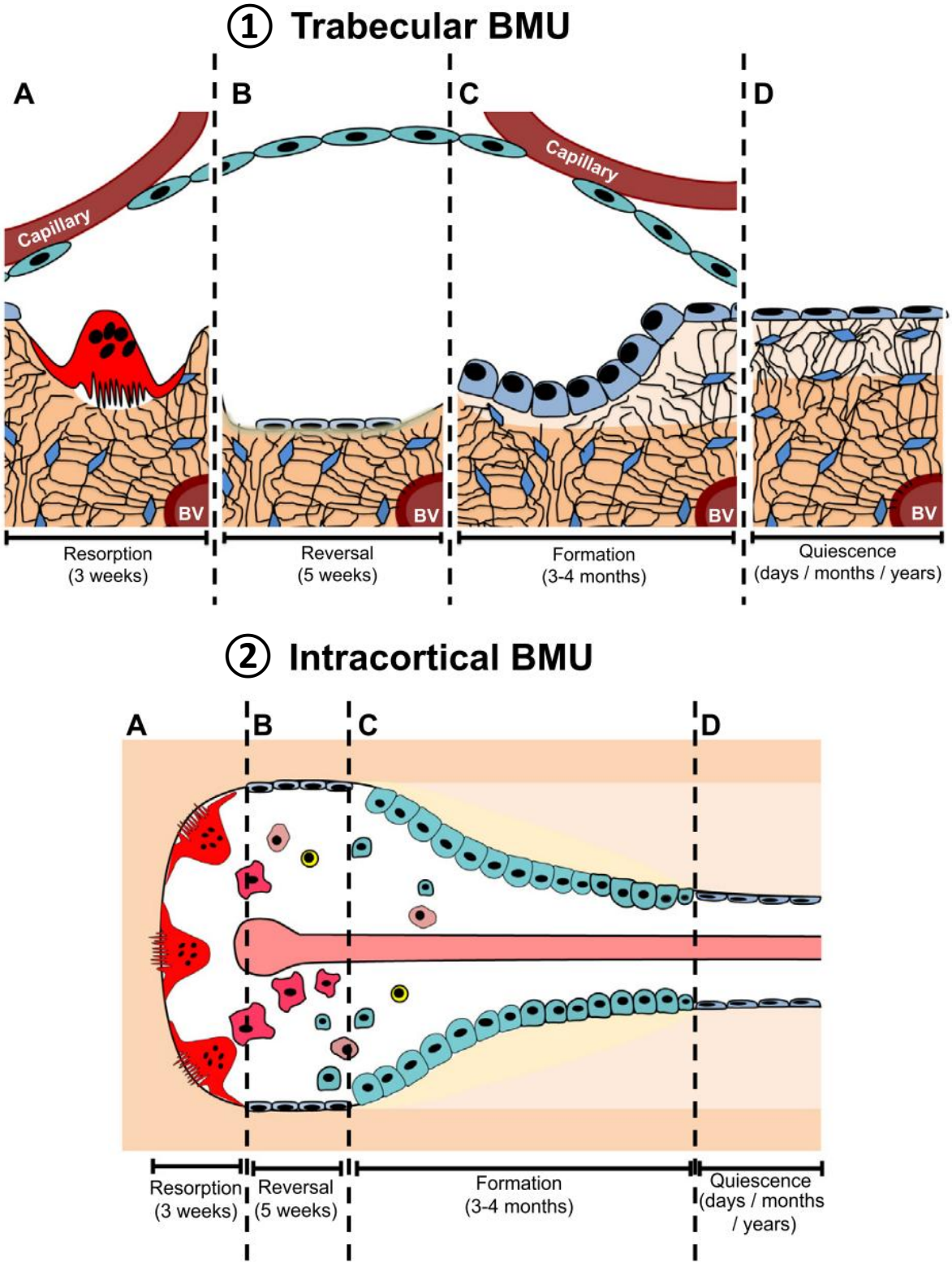

Figure 9: The bone multicellular unit. (from Sims and Martin, 2020a)

The BMU has two main shapes whether its (1) on trabecular bone or (2) in cortical bone.

Haversian canals (Figure 9). BMUs are distributed throughout the skeleton unevenly and asynchronously but not randomly, replacing bone where and when it is needed. Remodeling is a sequential mechanism that can be divided in three main phases, overlapping to some extent (Kenkre and Bassett, 2018; Sims and Martin, 2020a). First, osteoclasts differentiate and perform the resorption phase of the cycle. It is followed by a reversal phase initiating the switch from resorption to formation. Then, osteoblasts deposit new bone in the formation phase and the cycle ends by a return to a steady state. The whole cycle is 120 to 200 days long.

Initiation of the resorption phase is critical as it determines the area to be remodeled. To remove old bone, initiation is mostly orchestrated by osteocytes. They are the main source of RANK-L, secreted in response to mechanical stress alongside other mediators. Their apoptosis, if the matrix is damaged, can also produce pro-osteoclast signals. Systemic factors also promote remodeling but at non-specific sites. PTH for example induces resorption to increase blood calcium level. Those signals lead to the detachment of bone lining cells from the surface, as they form the canopy delimiting the BMU. Osteoclast precursors are recruited from the blood supply and differentiate. Activated osteoclasts resorb the area under the control of osteocytes, releasing both stimulating and inhibiting factors. Key proteins called coupling factors are released from the matrix, directly secreted, or even presented at the membrane of osteoclasts, influencing their own activity and survival and regulating osteoblast activation. These factors will be described later in detail. The high concentration of calcium released from the matrix is another inhibitor of the resorption activity. After approximately two weeks, this phase ends by the apoptosis of osteoclasts.

The reversal phase lasts four to five weeks. It is the least described to this day as it separates the main phases of resorption and formation. One of its functions is to prepare the surface for new bone deposition. Bone lining cells replace unmineralized matrix by the cement line, a non-collagenous mineralized matrix helping osteoblasts adhesion. Cement lines are markers of remodeled bone as there is no coupling in bone formation by modeling. The second role of the reversal phase is the actual recruitment of osteoblasts from the coupling signals emitted by osteoclasts. The cells synthesizing the cement line seem to be both targeting by the coupling signal from osteoclasts and relaying it to osteoblasts.

During the formation phase, osteoblasts first synthesize the osteoid matrix and then proceed to mineralize it. It is the longest process, with up to 4 months necessary to restore bone volume. Conversely to resorption, phosphate and calcium ion concentrations stimulate bone formation and as they are consumed the activity reduces. At the end of the cycles, osteoblasts are either entrapped in the matrix as osteocytes, becoming lining cells at the surface or disappearing via apoptosis. Once the canopy is brought back to the bone surface, the area is in quiescence until the next remodeling cycle.

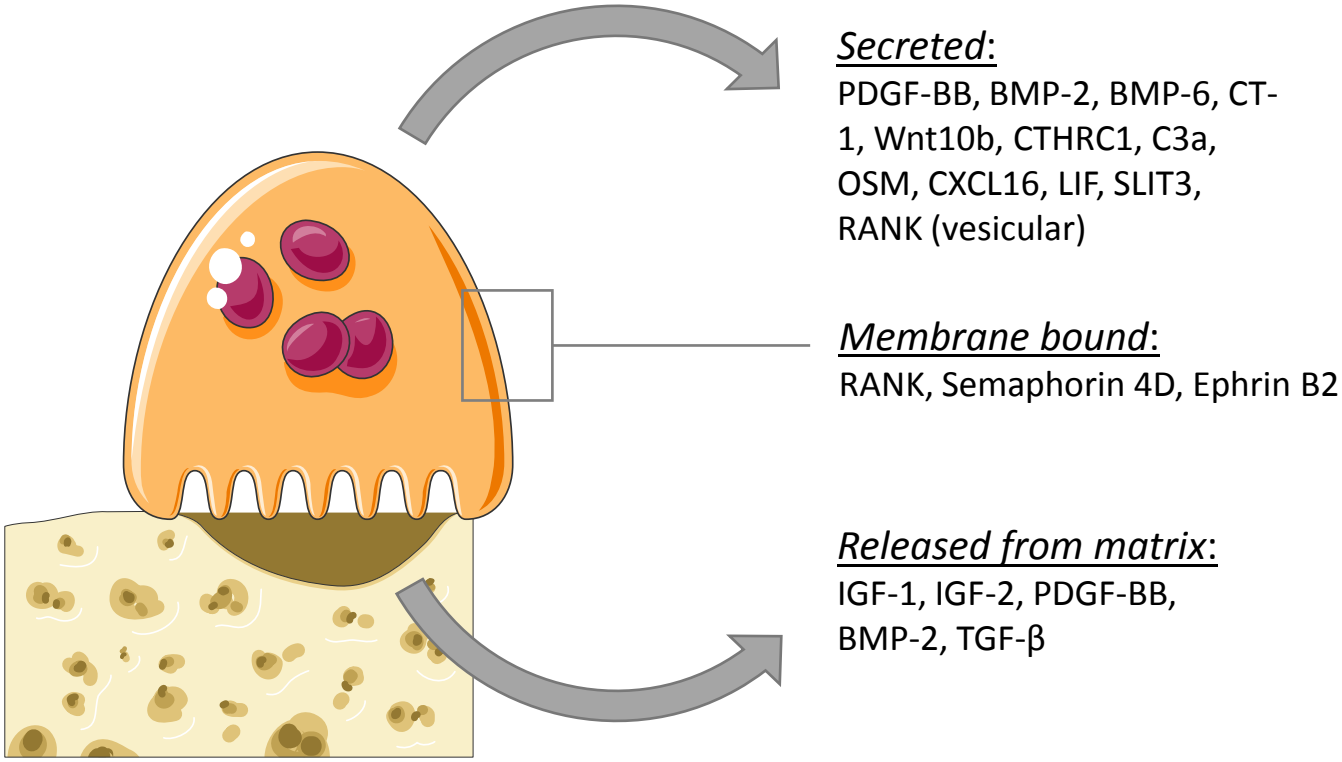

Figure 10: Osteoclast-derived coupling factors. (adapted from Sims and Martin, 2020b)

Coupling factors can be secreted, exposed or released from the matrix by resorbing osteoclasts.

b) Coupling factors

During resorption, osteoclasts produce "coupling factors" towards cells of the osteoblastic lineage to coordinate bone formation (Sims and Martin, 2020b & Figure 10). During resorption, some factors stored in the matrix are released. TGF-β and insulin-like growth factor 1 (IGF-1) are suspected to promote MSCs migration to the BMU while platelet-derived growth factor BB (PDGF-BB) could induce vessel formation, also important for progenitor's migration. Osteoclasts also directly secrete factors promoting the transition to bone formation such as sphingosin-1-phosphate (S1P), collagen triple helix repeat containing 1 (CTHRC1) or cytokines such as IL-6 and oncostatin M (OSM). In addition to this known mediators, the reverse signaling of vesicular RANK secreted by osteoclasts and activating osteogenic differentiation by binding RANKL at the membrane surface of osteoblast precursors was more recently described (Ikebuchi et al., 2018). Finally, some factors are just presented at the osteoclast membrane and require cell contact to effectively induce a signal, for example ephrinB2 or semaphoring D. All these factors have complex and sometimes indirect effects on osteoblast lineage cells.

C. Immune System & Bone

In healthy adults, production of blood cellular components, or hematopoiesis, takes place in the bone marrow (Rieger and Schroeder, 2012). Due to this localization and common regulatory cytokines, bone cells are influencing hematopoiesis and *vice versa*. Osteoclasts are even more connected to the immune system than other bone cells as they originate from the HSC. From this standpoint, they can be considered immune cells and retain some specific functions associated with immunity. In addition, fracture repair and material implantation involve immune reactions that must be considered to develop bone regenerative therapies. Given the interconnection of both fields, Arron and Choi (2000) proposed the term "osteoimmunology" as the study of the interaction between bone and the immune system. The following section is a glimpse at the complexity of the immune system and the diversity of its cells, with highlights on their relationship with bone cells. This peculiar relationship may also be essential to understand bone regeneration.

1. Immune Cells

a) HSC and Hematopoiesis

In common language, blood cellular components are divided into "red" blood cells (erythrocytes), "white" blood cells (all the immune cells) and platelets. Immune cells can be further dissociated in two lineages, myeloid and lymphoid. Generally, innate immunity is associated with the myeloid lineage and adaptive immunity with the lymphoid one but there are overlap and complex interactions between the two. All these cells derive from HSCs residing in a specific perivascular niche within the bone marrow associated with MSC (Morrison and Scadden, 2014; Pinho and Frenette, 2019 & Figure 11). MSCs are major regulators of HSCs and their differentiation in all branches of hematopoiesis (García-García

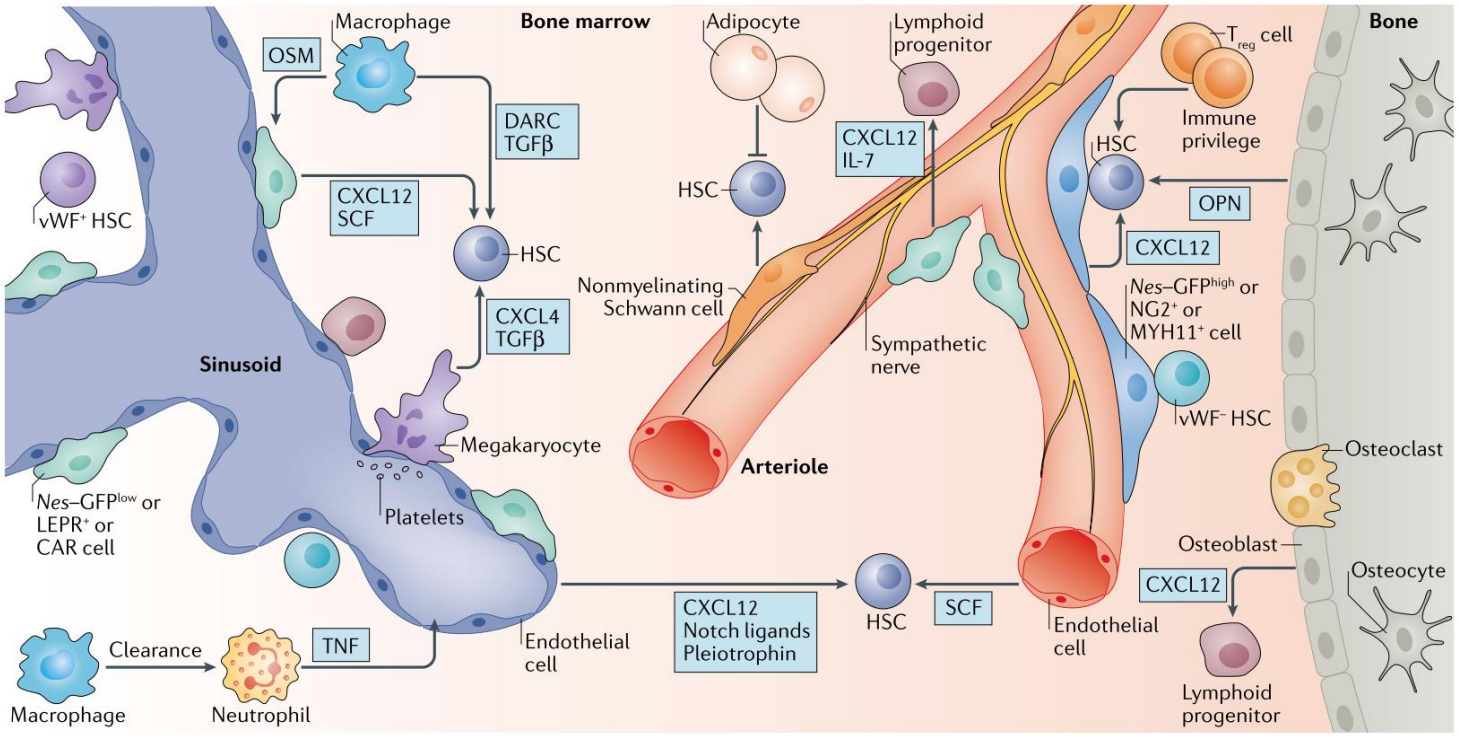

Figure 11: The bone marrow niche of hematopoietic stem cells. (from Pinho and Frenette, 2019)

A variety of immune and bone cells influence the maintenance and differentiation of hematopoietic stem cells (HSC) in their bone marrow niche. SDF-1/CXCL-12 = Stromal-Derived Factor 1, CAR cells = CXCL-12 abundant reticular cells, DARC = duffy antigen receptor for chemokines , LEPR = leptin receptor, OPN = osteopontin, OSM = oncostatin M, SCF = Stem Cell Factor, TGF = Transforming Growth Factor, TNF = Tumor Necrosis Factor, vWF = von Willebrand Factor.

et al., 2015). Adipose tissue being the other main component of marrow, it also influences various aspects of hematopoiesis as reviewed by Wang et al. (2018). Stem Cell Factor (SCF) and CXCL12 (or stromal cell-derived factor 1, SDF-1) are the main cytokines involved in HSCs self-renewal. The first step of differentiation is the loss of this ability, as HSCs become multipotent progenitors. Then, it is believed that this progenitor had to commit either to the lymphoid (T, B and Natural Killer cells) or erythro-myeloid lineage (erythrocytes, megakaryocytes, granulocytes and monocytic cells). A more recent "myeloid model" suggest that the potential of myeloid differentiation is conserved during some steps of lymphocytes differentiation (Kawamoto et al., 2010). Hematopoiesis tends to be schematized as a "tree" with HSC at its basis and differentiated cells on the branches, every bifurcation being a new progenitor with less multipotency. In reality, the differentiation axes seem interconnected and mature cells have phenotypic plasticity. As of today, many aspects of HSC differentiation and interaction with other cell types remain unknown.

b) Erythrocytes and Thrombocytes

A common megakaryocyte-erythroid progenitor downstream of the myeloid precursor gives rise to red blood cells and platelets. Erythrocytes have the essential role of distributing O_2 from the lungs throughout the body and carrying CO_2 back. Smaller than most other cells (around 7 µm in diameter and 2.5 µm of thickness), they also have a distinctive biconcave disk shape, are anucleated and lack most organelles. These characteristics allow them to pass through small capillaries while still having high hemoglobin content. Erythropoiesis main regulator is the erythropoietin (EPO), stimulating multiplication and survival of bone marrow erythroid progenitors derived from the HSC. EPO also seem to be involved in regulating bone cells in the marrow cavity (Suresh et al., 2020). These precursors will sequentially progress into various erythroblasts, undergoing limited division and drastic phenotypical changes. Most of the erythropoiesis happens in a specific niche of the bone marrow where macrophages regulate the maturation and phagocyte the expulsed nuclei (Palis, 2014).

Thrombocytes (Thon and Italiano, 2012), or platelets, are mainly responsible for hemostasis, i.e. preventing excessive bleeding by forming a blood clot (thrombus) when there is a lesion. Like erythrocytes, they do not have a nucleus but are even smaller (2-3 µm in diameter). Thrombocytes bud from megakaryocytes, large nucleated cells residing in the bone marrow with cellular extensions (proplatelets) dipped into blood vessels. Megakaryocyte differentiation is primarily directed by thrombopoietin (TPO), a growth factor that can also directly stimulate osteoclastogenesis (Bethel et al., 2015). In contrast, megakaryocytes themselves were shown to inhibit osteoclast formation and bone resorption *in vitro* (Beeton et al., 2006) while improving collagen expression and reducing the RANK-L/OPG ratio in osteoblasts (Bord et al., 2005). Recently, Kanagasabapathy et al. (2020) demonstrated in mice that megakaryocytes expression of RANK-L and TPO levels could be involved in age-related bone loss. As platelets are crucial early players upon injury,

their signals are essential to properly regenerate tissues afterwards. They are a major source of metabolites and proteins secreted form granules or lysosomes after platelet activation. Regarding tissue regeneration and inflammation, they can notably release coagulating factors, growth factors, such as PDGFs, vascular endothelial growth factor (VEGF) or hepatocyte growth factor, and cytokines, including angiopoietin 1 or several CXC and CC chemokines (CXCL-1/GROα, CXCL-8/IL-8, CCL-2/MCP-1, CCL-5/RANTES…). These mediators induce vasoconstriction, enhance migration and recruitment of immune cells involve in later stages of inflammation, regulate angiogenesis and more (Nurden, 2011). The multiple roles of their secretions and their central place in the response to tissue damage make them particularly interesting for regenerative therapies (Stellos et al., 2010).

c) Myeloid Cells

The myeloid lineage regroups diverse cell types from all granulocytes (basophils, eosinophils, and neutrophils) to mast cells and monocyte/macrophage lineage cells, including dendritic cells (DC) and osteoclasts. These highly specialized cells are mostly involved in innate immune response as they are activated by various unphysiological elements rather than targeting specific antigens. Therefore, they are also involved in the response to biomaterial surfaces. They have an important signaling activity, recruiting and regulating each other or participating in antigen presentation to activate the adaptive immunity.

Granulocytes (Geering et al., 2013) differentiate from myeloblasts, downstream of the common myeloid precursor, via multiple intermediate cell types. Two members of the CSF superfamily are involved in granulocytes development, granulocyte (G) -CSF and granulocyte/macrophage (GM) -CSF. G-CSF seems to be involved in granulopoiesis under physiological condition (during the steady-state) while GM-CSF is more associated with survival and activation of granulocytes (and macrophages) at an inflammation site. The mature form of granulocytes has a characteristic polylobed nucleus and cytoplasmic granules. The latter, released upon activation, contain cytokines to communicate with other immune cells or proteases and cytotoxins to destroy pathogens. All types of granulocytes seem to exhibit antigen-presenting abilities under specific conditions (Lin and Loré, 2017). Neutrophils are the most abundant granulocytes, representing around 60% of circulating white blood cells. They have a major role in driving the inflammatory reaction, releasing pro-inflammatory IL-6 or TNF, and its resolution by a variety of secretion such as apoptotic bodies and resolving mediators (Jones et al., 2016). In their interaction with bone cells, neutrophils were shown to inhibit osteogenic differentiation of MSC in co-cultures, supporting the detrimental effect of prolonged inflammation on bone regeneration (Bastian et al., 2018). Conversely, their inflammatory secretions could favor the development of osteoclasts, as shown by depleting them with an anti-Ly6G antibody in a mouse model of periodontitis (Kim et al., 2020).

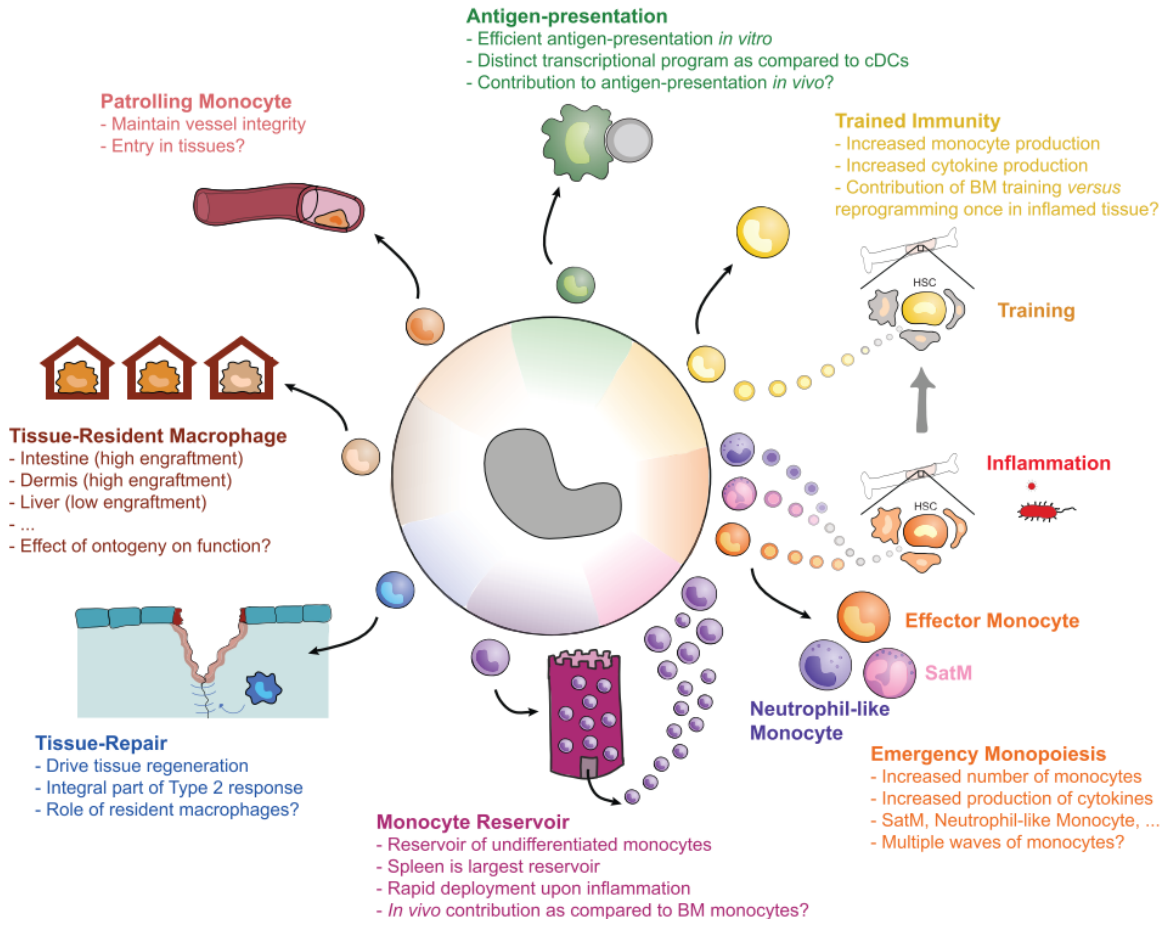

Figure 12: Diversity of monocyte functions (Guilliams et al., 2018)

Mast Cells are tissue-resident immune cells, closely resembling granulocytes but differentiating earlier from the myeloid stem cell (Franco et al., 2010). They are mostly studied in allergic reaction but are also involved in other inflammatory reaction. They are activated upon exposure to allergen, pathogens, or cytokine signals. They respond by degranulation, releasing preformed enzymes, growth factors and cytokines; that they can also directly secrete, such as interleukins-6, -9 and -13, and chemokines CXCL8, CCL2 and CCL5 (Theoharides et al., 2015). Many of these mediators can also interact with bone cells during physiological remodeling, fracture healing and bone disorders (reviewed in Ragipoglu et al., 2020). Using a mast cell deficient mice model, Kroner and colleagues (2017) notably shown that mast cells were an important source of pro-inflammatory cytokines after fracture. In their model, callus remodeling was impaired, and they observed reduced bone loss after ovariectomy, suggesting a positive regulation of osteoclastogenesis by mast cells. However, they did not report any abnormalities of bone formation or remodeling under physiological conditions. Systemic mastocytosis, a condition where clonal mast cells accumulate in various organs, is associated with osteoporosis in its indolent form but with increased bone mineral density in its advanced form (Riffel et al., 2020).

Monocytes account for 10% of circulating innate immune. Three types can be identified depending on their expression of the cluster of differentiation (CD) molecules 14 and 16: classical ($CD14^{high}$, $CD16^{-}$), intermediate ($CD14^{high}$, $CD16^{low}$) and non-classical ($CD14^{low}$, $CD16^{high}$). This classification seems limiting as it suggested strong differences in the CD expression while it seems to follow more of a “continuum”, even changing over time. They can be better distinguished by their multiple functions (Canè et al., 2019; Guilliams et al., 2018 & Figure 12): inflammatory monocyte, patrolling monocytes (involved in tissue repair), monocytic myeloid-derived suppressor cells (tumor development) or trained monocytes (innate immunity). This diversity contrasts with their previously thought function of undifferentiated intermediary between bone marrow precursors and dendritic cells or macrophages. Inflammatory monocytes can still differentiate into macrophages but also have distinct functions on their own.

Macrophages (Italiani and Boraschi, 2014) are major phagocytic cells, differentiating from circulating monocytes that infiltrate tissues upon inflammation. In monocyte/macrophages development and maturation, the two major cytokines are the steady-state expressed M-CSF and the inflammation-related GM-CSF. Other cytokines also participate in macrophages differentiation such as IL-4, also involved in T and B cell activation, and IL-34, second ligand of the MCSF receptor (CSF1R). The first step of macrophages activity is the recognition of microbe-associated molecular patterns (MAMP) from exogenous origin and damage-associated molecular patterns (DAMP) from cell debris needing to be cleared. Then, they proceed to engulf the targeted pathogen or dead cell in a phagosome. The content of the phagosome is later degraded by fusion with a lysosome. Macrophages exhibit a phenotypic diversity influenced by a variety of factors from their environment; a phenomenon described as macrophage polarization (Murray, 2017). As for

Inflammatory	***Profile***	Anti-inflammatory / Resolving Wound Healing
TNF, IFNγ, GM-CSF, LPS	***Stimulation***	IL-4, IL-13, M-CSF, TGF-β
MHCII, CD86, TLR4, HLA-DR	***Markers***	IL-4Rα, CD204, CD206
TNF, IL-6, IL-1, IL-12, IL-23, iNOS	***Secretions***	IL-10, TGF-β, VEGF

Figure 13: Simplified model of macrophage polarization.

monocytes, subtypes have been described, the two major being inflammatory “M1” macrophages and wound-healing “M2” macrophages, while in reality a spectrum of phenotypes between those extremes and changes throughout time are possible (Figure 13). As the primary cells involved in inflammation, macrophages are key players in wound healing (Kim and Nair, 2019). A second pool of macrophages, the tissue-residents, is present throughout the body and, in addition to their role during inflammation, participates in tissue development and homeostasis. Those macrophages could originate from both monocyte maturation and early embryonic progenitors already scattered in tissues. In bone, osteal macrophages, or OsteoMacs, have been shown to regulate bone cells activity, thus influencing remodeling (Chang et al., 2008; Pettit et al., 2008). As other macrophages, OsteoMacs are involved in tissue healing (Batoon et al., 2017) and essential players in the response to biomaterial (Miron and Bosshardt, 2016), therefore key cells to consider in designing therapies for bone regeneration.

Dendritic cells (DCs) are the major antigen presenting cells, linking the innate and adaptive immune systems. As reviewed by Collin and Bigley, (2018), three main subtypes have been described: plasmocytoid DC, classical (or myeloid) DC 1 and classical DC 2. Our understanding of the diversity of DCs and other immune cells will likely be broaden by cutting-edge techniques, as already demonstrated by Villani et al. (2017) who detected new subdivisions of DCs and monocytes through RNA sequencing. DCs are usually obtained *in vitro* by stimulation of monocytes with GM-CSF and IL-4. Evidences in mice showed that DCs are potential osteoclasts precursors both *in vitro* and *in vivo* (Wakkach et al., 2008). With human cells, Narisawa et al. (2020) reported higher bone resorption and stronger T cell stimulation with osteoclasts derived from DCs than with classical ones differentiated from monocytes. As part of their immunomodulatory function, MSCs seem to reduce DCs’ antigen uptake and migration ability while promoting an anti-inflammatory phenotype (Reis et al., 2018). As one possible path of monocyte differentiation, DCs also participate to the response to implanted materials and their (Keselowsky and Lewis, 2017).

d) Lymphoid Cells

Lymphoid cells are mostly involved in the response to pathogens and in building acquired immunity. The three main lymphoid cells are Natural Killer (NK) cells, B and T lymphocytes. As for most cells, their first description does not fully cover their multiple roles and internal diversity only being explored in recent years.

The major role of NK cells is to destroy virus-infected or tumoral cells by secreting cytotoxic granzymes and perforins. They also are a source of cytokine signals to coordinate the immune response. They can be distinguished from other lymphoid cells by their lack of rearranged antigen receptor as they do not need sensitization to be activated. In this regard, they are the most studied member of the recently identified subset of innate lymphoid cells (ILCs, Colonna, 2018). Conventional NK are circulating cells but tissue-resident ones were also described (Zhou et al., 2020). Hosting most of the hematopoiesis process, the bone

Chemokines	Other Name(s)	Receptor(s)	Influence on Osteoclasts	Influence on Osteoblasts
CXCL 1/2	GROα/β	CXCR 2	+	
CXCL 5	ENA-78	CXCR 2	+	
CXCL 8	IL-8	CXCR 1, 2	+	
CXCL 10	IP-10	CXCR 3	+	
CXCL 12	SDF-1, PBSF	CXCR 4	+	+
CX3CL 1	Fractalkine	CX3CR 1	+	
CCL 2	MCP-1	CCR 2	+	
CCL 3	MIP-1α, LD78α	CCR 1, 5	+	-
CCL 4	MIP-1β	CCR 5	+	
CCL 5	RANTES	CCR 1, 3, 5	-	+
CCL 11	Eotaxin	CCR 3	+	
CCL 20	LARC, MIP-3α	CCR 6	+	

Table 2: Chemokines influencing bone cells. (adapted from Murphy, 2018 and Brylka and Schinke, 2019) Overall positive (+) or negative (-) influence of chemokines on osteoclasts and osteoblasts development.

marrow is a tissue where resident NK are particularly studied to better understand their differentiation and self-renewing potential (Bonanni et al., 2019). While MSCs have been mostly reported as suppressive towards NK functions, Petri et al. (2017) recently suggested a more dynamic crosstalk. Short-term stimulation of MSCs by a viral MAMP led to activators of NKs through interferon secretion. With time, this effect switched toward a NK regulatory response as previously described.

Lymphocytes that mature in the thymus, T cells, are specialized in exogenous antigen recognition and therefore are the essential components of adaptive immunity. They regroup three major subtypes: cytotoxic T cells (T_c, $CD8^+$) destroying infected or mutated cells, helper T cells (T_h, $CD4^+$) assisting other lymphocytes and regulatory T cells (T_{reg}, $CD4^+$) mitigating the immune response by suppressing the activity of other T cells. The other type of lymphocytes, bone marrow-derived lymphocytes or B cells, are the producers of antibodies. Immature T lymphocytes are activated by the interaction with antigen presenting cells and T_h can then activate B cells in the secondary lymphoid organs. Subtypes of lymphocytes are long-lasting memory cells that can be remobilized by encountering a previously known antigen, thus accelerating the immune response. In relationship to bone, B cells seem to be indirectly, by production of RANK-L, and directly, by fusion of pro-B cells, involved in osteoclastogenesis through EPO signaling (Deshet-Unger et al., 2020). T lymphocytes were also associated to osteoclastogenesis as they express RANK-L (Horwood et al., 1999). More recently, Khassawna et al. (2017) demonstrated the direct role of T cells in directing mineral deposition by osteoblasts during fracture healing. Pro-inflammatory T cells were shown to directly stimulate osteoblast differentiation through IL-17 (Croes et al., 2016). MSCs are mostly suppressive towards lymphocyte and even promote T_{reg}, further participating in their immunomodulatory properties (Mougiakakos et al., 2011).

2. Cytokines & Bone Cells

The impact of immune cells on bone physiology often results from the responsiveness of bone cells to cytokines. Cytokines are primarily known as modulators of the maturation and activity of immune cells. They can be active at low levels and have singular pattern of cell activation and inhibition depending on the models and methods of analysis. In bone biology, they are particularly important during inflammation, after fracture or in longer lasting diseases. Osteoclasts, as a direct extension of the immune system, are bone cells particularly receptive to those signals. In addition to the essential RANK/RANK-L/OPG trio, other cytokines such as interleukins, chemokines and interferons influence bone cells (Lorenzo, 2020).

Chemokines (Murphy, 2018) are a subset of small secreted cytokines of characteristic tertiary structure, the chemokine fold. A limited number of chemokines can bind to a specific chemokine receptor. Most of the receptors (19 out of 23), the “typical” ones, are coupled with G protein while 4 “atypical” receptors are not. Depending on the arrangement of cysteines in their sequence, allowing the formation of disulfide bonds,

Cytokines	Receptor(s)	Influence on Osteoclasts	Influence on Osteoblasts
IL-1α/β	IL-1R1/-1R2	+	-
IL-4	IL-4R	-	-
IL-6	IL-6R, gp130	**Variable**	**Variable**
LIF	LIFR, gp130	**Variable**	**Variable**
OSM	OSMR, LIFR, gp130	-	+
IL-7	IL-7R, Common γ chain	**Variable**	**Variable**
IL-8	CXCR 1/2	+	
IL-10	IL-10R	-	-
IL-11	IL-11R, gb130	+	+

Cytokines	Receptor(s)	Influence on Osteoclasts	Influence on Osteoblasts
IL-12	IL-12R	-	
IL-13	IL-13R	-	-
IL-15	IL-15R	+	
IL-17	IL-17R	**Variable**	
IL-18	IL-18R	-	**Variable**
IL-23		+	
IL-33		-	
IL-34	CSF-1R	+	
IFN-α/β	IFNAR1	-	-
IFN-γ	IFNGR1, IFNGR2	**Variable**	**Variable**
TNF-α/β	TNFR1, TNFR2	+	**Variable**

Table 3: Cytokines influencing bone cells. (from Lorenzo, 2020)

Overall positive (+) or negative (-) influence of cytokines on osteoclasts and osteoblasts development.

chemokines are divided into 4 classes (C, CC, CXC and CX3C) with a specific letter differentiating the chemokine itself (the ligand, L) from the receptors (R). They are mostly involved in immune cells communication, especially chemotaxis, but some can have an impact on bone cell development and activity (Table 2, Brylka and Schinke, 2019).CXCL-12 (Gilbert et al., 2019) is particularly important in bone cells interaction with the immune system as a key regulator of the HSC niche. It can also favor osteoclast maturation as well as MSCs' osteogenic differentiation and participate in chondrocytes' regulation in the growth plate.

Interleukins (IL) are a heterogeneous group of cytokines, gathered by function and historical discovery more than structural similarities. In addition to their diverse primary functions on immune cells, they influence greatly the development of bone cells, especially under inflammatory conditions (Table 3, Amarasekara et al., 2018; Lorenzo, 2020). Many inflammatory cytokines such as TNF-α, IL-1 or IL-6 play a major role in the development of osteoclasts in inflammatory bone loss.

3. Fracture Healing

Fracture healing follows a sequence of events mixing inflammation, ossification and remodeling, where blood cells, immune cells and bone cells communicate and interact to restore pre-traumatic anatomy (Loi et al., 2016). As most wound healing mechanisms, it is initiated by the blood coagulation cascade forming the initial hematoma. The coagulation is associated with an inflammatory phase where immune cells clean the area from debris and delivers signals to move forward in the healing process. The actual repair phase depends on the anatomical site and type of fracture. Basically, with high stability and low complexity of the fracture, bone can be laid down directly to fill a small gap. In most cases, with a larger distance between bone ends, a cartilage callus is formed, and then replaced by bone which is further remodeled into the initial network of osteons (Figure 14).

Upon tissue injury, the first reaction of the body is the vasoconstriction to limit blood loss. Nonetheless, some blood will be in contact with the subendothelial tissue, triggering platelet aggregation and blood coagulation (Periayah et al., 2017). Formation of the hematoma is activated by the factors exposed from the ECM or released by damaged endothelial cells such as collagens and the Von Willebrand factor mediating platelets adhesion or the Tissue Factor initiating coagulation. Coagulation and platelet activation happen concurrently and stimulate one another. Thrombocytes undergo significant morphological changes, forming pseudopods to adhere to each and releasing factors by degranulation to enhance their own aggregation (thromboxane A2, ADP), modulate blood coagulation (factor V, VIII) and inflammation (Platelet Factor 4 / CXCL4, Neutrophil Activating Protein 2). The coagulation cascade is a series of protein (mostly serine protease) activating each other by cleavage, initiated mostly by the Tissue Factor. It ultimately leads to thrombin activation (factor IIa). Thrombin is another serine protease that transforms

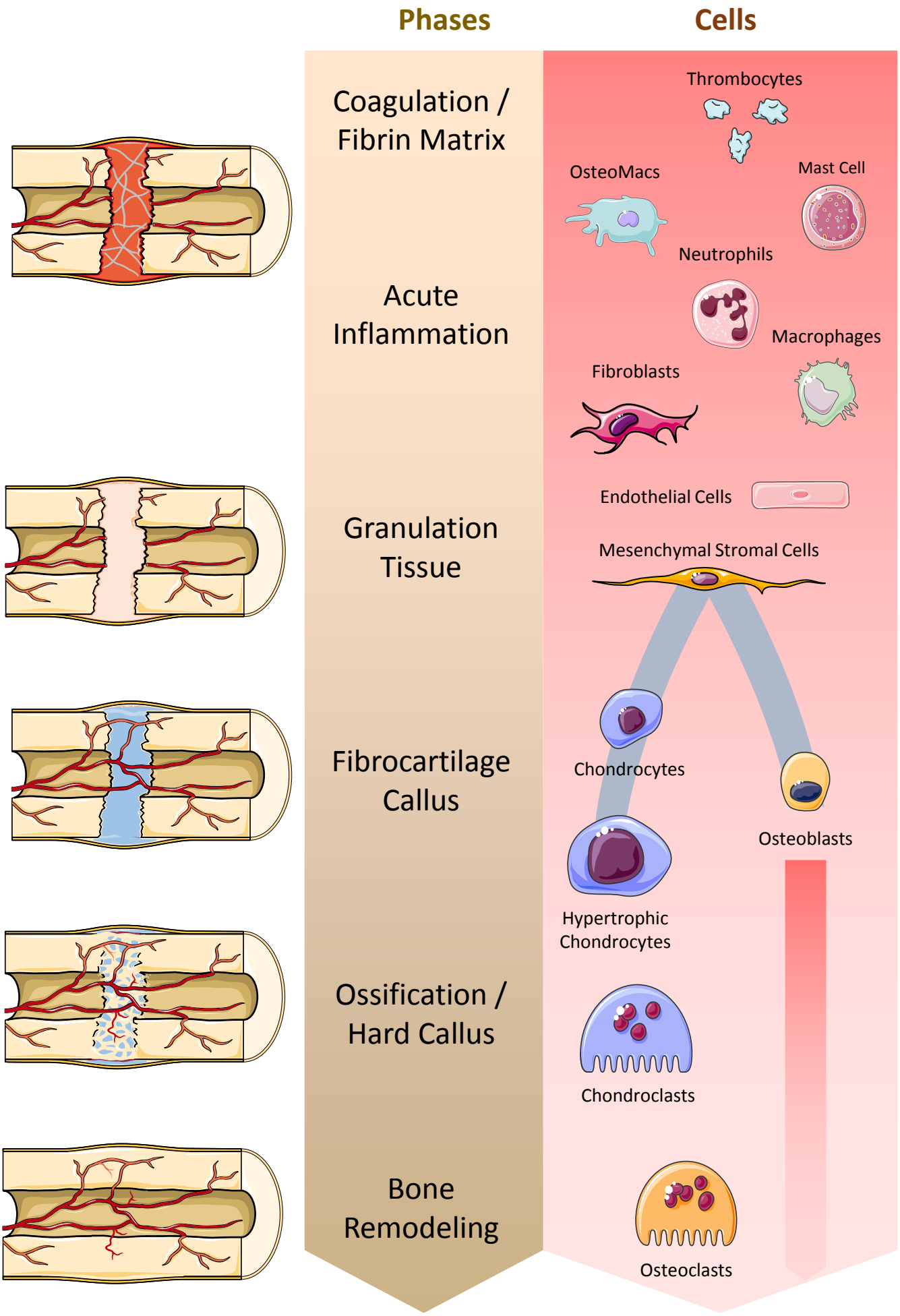

Figure 14: Phases of fracture healing.

insoluble fibrinogen into fibrin strands and participates in platelet activation. The fibrin matrix is the first step towards hemostasis and stabilization of the fracture.

The complement system is a humoral defense mechanism that is activated at the fracture site (Mödinger et al., 2018a). It is constituted of 35 circulating proteins, mostly produced by the liver. It has three activation pathways; the classical pathway involves antibody interaction; the lectin pathway is triggered by carbohydrate residues on bacterial membrane glycoproteins and the alternative pathway is activated by lipopolysaccharides and a broad variety of proteins. Active complement proteins enhance phagocytosis, perpetuate inflammation by neutrophils and macrophages recruitment or directly disrupt bacterial membrane by forming the membrane attack complex. In addition to their interactions with immune cells, complement proteins are present in the growth plate during development, expressed by bone cells and were found to influence their differentiation. Using knock-out mice models, Ehrnthaller et al. (2013) showed the importance of complement activation for proper callus formation after a fracture. Particularly, they demonstrated that expression of the receptor for complement protein C5a (C5aR1) was locally upregulated in osteoblasts and osteoclasts upon injury (Ignatius et al., 2011). However, an osteoblast-specific overexpression of this receptor impaired bone healing, suggesting a tight regulation of the complement proteins for efficient regeneration (Bergdolt et al., 2017).

Acute inflammation is led by OsteoMacs and mast cells already at the injury site and circulating neutrophils and monocytes attracted by signals from those tissue macrophages, activated platelets and damaged cells. These neutrophils seem to mostly serve as mediator with monocytes that they recruit via secretion of IL-6 and monocyte chemotactic protein 1 (MCP-1/CCL2). At this stage, macrophages have more of a pro-inflammatory phenotype, secreting additional IL-6 and CCL2 but also IL-1β and TNFα. Their main role is to phagocyte dead cells, debris and degrades the fibrin matrix while participating in the recruitment of fibroblasts, MSCs and endothelial cells. To do so, they release from the matrix or directly secrete a plethora of growth factors such as TGF-β family members, FGF-2, and VEGF. In particular, BMPs are a major source of chemotactic and osteogenic signals during fracture healing (Dumic-Cule et al., 2018). Additionally, OSM was proved to be a major osteogenic cytokine directly expressed by macrophages (Guihard et al., 2012, 2015). In this regard, this acute phase is essential. However, prolonged inflammation would be detrimental to the healing process as it will support osteoclasts development, unbalancing the equilibrium between bone formation and resorption (Claes et al., 2012).

Resolution of the inflammatory phase allows formation of a temporary granulation tissue, mostly composed of type III collagen produced by fibroblasts. At the same time, endothelial cells initiate neovascularization. Early on, the central area is still poorly supplied in O_2 and this hypoxia is one of the drivers of MSCs differentiation towards chondrocytes. The production of cartilage matrix leads to better stabilization of the fracture site by

forming the fibrocartilage callus. Concurrently, at the periosteum, direct intramembranous ossification occurs by osteoblastic differentiation of MSCs. By the same mechanism as endochondral ossification, chondrocytes eventually turn hypertrophic and leave empty spaces in the cartilage matrix for vessel growth. Precursors of chondro/osteoclasts and osteoblasts are carried to this ossification center and work in cooperation to replace cartilage by bone. Once the callus is fully ossified (hard callus), the original bone shape is restored by remodeling. The synchronization of these events, coordinated by complex cell communication and cell-matrix interactions, is essential to achieve complete healing. Logically, several signaling molecules were tested has therapeutic agents to shorten the healing period, such as BMPs or FGF-2, but without meaningful clinical results for now (Einhorn and Gerstenfeld, 2014).

4. Foreign Body Reaction

The "foreign body reaction" (Anderson et al., 2008) is the inflammatory response against an exogenous object perforating a tissue, a splinter from a piece of wood or an implanted medical device for example. It is a multistep process leading to the formation of a fibrous capsule isolating the foreign body from the adjacent tissue. In the case of implanted materials for bone regeneration, it needs to be turned into bone matrix. Therefore, understanding the reaction of the immune system to the biomaterial surface is crucial to develop efficient therapies.

As in fracture healing, the foreign body reaction is initiated by vessels and tissues disruption due to the surgery. Blood coagulation, complement activation (Mödinger et al., 2018b) and interaction of the implanted biomaterial surface with plasma proteins lead to the formation of a provisional fibrin matrix (Klopfleisch and Jung, 2017). In the beginning of the acute inflammation, the first immune cells involved are neutrophils and mast cells. They recruit other immune cells, including macrophages, to the site trough secretion of inflammatory signals. The adsorbed plasma and ECM proteins on the biomaterial provide attachment point for macrophages via integrins. This is where the material properties play a key role as they will influence protein adsorption, therefore macrophage reaction to the surface. Integrin binding induce cytoskeletal rearrangement and various intracellular signaling in macrophages. Under the right inflammatory conditions and on surfaces favorable for adhesion, macrophages can then fuse into multi-nucleated giant cells (MNGCs). The reason for cell fusion remains unclear but it has been suggested that it could either be an escape route from apoptosis or a way for macrophages to phagocyte larger particles. *In vitro*, IL-4 and IL-13 were shown to induce this fusion through upregulation of mannose receptors and the involvement of IL-4 was confirmed *in vivo*. In contrast with anterior hypothesis, Rodriguez et al. (2009) observed a comparable foreign body reaction in BALB/c nude mice compared to wild-type ones, even with fewer total leukocytes at the implant site. T cells were therefore not essential for MNGCs fusion. Instead, mast cells are suspected to be important producers of IL-4 and IL-13 (McLeod et al., 2015).

In the long run, MNGCs can either completely degrade the foreign material or lead to the formation of a collagenous capsule around the implant, isolating it from nearby tissues. In the second case, the environment close to the implant should still be inflammatory as MNGCs continue to secrete reactive oxygen species and degradation enzymes, preventing complete healing. *In vitro*, ten Harkel et al. (2015) showed very superficial degradation of an hydroxyapatite coating by MNGCs compared to osteoclasts, suggesting that they could slowly degrade implanted CaP materials. Both processes of fracture healing and foreign body reaction, bringing together immune and bone cells, are to consider for the design of bone regeneration strategies.

D. Bone Regeneration Strategies

In addition to trauma-induced fractures, diseases such as osteoporosis or osteogenesis imperfecta can provoke bone abnormalities or make it prone to fragility fractures. Bone sarcomas can induce abnormal osteolysis by osteoclast hyperactivation and the treatments include, in most cases, surgical resection of the tumor resulting in a bone defect needing to be filled. The gold standard for non-unions and skeletal defects healing is autologous bone grafts. Despite its effectiveness, this technique has numerous drawbacks leading to the development of innovative therapeutic strategies. Most of them combine bone substitutes, such as CaP materials, and osteogenic factors or MSCs.

1. Bone grafts

Following the “diamond concept”, bone grafts efficacy is based on four major properties that need to be taken into account in the design of biomaterial-based therapies: osteoconduction, mechanical strength, osteoinduction and osteogenesis (Albrektsson and Johansson, 2001; Fillingham and Jacobs, 2016; Giannoudis et al., 2007). A material is osteoconductive if it allows new bone formation on it. Its composition and surface properties are compatible with the survival and growth of bone cells and it should lead to osseointegration of the implant if those cells are activated. Mechanical strength is essential given the shear and compression stresses the implant may have to sustain depending on the anatomical region of implantation. Osteoinduction is the ability to recruit and activate bone cells at the implantation site. Finally, a graft is osteogenic if it contains viable bone cells (MSCs, osteoblasts, osteocytes) capable of producing new bone.

A variety of harvesting sites and surgical technics are used for autologous bone grafting depending on the defect location, size and shape (Jakoi et al., 2015). The ratio of cortical to trabecular bone needs to be considered, as cortical bone gives more stability but less marrow, therefore less osteogenic cells. Cancellous bone from the iliac crest is the most frequent filling for non-unions, the lack of strength being compensated by immobilization. Obviously, large defect are challenging to manage and require complex surgery technics as vascularization becomes a crucial factor to consider (Vidal et al., 2020). In mandibular reconstruction for example, transplantation of whole segments of the fibula associated with

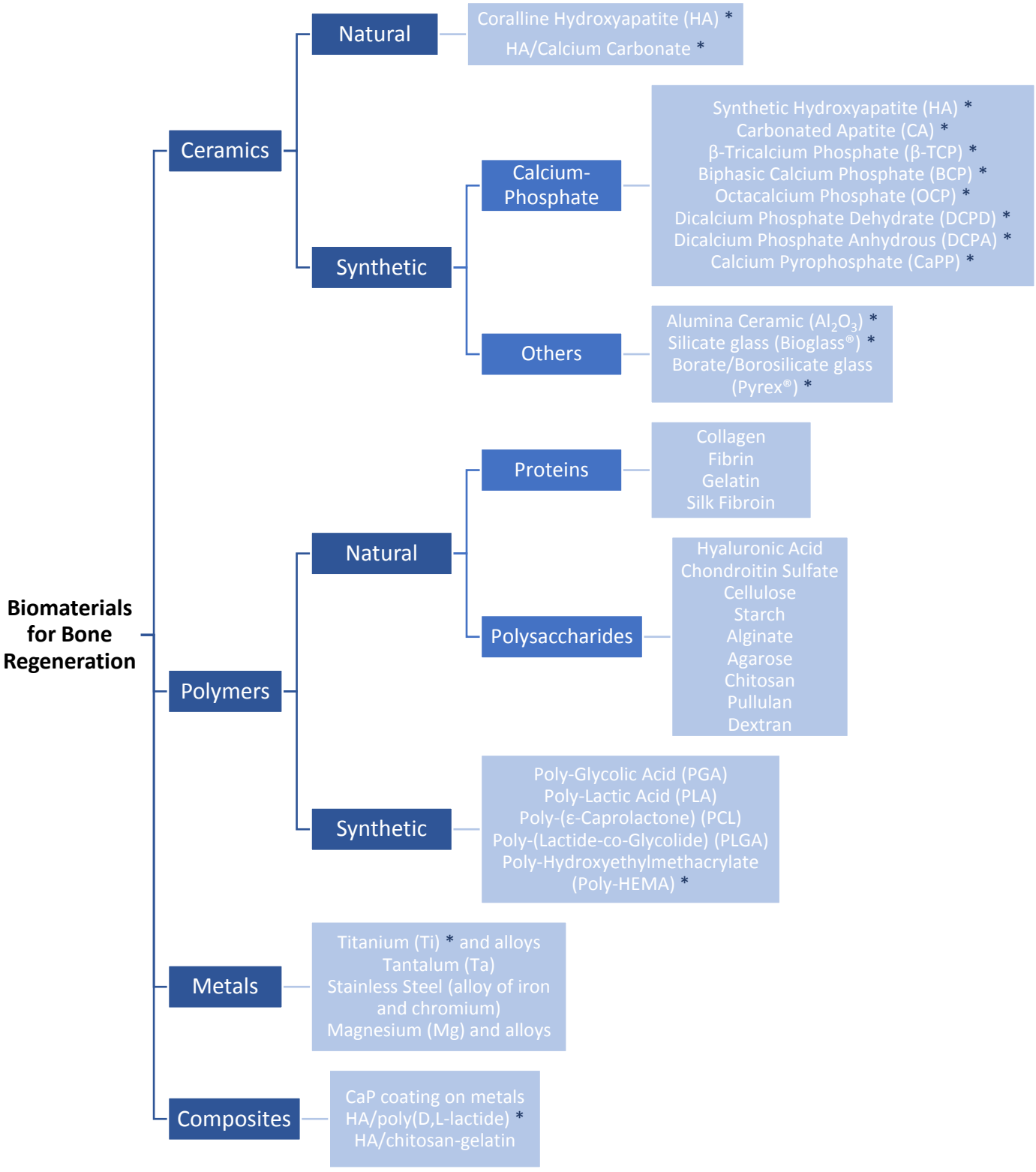

Figure 15: Materials for bone regeneration.
(adapted from Barradas et al., 2011 and García-Gareta et al., 2015)

Materials with inherent osteogenic properties in animal models are indicated by *.

their original vasculature are successfully used. Surgery planning based on 3D reconstruction from computed tomography scan could improve the treatment of those difficult cases (Wang et al., 2016).

The major limitations of bone grafting are the amount of bone available, the complexity of the surgery, the pain and morbidity associated with the donor site. Cadaveric bone can be used as an allograft, avoiding the complications related to the harvesting site and reducing the operative time. Also available in larger quantity, it is practical alternative for large defect reconstruction. However, this type of graft can be responsible for disease transmission even with donor screening and quality control during preservation (Zamborsky et al., 2016). Bone substitutes from other species, xenografts, are also studied to overcome the limited bone volume available but this type of procedure is prone to poor integration or even rejection. Overall, autologous bone grafting showed unmatched effectiveness in clinical trials with an union rate of 91% (Azi et al., 2016).

2. Biomaterial-based Therapies

Strategies using synthetic substitutes in lieu of bone grafts can be divided in three categories, based on their risk level, determining the regulatory path for their validation. Bone substitutes, alone or with only modifications of the surface properties with a coating or chemical treatment, are the simplest systems entering the Food and Drug Administartion (FDA) classification system as medical device of class II. They are usually studied for small defect reconstruction as they do not carry osteogenic elements. There development is also driven by the availability of 3D printing for numerous materials, allowing personalized manufacturing of implants. The adjunction to the biomaterials of growth factors, peptides from ECM proteins or other small proteins brings the product to a medical device of class III. Finally, an implant containing stem cell cells is not considered a medical device by the FDA and enters the regulation of cellular and gene therapy product. In Europe, medical devices need to obtain a CE mark rather than being evaluated by an agency. Cell therapies are also treated separately and considered “advanced therapeutic medicinal products”. (Ho-Shui-Ling et al., 2018)

a) Biomaterials

Biocompatible materials are the basis of bone regeneration strategies as they physically fill defects and are the support for new bone growth. The essential property required is therefore osteoconductivity. Four types of materials are mainly used: metals, polymers, ceramics and composites of the previous three (García-Gareta et al., 2015 & Figure 15).

Metals have been historically used in prosthetics for their strength and durability. However, they can be associated with toxicity due to the release of metallic ions and a lack of osteoconductivity leading poor osseointegration and implant loosening. Coating titanium implants with titanium dioxide (TiO_2) enhance cell adhesion and biocompatibility. Titanium

showed osteoinductive properties only after chemical (NaOH) and heat treatment, creating micro-pores on the surface. Tantalum, used effectively in hip replacement, could also have improved biocompatibility after tantalum oxide (Ta_2O_5) coating. Magnesium is being studied primarily for the effect of its released ions Mg2+ on bone metabolism and its elasticity closer to bone's compared to other metals.

Polymers are, in some ways, the opposite of metals. On the one end, they often display poor mechanical strength and high degradation rate but on the other hand, they are highly versatile, malleable and can be rapidly replaced by new matrix from host cells. Obviously, cells have high affinity with natural polymers, such as collagen or chitosan, leading to proper integration. Complex ECM can be recreated by combining them. The development of synthetic polymers broadens the available micro- (surface structure, porosity) and macro-properties (size, shape, mechanical strength) of polymer-based material. The drawbacks of those new molecules are the acidic products and small particles from dissolution that can trigger an inflammatory reaction.

CaP ceramics are a middle ground between the previous two. Their composition, closely resembling the inorganic phase of bone, allows for both superior mechanical strength than polymers and better osteoconduction than metals. Their biomimetic characteristics lead to early and extensive analysis of those materials and the diversification of their composition. Compared to other materials, most studies found some favorable conditions for osteoinduction with CaP alone They are obtained either by solid state reaction at high temperature (sintered CaP) or by precipitation from an aqueous solution at lower temperature (biomimetic CaP); HA being the only one that can be obtain by both methods. Their major disadvantage is their brittleness due to their lack of elasticity, given by the organic phase in natural bone. They are mostly used as blocks or granules that participate in this fragility and can make them unpractical in the operative room. Combining CaP with various proteins and synthesizing them as easier implantable devices are the main challenges of their development in upcoming years. (Ginebra et al., 2018)

All physical and chemical properties of a material can influence integration and bone formation in one way or the other. Macro-porosity permits vessels ingrowth. Chemical composition and micro-architecture of the surface can influence immune cell response and degradation rate (Sheikh et al., 2015). Ions released during degradation can either be chemotactic for bone cells or completely toxic. Some materials are more suitable than others to deliver growth factors and osteogenic cells. In the case of implanted cells, they are also influenced by all the properties of the biomaterial, even the material stiffness could alter their phenotype (Darnell et al., 2018). In the end, all materials carry some disadvantages and are best suited for different applications. Composites allow counterbalancing the weaknesses of one material by the properties of another. For example, CaP coating on metals increases the osseointegration of the most mechanically stable type of implants (Su et al., 2019). Mixing polymers with CaP ceramics in an attempt to

mimic the bone dual composition seem promising, especially as a mean to deliver growth factor, but no composite got close to the mechanical properties of bone for now (Yunus Basha et al., 2015).

b) Osteogenic Factors

Some of the materials presented above demonstrated osteoinductive properties when implanted alone in ectopic sites (intramuscularly or subcutaneously) in animal models (Barradas et al., 2011). However, osteoinductivity is overall the weakest property of any biocompatible material as it associates modulation of inflammation and chemotactic signals towards bone cells. This complex property of bone grafts is conveyed by bone cells and the signaling proteins they express. Therapeutic use of growth factors often requires the design of specialized biomaterials for efficient delivery (De Witte et al., 2018). The proteins can be adsorbed or bound at the surface, entrapped in the material or incorporated into nano/microspheres. The objective is to avoid fast clearance of the active molecules, as observed with injections, without bringing supraphysiological doses that could have adverse effects. The material should also retain its osteoconductive and mechanical properties. Given their malleability, polymers are the most promising for these applications. For example, Witzler et al. (2019) reviewed the polysaccharides that could be used in the design of such materials. However, CaP and metallic surfaces can also be functionalized or coated to enhance their osteogenic potential.

Given their implication in bone metabolism and fracture healing, BMPs are among the most promising growth factors in regenerative therapies (Salazar et al., 2016). Recombinant human BMP-2 has received FDA approval for several applications already (Schmidt-Bleek et al., 2016). As various BMPs are expressed throughout the healing process of fractures, sequential administration or delayed release from the material may be optimal to match the phases of regeneration. Several other products associating bioactive molecules and biomaterials are being developed or already commercialized, as reviewed by Ho-Shui-Ling et al. (2018). In addition to recombinant growth factors such as PDGFs or BMPs (-2, -6 or -7) some contain PTH or the collagen-derived peptide P-15, favoring stem cell adhesion and differentiation. The use of VEGF in combination with other factors could also be interesting as vascularization is a critical parameter, bringing in stem cells and releasing growth factors (Hu and Olsen, 2016).

Although easier from a technical and regulatory point of view, the addition of growth factors to a material cannot recapitulate the complexity of signals emitted by cells over time. Platelet rich plasma (PRP) and bone marrow aspirate concentrate (BMAC) are raw mixtures containing cells, growth factors and other proteins explored as intermediate between purified factors and *in vitro* expanded cells. (Yamaguchi et al., 2019). Both are fairly practical to prepare and showed promising results in bone and cartilage regeneration. However, both have their limitations as PRP preparation still needs to be standardize and BMAC collection is an invasive intervention. In addition, BMAC efficacy seems closely

Source	Surface Markers	Lineage Differentiation
Bone marrow	Positive: SH2, SH3, CD29, CD44, CD49e, CD71, CD73, CD90, CD105, CD106, CD166, CD120a, CD124 Negative: CD34, CD45, CD19, CD3, CD31, CD11b, HLA-DR	Adipogenic, Chondrogenic, Osteogenic
Umbilical cord / Umbilical cord blood	Positive: CK8, CK18, CK19, CD10, CD13, CD29, CD44, CD73, CD90, CD105, CD106, HLA-I, HLA-II Negative: CD14, CD31, CD33, CD34, CD45, CD38, CD79, CD133, vWF, HLA-DR	Adipogenic, Chondrogenic, Osteogenic, Endothelial-like cells, Neuron-like cells
Wharton's jelly	Positive: CD13, CD29, CD44, CD73, CD90, CD105, HLA-I Negative: CD14, CD34, CD45, CD31, HLA II	Adipogenic, Osteogenic
Adipose tissue	Positive: CD13, CD29, CD44, CD73, CD90, CD105, CD166, HLA-I, HLA-ABC Negative: CD10, CD14, CD24, CD31, CD34, CD36, CD38, CD45, CD49d, CD117, CD133, SSEA4, CD106, HLA- II, HLA-DR	Adipogenic, Chondrogenic, Osteogenic, Neurogenic, Muscular
Amniotic fluid	Positive: SH2, SH3, SH4, CD29, CD44, CD49, CD54, CD58, CD71, CD73, CD90, CD105, CD123, CD166, HLA-ABC. Negative: CD10, CD11, CD14, CD31, CD34, CD49, CD50, CD117, HLA-DR, DP, DQ, EMA.	Adipogenic, Osteogenic, Neurogenic
Dental tissues	Positive: CD29, CD44, CD90, CD105, CD, SH2, SH3, HLA- DR, CD117, CD146, DPSC- EZ, DPSC-OG Negative: CD10, CD14, CD34, CD45, HLA-DR, Stro-1, NGFR	Adipogenic, Chondrogenic, Myogenic, Osteogenic
Skin	Positive: CD90, CD73, CD105, SSEA4 Negative: CD14, CD45, CD34, c- kit, CD133, SSEA3, Oct-4, TRA 1–60, TRA 1–81, HLA-DR	Adipogenic, Myogenic, Osteogenic
Placenta	Positive: CD29, CD44, CD73, CD90, CD105 Negative: CD45, CD34, HLA-DR	Adipogenic, Endothelial-like cells, Neurogenic, Osteogenic
Salivary gland	Positive: CD13, CD29, CD44, CD49f, Thy-1, CD90, CD104, p75NGFR, b2-microglobulin, CD130 Negative: CD34, CD38, CD45, CD133	Adipogenic, Chondrogenic, Osteogenic, Pancreatic endocrine
Synovial fluid	Positive: CD10, CD166, CD44, CD54, CD90, CD105, CD147, D7-FIB, STRO-1 Negative: CD31, CD34, CD45, CD106, CD117, CD166, VEGFR2, Flk-1, CXCR4, BMPR-1A, NGFR	Adipogenic, Chondrogenic, Osteogenic

Table 4: Main sources of MSCs for regenerative medicine, their surface markers and differentiation potential. (adapted from Mushahary et al., 2018)

correlated to the number of stem cells, therefore may not be as efficient as a higher number of expanded cells obtained from a similar bone marrow aspiration.

c) Stem cells

The need for a precise classification of MSCs (Dominici et al., 2006) came from the increasing interest around their potential uses in regenerative therapies. Defining what makes a MSC is essential to ensure reproducible and safe clinical applications. MSCs and their derived culture media or isolated extracellular vesicles have potential applications for regenerative therapies of multiple organs and tissues such as nerves, heart, liver, cornea, cartilage or, of course, bone (Han et al., 2019). As for bone regeneration, most applications emerged from the identification of MSCs differentiation potential into cells of those targeted tissues. However, their major role as immune-modulators is now being recognize and increasingly studied for the treatment of immune-related diseases such as multiple sclerosis, Crohn's disease or graft versus host disease (Wang et al., 2018b).

For bone regeneration, MSCs are classically isolated from the bone marrow by their ability to attach to plastic surfaces, as they were originally discovered (Owen and Friedenstein, 1988). As reviewed by Mushahary et al. (2018), MSC-like cells can be isolated from multiple tissues but have different surface markers and differentiation potential (Table 4). In the same vein as the discovery of the skeletal stem cell subset, these differences suggest tissue-specific subtypes. Their distinct differentiation capacities could also favor the use of certain tissue-derived MSCs based on the desired application, especially the receiving tissue. However, this can conflict with the isolation procedure as some sources of MSCs are more easily available than others. For example, adipose tissue-derived stem cells (ATSC) could offer a great alternative in bone regeneration therapies as this tissue can be accessed with minimally invasive procedures compared to the bone marrow (Barba et al., 2017). ATSCs meet the criteria for MSCs *in vitro* and enhance calvarial defect bridging in mice without the need of an osteogenic priming (Carvalho et al., 2014). However, when compare to bone marrow MSCs, a previous study from our lab demonstrated less efficient ectopic bone formation (Brennan et al., 2017). Similarly, Xu et al. (2017) reported lower osteogenic differentiation potential *in vitro,* and lesser ectopic and orthotopic bone formation *in vivo* with ATSCs compared to bone marrow MSC. The gain from a high yield and less invasive harvesting procedure compared to a potential loss in efficacy still needs to be weighted in clinical applications.

Other sources of MSC have been evaluated in preclinical models. A pilot study by Wang et al. (2015) evaluated, alongside bone marrow MSCs and in combination with calcium phosphate cement, the use of umbilical cord MSCs and induced pluripotent stem cells (iPSCs) for the repair of a cranial defect in rat. Both cell types evaluated showed similar angiogenic and bone inducing properties as bone marrow MSCs. A range of dental stem cells (from the pulp, the apical papilla, the follicle…) are studied for bone regeneration, particularly for specific craniofacial reconstruction given their origin and limited availability

(Ercal et al., 2018). Genetically engineering MSCs is a future perspective to compensate for their unfavorable origin or enhance further their osteoinductive properties, by specifically increasing the secretion of desired mediators or improve their proliferation *in vitro* to ameliorate the yield of amplification (Freitas et al., 2019). Obviously, these projects still face major safety and regulatory limitations for now.

The mechanism by which MSCs induce bone formation is discussed in detail in the following review article. We gathered data from *in vitro* and preclinical studies, highlighting the influence of macrophages and osteoclasts in the success of bone regeneration strategies using CaP materials in combination with MSCs. Characteristics of CaP materials (micro- and macro-porosity, surface roughness and chemical composition) direct immune response and therefore bone regeneration. The host response is further modulated by the crosstalk between immune cells and implanted MSCs. Undoubtedly, the inflammatory and hypoxic environment of the implantation site greatly influence MSCs' secretion. Taken together, these observations built our working hypothesis that MSCs, particularly under stressful conditions, release immunomodulatory mediators reducing inflammation and turning the foreign body reaction against CaP materials into osteoclast formation, initiating local bone remodeling.

frontiers in Immunology

REVIEW
published: 02 April 2019
doi: 10.3389/fimmu.2019.00663

Immune Modulation by Transplanted Calcium Phosphate Biomaterials and Human Mesenchymal Stromal Cells in Bone Regeneration

Paul Humbert[1], *Meadhbh Á. Brennan*[1,2], *Noel Davison*[3,4], *Philippe Rosset*[1,5], *Valérie Trichet*[1], *Frédéric Blanchard*[1]* *and Pierre Layrolle*[1]

[1] *Laboratory Phy-Os, Inserm UMR1238, University of Nantes, Nantes, France,* [2] *Harvard School of Engineering and Applied Sciences, Harvard University, Cambridge, MA, United States,* [3] *MERLN Institute for Technology-Inspired Regenerative Medicine, Maastricht University, Maastricht, Netherlands,* [4] *Instructure Labs, B.V., The Hague, Netherlands,* [5] *Centre Hospitalier Universitaire de Tours, Tours, France*

OPEN ACCESS

Edited by:
Claudine Blin-Wakkach, UMR7370 Laboratoire de Physio Médecine Moléculaire (LP2M), France

Reviewed by:
Catarina R. Almeida, University of Aveiro, Portugal
Yasser Mohamed El-Sherbiny, Nottingham Trent University, United Kingdom
Aisling Dunne, Trinity College Dublin, Ireland

***Correspondence:**
Frédéric Blanchard
frederic.blanchard@univ-nantes.fr

Specialty section:
This article was submitted to Inflammation, a section of the journal Frontiers in Immunology

Received: *11 December 2018*
Accepted: *11 March 2019*
Published: *02 April 2019*

Citation:
Humbert P, Brennan MÁ, Davison N, Rosset P, Trichet V, Blanchard F and Layrolle P (2019) Immune Modulation by Transplanted Calcium Phosphate Biomaterials and Human Mesenchymal Stromal Cells in Bone Regeneration. Front. Immunol. 10:663. doi: 10.3389/fimmu.2019.00663

A wide variety of biomaterials have been developed as both stabilizing structures for the injured bone and inducers of bone neoformation. They differ in chemical composition, shape, porosity, and mechanical properties. The most extensively employed and studied subset of bioceramics are calcium phosphate materials (CaPs). These materials, when transplanted alongside mesenchymal stem cells (MSCs), lead to ectopic (intramuscular and subcutaneous) and orthotopic bone formation in preclinical studies, and effective fracture healing in clinical trials. Human MSC transplantation in pre-clinical and clinical trials reveals very low engraftment in spite of successful clinical outcomes and their therapeutic actions are thought to be primarily through paracrine mechanisms. The beneficial role of transplanted MSC could rely on their strong immunomodulatory effect since, even without long-term engraftment, they have the ability to alter both the innate and adaptive immune response which is critical to facilitate new bone formation. This study presents the current knowledge of the immune response to the implantation of CaP biomaterials alone or in combination with MSC. In particular the central role of monocyte-derived cells, both macrophages and osteoclasts, in MSC-CaP mediated bone formation is emphasized. Biomaterial properties, such as macroporosity and surface microstructure, dictate the host response, and the ultimate bone healing cascade. Understanding intercellular communications throughout the inflammation, its resolution and the bone regeneration phase, is crucial to improve the current therapeutic strategies or develop new approaches.

Keywords: osteoimmunology, mesenchymal stromal cell, calcium phosphate biomaterial, bone regeneration, osteoclast, immune modulation

INTRODUCTION

Bone regeneration strategies remain a critical challenge in the treatment of delayed union and non-union fractures (1), bone loss due to tumor resection (2), metabolic bone diseases, or to heritable skeletal dysplasia such as *osteogenesis imperfecta*. Autologous bone grafting is the current clinical gold standard to repair large bone defects. This entails harvesting the patient's own bone

fragments, and transplanting them to the site of injury (3). There are ∼2.2 million bone graft procedures performed annually worldwide, including 1 million procedures in Europe (4). Indeed, after blood, bone is the most frequently transplanted tissue. The significant disadvantages of bone grafting, including the severe pain and morbidity endured by patients as a consequence of the bone harvest site, have prompted advances in the development of synthetic biomaterials targeting bone repair. Human bone comprises ∼70% of calcium phosphate (CaP) mineral; therefore CaPs are the biomaterials of choice to heal injured bone. They were first introduced in the 1920s as materials to facilitate bone repair (5) and have since undergone intense chemical and physical developments aimed at optimizing porosity, surface architecture, resorption rates, and mechanical strength in order to improve their bone healing capacities. Despite these advances in biomaterial design, CaPs still lack adequate osteogenecity to heal large, critical sized bone defects, and thus cell therapy has been employed for bone defect treatment with biomaterial bone substitutes such as CaPs to increase bone regeneration efficiency. Mesenchymal stromal stem cells (MSCs), derived primarily from the bone marrow and isolated by adherence to plastic, show great capacity for bone healing in unison with CaPs (6, 7). Although it is yet to be adopted into standard clinical practice, this state-of-the-art cell therapy is currently the most promising regenerative medicine strategy and has demonstrated successful bone healing in patients in clinical trials (8). The initial premise that MSCs, through cellular differentiation, regenerated damaged tissue was largely disregarded following observations that very few transplanted cells survive and engraft (9–11). Few children with severe *osteogenesis imperfecta* have received allogenic bone marrow transplant or allogenic MSC and showed faster growth, higher bone mineral content and less bone fracture than before transplant (12–16). Such growth and mineralization improvements were associated with <5% of donor cell engraftment. Consequently, it is proposed that the therapeutic benefit of transplanted MSCs is largely through a paracrine mechanism that stimulates recruitment of host cells, which ultimately form the new bone tissue. The underlying mechanisms involved have yet to be delineated, however evidence to date reveals that roles of MSCs and their secretions such as modulating immune responses (17), attenuating inflammation, and promoting angiogenesis (18), together act to ultimately ameliorate healing and restore function. The host immune-modulatory response to both CaPs and MSCs, encompassing both innate and adaptive immunity, and how this contributes to bone healing in the context of tissue engineered implants is the focus of the current review.

OSTEOIMMUNOLOGY OF CALCIUM PHOSPHATE CERAMICS IN BONE REGENERATION

A wide variety of CaP biomaterials have been developed to fill bone defects as alternatives to autologous bone grafting. Synthetically synthesized ceramics mainly comprise sintered CaPs in order to achieve higher mechanical strength, including β-tricalcium phosphate (β -TCP), hydroxyapatite (HA), or their mixtures (biphasic calcium phosphate: BCP). These CaPs are therefore widely described in terms of their interactions with cells and tissues following implantation, as well as in relation to their bone forming abilities. Synthetic CaPs bioceramics are used successfully to fill bone defects in various clinical indications since they are considered biocompatible, bioactive and osteoconductive, thereby permitting guidance of the bone healing process (19). *In vivo*, the chemical and physical properties of the biomaterial dictate the host response and the ultimate bone healing cascade and osteoinduction has been achieved by various CaP ceramics, which demonstrate ectopic bone formation when implanted in the muscles or subcutaneously in animals [reviewed in (13)].While the interactions of these CaP materials with body fluids, cells, and tissues have been investigated at both the microscopic and ultrastructural levels, there is still a lack of understanding of the potential mechanisms leading to osteoinduction. Early on, the dissolution and precipitation of an apatite layer on CaP materials was identified as a potential major trigger for bone formation (20). It was further proposed that concentration of bone growth factors from body fluids, especially BMPs onto the biomaterial surface, attracts circulating stem cells to form bone tissue (21). The geometry of the biomaterial is certainly a critical parameter for bone induction. Studies demonstrate that in order for CaPs to exhibit osteoinductive properties, both a macroporous structure and surface microporosity are prerequisites. Micro- and macro-porous BCP biomaterials demonstrated the ability to induce mature lamellar bone tissue after 6 months without the addition of osteogenic cells or bone growth factors when implanted ectopically in sheep (22). Macro pores are introduced into CaPs by the addition of pore makers during the fabrication process. The importance of macrostructure in efficient osteoinduction is highlighted as bone formation occurs primarily in concavities (23). Microporosity is controlled by the sintering temperature, with lower sintering temperatures resulting in higher surface microporosity. Interestingly, the microporous CaPs bioceramics exhibited higher bone growth in critical size bone defects in goats compared with autologous bone grafts or the same CaPs bearing larger surface micropores and lower specific surface area (higher sintering temperature) (24). Increasing the microporosity increases the surface area thus possibly enhancing the dissolution/reprecipitation phenomenon (21). Further to biomaterial geometry, it has been speculated that low oxygen tension in the central region of the implants might provoke dedifferentiation of pericytes from blood vessels into osteoblasts (25). Most recently, Bohner and Miron added the idea that depletion of calcium and/or phosphate ions in the center of an implanted material could induce bone formation *via* the calcium-sensing of immune and bone cells (26).

In early reports, bone induction by CaPs ceramics was thought to be limited to the muscles of large animals such as rabbits, sheep, goats, dogs, and baboon, until Barradas et al. screened various different mouse strains and found osteoinduction by CaPs ceramics in FVB/NCrl mice (27). This study was a major step for further understanding the biological mechanisms of osteoinduction by these ceramics because there are abundant

immunohistochemistry protocols available for mice compared to large animals, not to mention their ease of handling and low cost.

Innate Immune Response to Calcium Phosphate Biomaterials

Various innate immune cells participate in the host-cell response to the implantation of CaP materials including mast cells, neutrophils, monocytes, macrophages, and multinucleated giant cells (MNGCs) (28). In addition to their role in the innate immune response, macrophages have tissue-specific functions. Osteal macrophages (so called OsteoMacs), a specific type of specialized macrophages residing in the periosteum and endosteum, are an important cell type for the regulation of bone healing (29) but less is known about their relationship with implanted biomaterials (30). Depletion of OsteoMacs in mice demonstrates their key role in regulating bone regeneration in normal bone healing in a bone injury model (31, 32), suggesting that resident macrophages may also possess the phenotypic capability to instruct bone regeneration upon implantation of biomaterials used for bone repair. Previous studies have documented that resident or infiltrating monocyte-derived macrophages present at early time points after tissue trauma or the implantation of a biomaterial are characterized as pro-inflammatory (M1 macrophages), typified by their secretion of inflammatory cytokines such as TNFα, IL-1, IL-6, and IL-12, while macrophages present at later time points exhibit a predominantly anti-inflammatory profile (M2 subtype) and promote healing by secretion of cytokines such as IL-10 and TGF-β, stimulating angiogenesis, and recruiting cells for tissue repair (33–36). Importantly, macrophage polarization can be switched between M1 and M2, rendering them highly sensitive and adaptive to their environment. Moreover, mounting evidence suggests that macrophage polarization occurs over a continuous spectrum, rendering the M1/M2 classification paradigm too simple to accurately characterize their dynamic phenotypic changes and plasticity *in vivo*. In any case, macrophages are among the first cells present at the site of CaP implantation and play an integral role in MSC migration and bone formation (**Table 1**). The infiltration of macrophages and the subsequent homing of MSCs and ectopic bone formation was observed after CaP implantation in mice (44). Interestingly, MSCs migration and osteogenic differentiation was significantly enhanced by conditioned media (CM) from macrophages cultured on BCP, compared to CM from macrophages cultured on tissue culture plastic (43, 44). Furthermore, it was shown that macrophage-secreted MCP-1 and MIP-1α were the effectors of enhanced MSC migration.

Osteoclasts, which originate from the same hematopoietic precursor as macrophages, are multi-nucleated cells capable of efficiently degrading both the organic and inorganic fractions of bone. Activated osteoclasts have a characteristic morphology including a ruffle border by which they secrete proteases, such as cathepsin K and matrix metalloproteinases, and release hydrogen ions by proton pumps to acidify the resorptive pit. Histologically, osteoclasts can be identified by intensely positive tartrate-resistant acid phosphatase (TRAP) activity, which relates to their functional activity in resorbing bone or mineralized substrates such as CaPs (45). Osteoclastogenesis is essentially regulated, both *in vivo* and *in vitro*, by the macrophage colony-stimulating factor (M-CSF) and the tripartite system constituted by the receptor activator of nuclear factor κB (RANK), its ligand (RANKL) and osteoprotegerin (OPG). M-CSF permits survival and proliferation of osteoclast-precursors, also allowing them to respond efficiently to RANKL stimulation. RANKL triggers differentiation into osteoclasts by binding RANK, while OPG can prevent the interaction as a decoy receptor for RANKL (46). Osteoclasts are important players in the bone healing cascade. Several studies have documented that osteoclast presence at the site of CaP implantation precedes new bone formation (39). Evidence to demonstrate the crucial interplay between osteoclasts and osteoblasts, in association with CaPs, was highlighted by several studies (**Table 1**). Bisphosphonates are a class of drug employed to inhibit bone resorption by induced osteoclast apoptosis (47). The first-line medical management for *osteogenesis imperfecta* is based on bisphosphonates to inhibit osteoclasts, while the disease relies on osteoblast dysfunction. Bisphosphonates allow an increase of bone mineral density and a 20% decrease of fractures in long-bone in the pediatric *osteogenesis imperfecta* population (48, 49). However, in CaP-mediated bone formation, several osteoclast depletion strategies including the administration of bisphosphonates highlight the important role of osteoclasts, suggesting that coupling mechanisms linking osteoclast resorption to osteogenesis may be involved (50). Of note, Takeshita et al. convincingly showed that osteoclasts in association with CaP or bone secrete CTHRC1, which enhances osteoblastogenesis, thereby coupling bone resorption to formation. CTHRC1-triggered bone turnover was attenuated when resorption was inhibited by bisphosphonate (alendronate) treatment, and OC-specific CTHRC1 KO mice led to reduced bone formation and lower bone mass (37). This concurs with findings by other groups that bisphosphonates inhibited osteoclasts and osteoinduction by CaPs in baboons (38) or rabbits (41). Furthermore, depletion of osteoclasts by local injection of liposome-encapsulated clodronate impeded heterotopic bone formation by intrinsically osteoinductive microstructured CaPs after subcutaneous implantation in mice (42). Surface microstructure stimulates osteoclastogenesis and therefore may be a primary trigger for subsequent *de novo* bone formation for certain CaPs which do not require the addition of MSCs or growth factors to induce bone formation (40). The biological mechanism by which osteoclasts stimulate subsequent osteogenesis in response to these microstructured CaPs is still not understood. Even more interesting, non-microstructured CaPs, which possess no intrinsic osteoinduction potential, have been show to induce heterotopic bone formation when first seeded with osteoclasts prior to implantation. Taken together, OC depletion and enrichment strategies combined with implanted CaPs points to an essential role of this cell type in inducing new bone formation

Distinct from osteoclasts, MNGCs are observed in human histological samples around various CaP bone substitutes and their presence correlates with a higher maintenance of bone

TABLE 1 | Implication of macrophages and osteoclasts in the bone formation induced by calcium phosphate biomaterials.

CaP biomaterial	*In vitro* and *in vivo* models	Outcome	References
Hydroxyapatite (HA)	*In vitro:* Osteoclasts (OCs) were differentiated from bone marrow monocytes from C57BL/6 mice. Primary osteoblasts (OBs) were derived from the calvaria. *Ex vivo:* Organ culture of explanted calvaria. *In vivo model:* C57BL/6mice	CTHRC1 protein is secreted by mature OCs. CTHRC1 mRNA expression is elevated in OCs cultured on HA compared to tissue culture plastic (TCP). CTHRC1 stimulates osteoblastogenesis (gene expression and mineralized matrix deposition). CTHRC1 expression and bone turnover *in vivo* was increased by RANKL injections and conversely decreased by alendronate treatment. OC-specific CTHRC1 KO mice led to reduced bone formation and lower bone mass.	(37)
Coral derived calcium carbonate (CC)/ HA constructs	*In vivo model:* Intramuscular implantation in Chacma baboons	Osteoinduction of biomaterials was inhibited by preloading constructs with the bisphosphonate zoledronate.	(38)
β-TCP	*In vivo model:* Intramuscular implantation in female beagle dogs	CaP induces the formation of TRAP and Cathepsin K positive, multinucleated cells on the biomaterial, and their presence precedes ectopic bone formation	(39)
β-TCP with different surface microstructures	*In vitro:* Osteoclasts were differentiated from a murine macrophage cell line RAW264.7 Human MSCs were isolated from bone marrow harvested from femoral heads. *In vivo model:* Intramuscular implantation in male mongrel dogs	*In vitro*, CaPs with submicron-scale surfaces lead to increased differentiation of OCs and higher secretions of factors that induced osteogenic differentiation of MSCs. *In vivo*, submicro-structured CaPs formed bone and OCs presence was significant, whereas micro-structured CaPs formed no bone and OC presence was spare.	(40)
β-TCP	*In vivo model:* Rabbit femoral condyles	Loading of Alendronate (bisphosphonate) onto β-TCP inhibited the presence of TRAP-positive cells on the surface of the biomaterial and abrogated the CaP-mediated bone formation.	(41)
β-TCP	*In vivo model:* FVB/NCrl strain mice	CaPs induced osteoclastogenesis and ectopic bone formation. Depletion of osteoclasts by local injection of liposome-encapsulated clodronate impeded bone formation by CaPs.	(42)
Biphasic calcium phosphate (BCP) HA/ β-TCP composite	*In vitro:* Mouse macrophage cell line RAW264.7. Mouse bone marrow-derived MSCs.	Macrophages upregulated gene expression of inflammatory factors (IL-1, IL-6, MCP-1) and growth factors (EGF, PDGF, and VEGF) as a consequence of their CaP substrate. This macrophage conditioned media (CM) increased MSC migration and osteogenic differentiation (osteogenic gene expression and mineralized matrix deposition).	(43)
BCP (HA/ β-TCP)	*In vitro:* Mouse macrophage cell line RAW264.7. Mouse bone marrow-derived MSCs. *In vivo model:* Implantation into thigh muscle of male BALB/c mice.	BCP implantation *in vivo* caused infiltration of macrophages to the site, followed by homing of MSCs and subsequent ectopic bone formation. BMSCs migrated significantly faster under stimulation by CM from macrophages cultured on BCP, compared to CM from macrophages cultured on TCP. Secretion of MCP-1 and MIP- 1α by macrophages was increased by culture on BCP and were shown to be the effectors of enhanced migration since blocking these in macrophage CM had inhibited MSC migration.	(44)

mass in grafted sites (51). Such MNGCs are formed by fusion of monocytes/macrophages on various bone substitutes not surrounded by bone. Histologically, they are slightly TRAP positive and occasionally associated with small resorption lacunae, indicating a potential osteoclast-like activity. *In vitro*, they can be obtained by stimulation of monocytes with IL-4 and IL-13 (52, 53). These *in vitro* generated MNGCs can dissolve hydroxyapatite, although not as efficiently as osteoclasts, but they cannot digest the bone matrix (54). The case *in vivo* may however be more complex, particularly since mononucleated and fused macrophages found at the surface of implanted biomaterials or wounds may express a variety of markers spanning both classical M1 and alternatively activated M2 phenotypes.

Dendritic cells (DC) have been described as the scavenging sentinel cells also responsible for identifying foreign materials and organisms in the host. Although 25% of monocytes present at the site of injury or inflammation differentiate into DCs, the current knowledge of how DCs interact with biomaterials is incomplete—particularly whether they interact with the foreign body distinctly or in concert with macrophages and MNGCs (55). This is compounded by the heterogeneity of DC subsets, similar to macrophages (56). Still, it is clear that DCs also possess

phagocytic ability and can readily internalize CaP particles or polymeric beads. Such particle internalization causes DCs to secrete inflammatory cytokines as well as migrate back to the lymph nodes and instruct the adaptive immune response through T cell priming (55, 57). Because these cells interrogate and recognize foreign bodies as well as prolifically express surface antigens, DCs represent an important bridge between the innate and adaptive immune system and may mediate the polarization or transition between inflammatory or anti-inflammatory adaptive immunity. Illustrating this immune-modulatory role, DCs have been implicated with suppression of a chronic inflammatory response to implanted biomaterials and thus may play a key role in mediating the transition from fibrous encapsulation to functional tissue regeneration, and as the case may be with CaPs implanted in bony locations, the regeneration of bone tissue. Similar to macrophages, DCs have been shown to distinctly respond to biomaterial surface chemistry, hydrophobicity, and topography which direct activated vs. suppressive states of DCs (58). Some work has been conducted to explore the role of DCs in mediating the innate and adaptive immune response to subcutaneously implanted polymeric materials *in vivo* (59), but less is known about how DCs may interact with resorbable biomaterials such as calcium phosphates, particularly those that are too large to phagocytose.

These studies emphasize the crucial role of the innate immune system and osteoclastogenesis in modulating and facilitating bone healing and how CaP biomaterial properties such as surface microporosity significantly affect such responses. It should be noted that the combination of CaP biomaterial and natural (collagen, fibrinogen etc.) or synthetic polymers are also developed to influence the osteoinductive capacities of the implant (60) and could therefore influence the immune response. In spite of the significant improvements in CaPs, yielding well tolerated, osteoconductive biomaterials with some osteoinductive capability, most CaPs still lack adequate osteoinduction capacity for regenerating large bone defects. Therefore, they are generally employed for treating small bone defects, to supplement autologous bone grafting, or, increasingly, as scaffolds to deliver cells or growth factors targeting bone repair (61, 62).

OSTEOIMMUNOMODULATION AND OSTEOINDUCTION BY MSC/CaP COMBINATIONS

Bone marrow derived mesenchymal stromal cells may overcome the challenges of autologous bone grafting for the regeneration of large defects. Transplanted in unison with CaP bioceramics, MSCs achieve ectopic (intramuscular and subcutaneous) (7, 9, 63) and orthotopic bone formation and critical-sized defect healing in preclinical studies, and efficient fracture healing and bone augmentation in clinical trials (64, 65). The key role of implanted MSCs was initially thought to be their differentiation into bone forming osteoblast cells and studies observing transplanted MSCs within osteocyte lacunae of newly formed bone support this hypothesis (6, 66–68). However, in general, cell engraftment of transplanted MSCs is very low or completely absent, in spite of successful outcomes (10, 11, 69), leading to the contention that the therapeutic benefit of transplanted MSCs is largely through a paracrine mechanism. These conflicting observations of the fate of transplanted MSCs is present throughout the literature and could be caused by a multitude of reasons such as initial cell dosage, biomaterial scaffold employed, implantation site, and host immune response. In our own hands, we have observed instances of some, albeit a small proportion, transplanted MSCs present in newly formed bone (9), and others where cell engraftment was not detected (10), while both resulted in ectopic bone formation. Although not quantified, it appears the transplanted MSCs persisted in outcomes of abundant bone formation and interestingly human MSCs resided in osteocyte lacunae in the vicinity of host (mice) osteocytes, with host osteocytes representing the larger proportion (9). MSCs secrete a vast array of paracrine factors into their conditioned media (MSC-CM) *in vitro* and interestingly, administration of MSC-CM *in vivo*, induces healing in many tissues including bone (70–72) providing evidence that the MSC secretome can initiate the bone tissue regeneration cascade. The MSC secretome comprises all factors secreted by MSCs, including soluble secretions (cytokines, growth factors, chemokines, and hormones) as well as vesicular secretions, or extracellular vesicles (EVs), which encompass exosomes, microvesicles, and apoptotic bodies. EVs are nanoparticles (ranging in size from 30 to 1,000 nm) that are secreted by all cells and carry bioactive cargo from the parental cells including lipids, proteins, RNA, and DNA (73, 74). It was recently reported that EVs secreted by MSCs have therapeutic potential in preclinical studies targeting bone repair (75–78). While not yet investigated in the context of bone regeneration, it has been observed in other settings that EVs secreted from MSCs mimic the immune-regulatory function of MSCs (79).

The Immune System Influences MSC-Based Bone Regeneration

Several studies have observed that MSCs enhance bone repair by modulating the foreign body response to CaPs. Macrophages are an important innate immune cell population for the regulation of MSC-based bone regeneration. Interestingly, it was observed that the mobilization of macrophages to the site of CaP implantation was significantly enhanced by MSC transplantation prior to MSC-mediated ectopic bone formation (10, 17). Early studies indicated that inflammatory macrophages suppressed osteoblastogenesis, through secretion of TNFα and IL1b [reviewed in (50)]. However, in contrast to this, both Tour et al. (17) and Gamblin et al. (10) independently observed that transplanted MSCs led to a M1 dominant macrophage phenotype, which was followed by bone formation. In line with these *in vivo* studies, several *in vitro* studies have demonstrated the impact of M1 macrophages on enhancing the osteogenic differentiation of MSCs. We previously demonstrated that inflammatory M1 macrophages secrete Oncostatin M (OSM) to improve osteoblastogenesis *in vitro* (80). In addition, OSM production by macrophages

sustained bone regeneration in a mouse model of tibia injury (81). Furthermore, MSCs treated with conditioned media (CM) from lipopolysaccharide (LPS) stimulated monocytes exhibited increased osteogenic differentiation (82), an effect partially imparted by extracellular vesicles secreted by the activated monocytes (83). Conversely, other *in vitro* studies have reported that M2, and not M1 macrophages, enhanced osteogenic differentiation of MSCs (84). The exact role of resident vs. monocyte-derived macrophages or of M1 vs. M2 alternatively activated macrophages in response to transplanted MSCs are still not clear. The M1/M2 paradigm is certainly a key for successful bone regeneration, since resolution of inflammation and tissue repair are tightly linked (85). Interestingly, M1 and M2 macrophages were both recently demonstrated to modulate MSC osteogenic differentiation but in disparate manners, whereby M1 macrophages enhanced early osteogenic differentiation without any effect on matrix mineralization, which was subsequently enhanced by M2 macrophages (86). In addition, it was demonstrated that macrophages preferentially recruit fibroblasts over MSCs. Pre-incubation of macrophages with immunomodulatory MSCs impairs fibroblast recruitment (87). Taken together, these studies indicate that macrophage polarization is important for distinct roles in the bone healing cascade by MSCs in association with CaPs, much like how normal tissue repair encompasses a transition from a pro-inflammatory status to a pro-reparative status.

Osteoclasts also play a central role in the regulation of MSC-based bone regeneration. It was demonstrated *in vitro* that osteoclasts secrete factors (S1P, BMPs, WNTs etc.) which induce MSC migration and osteogenic differentiation (88, 89). Interestingly, MSCs transplanted with BCP were shown to positively influence the foreign body reaction by attracting circulating monocytes and inducing their differentiation into osteoclasts, thus favoring bone formation. Importantly, depletion of osteoclasts by local injection of clodronate or injection of neutralizing anti-RANKL antibodies impeded bone formation, highlighting the imperative role of osteoclasts in MSC-mediated bone formation (10).

The adaptive immune system also plays an important role in MSC-modulated bone regeneration, which was elegantly shown by Liu et al. (90) and is discussed in detail in **Table 2**. Briefly, MSCs together with CaP particles induced ectopic bone formation in immuno-deficient mice but failed to do so in immune competent C57BL/6 mice (90). Moreover, infusion of CD4+ T cells in nude mice blocked ectopic bone formation through secretion of TNFα and IFNγ, which inhibited MSC differentiation and induced MSC apoptosis (90, 92). Interestingly, infusion of CD4+ CD25+ Treg abolished TNFα and IFNγ production and improved MSC-mediated bone regeneration in critical-sized calvarial bone defects in C57BL/6 mice (90). These observations were corroborated by findings that MSC from immune-competent mice formed ectopic bone in immune deficient mice, but much less in syngenic mice with the initiation of an inflammatory reaction involving Th1, Th2, and cytotoxic T-cell responses (91). Collectively these data demonstrate that modulation of both the innate and adaptive host immune response facilitates MSC-based bone regeneration.

IMPACT OF MSC STRESS ON IMMUNOMODULATION

As indicated above, implantation of MSCs with CaP results in the local recruitment of various innate immune cells including mast cells, neutrophils, monocytes, macrophages, and several types of multinucleated giant cells. An exhaustive overview of how MSC influence the innate and adaptive immune system is outside the scope of this review. Rather, we focus on how transplanted MSCs in association with CaPs may modulate the immune system by focusing on the conditions that MSCs encounter following transplantation and the potential impact that these cell stresses can have on MSCs immunomodulation.

MSC Influence the Innate and Adaptive Immune System

Since MSCs express low levels of MHC-II and costimulatory molecules (CD40, CD80, CD86), but substantial amount of the tolerogenic HLA-G molecule, they are considered as immunoprivileged cells, and thus would be ideal for tissue repair even in allogeneic transplantation (92, 93). Moreover, the discovery of the immunomodulatory roles of MSCs fostered their therapeutic use to suppress inflammation and limit pathogenic immune responses in graft-vs-host and auto-immune diseases such as multiple sclerosis, diabetes, and rheumatoid arthritis. Indeed, MSCs tend to limit macrophage polarization to M1, favoring M2 polarization. They also favor the generation of regulatory dendritic cells. They inhibit mast cells degranulation and NK cell effector functions (**Figure 1**). MSC production of PGE2, IL-6, TGFβ, and IDO for example has a key role in these suppressive effects on innate immune cells (93, 94). With regard to adaptive immune cells, MSCs favor the development of Th2 and Treg cells, with suppression of CD4+ T cells proliferation and polarization toward Th1 and Th17 cells. They also inhibit B cell activation, proliferation, and differentiation into plasma cells. These suppressive effects depend on MSCs production of NO, TGFβ, PGE2, IL-10, and ligation of PD-1/PD-L1 for example (93, 94). Interestingly, culture of MSC on BCP did not impair their suppressive effect toward T, B, and Natural Killer (NK) cells (95). Extracellular vesicles produced by MSC are also implicated in immunomodulation (96). It is important to note that the immunosuppressive effect of MSCs when delivered systemically is well documented, but the possible role of MSCs in regulating the innate and adaptive immune responses when delivered locally to regenerate bone remains elusive.

Impact of Stressful Conditions on MSCs Phenotype/Secretome

Because MSCs disappear shortly after implantation with CaP, it is important to consider the impact of cell stress or cell death on MSCs immunomodulation activity. The primary factors responsible for the large cell death of transplanted BMSCs include the ischemic environment and the lack of glucose that the BMSCs encounter (97–100). It is unclear the exact means of MSCs death after implantation with CaP

TABLE 2 | Osteoimmunology of mesenchymal stem cells transplantation with calcium phosphate biomaterials.

CaP Biomaterial	MSC origin	*In vitro* and *In vivo* models	Outcome	References
BCP (HA/β-TCP)	Human bone marrow derived MSCs	*In vivo model:* Intramuscular implantation in immunocompromised nude NMRI Nu/Nu female mice	Both macrophage and osteoclast presence at the CaP site was significantly enhanced by MSC transplantation. Their presence preceded MSC-mediated ectopic bone formation. Depletion of osteoclasts by local injection of clodronate impeded bone formation, highlighting the imperative role of osteoclasts in MSC-mediated bone formation	(10)
HA	Rat (Lewis) bone marrow derived MSCs	*In vivo model:* Rat calvaria critical-sized defects	MSCs increase bone formation by modulating (both up- and down-regulation) the foreign body reaction. MSCs increased macrophage presence at the CaP implantation site and enhanced bone healing. However, MSCs reduced the immune cell presence (macrophages and eosinophils at the site when the scaffold was delivered with extracellular matrix produced by fibroblasts (dermis of Sprague-Dawley rats), indicating that MSCs modulate the host immune response depending on the environment with the aim of positively influencing the tissue healing cascade.	(17)
BCP (HA/β-TCP)	Bone marrow MSCs C57BL/6-Tg (CAG-EGFP)1Osb/J mice	*In vivo model:* Subcutaneous and calvaria implants. Female C3H/HeJ, C57BL6J, B6.129S7-Ifng^{tm1Ts}/J, C57BL/6-Tg(CAG-EGFP)1Osb/J, B6.MRL-Fas^{lpr}/J, immunocompromised nude mice (Beige nude/nudeXIDIII).	Firstly, MSC transplantation with CaP formed ectopic bone in nude mice but not in C57BL/6 mice. Interestingly CD8+ T cells, and CD4+ T cell infusion into nude mice partially and totally blocked bone formation, respectively. Inhibition of MSC-mediated bone formation in C57BL/6 was caused by interferon (IFN)-γ induced down-regulation of the runt-related transcription factor 2 (Runx-2) pathway and tumor necrosis factor (TNF)-α-induced MSC apoptosis. Treatment with IFN-γ and TNF-α also inhibited MSC-mediated bone formation in nude mice and interestingly antibodies to neutralize IFN-γ and TNF-α, as well as infusion of Treg cells rescued bone formation by transplanted MSCs in C57BL/6 mice. Together, this reveals that pro-inflammatory T cells inhibit transplanted MSC-mediated bone repair.	(90)
BCP (HA/β-TCP)	Bone marrow MSCs from C57BL/6 mice	*In vivo model:* Subcutaneous implantation in C57BL/6 and immunocompromised nude mice (NMRI Nu/Nu)	MSC transplantation into nude mice led to abundant ectopic bone and bone marrow formation, whereas MSC transplantation into syngenic C57BL/6 mice resulted in only minor quantities of ectopic bone formation and significant quantities of multinucleated giant cells (MNGCs). MSCs survived for a shorter duration in immune-competent mice and the implant site was characterized by Th1, Th2, and cytotoxic T-lymphocyte activation, highlighting the benefit T-lymphocyte absence in nude mice for bone formation.	(91)

but senescence, apoptosis, necrosis, or other types of cell death could presumably be implicated which can have a profound effect on MSC-mediated immunomodulation. MSCs are considered relatively resistant to programmed apoptosis and prefer senescent growth arrest or autophagy to cell death (101). In general, necrotic (necroptotic, pyroptotic) cell death is associated with inflammation and exacerbated immune responses, whereas apoptosis avoids an inflammatory response and rather contributes to its resolution. For example, Laing et al. demonstrated that systemic injection of H_2O_2-induced apoptotic MSCs is more efficient than injection of live MSCs to induce a robust immune suppressive reaction in an ovalbumin induced model of allergic airway inflammation (102). Similarly, Galleu et al. showed that after infusion of apoptotic MSCs in a murine model of graft-vs-host disease, recipient phagocytes engulf apoptotic MSCs and produce IDO, which is ultimately necessary for effecting immunosuppression (103). The authors also observed that cytotoxic cells, such as CD8+ T lymphocytes and NK cells, induce MSCs apoptosis through perforin, granzyme B, and FasL, and that PBMCs from patients that responded to MSC therapy had more cytotoxic activity against MSCs. Another level of complexity is that when apoptotic cells are not cleared in an efficient and timely manner, they progress to secondary necrosis and lose their membrane integrity. This results in a leakage of immunostimulatory, danger associated molecular patterns (DAMPs) such as HMGB1 and nucleosomes (104, 105). They induce an inflammatory response which can become chronic and even induce an adaptive immune response, a situation that would

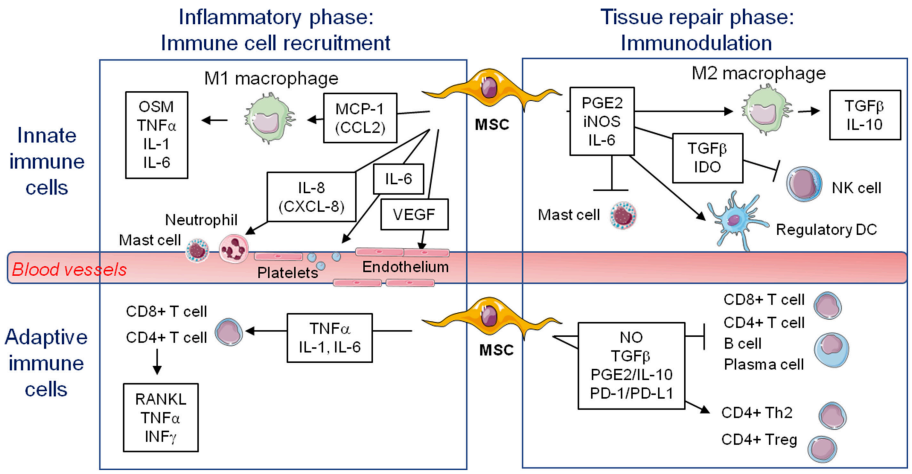

FIGURE 1 | Known immunomodulatory secretions from mesenchymal stem cells favoring (↑) or inhibiting (-) various cells potentially involved in bone formation on a biomaterial during early inflammation or the later stage of tissue repair. MSC, mesenchymal stem cell; M1, pro-inflammatory macrophages; M2, alternatively activated macrophages; NK, natural killer; DC, dendritic cell; OSM, oncostatin M; TNFα, tumor necrosis factor alpha; IL, interleukin; VEGF, vascular endothelial growth factor; PGE2, prostaglandin E2; iNOS, inducible nitric oxide synthase; TGFβ, transforming growth factor beta; IDO, indoleamine 2,3-dioxygenase; RANKL, receptor activator of nuclear factor kappa-B ligand; IFNγ, interferon gamma; NO, nitric oxide; PD-1/PD-L1, programmed cell death protein 1/programmed cell death-ligand 1.

presumably preclude local bone formation. Additional studies are mandatory in the context of bone regeneration induced by MSC-CaP combination.

Upon aging and in age-related deficiencies, compromised MSC-mediated immunological responses have been observed and attributed to MSC senescence. Senescence by replicative exhaustion or genotoxic stress during *ex vivo* culturing was also demonstrated (69). Acute, transient senescence induced by cell stresses such as hypoxia is presumably beneficial, because senescent cells secrete a plethora of molecules as part of the senescence-associated secretory phenotype (SASP), leading to rapid MSC clearance by immune cells, modulation of innate and adaptive immune cells, followed by tissue healing and regeneration (106). However, when chronic senescence occurs, for example upon aging, it impacts on the SASP, the local microenvironment and causes local and/or systemic inflammation.

The modifications of the secretome of MSCs induced by various stimuli, either mimicking physiological situations such as hypoxia and inflammatory stress or specific *in vitro* culture conditions to enhance the immunomodulatory properties of the cells, were previously widely reviewed (107–109). Those stresses could also alter the production and composition of EVs (110–112). Hypoxia is a main characteristic of the natural environment of MSCs and a major difference with *in vitro* culture. Overall, culture under low-oxygen atmosphere results in higher proliferation rate, survival, differentiation potential, and immune modulating secretions (113). For example, Paquet et al. (114) reported an upregulation of proangiogenic and chemotactic mediators (VEGF-A/-C, IL-8, MCP-1, and RANTES) and a downregulation of inflammatory mediators (IL-1b, IL-6, IL-15, IL-1Ra) with close to anoxic conditions (0.1% O_2). An artificial overexpression of the hypoxia-inducible factor 1 (HIF-1) in dental stem cells leads to an improved resistance to NK cells, an upregulation of CXCL12, CCL5, and IL-6 as well as a downregulation of CXCL10 (115).

Inflammatory stress is also characteristic of an implantation site and is mimicked *in vitro* by exogenous addition of LPS, TNFα, and/or IFNγ, usually termed MSC priming. When primed with inflammatory cytokines, MSCs increase their suppressive capacities (95). MSCs express constitutively many mitogenic growth factors, chemokines and matrix metalloproteinases at various levels. They are sensors and modulators of their microenvironment; i.e., MSC response to TNFα by increasing expression of some growth factor receptors, growth factors, chemokines, and matrix metalloproteases (116). Just as hypoxia, MSCs stimulated with LPS or TNFα produced more VEGF and FGF2 but also more HGF and IGF-1 via the activation of NFκB (117). Stimulation with IFNγ increases the expression of anti-inflammatory and regenerative molecules such as IDO, TGFβ or PGE2 for example (60). The addition of hypoxia to a TNFα and IFNγ stimulation on adipose-derived stem cells did not impair their higher secretion of immunomodulatory molecules IDO and PD-L1 (118).

PROPOSED MECHANISM OF BONE FORMATION AFTER MSC-CAP IMPLANTATION

It has been shown in many studies that only the combination of CaP and MSCs has the ability to induce abundant bone formation. MSCs have numerous, complex, and sometimes antagonist effects on the immune system depending on the physiological context. Their role in bone regeneration on CaP biomaterials remains unclear but evidence indicate that their immunomodulatory properties are involved. We previously highlighted the crucial role that osteoclasts seem to play and

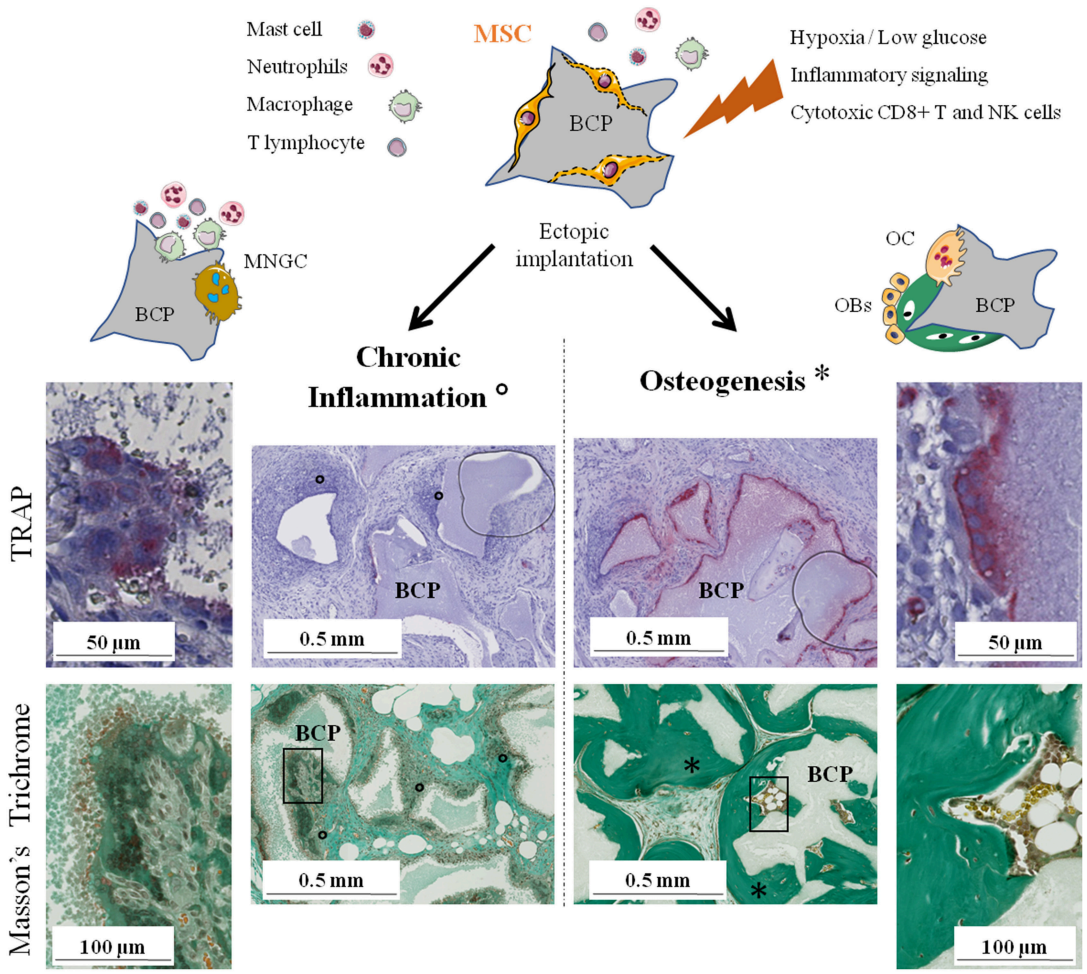

FIGURE 2 | The two possible outcomes of subcutaneous implantation of mesenchymal stem cells on calcium phosphate ceramic in mice. Histology of the implants: TRAP staining for osteoclasts detection after 4 weeks and Masson's trichrome to evaluate bone formation after 8 weeks. On the left, chronic inflammation (o) with formation of TRAP negative MNGCs followed by fibrous encapsulation and no sign of bone formation. On the right, osteoclastogenesis on the biomaterial followed by abundant bone formation (*). NK, natural killer; BCP, biphasic calcium phosphate; MNGC, multi-nucleated giant cell; OC, osteoclast; OBs, osteoblasts; TRAP, tartrate-resistant acid phosphatase.

the rapid disappearance of implanted MSCs before new bone is formed. Therefore, we hypothesize that MSCs, through their dialogue with various cells of the immune system, favor osteoclastogenesis on lieu of MNGCs formation, i.e., inducing a switch from chronic inflammation and fibrous encapsulation to bone formation via the recruitment and differentiation of new MSCs or skeletal stem cells in the bone remodeling process (**Figure 2**).

In detail, the environment just after implantation consists of the biomaterial exhibiting specific properties (chemical composition, micro-/macro-porosity, topography) and the MSCs adhering and reacting to it. Neutrophils, mast cells and macrophages are the first immune cells in contact with the implant, the latter mostly polarizing toward the inflammatory M1 phenotype (28). Therefore, inflammatory cytokines, ions released by the biomaterial, lack of O_2 (98), and nutrients (97), presence of cytotoxic CD8+ T and NK cells are all environmental factors influencing MSCs' behavior in the early stages of implantation. Most of those stresses were individually found to increase the production of pro- or anti-inflammatory molecules by MSCs (107–109). Given the osteogenic effect of the biomaterial (119) and the M1 population of macrophages (86), implanted MSCs might also express some markers of early osteoblast precursors. Eventually, MSCs will disappear by senescence, apoptosis and/or necrosis, releasing novel pro- and anti-inflammatory signals. Clearance of dead MSC by immune cells would also modulate the innate and adaptive immune system.

We believe that the secretions from those highly stimulated MSCs directly or indirectly (through modulation of innate and adaptive immune cells) favor the formation of osteoclasts at the expense of MNGCs. Indeed, MSC-based bone formation was significantly altered by anti-RANKL mAB (10) or clodronate (42) administration. While clodronate also affects MNGCs, the

anti-RANKL mAB is specifically restricting osteoclastogenesis. Due to their common origin and similar morphology, osteoclasts, and MNGCs are difficult to distinguish. Theoretically, both osteoclasts and MNGCs can arise from the fusion of circulating monocytes, M1/M2 macrophages or even of dendritic cells. An in depth description of the known differences between osteoclasts and MNGCs have already been well reviewed (120). Both cell types share a lot of markers but they can be differentiated by expression of the calcitonin receptor and RANK only in osteoclasts, or CD86 (B7-2), CD206, and HLA-DR only present in MNGCs. Interestingly, MNGCs are able to express low levels of TRAP a few days after formation (both *in vitro* and *in vivo*) while there seem to be two distinct populations expressing or not Cathepsin K (121, 122). Miron et al. also discussed the polarization potential of MNGCs, in parallel with the polarization of macrophages, with a proposed distinction between pro-inflammatory M1-MNGCs that were also called foreign body giant cells (FBGCs) and wound-healing M2-MNGCs. It is impossible to state whether the suggested M2-MNGCs are the MNGCs observed in close contact to the CaP materials leading to bone formation or if M2-MNGCs can differentiate further into true osteoclasts even if this last statement seems unlikely due to their unresponsiveness to RANKL *in vitro* (54). In our hypothesis, M2-MNGCs are likely to be involved in late stages of chronic inflammation, leading to fibrous encapsulation. In any case, there is an urgent need to better characterize those MNGCs and to discover the cell communications involved in their formation.

Preliminary results showed that conditioned media from MSC culture could have a positive direct impact on osteoclastogenesis (123). This effect of MSCs could rely on enhanced secretion or membrane expression of RANKL. Activated T cells were also reported to increase osteoclastogenesis *in vitro* (124) but they cannot be the main source of RANKL in MSC-based bone formation as many successful experiments were carried out in Nude mice. Also, a number of factors are known to influence osteoclastogenesis, primarily by modifying RANKL/RANK signaling (125). *In vitro*, TGFβ (a known product of MSC but also Treg) promote osteoclast formation from RANKL stimulated precursors but also decreases RANKL expression in osteoblasts resulting in fewer osteoclasts in co-culture (126). In mice, activation of the non-canonical Wnt pathway by Wnt5a in osteoclast precursors increases the production of RANK (127). These are only few examples of molecules that could be implicated in the MSC-osteoclast communications and future studies will certainly better delineate this key step toward MSC-CaP induced bone formation.

As the newly formed bone comes mostly from host osteoblasts, it entails recruitment and differentiation of new MSCs or the newly characterized subset of skeletal stem cells [SSC, (128)]. We hypothesize that osteoclasts might be the essential attractor for those cells, setting off a local bone remodeling cycle. The basic mechanisms and the major signaling molecules involved in the osteoclast-osteoblast crosstalk during the physiological coupling of bone resorption and formation are well described (129, 130). Osteoclasts are known to release growth factors from the degradation of bone matrix and, most importantly in our case, to express chemotactic and osteogenic coupling factors toward cell of the osteoblastic lineage such as BMP6, WNT10b, and S1P (131). The CTHRC1 protein, expressed by mature osteoclasts, promote osteoblastic differentiation *in vitro* and an osteoclast-specific KO induce

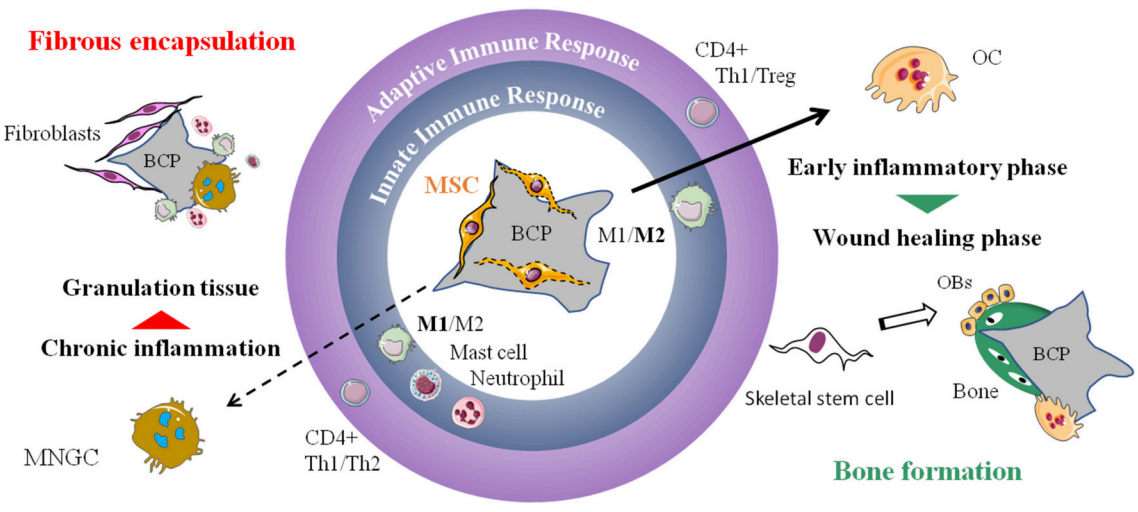

FIGURE 3 | Proposed mechanism of MSC-CaP immune modulation leading to bone formation. The local innate and adaptive immune response will determine the fate of the implanted biomaterial (central part of the drawing). On the left, is displayed the classical foreign body reaction characterized by activation of M1 macrophages, mast cells, neutrophils, Th1, and Th2 CD4+ lymphocytes. It leads to the formation of MNGCs, chronic inflammation and subsequent fibrous encapsulation of the implant. On the right, adjunction of MSCs to the biomaterial favor M2 macrophages, Th1, Treg, and osteoclastogenesis followed by recruitment of new stem cells, likely from the skeletal subtype, that differentiate into bone forming osteoblasts. MSC, mesenchymal stem cell; BCP, biphasic calcium phosphate; M1, pro-inflammatory macrophages; M2, alternatively activated macrophages; Th1/Th2/Treg, type 1 helper/type 2 helper/regulatory T cells; MNGC, multi-nucleated giant cell; OC, osteoclast; OBs, osteoblasts.

a low bone mass phenotype in mice (37). More recently, an important study unveiled a reverse signaling mechanism whereby osteoclasts secrete extracellular vesicles expressing RANK which are able to stimulate membrane RANKL on the surface of osteoblasts to induce bone formation (132). Also, as osteoclasts can degrade the biomaterial, they modulate the local calcium and phosphate concentrations, thus influencing the deposition of the apatite layer and the calcium sensing of other cell types (26, 133).

Simultaneously to this main phenomenon, MSCs are likely to induce a switch from M1 macrophages to the M2 phenotype, the formation of regulatory dendritic cells and the suppression of B, NK, CD4+, and CD8+ T cells while promoting Th2 and Treg cells. The timing of activation of the various cells is critical as the initial acute inflammation is necessary to recruit all the immune cells but is detrimental if it becomes chronic and favors the formation of MNGCs. The M1/M2 balance of macrophages phenotype has a key role in this switch to resolve inflammation and move on to bone formation (85, 134). Moreover, the M2 phenotype favored by MSCs is thought to help in late stages of osteoblastic differentiation and mineralization (86). The stressful conditions and, eventually, the apoptosis of implanted MSCs might increase their inherent immunomodulatory properties.

CONCLUSION

The implantation of CaP biomaterials in combination with MSCs emphasizes the central role of the host immune system in bone regeneration. It is important to consider that the cellular events hypothesized here may only occur on an osteoconductive CaP material. The implanted MSCs potentiate the effect of the biomaterial allowing ectopic bone formation by creating a bone-like microenvironment. We highlighted here the pivotal role that macrophages and osteoclasts play in the multistep process of bone formation induced by MSC-CaP implantation (**Figure 3**) but this complex mechanism is just beginning to be explored. Over the course of several weeks, multiples cells types and molecules appear implicated in a coordinated manner before bone is formed. Any dysregulation would lead to unwanted chronic inflammation and fibrosis. A better comprehension of these spatiotemporal cell communications is mandatory to reach more efficient bone healing and develop better cell-free approaches.

AUTHOR CONTRIBUTIONS

All authors participated in the literature search, organization, writing, reviewing, and proofreading of the manuscript. PH, ND, VT, and FB designed the figures. MB and PL created the tables.

FUNDING

This work is financially supported by the European Commission through the H2020 project ORTHOUNION (Grant Agreement: 733288). PH receives a PhD fellowship from the Regional Council Pays de la Loire and the ORTHOUNION project. MB benefits from a Marie Skłodowska-Curie Individual Fellowships from the European Commission through the H2020 project PARAGEN (Project ID: 708711).

REFERENCES

1. Stanovici J, Le Nail L-R, Brennan MA, Vidal L, Trichet V, Rosset P, et al. Bone regeneration strategies with bone marrow stromal cells in orthopaedic surgery. *Curr Res Transl Med.* (2016) 64:83–90. doi: 10.1016/j.retram.2016.04.006
2. Abe K, Yamamoto N, Hayashi K, Takeuchi A, Miwa S, Igarashi K, et al. The usefulness of wide excision assisted by a computer navigation system and reconstruction using a frozen bone autograft for malignant acetabular bone tumors: a report of two cases. *BMC Cancer*. (2018) 18:1036. doi: 10.1186/s12885-018-4971-8
3. Ahlmann E, Patzakis M, Roidis N, Shepherd L, Holtom P. Comparison of anterior and posterior iliac crest bone grafts in terms of harvest-site morbidity and functional outcomes. *J Bone Joint Surg Am*. (2002) 84–A:716–20. doi: 10.2106/00004623-200205000-00003
4. Giannoudis PV, Dinopoulos H, Tsiridis E. Bone substitutes: an update. *Injury*. (2005) 36:S20–7. doi: 10.1016/j.injury.2005.07.029
5. Albee FH. Studies in bone growth triple calcium phosphate as a stimulus to osteogenesis. *Ann Surg*. (1920) 71:32–9.
6. Mankani MH, Kuznetsov SA, Wolfe RM, Marshall GW, Robey PG. *In vivo* bone formation by human bone marrow stromal cells: reconstruction of the mouse calvarium and mandible. *Stem Cells*. (2006) 24:2140–9. doi: 10.1634/stemcells.2005-0567
7. Mankani MH, Kuznetsov SA, Robey PG. Formation of hematopoietic territories and bone by transplanted human bone marrow stromal cells requires a critical cell density. *Exp Hematol*. (2007) 35:995–1004. doi: 10.1016/J.EXPHEM.2007.01.051
8. Granchi D, Gómez-Barrena E, Rojewski M, Rosset P, Layrolle P, Spazzoli B, et al. Changes of bone turnover markers in long bone nonunions treated with a regenerative approach. *Stem Cells Int*. (2017) 2017:1–11. doi: 10.1155/2017/3674045
9. Brennan MÁ, Renaud A, Amiaud J, Rojewski MT, Schrezenmeier H, Heymann D, et al. Pre-clinical studies of bone regeneration with human bone marrow stromal cells and biphasic calcium phosphate. *Stem Cell Res Ther*. (2014) 5:114. doi: 10.1186/scrt504
10. Gamblin A-L, Brennan MA, Renaud A, Yagita H, Lézot F, Heymann D, et al. Bone tissue formation with human mesenchymal stem cells and biphasic calcium phosphate ceramics: the local implication of osteoclasts and macrophages. *Biomaterials*. (2014) 35:9660–7. doi: 10.1016/j.biomaterials.2014.08.018
11. Giannoni P, Scaglione S, Daga A, Ilengo C, Cilli M, Quarto R. Short-time survival and engraftment of bone marrow stromal cells in an ectopic model of bone regeneration. *Tissue Eng Part A*. (2010) 16:489–99. doi: 10.1089/ten.tea.2009.0041
12. Otsuru S, Gordon PL, Shimono K, Jethva R, Marino R, Phillips CL, et al. Transplanted bone marrow mononuclear cells and MSCs impart clinical benefit to children with osteogenesis imperfecta through different mechanisms. *Blood*. (2012) 120:1933–41. doi: 10.1182/blood-2011-12-400085
13. Götherström C, Westgren M, Shaw SWS, Åström E, Biswas A, Byers PH, et al. Pre- and postnatal transplantation of fetal mesenchymal stem cells in osteogenesis imperfecta: a two-center experience. *Stem Cells Transl Med*. (2014) 3:255–64. doi: 10.5966/sctm.2013-0090
14. Le Blanc K, Götherström C, Ringdén O, Hassan M, McMahon R, Horwitz E, et al. Fetal mesenchymal stem-cell engraftment in bone after *in utero* transplantation in a patient with severe osteogenesis imperfecta. *Transplantation*. (2005) 79:1607–14. doi: 10.1097/01.TP.0000159029.48678.93

15. Horwitz EM, Gordon PL, Koo WKK, Marx JC, Neel MD, McNall RY, et al. Isolated allogeneic bone marrow-derived mesenchymal cells engraft and stimulate growth in children with osteogenesis imperfecta: implications for cell therapy of bone. *Proc Natl Acad Sci USA*. (2002) 99:8932–7. doi: 10.1073/pnas.132252399
16. Horwitz EM, Prockop DJ, Fitzpatrick LA, Koo WWK, Gordon PL, Neel M, et al. Transplantability and therapeutic effects of bone marrow-derived mesenchymal cells in children with osteogenesis imperfecta. *Nat Med*. (1999) 5:309–13. doi: 10.1038/6529
17. Tour G, Wendel M, Tcacencu I. Bone marrow stromal cells enhance the osteogenic properties of hydroxyapatite scaffolds by modulating the foreign body reaction. *J Tissue Eng Regen Med*. (2014) 8:841–9. doi: 10.1002/term.1574
18. Qi X, Zhang J, Yuan H, Xu Z, Li Q, Niu X, et al. Exosomes secreted by human-induced pluripotent stem cell-derived mesenchymal stem cells repair critical-sized bone defects through enhanced angiogenesis and osteogenesis in osteoporotic rats. *Int J Biol Sci*. (2016) 12:836–49. doi: 10.7150/ijbs.14809
19. Barradas AMCA, Yuan H, van Blitterswijk CAC, Habibovic P. Osteoinductive biomaterials: current knowledge of properties, experimental models and biological mechanisms. *Eur Cells Mater*. (2011) 21:407–29. doi: 10.22203/eCM.v021a31
20. Daculsi G, Legeros RZ, Nery E, Lynch K, Kerebel B. Transformation of biphasic calcium phosphate ceramics *in vivo*: ultrastructural and physicochemical characterization. *J Biomed Mater Res*. (1989) 23:883–94. doi: 10.1002/jbm.820230806
21. Habibovic P, Yuan H, van der Valk CM, Meijer G, van Blitterswijk CA, de Groot K. 3D microenvironment as essential element for osteoinduction by biomaterials. *Biomaterials*. (2005) 26:3565–75. doi: 10.1016/j.biomaterials.2004.09.056
22. Le Nihouannen D, Daculsi G, Saffarzadeh A, Gauthier O, Delplace S, Pilet P, et al. Ectopic bone formation by microporous calcium phosphate ceramic particles in sheep muscles. *Bone*. (2005) 36:1086–93. doi: 10.1016/j.bone.2005.02.017
23. Ripamonti U, Roden LC, Ferretti C, Klar RM. Biomimetic matrices self-initiating the induction of bone formation. *J Craniofac Surg*. (2011) 22:1859–70. doi: 10.1097/SCS.0b013e31822e83fe
24. Fellah BH, Gauthier O, Weiss P, Chappard D, Layrolle P. Osteogenicity of biphasic calcium phosphate ceramics and bone autograft in a goat model. *Biomaterials*. (2008) 29:1177–88. doi: 10.1016/j.biomaterials.2007.11.034
25. Diaz-Flores L, Gutierrez R, Lopez-Alonso A, Gonzalez R, Varela H. Pericytes as a supplementary source of osteoblasts in periosteal osteogenesis. *Clin Orthop Relat Res*. (1992)280–6.
26. Bohner M, Miron RJ. A proposed mechanism for material-induced heterotopic ossification. *Mater Today*. (2018) 22:132–41. doi: 10.1016/j.mattod.2018.10.036
27. Barradas AMC, Yuan H, van der Stok J, Le Quang B, Fernandes H, Chaterjea A, et al. The influence of genetic factors on the osteoinductive potential of calcium phosphate ceramics in mice. *Biomaterials*. (2012) 33:5696–705. doi: 10.1016/j.biomaterials.2012.04.021
28. Anderson JM, Rodriguez A, Chang DT. Foreign body reaction to biomaterials. *Semin Immunol*. (2008) 20:86–100. doi: 10.1016/j.smim.2007.11.004
29. Batoon L, Millard SM, Raggatt LJ, Pettit AR. Osteomacs and bone regeneration. *Curr Osteoporos Rep*. (2017) 15:385–95. doi: 10.1007/s11914-017-0384-x
30. Miron RJ, Bosshardt DD. OsteoMacs: key players around bone biomaterials. *Biomaterials*. (2016) 82:1–19. doi: 10.1016/j.biomaterials.2015.12.017
31. Alexander KA, Chang MK, Maylin ER, Kohler T, Müller R, Wu AC, et al. Osteal macrophages promote *in vivo* intramembranous bone healing in a mouse tibial injury model. *J Bone Miner Res*. (2011) 26:1517–32. doi: 10.1002/jbmr.354
32. Batoon L, Millard SM, Wullschleger ME, Preda C, Wu AC-K, Kaur S, et al. CD169 + macrophages are critical for osteoblast maintenance and promote intramembranous and endochondral ossification during bone repair. *Biomaterials*. (2017) 2017:33. doi: 10.1016/j.biomaterials.2017.10.033
33. Mantovani A, Sica A, Sozzani S, Allavena P, Vecchi A, Locati M. The chemokine system in diverse forms of macrophage activation and polarization. *Trends Immunol*. (2004) 25:677–86. doi: 10.1016/j.it.2004.09.015
34. Mantovani A, Sozzani S, Locati M, Allavena P, Sica A. Macrophage polarization: tumor-associated macrophages as a paradigm for polarized M2 mononuclear phagocytes. *Trends Immunol*. (2002) 23:549–55. doi: 10.1016/S1471-4906(02)02302-5
35. Jones JA, Chang DT, Meyerson H, Colton E, Kwon IK, Matsuda T, et al. Proteomic analysis and quantification of cytokines and chemokines from biomaterial surface-adherent macrophages and foreign body giant cells. *J Biomed Mater Res Part A*. (2007) 83A:585–96. doi: 10.1002/jbm.a.31221
36. Badylak SF, Valentin JE, Ravindra AK, McCabe GP, Stewart-Akers AM. Macrophage phenotype as a determinant of biologic scaffold remodeling. *Tissue Eng Part A*. (2008) 14:1835–42. doi: 10.1089/ten.tea.2007.0264
37. Takeshita S, Fumoto T, Matsuoka K, Park K, Aburatani H, Kato S, et al. Osteoclast-secreted CTHRC1 in the coupling of bone resorption to formation. *J Clin Invest*. (2013) 123:3914–24. doi: 10.1172/JCI69493
38. Ripamonti U, Klar RM, Renton LF, Ferretti C. Synergistic induction of bone formation by hOP-1, hTGF-β3 and inhibition by zoledronate in macroporous coral-derived hydroxyapatites. *Biomaterials*. (2010) 31:6400–10. doi: 10.1016/j.biomaterials.2010.04.037
39. Kondo N, Ogose A, Tokunaga K, Umezu H, Arai K, Kudo N, et al. Osteoinduction with highly purified β-tricalcium phosphate in dog dorsal muscles and the proliferation of osteoclasts before heterotopic bone formation. *Biomaterials*. (2006) 27:4419–27. doi: 10.1016/j.biomaterials.2006.04.016
40. Barrère-de Groot F, de Bruijn, Everts V, Davison N, Yuan H, Luo X, et al. Submicron-scale surface architecture of tricalcium phosphate directs osteogenesis *in vitro* and *in vivo*. *Eur Cells Mater*. (2016) 27:281–97. doi: 10.22203/ecm.v027a20
41. Tanaka T, Saito M, Chazono M, Kumagae Y, Kikuchi T, Kitasato S, et al. Effects of alendronate on bone formation and osteoclastic resorption after implantation of beta-tricalcium phosphate. *J Biomed Mater Res A*. (2010) 93:469–74. doi: 10.1002/jbm.a.32560
42. Davison NL, Gamblin A-L, Layrolle P, Yuan H, de Bruijn JD, Barrère-de Groot F. Liposomal clodronate inhibition of osteoclastogenesis and osteoinduction by submicrostructured beta-tricalcium phosphate. *Biomaterials*. (2014) 35:5088–97. doi: 10.1016/j.biomaterials.2014.03.013
43. Wang J, Liu D, Guo B, Yang X, Chen X, Zhu X, et al. Role of biphasic calcium phosphate ceramic-mediated secretion of signaling molecules by macrophages in migration and osteoblastic differentiation of MSCs. *Acta Biomater*. (2017) 51:447–60. doi: 10.1016/j.actbio.2017.01.059
44. Wang M, Chen F, Wang J, Chen X, Liang J, Yang X, et al. Calcium phosphate altered the cytokine secretion of macrophages and influenced the homing of mesenchymal stem cells. *J Mater Chem B*. (2018) 6:4765–74. doi: 10.1039/C8TB01201F
45. Hayman AR. Tartrate-resistant acid phosphatase (TRAP) and the osteoclast/immune cell dichotomy. *Autoimmunity*. (2008) 41:218–23. doi: 10.1080/08916930701694667
46. Feng W. Osteoclastogenesis and osteoimmunology. *Front Biosci*. (2014) 19:758. doi: 10.2741/4242
47. Drake MT, Clarke BL, Khosla S. Bisphosphonates: mechanism of action and role in clinical practice. *Mayo Clin Proc*. (2008) 83:1032–45. doi: 10.4065/83.9.1032
48. Shi CG, Zhang Y, Yuan W. Efficacy of bisphosphonates on bone mineral density and fracture rate in patients with osteogenesis imperfecta: a systematic review and meta-analysis. *Am J Ther*. (2016) 23:e894-904. doi: 10.1097/MJT.0000000000000236
49. Biggin A, Munns CF. Long-term bisphosphonate therapy in osteogenesis imperfecta. *Curr Osteoporos Rep*. (2017) 15:412–8. doi: 10.1007/s11914-017-0401-0
50. Sims NA, Martin TJ, Quinn JMW. Coupling: the influences of immune and bone cells. In: Lorenzo J, Horowitz MC, Choi Y, Takayanagi H, Schett G, editors. *Osteoimmunology: Interactions of the Immune and Skeletal Systems*. London: Academic Press. p. 169–85. Available online at: https://www.sciencedirect.com/science/article/pii/B9780128005712000219 doi: 10.1016/B978-0-12-800571-2.00010-4
51. Jensen SS, Gruber R, Buser D, Bosshardt DD. Osteoclast-like cells on deproteinized bovine bone mineral and biphasic calcium phosphate: light

and transmission electron microscopical observations. *Clin Oral Implants Res*. (2015) 26:859–64. doi: 10.1111/clr.12376
52. DeFife KM, Jenney CR, McNally AK, Colton E, Anderson JM. Interleukin-13 induces human monocyte/macrophage fusion and macrophage mannose receptor expression. *J Immunol*. (1997) 158:3385–90.
53. McNally AK, Jones JA, MacEwan SR, Colton E, Anderson JM. Vitronectin is a critical protein adhesion substrate for IL-4-induced foreign body giant cell formation. *J Biomed Mater Res Part A*. (2008) 86A:535–43. doi: 10.1002/jbm.a.31658
54. ten Harkel B, Schoenmaker T, Picavet DI, Davison NL, de Vries TJ, Everts V. The foreign body giant cell cannot resorb bone, but dissolves hydroxyapatite like osteoclasts. *PLoS ONE. (*2015) 10:e0139564. doi: 10.1371/journal.pone.0139564
55. Randolph GJ, Inaba K, Robbiani DF, Steinman RM, Muller WA. Differentiation of phagocytic monocytes into lymph node dendritic cells *in vivo*. *Immunity*. (1999) 11:753–61. doi: 10.1016/S1074-7613(00)80149-1
56. Merad M, Sathe P, Helft J, Miller J, Mortha A. The dendritic cell lineage: ontogeny and function of dendritic cells and their subsets in the steady state and the inflamed setting. *Annu Rev Immunol*. (2013) 31:563–604. doi: 10.1146/annurev-immunol-020711-074950
57. Sokolova V, Knuschke T, Kovtun A, Buer J, Epple M, Westendorf AM. The use of calcium phosphate nanoparticles encapsulating Toll-like receptor ligands and the antigen hemagglutinin to induce dendritic cell maturation and T cell activation. *Biomaterials*. (2010) 31:5627–33. doi: 10.1016/j.biomaterials.2010.03.067
58. Keselowsky BG, Lewis JS. Dendritic cells in the host response to implanted materials. *Semin Immunol*. (2017) 29:33–40. doi: 10.1016/j.smim.2017.04.002
59. Vasilijić S, Savić D, Vasilev S, Vučević D, Gašić S, Majstorović I, et al. Dendritic cells acquire tolerogenic properties at the site of sterile granulomatous inflammation. *Cell Immunol*. (2005) 233:148–57. doi: 10.1016/J.CELLIMM.2005.04.007
60. Michel J, Penna M, Kochen J, Cheung H. Recent advances in hydroxyapatite scaffolds containing mesenchymal stem cells. *Stem Cells Int*. (2015) 2015:305217. doi: 10.1155/2015/305217
61. Miron RJ, Zhang YF. Osteoinduction. *J Dent Res*. (2012) 91:736–44. doi: 10.1177/0022034511435260
62. García-Gareta E, Coathup MJ, Blunn GW. Osteoinduction of bone grafting materials for bone repair and regeneration. *Bone*. (2015) 81:112–21. doi: 10.1016/J.BONE.2015.07.007
63. Brennan MA, Renaud A, Guilloton F, Mebarki M, Trichet V, Sensebé L, et al. Inferior *in vivo* osteogenesis and superior angiogeneis of human adipose-derived stem cells compared with bone marrow-derived stem cells cultured in xeno-free conditions. *Stem Cells Transl Med*. (2017) 6:2160–72. doi: 10.1002/sctm.17-0133
64. Gjerde C, Mustafa K, Hellem S, Rojewski M, Gjengedal H, Yassin MA, et al. Cell therapy induced regeneration of severely atrophied mandibular bone in a clinical trial. *Stem Cell Res Ther*. (2018) 9:213. doi: 10.1186/s13287-018-0951-9
65. Gómez-Barrena E, Rosset P, Gebhard F, Hernigou P, Baldini N, Rouard H, et al. Feasibility and safety of treating non-unions in tibia, femur and humerus with autologous, expanded, bone marrow-derived mesenchymal stromal cells associated with biphasic calcium phosphate biomaterials in a multicentric, non-comparative trial. *Biomaterials*. (2018) 196:100–8. doi: 10.1016/j.biomaterials.2018.03.033
66. Fang D, Seo B-M, Liu Y, Sonoyama W, Yamaza T, Zhang C, et al. Transplantation of mesenchymal stem cells is an optimal approach for plastic surgery. *Stem Cells*. (2007) 25:1021–8. doi: 10.1634/stemcells.2006-0576
67. Hasegawa N, Kawaguchi H, Hirachi A, Takeda K, Mizuno N, Nishimura M, et al. Behavior of transplanted bone marrow–derived mesenchymal stem cells in periodontal defects. *J Periodontol*. (2006) 77:1003–7. doi: 10.1902/jop.2006.050341
68. Oshima Y, Watanabe N, Matsuda K, Takai S, Kawata M, Kubo T. Behavior of transplanted bone marrow-derived GFP mesenchymal cells in osteochondral defect as a simulation of autologous transplantation. *J Histochem Cytochem*. (2005) 53:207–16. doi: 10.1369/jhc.4A6280.2005
69. Tasso R, Augello A, Boccardo S, Salvi S, Caridà M, Postiglione F, et al. Recruitment of a host's osteoprogenitor cells using exogenous mesenchymal stem cells seeded on porous ceramic. *Tissue Eng Part A*. (2009) 15:2203–12. doi: 10.1089/ten.tea.2008.0269
70. Ando Y, Matsubara K, Ishikawa J, Fujio M, Shohara R, Hibi H, et al. Stem cell-conditioned medium accelerates distraction osteogenesis through multiple regenerative mechanisms. *Bone*. (2014) 61:82–90. doi: 10.1016/j.bone.2013.12.029
71. Xu J, Wang B, Sun Y, Wu T, Liu Y, Zhang J, et al. Human fetal mesenchymal stem cell secretome enhances bone consolidation in distraction osteogenesis. *Stem Cell Res Ther*. (2016) 7:134. doi: 10.1186/s13287-016-0392-2
72. Osugi M, Katagiri W, Yoshimi R, Inukai T, Hibi H, Ueda M. Conditioned media from mesenchymal stem cells enhanced bone regeneration in rat calvarial bone defects. *Tissue Eng Part A*. (2012) 18:1479–89. doi: 10.1089/ten.tea.2011.0325
73. Skog J, Würdinger T, van Rijn S, Meijer DH, Gainche L, Curry WT, et al. Glioblastoma microvesicles transport RNA and proteins that promote tumour growth and provide diagnostic biomarkers. *Nat Cell Biol*. (2008) 10:1470–6. doi: 10.1038/ncb1800
74. Valadi H, Ekström K, Bossios A, Sjöstrand M, Lee JJ, Lötvall JO. Exosome-mediated transfer of mRNAs and microRNAs is a novel mechanism of genetic exchange between cells. *Nat Cell Biol*. (2007) 9:654–9. doi: 10.1038/ncb1596
75. Furuta T, Miyaki S, Ishitobi H, Ogura T, Kato Y, Kamei N, et al. Mesenchymal stem cell-derived exosomes promote fracture healing in a mouse model. *Stem Cells Transl Med*. (2016) 5:1620–30. doi: 10.5966/sctm.2015-0285
76. Xie H, Wang Z, Zhang L, Lei Q, Zhao A, Wang H, et al. Extracellular vesicle-functionalized decalcified bone matrix scaffolds with enhanced pro-angiogenic and pro-bone regeneration activities. *Sci Rep*. (2017) 7:45622. doi: 10.1038/srep45622
77. Zhang J, Liu X, Li H, Chen C, Hu B, Niu X, et al. Exosomes/tricalcium phosphate combination scaffolds can enhance bone regeneration by activating the PI3K/Akt signaling pathway. *Stem Cell Res Ther*. (2016) 7:136. doi: 10.1186/s13287-016-0391-3
78. Otsuru S, Desbourdes L, Guess AJ, Hofmann TJ, Relation T, Kaito T, et al. Extracellular vesicles released from mesenchymal stromal cells stimulate bone growth in osteogenesis imperfecta. *Cytotherapy*. (2018) 20:62–73. doi: 10.1016/j.jcyt.2017.09.012
79. Burrello J, Monticone S, Gai C, Gomez Y, Kholia S, Camussi G. Stem cell-derived extracellular vesicles and immune-modulation. *Front Cell Dev Biol*. (2016) 4:83. doi: 10.3389/fcell.2016.00083
80. Guihard P, Danger Y, Brounais B, David E, Brion R, Delecrin J, et al. Induction of osteogenesis in mesenchymal stem cells by activated monocytes/macrophages depends on oncostatin M signaling. *Stem Cells*. (2012) 30:762–72. doi: 10.1002/stem.1040
81. Guihard P, Boutet M-A, Brounais-Le Royer B, Gamblin A-L, Amiaud J, Renaud A, et al. Oncostatin M, an inflammatory cytokine produced by macrophages, supports intramembranous bone healing in a mouse model of tibia injury. *Am J Pathol*. (2015) 185:765–75. doi: 10.1016/J.AJPATH.2014.11.008
82. Omar OM, Granéli C, Ekström K, Karlsson C, Johansson A, Lausmaa J, et al. The stimulation of an osteogenic response by classical monocyte activation. *Biomaterials*. (2011) 32:8190–204. doi: 10.1016/j.biomaterials.2011.07.055
83. Ekström K, Omar O, Granéli C, Wang X, Vazirisani F, Thomsen P. Monocyte exosomes stimulate the osteogenic gene expression of mesenchymal stem cells. *PLoS ONE.* (2013) 8:e75227. doi: 10.1371/journal.pone.0075227
84. Gong L, Zhao Y, Zhang Y, Ruan Z. The macrophage polarization regulates MSC osteoblast differentiation *in vitro*. *Ann Clin Lab Sci*. (2016) 46:65–71.
85. Pajarinen J, Lin T, Gibon E, Kohno Y, Maruyama M, Nathan K, et al. Mesenchymal stem cell-macrophage crosstalk and bone healing. *Biomaterials*. (2018) 196:80–9. doi: 10.1016/j.biomaterials.2017.12.025
86. Zhang Y, Böse T, Unger RE, Jansen JA, Kirkpatrick CJ, van den Beucken JJJP. Macrophage type modulates osteogenic differentiation of adipose tissue MSCs. *Cell Tissue Res*. (2017) 369:273–86. doi: 10.1007/s00441-017-2598-8
87. Caires HR, Barros da Silva P, Barbosa MA, Almeida CR. A co-culture system with three different primary human cell populations reveals that biomaterials and MSC modulate macrophage-driven fibroblast recruitment. *J Tissue Eng Regen Med*. (2018) 12:e1433–40. doi: 10.1002/term.2560

88. Quint P, Ruan M, Pederson L, Kassem M, Westendorf JJ, Khosla S, et al. Sphingosine 1-phosphate (S1P) receptors 1 and 2 coordinately induce mesenchymal cell migration through S1P activation of complementary kinase pathways. *J Biol Chem*. (2013) 288:5398–406. doi: 10.1074/jbc.M112.413583
89. Pederson L, Ruan M, Westendorf JJ, Khosla S, Oursler MJ. Regulation of bone formation by osteoclasts involves Wnt/BMP signaling and the chemokine sphingosine-1-phosphate. *Proc Natl Acad Sci*. (2008) 105:20764–9. doi: 10.1073/pnas.0805133106
90. Liu Y, Wang L, Kikuiri T, Akiyama K, Chen C, Xu X, et al. Mesenchymal stem cell–based tissue regeneration is governed by recipient T lymphocytes via IFN-γ and TNF-α. *Nat Med*. (2011) 17:1594–601. doi: 10.1038/nm.2542
91. Bouvet-Gerbettaz S, Boukhechba F, Balaguer T, Schmid-Antomarchi H, Michiels J-F, Scimeca J-C, et al. Adaptive immune response inhibits ectopic mature bone formation induced by BMSCs/BCP/plasma composite in immune-competent mice. *Tissue Eng Part A*. (2014) 20:2950–62. doi: 10.1089/ten.tea.2013.0633
92. Su Y, Shi S, Liu Y. Immunomodulation regulates mesenchymal stem cell-based bone regeneration. *Oral Dis*. (2014) 20:633–6. doi: 10.1111/odi.12248
93. Najar M, Raicevic G, Crompot E, Fayyad-Kazan H, Bron D, Toungouz M, et al. The immunomodulatory potential of mesenchymal stromal cells. *J Immunother*. (2016) 39:45–59. doi: 10.1097/CJI.0000000000000108
94. Glenn JD. Mesenchymal stem cells: emerging mechanisms of immunomodulation and therapy. *World J Stem Cells*. (2014) 6:526. doi: 10.4252/wjsc.v6.i5.526
95. Bassi G, Guilloton F, Menard C, Di Trapani M, Deschaseaux F, Sensebé L, Schrezenmeier H, et al. Effects of a ceramic biomaterial on immune modulatory properties and differentiation potential of human mesenchymal stromal cells of different origin. *Tissue Eng Part A*. (2015) 21:767–81. doi: 10.1089/ten.tea.2014.0269
96. Giebel B, Kordelas L, Börger V. Clinical potential of mesenchymal stem/stromal cell-derived extracellular vesicles. *Stem Cell Investig*. (2017) 4:84. doi: 10.21037/sci.2017.09.06
97. Deschepper M, Manassero M, Oudina K, Paquet J, Monfoulet L-E, Bensidhoum M, et al. Proangiogenic and prosurvival functions of glucose in human mesenchymal stem cells upon transplantation. *Stem Cells*. (2013) 31:526–35. doi: 10.1002/stem.1299
98. Becquart P, Cambon-Binder A, Monfoulet L-E, Bourguignon M, Vandamme K, Bensidhoum M, et al. Ischemia is the prime but not the only cause of human multipotent stromal cell death in tissue-engineered constructs *in vivo*. *Tissue Eng Part A*. (2012) 18:2084–94. doi: 10.1089/ten.tea.2011.0690
99. Potier E, Ferreira E, Meunier A, Sedel L, Logeart-Avramoglou D, Petite H. Prolonged hypoxia concomitant with serum deprivation induces massive human mesenchymal stem cell death. *Tissue Eng*. (2007) 13:1325–31. doi: 10.1089/ten.2006.0325
100. Moya A, Paquet J, Deschepper M, Larochette N, Oudina K, Denoeud C, et al. Human mesenchymal stem cell failure to adapt to glucose shortage and rapidly use intracellular energy reserves through glycolysis explains poor cell survival after implantation. *Stem Cells*. (2018) 36:363–76. doi: 10.1002/stem.2763
101. Nicolay NH, Perez RL, Saffrich R, Huber PE, Nicolay NH, Perez RL, et al. Radio-resistant mesenchymal stem cells: mechanisms of resistance and potential implications for the clinic. *Oncotarget*. (2015) 6:19366–80. doi: 10.18632/oncotarget.4358
102. Laing AG, Riffo-Vasquez Y, Sharif-Paghaleh E, Lombardi G, Sharpe PT. Immune modulation by apoptotic dental pulp stem cells *in vivo*. *Immunotherapy*. (2018) 10:201–11. doi: 10.2217/imt-2017-0117
103. Galleu A, Riffo-Vasquez Y, Trento C, Lomas C, Dolcetti L, Cheung TS, et al. Apoptosis in mesenchymal stromal cells induces *in vivo* recipient-mediated immunomodulation. *Sci Transl Med*. (2017) 9:eaam7828. doi: 10.1126/scitranslmed.aam7828
104. Sachet M, Liang YY, Oehler R. The immune response to secondary necrotic cells. *Apoptosis*. (2017) 22:1189–204. doi: 10.1007/s10495-017-1413-z
105. Bianchi ME, Crippa MP, Manfredi AA, Mezzapelle R, Rovere Querini P, Venereau E. High-mobility group box 1 protein orchestrates responses to tissue damage via inflammation, innate and adaptive immunity, and tissue repair. *Immunol Rev*. (2017) 280:74–82. doi: 10.1111/imr.12601
106. Lunyak VV, Amaro-Ortiz A, Gaur M. Mesenchymal stem cells secretory responses: senescence messaging secretome and immunomodulation perspective. *Front Genet*. (2017) 8:1–21. doi: 10.3389/fgene.2017.00220
107. Madrigal M, Rao KS, Riordan NH. A review of therapeutic effects of mesenchymal stem cell secretions and induction of secretory modification by different culture methods. *J Transl Med*. (2014) 12:260. doi: 10.1186/s12967-014-0260-8
108. Sisakhtnezhad S, Alimoradi E, Akrami H. External factors influencing mesenchymal stem cell fate *in vitro*. *Eur J Cell Biol*. (2017) 96:13–33. doi: 10.1016/j.ejcb.2016.11.003
109. Silva LHA, Antunes MA, Dos Santos CC, Weiss DJ, Cruz FF, Rocco PRM. Strategies to improve the therapeutic effects of mesenchymal stromal cells in respiratory diseases. *Stem Cell Res Ther*. (2018) 9:45. doi: 10.1186/s13287-018-0802-8
110. Xue C, Shen Y, Li X, Li B, Zhao S, Gu J, et al. Exosomes derived from hypoxia-treated human adipose mesenchymal stem cells enhance angiogenesis through the PKA signaling pathway. *Stem Cells Dev*. (2018) 27:456–65. doi: 10.1089/scd.2017.0296
111. Ban J-J, Lee M, Im W, Kim M. Low pH increases the yield of exosome isolation. *Biochem Biophys Res Commun*. (2015) 461:76–9. doi: 10.1016/j.bbrc.2015.03.172
112. Eldh M, Ekström K, Valadi H, Sjöstrand M, Olsson B, Jernås M, et al. Exosomes communicate protective messages during oxidative stress; possible role of exosomal shuttle RNA. *PLoS ONE*. (2010) 5:e15353. doi: 10.1371/journal.pone.0015353
113. Ejtehadifar M, Shamsasenjan K, Movassaghpour A, Akbarzadehlaleh P, Dehdilani N, Abbasi P, et al. The effect of hypoxia on mesenchymal stem cell biology. *Adv Pharm Bull*. (2015) 5:141–9. doi: 10.15171/apb.2015.021
114. Paquet J, Deschepper M, Moya A, Logeart-Avramoglou D, Boisson-Vidal C, Petite H. Oxygen tension regulates human mesenchymal stem cell paracrine functions. *Stem Cells Transl Med*. (2015) 4:809–21. doi: 10.5966/sctm.2014-0180
115. Martinez VG, Ontoria-Oviedo I, Ricardo CP, Harding SE, Sacedon R, Varas A, et al. Overexpression of hypoxia-inducible factor 1 alpha improves immunomodulation by dental mesenchymal stem cells. *Stem Cell Res Ther*. (2017) 8:208. doi: 10.1186/s13287-017-0659-2
116. Ponte AL, Marais E, Gallay N, Langonné A, Delorme B, Hérault O, et al. The *in vitro* migration capacity of human bone marrow mesenchymal stem cells: comparison of chemokine and growth factor chemotactic activities. *Stem Cells*. (2007) 25:1737–45. doi: 10.1634/stemcells.2007-0054
117. Crisostomo PR, Wang Y, Markel TA, Wang M, Lahm T, Meldrum DR. Human mesenchymal stem cells stimulated by TNF-α, LPS, or hypoxia produce growth factors by an NFκB- but not JNK-dependent mechanism. *Am J Physiol Physiol*. (2008) 294:C675–82. doi: 10.1152/ajpcell.00437.2007
118. Roemeling-van Rhijn M, Mensah FKF, Korevaar SS, Leijs MJ, van Osch GJVM, IJzermans JNM, et al. Effects of hypoxia on the immunomodulatory properties of adipose tissue-derived mesenchymal stem cells. *Front Immunol*. (2013) 4:1–8. doi: 10.3389/fimmu.2013.00203
119. Cordonnier T, Layrolle P, Gaillard J, Langonné A, Sensebé L, Rosset P, et al. 3D environment on human mesenchymal stem cells differentiation for bone tissue engineering. *J Mater Sci Mater Med*. (2010) 21:981–7. doi: 10.1007/s10856-009-3916-9
120. Miron RJ, Zohdi H, Fujioka-Kobayashi M, Bosshardt DD. Giant cells around bone biomaterials: osteoclasts or multi-nucleated giant cells? *Acta Biomater*. (2016) 46:15–28. doi: 10.1016/j.actbio.2016.09.029
121. Ahmed GJ, Tatsukawa E, Morishita K, Shibata Y, Suehiro F, Kamitakahara M, et al. Regulation and biological significance of formation of osteoclasts and foreign body giant cells in an extraskeletal implantation model. *Acta Histochem Cytochem*. (2016) 49:97–107. doi: 10.1267/ahc.16007
122. Khan UA, Hashimi SM, Bakr MM, Forwood MR, Morrison NA. Foreign body giant cells and osteoclasts are TRAP positive, have podosome-belts and both require OC-STAMP for cell fusion. *J Cell Biochem*. (2013) 114:1772–8. doi: 10.1002/jcb.24518
123. Ogata K, Katagiri W, Hibi H. Secretomes from mesenchymal stem cells participate in the regulation of osteoclastogenesis *in vitro*. *Clin Oral Investig*. (2017) 21:1979–88. doi: 10.1007/s00784-016-1986-x

124. Horwood NJ, Kartsogiannis V, Quinn JMW, Romas E, Martin TJ, Gillespie MT. Activated T lymphocytes support osteoclast formation *in vitro*. *Biochem Biophys Res Commun*. (1999) 265:144–50. doi: 10.1006/bbrc.1999.1623
125. Martin TJ, Sims NA. RANKL/OPG; critical role in bone physiology. *Rev Endocr Metab Disord*. (2015) 16:131–9. doi: 10.1007/s11154-014-9308-6
126. Quinn JMW, Itoh K, Udagawa N, Häusler K, Yasuda H, Shima N, et al. Transforming growth factor β affects osteoclast differentiation via direct and indirect actions. *J Bone Miner Res*. (2001) 16:1787–94. doi: 10.1359/jbmr.2001.16.10.1787
127. Maeda K, Kobayashi Y, Udagawa N, Uehara S, Ishihara A, Mizoguchi T, et al. Wnt5a-Ror2 signaling between osteoblast-lineage cells and osteoclast precursors enhances osteoclastogenesis. *Nat Med*. (2012) 18:405–12. doi: 10.1038/nm.2653
128. Chan CKF, Gulati GS, Sinha R, Tompkins JV, Lopez M, Carter AC, et al. Identification of the human skeletal stem cell. *Cell*. (2018) 175:43–56.e21. doi: 10.1016/J.CELL.2018.07.029
129. Sims NA, Martin TJ. Coupling the activities of bone formation and resorption: a multitude of signals within the basic multicellular unit. *Bonekey Rep*. (2014) 3:1–10. doi: 10.1038/bonekey.2013.215
130. Matsuo K, Irie N. Osteoclast–osteoblast communication. *Arch Biochem Biophys*. (2008) 473:201–9. doi: 10.1016/j.abb.2008.03.027
131. Henriksen K, Karsdal MA, John Martin T. Osteoclast-derived coupling factors in bone remodeling. *Calcif Tissue Int*. (2014) 94:88–97. doi: 10.1007/s00223-013-9741-7
132. Ikebuchi Y, Aoki S, Honma M, Hayashi M, Sugamori Y, Khan M, et al. Coupling of bone resorption and formation by RANKL reverse signalling. *Nature*. (2018) 561:195–200. doi: 10.1038/s41586-018-0482-7
133. Cianferotti L, Gomes AR, Fabbri S, Tanini A, Brandi ML. The calcium-sensing receptor in bone metabolism: from bench to bedside and back. *Osteoporos Int*. (2015) 26:2055–71. doi: 10.1007/s00198-015-3203-1
134. Chen Z, Klein T, Murray RZ, Crawford R, Chang J, Wu C, et al. Osteoimmunomodulation for the development of advanced bone biomaterials. *Mater Today*. (2016) 19:304–21. doi: 10.1016/j.mattod.2015.11.004

Conflict of Interest Statement: ND is employed by Instructure Labs, B.V.

The remaining authors declare that the research was conducted in the absence of any commercial or financial relationships that could be construed as a potential conflict of interest.

Objectives

Based on these evidences, this project aims to further study the suspected central role of osteoclasts in the process of bone regeneration induced by the combination of CaP materials and MSCs. The precise underlying mechanism remains unknown; therefore the stimulating factors leading to osteoclasts formation have to be identified. As they lead to efficient bone formation, implanted MSCs are the first suspected source of pro-osteoclastogenic mediators. Then, if coupling factors from osteoclasts can locally initiate remodeling, there were not yet identified in this context. Additionally, the material composition may yield bone formation depending on osteoclasts attraction and their subsequent phenotype.

The first chapter presents a draft article for an *in vitro* approach studying the effect of the secretome from human MSCs on osteoclasts. The goal was to identify pro-osteoclastogenic mediators that could be secreted by MSCs. Given their rapid clearance after implantation, the effect of apoptosis on MSCs' secretome was particularly analyzed. Additional valuable results are presented, particularly experiments replacing bone marrow MSCs by adipose-derived MSCs or fibroblasts.

In a second part, the development of osteoclasts on various CaP materials and the osteogenic effect of their secreted factors were evaluated *in vitro*. This collaborative project also permitted to compare our models, with human cells, to the use of mouse cells. An ongoing experiment in nude mice will allow us to link our *in vitro* observation with osteoclast and bone formation *in vivo* to strengthen our conclusion.

Finally, other preliminary experiments *in vivo* will be presented to fuel the discussion on the future of cell therapies. We first attempted to substitute human MSCs by their conditioned culture media or specifically isolated extracellular vesicles in a subcutaneous bone formation model in nude mice. Also, we tried to transpose this model in rats with syngenic and allogenic MSCs to evaluate potential difference in immune response.

Chapter I:
Effect of MSC-derived factors on osteoclastogenesis *in vitro*

Apoptotic mesenchymal stromal cells support osteoclastogenesis *in vitro* through secretion of CXCR-1 and CXCR-2 ligands.

Running title: Apoptotic MSCs stimulate osteoclasts *in vitro*

Paul Humbert[1°], Meadhbh Á. Brennan[1,2], Julien De Lima[1], Régis Brion[1,3], Annie Adrait[4], Céline Charrier[1], Bénédicte Brulin[1], Valérie Trichet[1], Yohann Couté[4], Frédéric Blanchard[1*], Pierre Layrolle[1*]

1. INSERM, UMR 1238, Phy-OS, Bone Sarcoma and Remodeling of Calcified Tissues, School of Medicine, University of Nantes, 44000 Nantes, France
2. Regenerative Medicine Institute, School of Medicine, and Bioengineering department, School of Engineering, National University of Ireland, Galway, Ireland.
3. CHU Nantes, 44000 Nantes, France
4. Université Grenoble Alpes, CEA, INSERM, IRIG, BGE, F-38000 Grenoble, France

° Corresponding author
* Co-senior authors

Contributions:

P.H. performed experiments, analyzed the data and drafted the manuscript; J.D.L., R.B., C.C. and B.B. provided technical support; R.B. performed the multiplex experiment; A.A. and Y.C. performed and analyzed the MS experiment; P.H., Y.C., V.T., M.Á.B., F.B. and P.L. revised the manuscript; F.B. and P.L. designed the study.

Abstract:

In bone regeneration induced by the combination of mesenchymal stromal cells and calcium-phosphate materials, osteoclasts emerge as a possible key element linking initial inflammation and subsequent bone formation. Favorable outcomes are observed despite only short-term engraftments of implanted cells, highlighting their major paracrine function and the possible implication of cell death in modulating their secretions. In this work, we focused on the communication from mesenchymal stromal cells towards osteoclasts-like cells *in vitro*. Mesenchymal stromal cells grown on a calcium-phosphate biomaterial or undergoing induced apoptosis produced a conditioned media favoring the development of osteoclasts from human CD14+ monocytes. On the contrary, mesenchymal stromal cells' apoptotic secretion inhibited the development of inflammatory multinucleated giant cells formed after IL-4 stimulation. Components of mesenchymal stromal cells' secretome before and after apoptotic stress were compared using mass spectrometry-based quantitative proteomics and a complementary immunoassay for major cytokines. CXCR-1 and CXCR-2 ligands, primarily IL-8/CXCL-8 but also the growth-regulated proteins CXCL-1, -2 or -3, were identified as the major players of mesenchymal stromal cells' pro-osteoclastic effect. These findings support our working hypothesis implicating osteoclasts as a central player in bone regeneration induced by the combination of mesenchymal stromal cells and calcium-phosphate materials, and suggest that apoptosis plays an important role in mesenchymal stromal cells' effectiveness. The identification of key mediators is essential to rationally design future therapies.

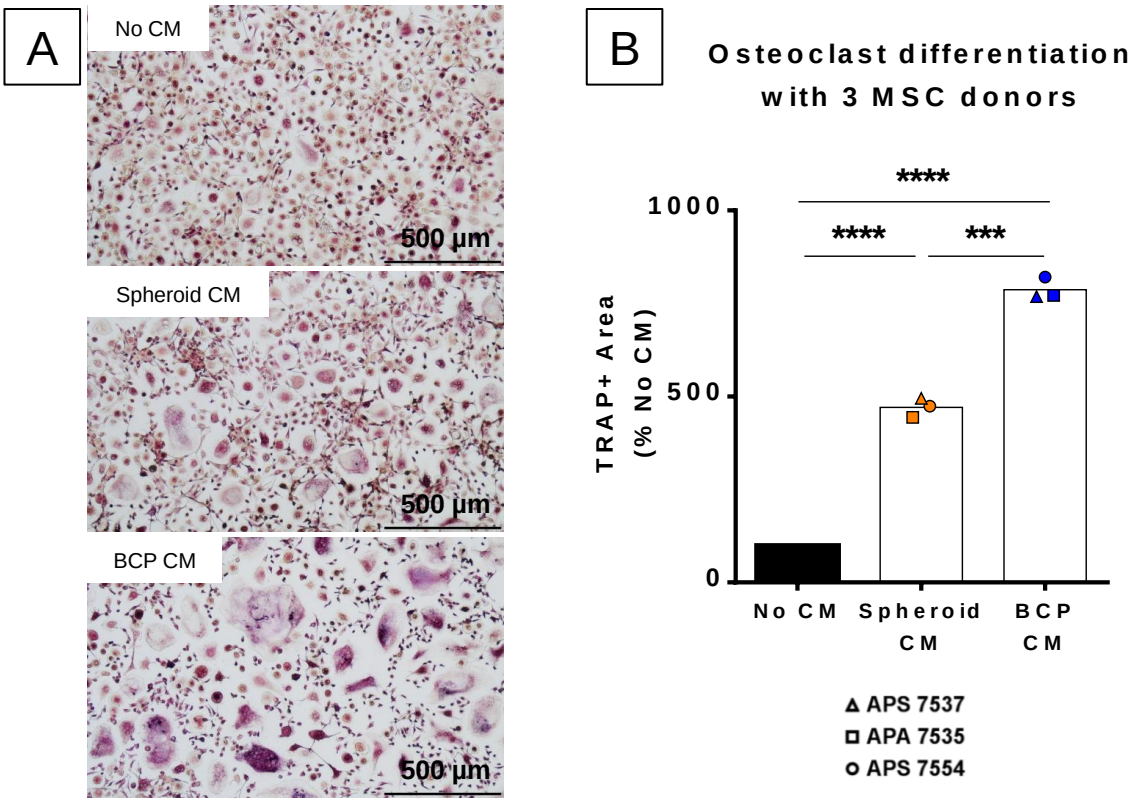

Figure 1: Osteoclastogenesis is enhanced *in vitro* by CM from MSCs culture on BCP material. (A) Microscopic images of TRAP stained osteoclasts culture without CM, with CM from MSC spheroids (Spheroid CM) or MSCs on BCP material (BCP CM). (B) Quantification by image analysis of TRAP+ area after 8 days of osteoclast differentiation with spheroid or BCP CM from three MSC donors, normalized to the TRAP+ area without CM. Statistical analysis by repeated measure ANOVA followed by Tukey's multiple comparison test, *** for p-value < 0.001, **** for p-value < 0.0001.

Introduction:

The combination of culture-expanded autologous mesenchymal stromal cells (MSCs) from bone marrow and calcium-phosphate (CaP) materials has been increasingly studied for bone regeneration therapies. It has proven efficacy in preclinical models[1], in both ectopic and orthotopic sites, and in clinical trials for the treatment of non-unions[2,3] as well as maxilla-facial defects[4]. The ongoing ORTHOUNION European project aims to evaluate the efficacy and the cost effectiveness of this cell therapy in comparison to autologous bone grafting.[5] Despite promising results, and although the clinical use of autologous MSCs resolve many of the limitations of bone grafting, it also presents some major challenging issues. While less invasive than bone harvesting for autologous grafting, bone marrow aspiration remains a surgical procedure comprising risks. The variability between donors may alter the expansion efficiency and the clinical outcome. The use of living cells comes with substantial regulatory constraints[6] and the cost efficiency of the procedure still remains to be evaluated. Therefore, a better understanding of the exact mechanism of osteoinduction by MSC-CaP therapies is essential to rationally design future cell-free approaches for bone regeneration and improve further patients care.

Both the biomaterial properties (including porosity, surface structure, chemical composition)[7] and the cells' characteristics (including tissue of origin, passage, dose)[8,9] are important in modulating the host response and directing the outcome of implantation. From our own experimental observations[10], together with an in-depth review of the literature on this topic, we recently presented a hypothetical mechanism of bone formation whereby osteoclasts are key cells that turn the early inflammatory reaction towards a bone formatting cascade.[11] In successful bone forming conditions, a rapid death of implanted MSCs was observed[12], along with early osteoclast formation on the biomaterial.[10] We postulated that stressed MSCs on CaP materials can locally direct myeloid cell differentiation, i.e. favor the development of osteoclasts instead of multinucleated giant cells (MNGCs), typical of the foreign body reaction. Consistent with the plasticity of macrophages, two different phenotypes of MNGCs could favor either inflammation or wound healing.[13] However, osteoclasts are the physiological multinucleated cells of bone responsible for its resorption and, most importantly here, the major sources of coupling factors with osteoblast lineage cells.[14] Once formed on the surface of the biomaterial, they could attract new skeletal stem cells and participate in their differentiation into bone forming osteoblasts while MNGCs would favor fibrosis.

MSCs secrete a variety of immunomodulatory factors[15], essential to attenuate initial host reaction against the biomaterial and avoid chronic inflammation. Death of implanted cells is mostly attributed to a lack of oxygen[16] and nutrients[17]. These factors, and other stresses such as the inflammatory environment, the reaction to the biomaterial surface or the mechanical constrain, influence MSCs to such an extent that MSC pre-conditioning before implantation is being explored to enhance their therapeutic potential.[18,19] In addition, *in vitro* collection of MSCs' secretions after stimulation could represent a valuable clinical tool. Apoptosis itself is a source of immunomodulatory signals that could be involved in MSC-based therapies.[20]

MSCs have been described as either supportive[21,22] or suppressive[23,24] towards osteoclastogenesis depending on the culture conditions and the cell source. In this study, we

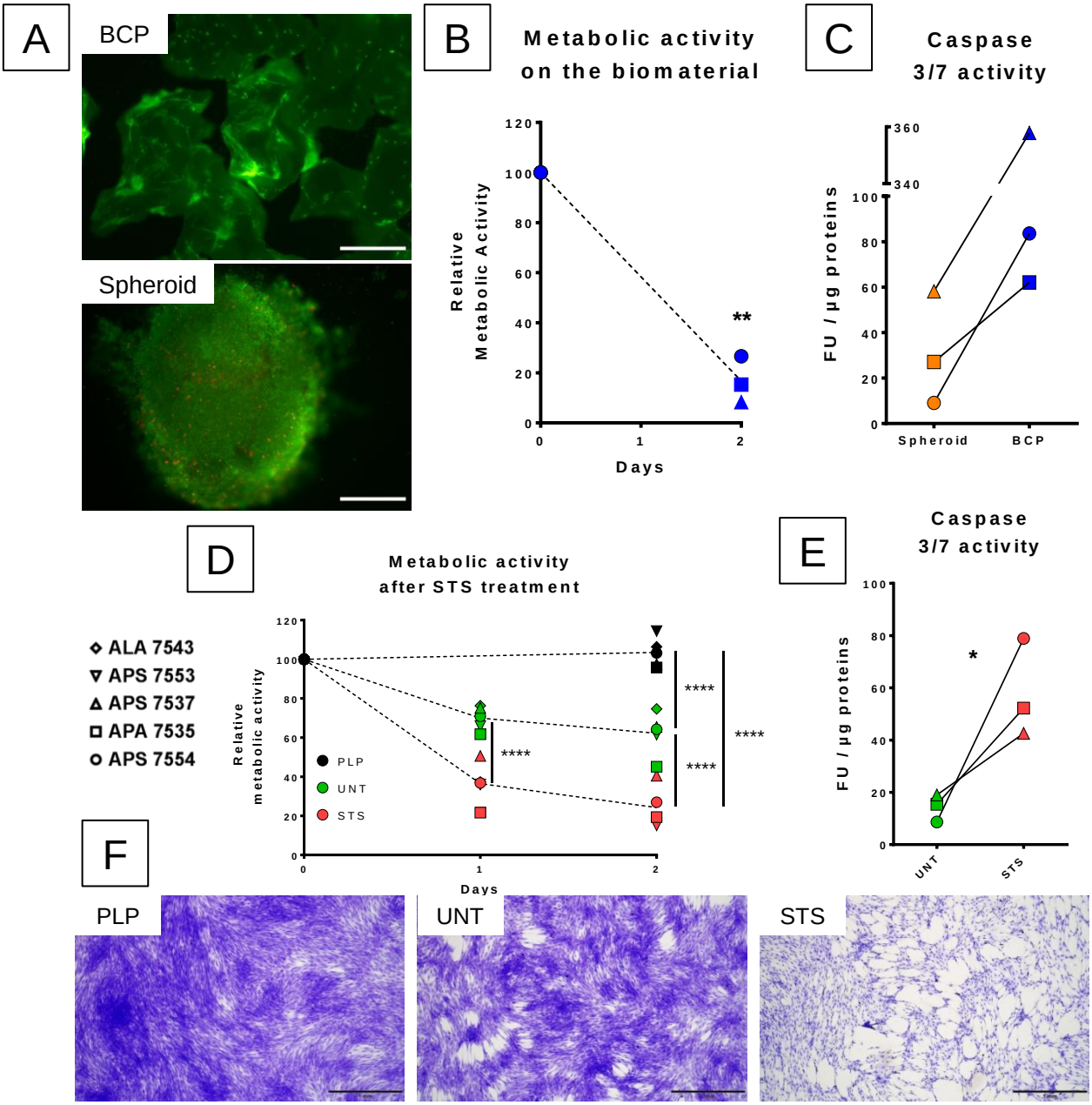

Figure 2: MSCs seeded on BCP material undergo apoptosis, reproduced in 2D by a staurosporine treatment. (A) LIVE/DEAD® staining at 48 hours of MSCs seeded on BCP particules or in spheroid form. (B) Metabolic activity measured by resazurin assay after 48h of MSCs from three donors on the BCP material, normalized to the value after seeding. Statistical analysis by one-sided paired t-test, ** for p-value < 0.01 (C) Caspase 3/7 activity per µg of proteins extracted from spheroid or BCP cultures of three MSC donors. (D) Metabolic activity measured by resazurin assay after 24 and 48 hours of MSCs from five donors, in complete media (PLP) in serum-free media (untreated, UNT) or in serum-free media after a 4h 0.1µM STS treatment (STS), normalized to the value before treatment. Statistical analysis by repeated measure ANOVA followed by Tukey's multiple comparison test, **** for p-value < 0.0001. (E) Caspase 3/7 activity per µg of proteins extracted from untreated (UNT) or or STS-treated (STS) cultures of three MSC donors. Statistical analysis by one-sided paired t-test, * for p-value < 0.05. (F) Crystal violet staining of MSCs after 48 hours in complete media (PLP), serum-free media (UNT) or serum-free media after STS-treatment (STS).

explored the effect of MSCs' secretion on osteoclasts and MNGCs *in vitro,* using primary human cells. Conditioned media (CM) from human bone marrow MSCs were initially collected after cell seeding on the biphasic calcium phosphate (BCP) material used in the ORTHOUNION clinical trial. This model was later simplified into a two-dimensional culture where apoptotic stress was induced by a staurosporine (STS) treatment. We explored the composition of the CMs by high-throughput proteomic analysis using bottom-up mass spectrometry (MS)-based analysis and multiplex immunoassay. The implication of major candidates was evaluated using neutralizing antibodies targeting cytokine and chemokine receptors on the osteoclast membrane.

Results:

MSCs' secretome on BCP is pro-osteoclastogenic

In order to study the secretions of MSCs in contact with the biomaterial, short duration (48 hours) cell cultures were performed before recovering the CM. To be consistent with *in vivo* implantation, a large number of cells (400 000) were seeded on biomaterial granules (50 mg) in a small volume (500 µL) of serum-free media. The use of MSC spheroids as a control allowed us to preserve the cell/volume ratio, essential as the CM is later used in an osteoclast culture. The CMs were centrifuged to avoid adding dead cells or debris to the osteoclast differentiation test. Osteoclasts were differentiated from human CD14+ monocytes stimulated with recombinant human M-CSF and RANK-L. As shown in Figure 1.A, addition of CM from MSC spheroid cultures significantly increased the number and size of osteoclasts. CM from MSC/BCP cultures had an even stronger effect leading to the formation of huge and strongly TRAP+ multinucleated cells. This effect was consistent with three different MSC donors, confirming the pro-osteoclastogenic effect of MSCs' secretions on BCP (Figure 1.B). Also, increasing the exogenous RANK-L concentration two to four times did not change the size and shape of osteoclasts formed (data not shown), ensuring saturating conditions in this major cytokine. CM obtained on BCP granules without cells did not have any effect on osteoclasts either (data not shown), confirming that MSC-secreted factors other than RANK-L were responsible for the phenotypical changes in osteoclasts.

MSCs grown in vitro on BCP are undergoing apoptosis

After two days of culture, Live/Dead staining (Figure 2.A) showed living MSCs attached on the biomaterial surface and almost no dead cells, however cell density appeared lower than what would be expected according to the quantity of cells seeded. Dead cells may have been removed with the collected media or washed away during the staining protocol. In the MSC spheroid, cells were visible as a cohesive mass, entrapped by the secreted matrix, and only sporadic dead cells were observed. As shown in Figure 2.B, 48 hours after seeding, the metabolic activity measured from MSCs on BCP dropped to around 20 % of its initial value, corroborating the fluorescent images. The metabolic activity of the cells could only be recorded on the MSC/BCP culture, as the reagent did not diffuse efficiently inside the MSC spheroids, indicating that the MSC spheroid culture may not be a good control in this instance as it might also prevent the diffusion of soluble mediators into the CM. In line with these results, it was found that caspase 3/7 activity was higher in cell lysate from cells grown on BCP compared to spheroids prepared from the three MSC donors, suggesting an increased apoptosis for MSCs grown on the biomaterial (Figure 2.C).

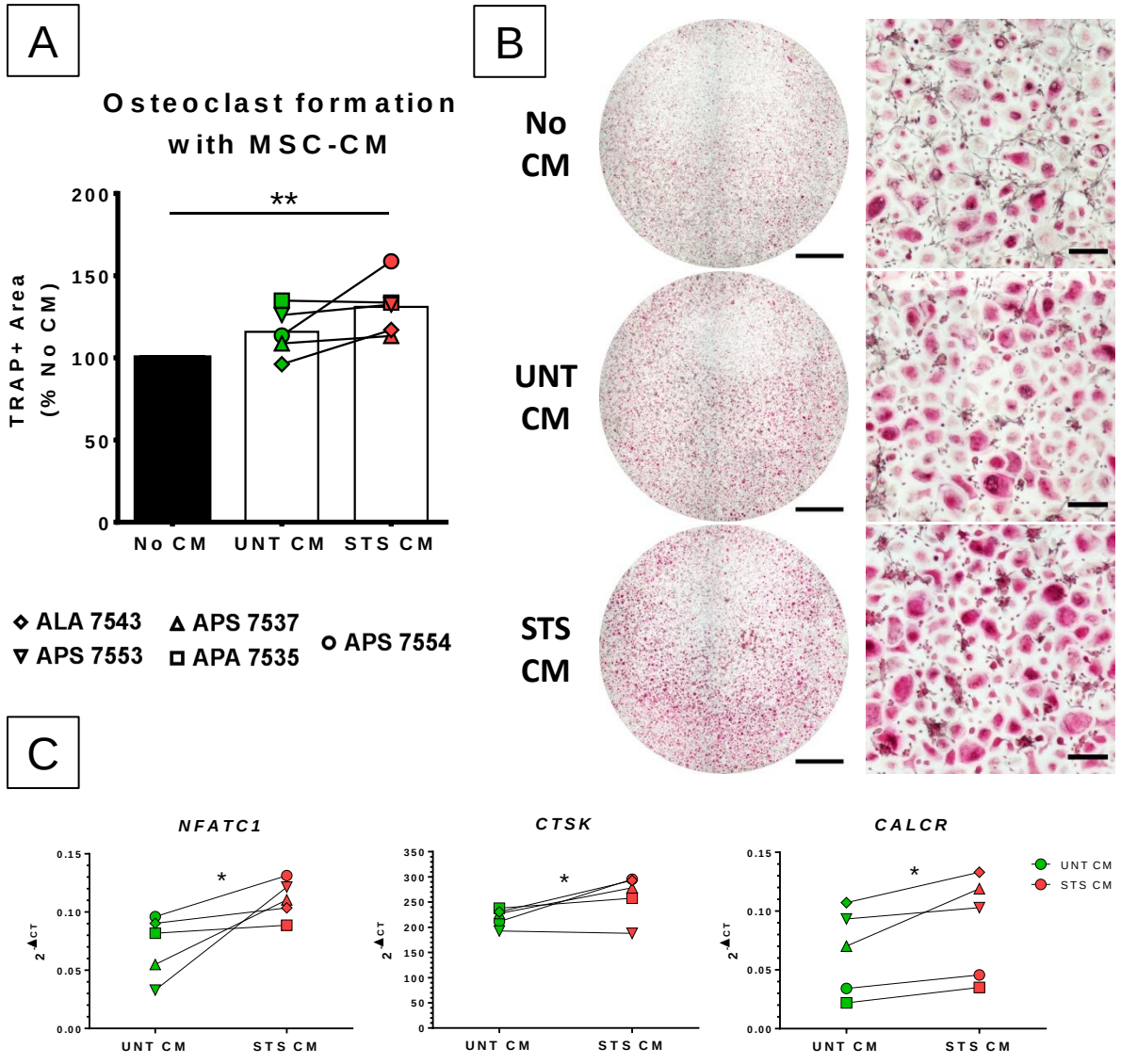

Figure 3: CM from STS-treated MSCs exhibit pro-osteoclastogenic properties. (A) Quantification by image analysis of TRAP+ area after 8 days of osteoclast differentiation with UNT or STS CM from five MSC donors with two or three CD14+ donors, normalized to the TRAP+ area without CM. Statistical analysis by repeated measure ANOVA followed by Tukey's multiple comparison test, ** for p-value < 0.01 (B) Full well (scale bar = 2 mm) and close-up (scale bar = 200 µm) images of TRAP-stained osteoclasts at 8 days of differentiation without CM, with UNT-CM and STS-CM. (D) Comparative expression of differentiation markers in osteoclasts treated with UNT or STS-CM from five MSC donors. Statistical analysis by one-sided paired t-test, * for p-value < 0.05.

To further investigate the implications of MSCs undergoing apoptosis and to simplify the model, MSCs in a classical 2D culture were subjected to a staurosporine (STS) treatment, artificially inducing cell death by apoptosis. STS is an inhibitor of protein kinases, widely used for *in vitro* induction of apoptosis by activation of caspase-3-like proteases.[25] A mild treatment with 0.1 µM STS during 4 hours in serum-free conditions caused a loss of metabolic activity in MSCs from five human donors of 60 % at 24 hours and 80 % at 48 hours (Figure 2.D). In parallel, culture of the same cells in serum-free conditions without STS also exhibited a diminished metabolic activity, less drastic compared to treated cells, averaging 75 % and 60 % of their initial value at 24 and 48 hours, respectively. In contrast, in cells grown with complete culture media containing platelet lysate, metabolic activity was maintained after 2 days (Figure 2.D). Importantly, MSCs treated with STS showed a significant increase, of two to eight-folds, in caspase 3/7 activity per µg of proteins compared to untreated cells, confirming their death by apoptosis (Figure 2.E). A crystal violet staining allowed visualization of healthy cell morphologies in complete or serum-free media while revealing rounded cells and cell layer disruption after STS treatment (Figure 2.F). These data indicated that STS treatment mirrored the apoptotic stress induced by seeding MSCs in large numbers on BCP materials and could facilitate the production of CM in more controlled conditions.

Supernatants from apoptotic MSCs favor osteoclasts but inhibit MNGCs

CM of untreated MSCs (UNT-CM) and STS-treated MSCs (STS-CM) were used in osteoclasts and MNGCs cultures. Results obtained from five MSCs donors and two to three CD14+ monocytes donors indicated that STS-CMs significantly favor osteoclastogenesis in comparison to cultures without CM (Figure 3.A). In comparison to UNT-CM, two STS-CMs (donors APS 7554 and ALA 7543) strongly stimulated osteoclastogenesis, whereas two only slightly induced it (donors APS 7553 and APS 7537) and one did not (APA 7535). The number of donors was too small to analyze this variability further but CMs obtained with MSCs from donor APS 7554 consistently showed a significant stronger pro-osteoclastogenic effect after STS treatment, using CD14+ monocytes from three different donors (Figure 3.B). To confirm the superior effect of STS-CMs compared to UNT-CM on osteoclastogenesis, the expression of specific genes was evaluated using RT-qPCR in osteoclasts stimulated with the CM from the five MSCs donors. A significant over-expression of three markers of osteoclast differentiation was observed with STS-CMs compared to UNT-CM (Figure 3.D): cathepsin K (*CTSK*), nuclear factor of activated T cells 1 (*NFATC1*) and the calcitonin receptor (*CALCR*). The expression of other osteoclast markers, such as dendrocyte expressed seven transmembrane protein (*DCSTAMP*) and matrix metallopeptidase 9 (*MMP9*), was not modulated between the two conditions (data not shown). With the MSC donor APS 7554, gene expression analysis (Supplementary Figure 1) confirmed the consistent overexpression of classical markers of differentiation (*NFATC1*, *CTSK*, *CALCR* & *ACP5/TRAP*) in osteoclasts grown with STS-CM compared to osteoclasts cultured in absence of CM. STS-CM treated osteoclasts also had a modulated inflammatory phenotype with increased expression of *TNFRSF11B/OPG* and *IL-8/CXCL-8* but reduced *TNF*, *IL1B* and *IL10*.

We then tested the impact of STS-CM on MNGC formation. For this, MNGCs culture conditions were validated based on the literature (GM-CSF & IL-4, both 50 ng/mL)[26] and followed the same timing as used for osteoclast differentiation. MNGCs formation was assessed with the same staining protocol used for osteoclasts as they also express the TRAP

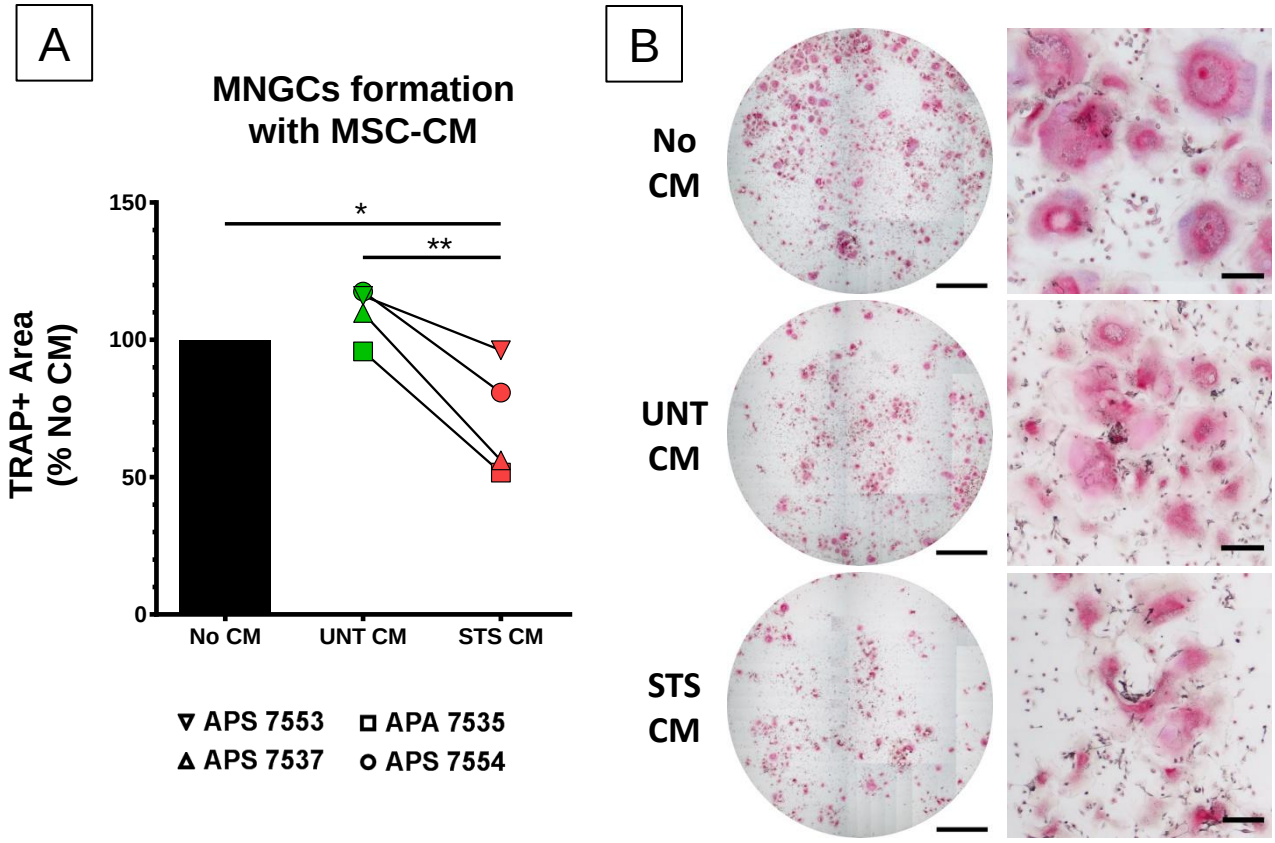

Figure 4: CM from STS-treated MSCs inhibit the development of GM-CSF/IL-4 induced MNGCs. (A) Quantification by image analysis of TRAP+ area after 8 days of MNGC differentiation with UNT or STS CM from four MSC donors, normalized to the TRAP+ area without CM. Statistical analysis by repeated measure ANOVA followed by Tukey's multiple comparison test, * for p-value < 0.05, ** for p-value < 0.01. (B) Full well (scale bar = 2 mm) and close-up (scale bar = 200 µm) images of TRAP-stained MNGCs at 8 days of differentiation without CM, with UNT-CM and STS-CM.

enzyme. DAPI/Phalloidin staining confirmed their multinucleation and a brief comparison with osteoclasts' gene expression profile revealed low expression of osteoclast-specific markers (*NFATC1*, *CTSK*, *CALCR*, *MMP9*) but higher expression of cytokines such as *IL-6*, *IL-1B* or *IL-10* and of the protein essential for cell fusion DC-Stamp (Supplementary Figure 2). Using four MSCs donors, we showed that STS-CM significantly inhibited the formation of MNGCs compared to UNT-CM (Figure 4). Therefore, CMs from MSC cultures after induction of apoptosis have opposite effects on CD14+ monocytes fate; inhibiting MNGC differentiation of CD14+ monocytes stimulated with GM-CSF and IL-4 while promoting osteoclast differentiation with M-CSF and RANK-L.

MSCs undergoing apoptosis have an altered secretion profile

To better characterize the secretion profile of MSCs, we performed high-throughput proteomic analysis using MS-based analysis and multiplex immunoassay. MS-based quantitative analyses of the proteins contained in CM from 3 MSC donors in UNT or STS conditions led to the identification and quantification in the three replicates of one condition of 1420 proteins. Statistical analysis highlighted 181 proteins with a differential abundance, 76 being more abundant in STS-CM and 105 being more abundant in UNT-CM (fold change ≥ 2 and p-value ≤ 0.03, Figure 5.A, Supplementary Table 1). Among the classical soluble mediators (cytokines, chemokines and growth factors), 2 cytokines of the IL-6 family were enriched in STS-CM (CRLF1 and IL-11), 13 mediators were unchanged (such as TGFB1, BMP-1, IGF2, CXCL-12 or IL-6) and 5 were downregulated (such as PDGF-D, M-CSF or OPG) (Table 1). Bioinformatic analyses (Supplementary Table 2) emphasized that STS-CMs were enriched in apoptosis-linked pathways, notably through proteins that are associated to the cytoskeleton (GSN, ROCK1), and in the interleukin-12 signaling pathway (e.g. CRLF1). On the contrary, UNT-CM enriched proteins were linked to the extracellular matrix, with components such as collagens (e.g. COL1A1) or proteoglycans (e.g. LUM), and its degradation (e.g. MMP1). These findings were consistent with a classical MSC phenotype in the untreated condition while STS treatment induced an apoptotic stress.

In addition, the CMs from 5 MSC donors were analyzed by a multiplex immunoassay towards 45 cytokines. Among the targeted proteins, 22 were detected in at least one sample but only 9 with a value above the lowest standard point. Figure 5.B present the six well-detected proteins for which a statistical analysis could be conducted. Three were statistically enriched in STS-CM; GROα/CXCL-1 with only 3 values above the lowest standard point but always in STS-CMs (3.5-fold increase, $p<0.05$), IL-8/CXCL-8 (4-fold increase, $p<0.05$) and PDGF-AA (3-fold increase, $p<0.01$). The only protein detected in both the immunoassay and MS-based analysis was IL-6, whose concentration did not change between the UNT and STS conditions. VEGF concentration was also found to be equivalent between UNT- and STS-CMs. MCP-1/CCL-2 was the only cytokine depleted in STS-CM (9-fold decrease, $p<0.01$). Other cytokines were only detected at low levels (close or below the lowest standard point), thus conclusions on their regulation should be drawn with caution. GROβ/CXCL-2 and basic Fibroblast Growth Factor (bFGF) were only detected in some STS-CM, suggesting an increased production or secretion during apoptosis. Eotaxin/CCL-11 was found downregulated in STS-CM but with only one value above the lowest standard point. All measurements for FMS-like tyrosine kinase 3 ligand (FLT3L) were below the lowest standard but it could be enriched in STS-CM.

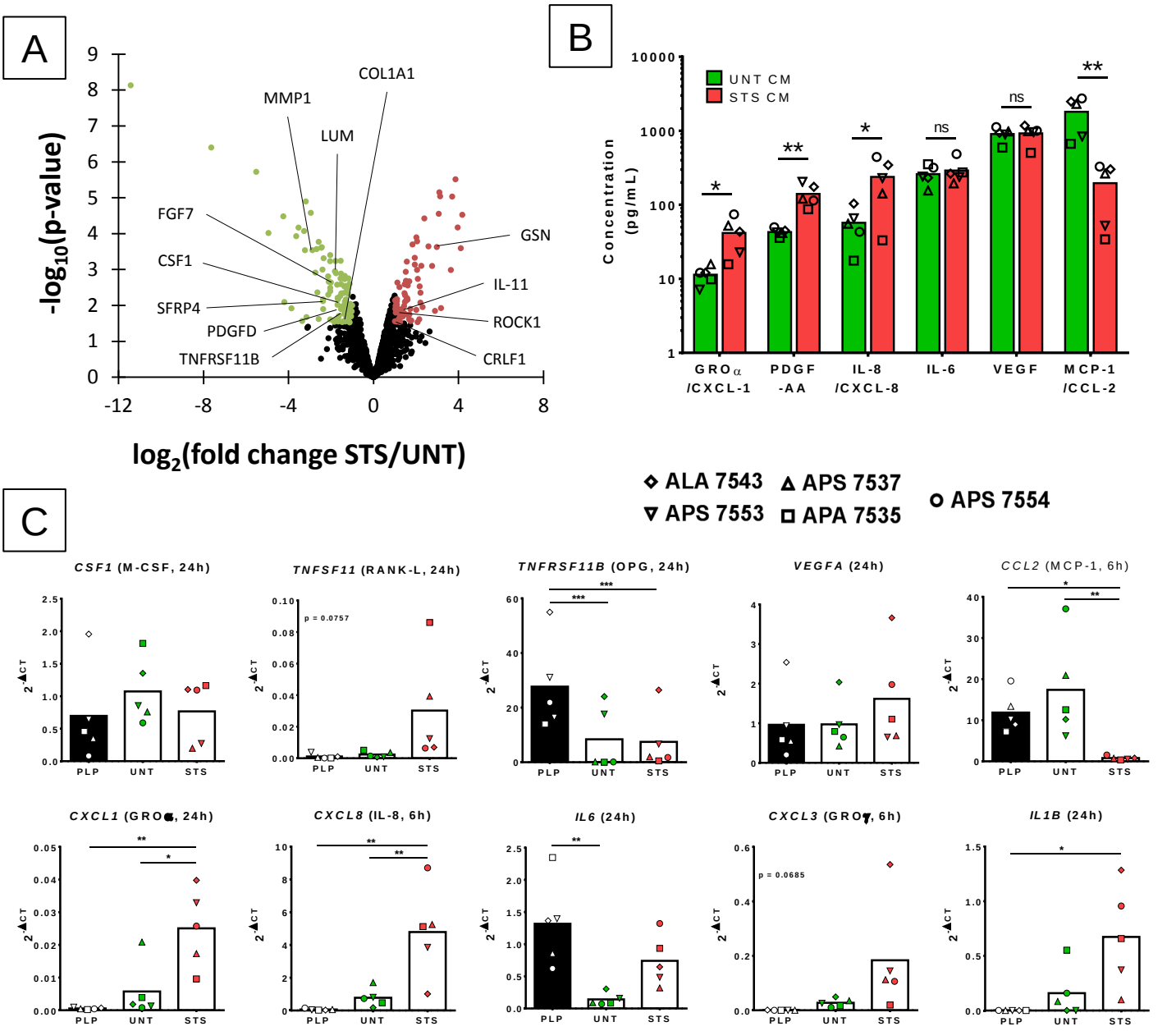

Figure 5: Soluble factors present in the media drastically change upon STS treatment. (A) Volcano plot displaying the differential abundance of proteins detected in STS-CM and UNT-CM by MS-based proteomics. The volcano plot represents the -log10 (p-value) on y axis plotted against the log2 (Fold Change STS/UNT) on x axis. Red and green dots represent proteins found more abundant respectively in STS-CM and UNT-CM (p-value ≤ 0.03 and fold change ≥ 2). (B) Quantification of cytokines concentration detected by multiplex immunoassay in UNT and STS-CM from 5 MSC donors. Statistical analysis by one-sided paired t-test, ns = not significant, * for p-value < 0.05, ** for p-value < 0.01. (C) Gene expression analysis in MSCs from five donors in complete media (PLP) or after 6 and 24 hours in serum-free media, with (STS) or without (UNT) STS-treatment. Statistical analysis by repeated measure ANOVA followed by Tukey's multiple comparison test, * for p-value < 0.05, ** for p-value < 0.01, *** for p-value < 0.001.

The expression of detected cytokines as well as other potential soluble modulators of osteoclastogenesis, such as M-CSF, RANK-L and osteoprotegerin (OPG), was evaluated by RT-qPCR at 6 and 24 hours after STS treatment (Figure 5.C and data not shown). *TNFSF11/RANKL* transcript seemed to be upregulated after STS treatment compared to either the untreated condition (serum-free media) or the basal condition in complete media, but the difference was not statistically significant, most probably because of a great variability between the replicates. M-CSF and OPG proteins were both reported as downregulated in STS-CM compared to UNT-CM by MS-base quantitative proteomics, but the expression of their transcript was found similar with or without treatment. These results suggest that the increased abundance of these proteins in UNT-CM compared to STS-CM is linked either to differential post-transcriptional regulations or enhanced secretion in UNT-CM. *TNFRSF11B/OPG* mRNA expression was however lower in serum-free conditions (UNT and STS) than in complete media. The RANK-L/OPG ratio could overall be more favorable to osteoclasts after STS treatment. Overexpression of GROα/CXCL-1, IL-8/CXCL-8 and downregulation of MCP-1/CCL-2 were confirmed at the transcriptional level. Similarly, *VEGFA* expression was unchanged in all tested conditions. *IL6* expression, stable after 6h, significantly dropped in serum-free untreated condition at 24h. Expression of *PDGFA* was below the detection limit and expression of *CXCL2* was detected at low level in only some STS-treated MSCs (data not shown). In addition, screening of other mediators revealed a potential overexpression of *CXCL3* (p=0.0685) and a significant one of *IL1B* (Figure 5.C).

Overall, radical changes of MSC secretions occur after STS treatment. The proteomic analysis illustrate that apoptotic cells lost their normal secretion profile while releasing intracellular components. Several mediators enriched in STS-CM could influence osteoclasts development.

Blocking CXCR-1/CXCR-2 abrogates the effect of MSC-CM but also alters basal osteoclastogenesis

To gain a deeper understanding of the cytokines involved in the communication between MSCs and osteoclasts, neutralizing antibodies were employed. For this experiment, CMs from the donor giving the most marked and reproducible results were used (APS 7554). Given the combined results of proteomics, multiplex analysis (Table 1) and RT-qPCR, and the literature on osteoclasts regulation, CXCR-1 and CXCR-2 were targets of choice as receptors for IL-8 and CXCL-1 to -3. The effect of IL-6 on osteoclasts is controversial[27] but since it is one of the most abundant cytokines and it shares the gp130 receptor with other detected cytokines such as LIF or IL-11, the effect of an anti-gp130 antibody was evaluated. An analysis by RT-qPCR confirmed that osteoclasts expressed the 3 receptors CXCR-1, CXCR-2 and gp130 (Supplementary Fig 2). As previously observed in Figure 3, STS-CM obtained with MSC donor APS 7554 significantly increased the TRAP area compared to the basal culture (Figure 6). Addition of an anti-CXCR-1 or anti-CXCR-2 but not anti-gp130 antibody erased the difference induced by STS-CM. Antibodies targeting CXCR-1 and -2 also impacted basal osteoclasts differentiation. Blocking CXCR-2 had an even more significant effect, possibly due to its ligands not utilizing CXCR-1, such as CXCL-1, -2 and -3. Consequently, GROα/CXCL-1 and IL-8/CXCL-8 seemed implicated in the activation of osteoclastogenesis as ligands of these two receptors upregulated in STS-CM.

Discussion:

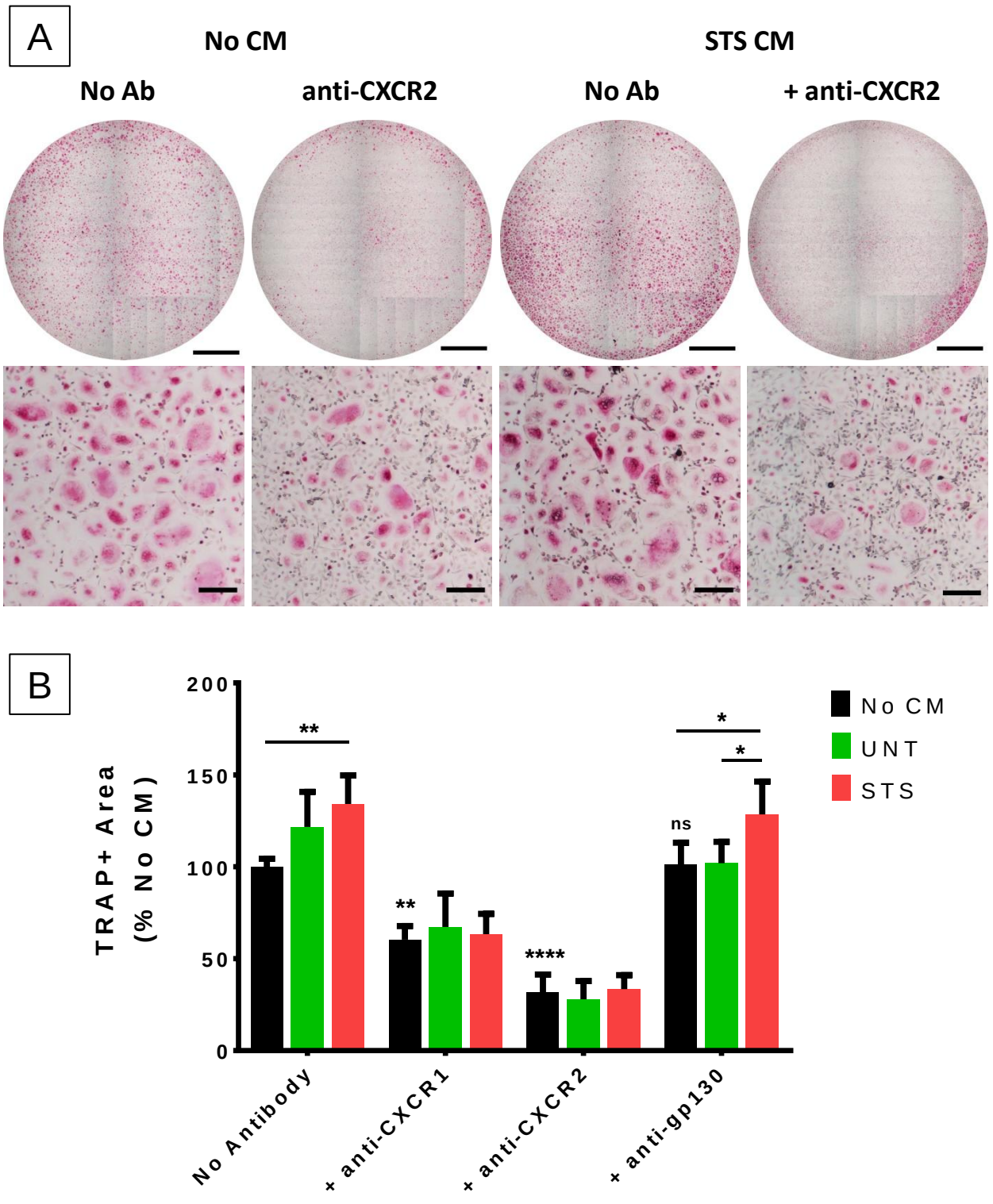

Figure 6: MSC-mediated induction of osteoclastogenesis is alleviated by an anti-CXCR1 or anti-CXCR2 antibody (Ab) but not anti-gp130. (A) Full well (scale bar = 2 mm) and close-up (scale bar = 200 µm) images of TRAP-stained osteoclasts at 8 days of differentiation with or without STS-CM and with or without anti-CXCR-2 antibody. (B) Quantification by image analysis of TRAP+ area after 8 days of osteoclast differentiation with UNT or STS-CM from MSC of donor APS 7554, with or without neutralizing antibodies towards CXCR-1, CXCR-2 or gp130, normalized to the TRAP+ area without CM and antibody. Representative experiment out of two. Statistical analysis by repeated measure ANOVA followed by Tukey's multiple comparison test, comparison between the conditions with the same antibody or with the control "No CM, No antibody", * for p-value < 0.05, ** for p-value < 0.01, **** for p-value < 0.0001.

This study demonstrated that MSCs seeded on a BCP material had a strong pro-osteoclastic effect. Similarly to an in vivo implantation, few cells survived on the biomaterial compared to the number seeded. Perhaps due to their high seeding concentration or to the interaction with the material, most cells went through apoptosis, as detected by caspases activity. This apoptosis could be replicated in a 2D model by STS treatment. The conditioned media from STS-treated culture retained this pro-osteoclastic characteristic, although significantly diminished in comparison to CM of MSCs seeded on the biomaterial. Conversely, they inhibited the formation of IL-4 stimulated MNGCs. A deep proteomic analysis could be performed, completed by a specific cytokine detection assay, to determine the major players of these communications between MSCs and myeloid cells. It was found that GROα/CXCL-1, GROβ/CXCL-2 and IL-8/CXCL-8 were significantly enriched in STS-CM, as well as *CXCL3* (GROγ) mRNA expression in STS-treated MSCs. Blocking them with specific antibodies against their receptors CXCR-1 or -2 confirmed their pivotal role in osteoclastogenesis. The RANK-L/OPG ratio was potentially increased after STS treatment. However, RANK-L is unlikely to be the major mediator of osteoclast stimulation in our assay as exogenous RANK-L concentrations were saturating. Also, it is primarily a transmembrane, cell surface associated cytokine and could be essential *in vivo* when MSCs are in direct contact with macrophages participating in the inflammatory reaction towards the biomaterial. Overall, we provide here evidences for a key role of several CXCL chemokines in the crosstalk between apoptotic MSCs and osteoclasts.

The major mediators of MSCs' stimulatory effect towards osteoclastogenesis seemed to be IL-8/CXCL-8 and other CXCR-2 ligands (CXCL-1, -2 and -3). This is supported by previous *in vitro* studies reporting positive effects of these CXCL chemokines on monocytes migration and osteoclasts differentiation [28–30]. Given the complexity of MSCs' secretome, these proteins may not be the only ones involved, and additional studies are warranted to identify additional players. Incidentally, there are most likely positive and negative regulators of osteoclastogenesis co-secreted by MSCs and neutralizing antibodies could therefore unbalance this equilibrium. This would explain why blockage of one of the two receptors for IL-8 was sufficient to suppress the stimulatory effect of the CM. In addition, osteoclasts self-stimulation, mostly based on IL-8/CXCL-8, is essential during osteoclastogenesis[31] and seem to be activated by STS-CM. The observed increase in *CXCL8/IL8* expression in osteoclast culture with STS-CM could either be due to a higher differentiation rate or to a specific improvement of autocrine signaling by MSCs' secretome through a different pathway. Also, IL-8 has been reported as an enhancer of bone regeneration by MSC recruitment[32] and could have a key role in regeneration beyond osteoclast differentiation.

The phenotype of osteoclasts formed in presence of STS-CM needs to be further investigated. In Supplementary Figure 1, we present preliminary data revealing differential expression of several cytokines in STS-CM treated osteoclasts. These changes could be involved in the complex processes allowing the transition from early inflammation to bone formation. A lower expression of *TNF* and *IL1B* is in line with a less inflammatory phenotype but it is associated with a reduced *IL10* expression, a major anti-inflammatory cytokine. Also, increased *TNFRSF11B/OPG* expression should inhibit osteoclasts, but higher *CXCL8/IL8* production could participate in their self-induction. Levels of these cytokines need to be more precisely measured at the protein level, which was complicated here due to the presence of MSC-CM. In addition, chemoattractant for skeletal stem cells and coupling factors should be measured as potential key proteins to revive the bone remodeling cycle

Upregulated	Unchanged	Downregulated
CRLF1	ADIPOQ	SFRP4
IL-11	LIF	FGF7
bFGF	TGFB1	PDGF-D
GROα/CXCL-1	TGFB2	CSF-1/M-CSF
GROβ/CXCL-2	PDGF-C	OPG/TNFRSF11B
IL-8/CXCL-8	BMP-1	Eotaxin/CCL-11
PDGF-AA	NOTCH3	MCP-1/CCL-2
	GDF6	
	MIF	
	IGF2	
	INHBA	
	SDF-1/CXCL-12	
	IL-6	
	RANTES	
	VEGF	

Table 1: Major soluble mediators differentially present in STS-CM compare to UNT-CM. Proteins detected by LC-MS (black),Bioplex experiment (blue) or both (green).

It is important to keep in mind that this communication with osteoclasts is not the only role of MSCs. It is well established that they have a strong immunomodulatory potential. Their crosstalk with macrophages, for example, has been particularly studied for bone regeneration applications[33]. The effect of MSCs' secretome during apoptosis on immune cells involved in early inflammation (macrophages, neutrophils or mast cells) should also be investigated to improve our understanding of the process of bone induction by MSC-CaP as a whole. Here, we limited our observations to the effect of artificial apoptosis but other parameters may participate to cell death or modulate the activity of implanted MSCs. Hypoxia, for example, was previously reported to impact MSCs' secretion profile, notably inducing the expression of IL-8 among other mediators[34]. The biomaterial is crucial in the interaction with host cells through mechanotransduction but its composition[35] and surface properties[36] also influence MSCs phenotype. Since MSCs could have a perivascular origin[37,38], one may relate this osteoinduction mechanism to fracture healing where blood vessels are disrupted after trauma releasing many MSCs in the microenvironment. These cells may then undergo apoptosis due to the lack of oxygen and nutriments and lead to osteoclasts differentiation rather than MNGCs, although the balance is tight.

In conclusion, these results showed that secretions from apoptotic MSCs globally favored osteoclastogenesis and inhibited formation of MNGCs *in vitro*. The effect on osteoclasts seems linked to IL-8 and other CXCL chemokines, ligands of the receptors CXCR-1 and -2. The mediators responsible for the effect on MNGCs remain to be determined. Here, we link for the first time the two main observations of preclinical experiments using MSCs for bone regeneration, i.e. MSCs clearance by apoptosis from the implantation site and osteoclasts formation preceding bone formation. Apoptosis is a key event in natural tissue regeneration through apoptosis-induced proliferation[39,40]. In bone regeneration, osteoclasts' apoptotic bodies improved defect bridging in mice[41] as well as osteogenic differentiation *in vitro*[42]. In the treatment of graft-versus-host disease, MSCs immunosuppressive function has been tightly linked to their apoptosis[43]. These observations support the hypothesis putting osteoclasts in the center of bone formation induced by MSC-CaP constructs and further question the relationship between osteoclasts and MNGCs. These insights into the mechanism of MSC-based bone regeneration may constitute an additional step towards cell free approaches[44].

Materials and Methods:

All cell culture manipulations were performed under sterile conditions. Cells were incubated in a humid atmosphere at 37°C, 5 % CO_2.

MSCs culture:

Bone marrow MSCs from five healthy donors were obtained from the Institut für Klinische Transfusionsmedizin und Immungenetik of Ulm, Germany, after receiving ethical approval and informed consent. Donors are encoded as follow, their age and sex specified in brackets: APS 7554 (22, male), APS 7553 (22, male), APS 7537 (28, female), ALA 7543 (23, male), APA 7542 (24, female) and APA 7535 (26, female). Cells were grown in αMEM (Gibco, 22571020) containing 1 % Penicillin/Streptomycin mixture (P/S, Eurobio, CABPES010U) and 5 % pooled human platelet lysate with heparin (1 IU/ml of final media).

Target	Primer Forward	Primer Reverse
ACP5 (TRAP)	AAGACTCACTGGGTGGCTTTG	GGCAGTCATGGGAGTTCAGG
BMP2	AGGACCTGGGGAGCAGCAA	GCTCTTTCAATGGACGTGTCCC
CALCR	CCCTTTGCTTCTATTGAGCTG	AAGAATTGGGGTTGGGTGAT
CD68	GAACCCCAACAAAACCAAG	GATGAGAGGCAGCAAGATG
CTSK	GCCAGACAACAGATTTCCATC	CAGAGCAAAGCTCACCACAG
CXCR1	GCAGCTCCTACTGTTGGACA	ATCCCACATCTGTGGATCTGT
CXCR2	GGCACAGTGAAGACATCGGT	TTAAATCCTGACTGGGTCGCTG
DCSTAMP	TGCATGCAAAGCTGCTTAAA	AGGACTGGAAGCCAGAAATG
IL6ST (gp130)	GGACCAAAGATGCCTCAACT	CTTGGACAGTGAATGAAGATCG
CCL2 (MCP-1)	GCAATCAATGCCCCAGTCAC	TCTTGAAGATCACAGCTTCTTTGG
CSF1 (M-CSF)	GTTTGTAGACCAGGAACAGTTGAA	CGCATGGTGTCCTCCATTAT
*CXCL1 (*GROα)	AATTCACCCCAAGAACATC	CTGTTCAGCATCTTTTCGAT
CXCL2 (GROβ)	GAACATCCAAAGTGTGAAGG	GATTTGCCATTTTTCAGC
CXCL3 (GROγ)	TCAAGAACATCCAAAGTGTG	GCTCCCCTTGTTCAGTATC
CXCL8 (IL-8)	CATACTCCAAACCTTTCCAC	TCAAAAACTTCTCCACAACC
CXCL12 (SDF-1)	CCAAACTGTGCCCTTCAGAT	TGGCTGTTGTGCTTACTTGTTT
HPRT1	TGACCTTGATTTATTTTGCATACC	CGAGCAAGACGTTCAGTCCT
IL1B	CCGGGACTCACAGCAAAA	GGACATGGAGAACACCACTTG
IL6	TCCACAAGCGCCTTCGGTCCAG	CTCAGGGCTGAGATGCCGTCG
IL10	GCCTTGTCTGAGATGATCC	ACTCATGGCTTTGTAGATGC
ITGAV	ATTCTGTGGCTGTCGGAGAT	CCTTGCTGCTCTTGGAACTC
LIF	ACGCCACCTGTGCCATACGC	GCTCCCCCTGGGCTGTGTAATAGAG
MARCO	TCCCTAGCTGTGGTGGTCAT	CGCCTGCAGATTCAGAACTT
MMP9	GAACCAATCTCACCGACAG	GCCCCAGAGATTTCGACTC
NFATC1	GGTCTTCGGGAGAGGAGAAA	TGACGTTGGAGGATGCATAG
OSM	AGTACCGCGTGCTCCTTG	CCCTGCAGTGCTCTCTCAGT
TGFB1	GAGCCCAAGGGCTACCAT	GGGTTATGCTGGTTGTACAGG
TNF	CAGCCTCTTCTCCTTCCTGAT	GCCAGAGGGCTGATTAGAGA
TNFSF11 (RANK-L)	TCGTTGGATCACAGCACATCA	TATGGGAACCAGATGGGATGTC
TNFRSF11A (RANK)	CAGATGCCCACAGAAGATGAATAC	CCAGGCTCAGTGAGGAACAG
TNFRSF11B (OPG)	CAGCTCACAAGAACAGACTTTCC	TCGAAGGTGAGGTTAGCATGTC
VEGFA	CCTTGCTGCTCTACCTCCAC	CCACTTCGTGATGATTCTGC

Table 2: List of primers used in RT-qPCR experiments.

For 3D experiments, 400 000 cells were seeded in serum free media (αMEM, 1 %P/S), either on 50 mg of MBCP+ or in 15mL Falcon tubes and centrifuged (500g, 5min) to form spheroids. For experiments using staurosporine (STS, Santa Cruz, sc-3510), cells were seeded in T75 flasks and incubated until 80 to 90 % confluence was reached. The treatment consisted of 4 hours in 20 mL serum-free media containing 0.1 µM STS or without STS as a control (untreated, UNT). The flasks were then washed 3 times with PBS to remove excess STS and 20 mL of fresh serum-free media was added. The supernatants were collected after 48h, filtered at 0.22 µm, aliquoted and stored at -20°C until use.

Osteoclasts and MNGCs differentiation:

Circulating monocytes were isolated from concentrated peripheral blood of healthy individuals, provided by the Etablissement Français du Sang as leftovers of platelet donation. The blood was flushed out of the sorting system and diluted with PBS. This diluted solution was carefully deposited on an equivalent volume of Ficoll®-Paque Premium (GE Healthcare) and centrifuged (800g, 20min). PBMCs at the interface were recovered using a Pasteur pipette, wash 3 times with PBS and counted. CD14 positive cells were isolated using hCD14 MicroBeads (Miltenyi Biotec, 130-050-201) and LS Columns (Miltenyi Biotec, 130-042-401) according the manufacturer's instruction. CD14+ enriched cells were stored for up to six months in liquid nitrogen in vials of 10 million cells until use.

CD14+ monocytes were plated at 150, 000 cells/cm², either in 48-well plates for TRAP staining or in 24-well plates for RNA extraction. The media consisted of αMEM, 1 % P/S, 5 % fetal bovine serum supplemented with recombinant human Macrophage Colony-Stimulating Factor (rhMCSF, Miltenyi Biotec) at 25 ng/mL. This media was changed at day 2 and 5, and supplemented with 20 % conditioned media from MSC culture and either of 100 ng/mL recombinant human Receptor Activator of Nuclear factor Kappa-B Ligand (rhRANK-L, Miltenyi Biotec) for osteoclast differentiation or, recombinant human Granulocyte-Macrophage Stimulating Factor and Interleukin-4 (rhGM-CSF & rhIL-4, R&D Systems, both 50 ng/mL) for multinucleated giant cell formation. Neutralizing antibodies were also added at the media change, at 5 µg/mL (human CXCR-1, human CXCR-2 and human gp130 antibodies, R&D Systems). After 8 days, cells were either fixed in formalin for 20 minutes for TRAP staining or lysed for RNA extraction.

Viability and apoptosis assays:

The LIVE/DEAD® viability kit for mammalian cells (Invitrogen, L3224) was used to visualize the status of cells on the biomaterial and in spheroids. The samples were washed 3 times with PBS and incubated in culture conditions for 30 minutes in a PBS solution of the two reagents (calcein-AM for living cells and ethidium homodimer-1 for dead cells) diluted 2000 times. The staining solution was replaced by PBS and images were taken within 30min.

Metabolic activity was measured with a resazurin assay (Sigma-Aldrich, R7017). A 2 mM solution was prepared and diluted at 0.2 mM in culture media. The preparation was incubated 3 hours with the cells in culture conditions and the end-point fluorescence was measured on a microplate reader (Berthold). For Crystal Violet staining, cells were fixed for 5 minutes by addition of glutaraldehyde to the culture media (1 % final concentration). Fixed cells were washed twice in distilled water and stained for 5 minutes with a solution of Crysal

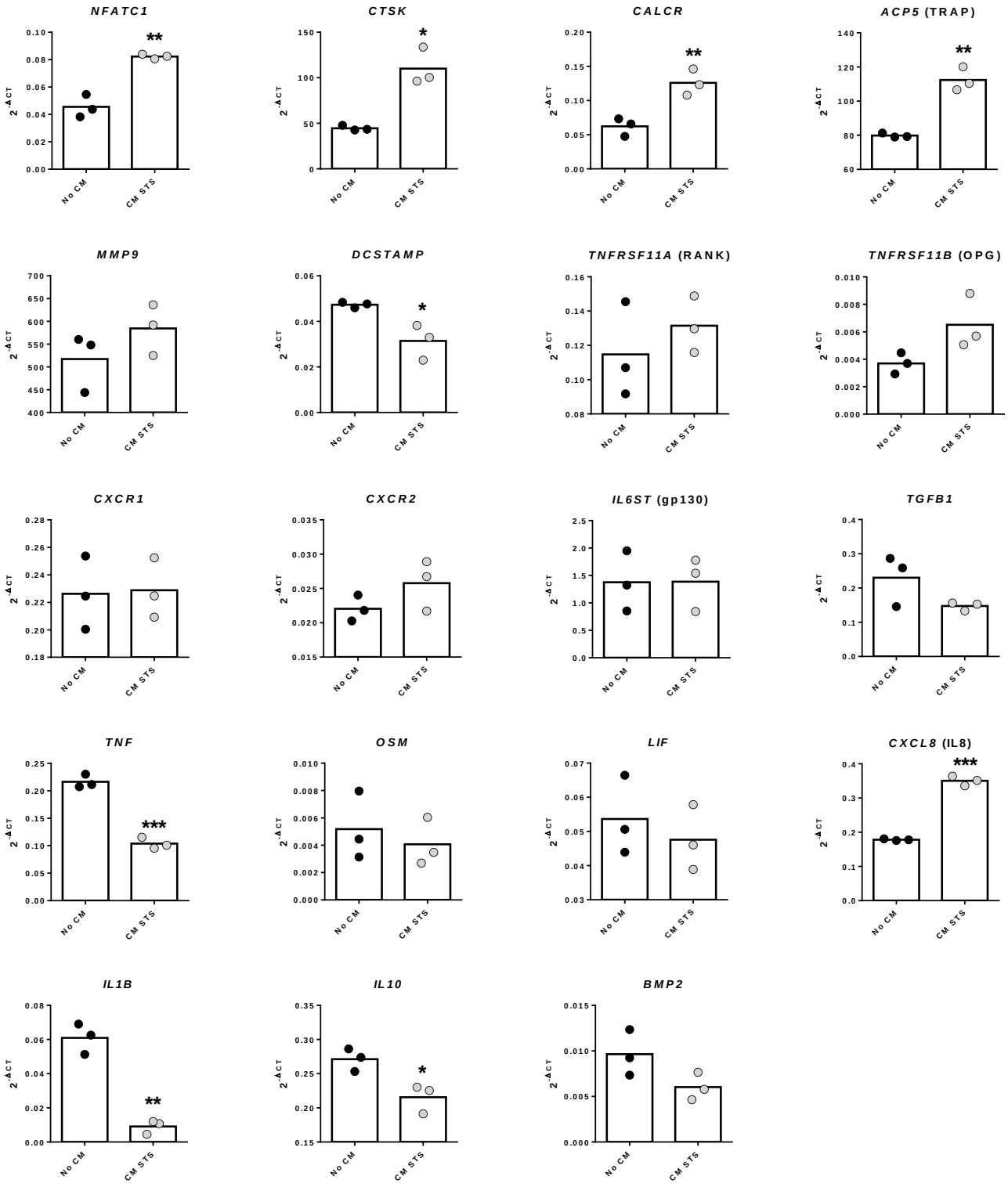

Supplementary Figure 1: Gene expression profile of osteoclasts cultured with or without STS-CM from donor APS 7554. Statistical analysis by one-sided unpaired t-test with Welch's correction, * = $p<0.05$.

Violet (Sigma-Aldrich, HT901) at 0.1 % in 20 % ethanol. After several washes in water, plates were let to dry before image acquisition.

Apoptosis was evaluated by measuring caspases activity with the kit Apo-ONE® Homogeneous Caspase-3/7 Assay (Promega, G7791). Proteins were extracted in RIPA buffer from attached cells and potential cells in the supernatant, retrieved by centrifugation. Samples were incubated at room temperature overnight with the kit's reagent diluted at 1/100 in the buffer before fluorescence measurement. Proteins were dosed with a bicinchoninic acid assay and bovine serum albumin was used as a standard.

TRAP Staining:

After fixation, cells were stored up to 2 weeks in PBS at 4°C or immediately stained. The wells were incubated for 30 minutes at 37°C in a buffer containing 40 mM Sodium Acetate, 10mM Sodium Tartrate at pH=5. The buffer was removed and a 1:1 mixture of acetone and 100 % ethanol was applied to the cell layer for 30 seconds. The samples were left to dry for 2 minutes before being incubated in a staining solution in buffer of 0.6 mg/mL Fast Red Violet LB salt (Sigma, 3381) and 100 µL/mL of a solution at 10 mg/mL Naphthol-AS-MX phosphate (Sigma, N4875) in N,N-dimethylformamide for 30 minutes. Wells were then washed with distilled water and dried for image acquisition.

RT-qPCR:

All steps followed the manufacturer's recommendations. RNA was extracted using the NucleoSpin RNA Plus kit (Macherey-Nagel, 740984.250). Reverse transcription was performed with the Maxima H Minus First Strand cDNA Synthesis Kit (Thermo Scientific, K1652). Real time PCR was carried out on a CFX96 (Bio-Rad) with SYBR® Select Master Mix (Applied Biosystems, 4472920) with *HPRT* as a reference gene and using the primers in Table 2.

BioPlex Assay:

For immunoassay detection of cytokine levels in the CM (UNT and STS) from five MSC donors, the Human XL Cytokine Discovery Base Kit (R&D Systems LUXLM000) was used on a Bio-Plex® 200 system (Bio-Rad), following the manufacturer's recommendations.

MS-based quantitative proteomics:

UNT-CMs and STS-CMs from three MSC donors were produced as previously described and concentrated 20-fold (from 20 to 1mL) in Amicon Ultra-15 3kD filters (Millipore). The final protein concentration was estimated by the bicinchoninic acid assay and samples were stored at -20°C, diluted in 1X Laemli buffer (from 4X stock solution). The proteins from each sample were stacked in a single band in the top of a SDS-PAGE gel (4-12 % NuPAGE, Life Technologies) and stained with Coomassie blue R-250 (Bio-Rad) before in-gel digestion using modified trypsin (Promega, sequencing grade) as previously described.[45] The resulting peptides were analyzed by online nanoliquid chromatography coupled to tandem MS (Ultimate 3000 RSLCnano and Q-Exactive HF, Thermo Scientific). Peptides were sampled on a 300 µm × 5 mm PepMap C18 precolumn (Thermo Scientific) and separated on a 75 µm × 250 mm C18 column (Reprosil-Pur 120 C18-AQ, 1.9 µm, Dr. Maisch) using a 240-

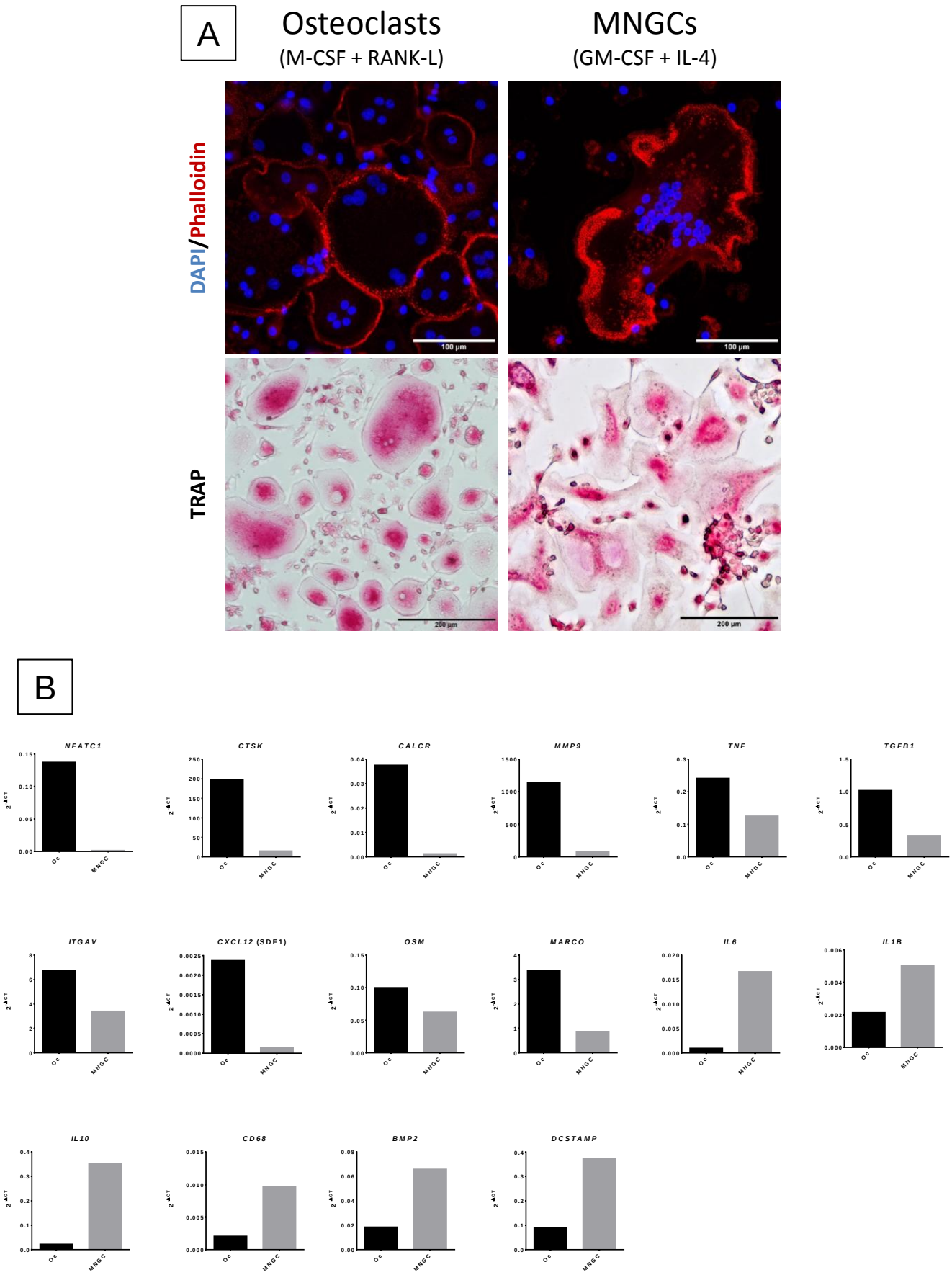

Supplementary Figure 2: *In vitro* model of MNGCs. (A) DAPI (nuclei, blue)/Phalloidin-AF546 (actin, red) fluorescent staining and TRAP staining for either osteoclasts obtained by M-CSF and RANK-L stimulation or MNGCs obtained with GM-CSF and IL-4 stimulation. (B) Gene expression in osteoclasts and MNGCs after 8 days of differentiation, n = 1.

min gradient. MS and MS/MS data were acquired using the Xcalibur software (Thermo Scientific).

Peptides and proteins were identified using Mascot (version 2.6.0, Matrix Science) through concomitant searches against Uniprot database (Homo sapiens taxonomy, September 2019 version), homemade classical contaminant database and the corresponding reversed databases. Trypsin/P was chosen as the enzyme and two missed cleavages were allowed. Precursor and fragment mass error tolerances were set at respectively at 10 and 25 mmu. Peptide modifications allowed during the search were: Carbamidomethyl (C, fixed), Acetyl (Protein N-term, variable) and Oxidation (M, variable). The Proline software[46] was used to filter the results: conservation of rank 1 peptides, peptide-spectrum-match score ≥ 25, peptide length ≥ 7 amino acids, false discovery rate of peptide-spectrum-match identifications < 1 % as calculated on peptide-spectrum-match scores by employing the reverse database strategy, and minimum of 1 specific peptide per identified protein group. Proline was then used to perform a compilation, grouping and MS1 quantification of the protein groups based on specific peptides.

Statistical analysis was performed using ProStaR.[47] Proteins identified in the reverse and contaminant databases, and proteins exhibiting less than three abundance values in one condition were discarded from the list. After log2 transformation, abundance values were normalized by median centering before missing value imputation (slsa algorithm for partially observed values in the condition and DetQuantile algorithm for totally absent values in the condition). Statistical testing was conducted using limma test. Differentially expressed proteins were sorted out using a log2 (fold change) cut-off of 1 and a p-value cut-off of 0.03, allowing to reach a FDR inferior to 5 % according to the Benjamini-Hochberg procedure.

Proteins found differentially abundant between UNT-CM and STS-CM were submitted to functional classification using PANTHER v.15.0[48]. Their enrichment in Reactome pathways was tested using Fisher's exact test. Enrichment was considered for a Bonferroni adjusted p-value < 0.05.

Statistical Analysis:

Data representation and statistical analysis were performed on GraphPad Prism software 6.0. Paired t-test was used to compare two groups of matching data. For comparison of three groups and more, repeated measure one- or two-way ANOVA was carried out, followed by Tukey's multiple comparison test. Differences were considered significant for p-value < 0.05 (*), very significant for p-value < 0.01 (**) and extremely significant for p-value < 0.001 (***) and p-value < 0.0001 (****).

Acknowledgements:

This work is financially supported by the European Commission through the H2020 project ORTHOUNION (Grant Agreement: 733288). PH received a PhD fellowship from the Regional Council Pays de la Loire and the ORTHOUNION project. Proteomic experiments were partly supported by the French National Agency for Research, grant number ANR-10-INBS-08-01 (Proteomics French Infrastructure). MÁB has received funding from the European Union's Horizon 2020 research and innovation programme under the Marie Skłodowska-Curie Individual Fellowship, grant agreement No 708711.

accession	log_2(fold change STS/UNT)	p-value
VPS29_HUMAN	4,18	2,99E-05
TES_HUMAN	4,10	2,55E-04
SMOC1_HUMAN	3,96	6,73E-05
TSK_HUMAN	3,86	3,06E-06
STX7_HUMAN	3,70	9,27E-06
PAMR1_HUMAN	3,64	1,03E-03
ADA15_HUMAN	3,17	1,19E-02
BOLA2_HUMAN	3,13	9,11E-06
DDX1_HUMAN	3,10	7,06E-06
TBCB_HUMAN	3,07	2,80E-05
GELS_HUMAN	2,98	2,36E-04
DENR_HUMAN	2,89	1,42E-02
PRKDC_HUMAN	2,76	7,94E-04
NECP2_HUMAN	2,58	2,26E-04
HNRDL_HUMAN	2,39	3,76E-05
2AAA_HUMAN	2,31	1,11E-02
IBP6_HUMAN	2,25	7,89E-04
MTAP_HUMAN	2,21	4,42E-03
ADDA_HUMAN	2,20	8,35E-03
IBP5_HUMAN	2,17	2,94E-03
EFHD2_HUMAN	2,15	2,43E-02
HNRPL_HUMAN	2,08	1,82E-03
KCC2D_HUMAN	2,07	2,92E-02
AL9A1_HUMAN	2,05	1,64E-04
PENK_HUMAN	2,05	1,02E-03
DHPR_HUMAN	2,01	1,27E-04
PSMD5_HUMAN	2,01	1,33E-02
SYQ_HUMAN	1,94	7,28E-04
GOPC_HUMAN	1,94	4,70E-04
OSTF1_HUMAN	1,83	2,00E-04
TSG6_HUMAN	1,77	2,62E-02
FUBP2_HUMAN	1,74	2,73E-02
SAP3_HUMAN	1,73	1,25E-02
SBDS_HUMAN	1,69	1,77E-02
GDS1_HUMAN	1,68	2,13E-03
IF4G1_HUMAN	1,67	2,41E-02
UBP5_HUMAN	1,65	1,89E-02
UBFD1_HUMAN	1,61	2,78E-03
AP3B1_HUMAN	1,60	6,88E-03
MINP1_HUMAN	1,58	6,28E-03
RS21_HUMAN	1,56	6,02E-04
YKT6_HUMAN	1,54	7,17E-03
METRL_HUMAN	1,52	2,07E-03
PP1A_HUMAN	1,51	1,16E-03
PA2G4_HUMAN	1,48	1,76E-02
ARHL2_HUMAN	1,48	5,20E-03
UGDH_HUMAN	1,48	7,96E-03
TIMP3_HUMAN	1,47	2,58E-03
GRP75_HUMAN	1,45	4,57E-03
SORCN_HUMAN	1,43	1,04E-02
ENPP1_HUMAN	1,43	1,60E-02
ARK72_HUMAN	1,38	2,02E-02
IL11_HUMAN	1,32	1,27E-02
CAB45_HUMAN	1,29	1,48E-02
DESP_HUMAN	1,24	2,91E-02

accession	log2(fold change STS/UNT)	p-value
ROCK1_HUMAN	1,24	1,42E-02
NONO_HUMAN	1,24	1,52E-02
FKBP3_HUMAN	1,23	2,55E-02
TETN_HUMAN	1,22	3,07E-03
VATB2_HUMAN	1,19	2,34E-02
BPNT1_HUMAN	1,19	1,64E-02
CATL1_HUMAN	1,15	1,25E-02
DBNL_HUMAN	1,14	1,46E-02
B2R582_HUMAN	1,13	1,46E-02
B4GT1_HUMAN	1,12	2,31E-03
IF2A_HUMAN	1,11	1,43E-02
CRIP2_HUMAN	1,10	6,67E-03
MTPN_HUMAN	1,10	7,62E-03
SODC_HUMAN	1,09	9,53E-03
ESYT1_HUMAN	1,09	2,82E-02
COPD_HUMAN	1,05	7,85E-03
NNMT_HUMAN	1,04	1,58E-02
CAPG_HUMAN	1,03	1,03E-02
VATA_HUMAN	1,02	1,25E-02
CNN1_HUMAN	1,01	7,22E-03
CRLF1_HUMAN	1,01	2,76E-02
UROK_HUMAN	-11,43	7,37E-09
OLM2B_HUMAN	-7,64	3,98E-07
PTX3_HUMAN	-5,52	1,90E-06
A0A0S2Z3V1_HUMAN	-4,95	9,59E-05
SDC4_HUMAN	-4,25	3,29E-05
LAMA2_HUMAN	-4,20	8,06E-03
PRS23_HUMAN	-3,87	1,20E-02
OMD_HUMAN	-3,64	1,18E-04
B2RCP7_HUMAN	-3,53	6,78E-05
CBPA4_HUMAN	-3,36	2,71E-02
SEM5A_HUMAN	-3,27	8,47E-05
B4DMA7_HUMAN	-3,23	2,89E-04
PAI1_HUMAN	-3,19	1,27E-05
ATS12_HUMAN	-3,16	2,11E-02
CO8A2_HUMAN	-2,96	2,63E-05
MMP1_HUMAN	-2,88	2,88E-04
MMP13_HUMAN	-2,74	1,22E-03
VCAM1_HUMAN	-2,68	2,69E-04
PODN_HUMAN	-2,64	4,34E-03
ITIH5_HUMAN	-2,59	2,39E-02
A1KY36_HUMAN	-2,59	1,69E-04
CO8A1_HUMAN	-2,46	2,47E-04
UNC5C_HUMAN	-2,44	2,38E-04
APOB_HUMAN	-2,40	1,00E-03
ASM_HUMAN	-2,38	7,57E-03
SFRP4_HUMAN	-2,38	6,79E-03
CO5A3_HUMAN	-2,37	1,27E-02
GAS6_HUMAN	-2,35	4,84E-04
CSTN2_HUMAN	-2,14	1,55E-03
EXT2_HUMAN	-2,13	5,03E-03
FGF7_HUMAN	-2,11	2,19E-03
LYOX_HUMAN	-2,05	5,85E-04
B4DRV4_HUMAN	-2,04	3,24E-03
TSP1_HUMAN	-2,04	3,96E-04
RARR2_HUMAN	-2,04	2,45E-02
RGMB_HUMAN	-2,04	4,01E-03
A1AG1_HUMAN	-2,01	2,29E-03
CERU_HUMAN	-1,85	2,86E-02
A0A024R6I7_HUMAN	-1,83	2,62E-02
LUM_HUMAN	-1,82	1,12E-03
TTHY_HUMAN	-1,79	5,78E-04
EXT1_HUMAN	-1,77	1,27E-03

accession	log2(fold change STS/UNT)	p-value
ISLR_HUMAN	-1,72	2,64E-03
PDGFD_HUMAN	-1,70	9,58E-03
ANGT_HUMAN	-1,69	6,15E-03
CSF1_HUMAN	-1,67	6,72E-03
PRELP_HUMAN	-1,67	6,30E-03
A0A024R884_HUMAN	-1,67	2,20E-02
ECM2_HUMAN	-1,67	2,80E-02
CO3A1_HUMAN	-1,63	1,95E-02
HEMO_HUMAN	-1,57	5,48E-03
BST1_HUMAN	-1,56	1,78E-03
SEM7A_HUMAN	-1,55	5,71E-04
OLFL3_HUMAN	-1,53	1,30E-03
IGK_HUMAN	-1,53	2,55E-03
CO5A2_HUMAN	-1,53	1,26E-02
IGHM_HUMAN	-1,52	4,61E-03
FST_HUMAN	-1,48	2,89E-02
HPT_HUMAN	-1,45	1,05E-02
ANT3_HUMAN	-1,45	1,23E-02
B4E1B2_HUMAN	-1,44	1,07E-02
SRGN_HUMAN	-1,44	2,82E-02
ITGBL_HUMAN	-1,41	4,51E-03
TR11B_HUMAN	-1,39	1,20E-02
GFRA1_HUMAN	-1,38	1,72E-02
A0A193CHR0_HUMAN	-1,38	2,93E-03
NRP1_HUMAN	-1,36	1,85E-03
COEA1_HUMAN	-1,36	1,51E-03
NEO1_HUMAN	-1,35	7,91E-03
A4_HUMAN	-1,34	1,54E-02
HBB_HUMAN	-1,34	2,80E-02
A2MG_HUMAN	-1,33	1,51E-02
Q6PIL8_HUMAN	-1,32	2,86E-03
ANXA1_HUMAN	-1,31	7,08E-03
TNR6C_HUMAN	-1,30	6,80E-03
A0A2U8J8P0_HUMAN	-1,29	2,39E-02
ULBP2_HUMAN	-1,29	2,45E-02
PRIO_HUMAN	-1,28	2,62E-02
A0A384MDQ7_HUMAN	-1,28	1,49E-02
Q53H26_HUMAN	-1,28	1,32E-02
ITB1_HUMAN	-1,28	2,22E-02
Q9UL78_HUMAN	-1,25	3,58E-03
TSP2_HUMAN	-1,25	3,38E-03
CO1A1_HUMAN	-1,23	2,20E-02
A2NB45_HUMAN	-1,23	2,34E-02
HPLN1_HUMAN	-1,22	2,54E-02
H0YMA5_HUMAN	-1,22	3,30E-03
IBP3_HUMAN	-1,21	3,37E-03
AFAM_HUMAN	-1,21	2,70E-02
TICN1_HUMAN	-1,20	4,67E-03
V9HW68_HUMAN	-1,20	9,94E-03
APOA1_HUMAN	-1,19	1,05E-02
HV374_HUMAN	-1,18	1,39E-02
A0A087WW33_HUMAN	-1,18	1,77E-03
A0A068LKQ2_HUMAN	-1,16	2,79E-02
D3DSX2_HUMAN	-1,14	1,63E-02
KV224_HUMAN	-1,13	1,12E-02
CSKP_HUMAN	-1,13	2,50E-03
GALT1_HUMAN	-1,13	2,97E-02
PGS2_HUMAN	-1,10	1,03E-02
COGA1_HUMAN	-1,10	1,30E-02
EDIL3_HUMAN	-1,10	9,03E-03
A0A0X9TD47_HUMAN	-1,06	2,01E-02
SDCB1_HUMAN	-1,03	1,46E-02
CO5A1_HUMAN	-1,01	1,00E-02

Supplementary Table 1: MS-based quantitative proteomic analysis of secretomes from untreated or STS-treated MSCs. Proteins from secretomes of untreated (UNT) and STS-treated MSCs (three biological replicates for each condition) were digested by trypsin and the resulting peptides analyzed by nanoLC-MS/MS. Peptides and proteins were then identified and their abundances extracted using dedicated computational tools (Mascot and Proline), before statistical analysis using ProStaR. In red, proteins found more abundant in STS-CM compared to UNT-CM (log2(fold change) ≥ 1 and p-value ≤ 0.03). In green, proteins found more abundant in UNT-CM compared to STS-CM (log2(fold change) ≤ -1 and p-value ≤ 0.03)

Conflict of Interests:

The authors declare no conflict of interest.

Contributions:

P.H. performed experiments, analyzed the data and drafted the manuscript; J.D.L., R.B., C.C. and B.B. provided technical support; R.B. performed the multiplex experiment; A.A. and Y.C. performed and analyzed the MS experiment; P.H., Y.C., V.T., M.Á.B., F.B. and P.L. revised the manuscript; F.B. and P.L. designed the study.

References:

1. Brennan, M. Á. *et al.* Pre-clinical studies of bone regeneration with human bone marrow stromal cells and biphasic calcium phosphate. *Stem Cell Res. Ther.* **5**, 114 (2014).

2. Gómez-Barrena, E. *et al.* Feasibility and safety of treating non-unions in tibia, femur and humerus with autologous, expanded, bone marrow-derived mesenchymal stromal cells associated with biphasic calcium phosphate biomaterials in a multicentric, non-comparative trial. *Biomaterials* **196**, 100–108 (2019).

3. Gómez-Barrena, E. *et al.* Early efficacy evaluation of mesenchymal stromal cells (MSC) combined to biomaterials to treat long bone non-unions. *Injury* **51**, S63–S73 (2020).

4. Gjerde, C. *et al.* Cell therapy induced regeneration of severely atrophied mandibular bone in a clinical trial. *Stem Cell Res. Ther.* **9**, 213 (2018).

5. Gómez-Barrena, E. *et al.* A Multicentric, Open-Label, Randomized, Comparative Clinical Trial of Two Different Doses of Expanded hBM-MSCs Plus Biomaterial versus Iliac Crest Autograft, for Bone Healing in Nonunions after Long Bone Fractures: Study Protocol. *Stem Cells Int.* **2018**, 1–13 (2018).

6. Viganò, M., Giordano, R. & Lazzari, L. Challenges of running a GMP facility for regenerative medicine in a public hospital. *Regen. Med.* **12**, 803–813 (2017).

7. Samavedi, S., Whittington, A. R. & Goldstein, A. S. Calcium phosphate ceramics in bone tissue engineering: A review of properties and their influence on cell behavior. *Acta Biomater.* **9**, 8037–8045 (2013).

8. Brennan, M. A. *et al.* Inferior In Vivo Osteogenesis and Superior Angiogeneis of Human Adipose-Derived Stem Cells Compared with Bone Marrow-Derived Stem Cells Cultured in Xeno-Free Conditions. *Stem Cells Transl. Med.* **6**, 2160–2172 (2017).

9. Chen, W. *et al.* Umbilical cord and bone marrow mesenchymal stem cell seeding on macroporous calcium phosphate for bone regeneration in rat cranial defects. *Biomaterials* **34**, 9917–9925 (2013).

10. Gamblin, A.-L. *et al.* Bone tissue formation with human mesenchymal stem cells and biphasic calcium phosphate ceramics: The local implication of osteoclasts and

A

Analysis Type:	PANTHER Overrepresentation Test (Released 20200728)
Annotation Version and Release Date:	Reactome version 65 Released 2019-12-22
Analyzed List:	Client Text Box Input (Homo sapiens)
Reference List:	Homo sapiens (all genes in database)
Test Type:	FISHER
Correction:	BONFERRONI
Bonferroni count:	2068

Reactome pathways	Homo sapiens - REFLIST (20851)	Client Text Box Input (75)	Client Text Box Input (expected)	Client Text Box Input (over/under)	Client Text Box Input (fold Enrichment)	Client Text Box Input (P-value)
Caspase-mediated cleavage of cytoskeletal proteins (R-HSA-264870)	12	3	0,04	+	69,5	4,03E-02
Gene and protein expression by JAK-STAT signaling after Interleukin-12 stimulation (R-HSA-8950505)	37	5	0,13	+	37,57	8,19E-04
Apoptotic cleavage of cellular proteins (R-HSA-111465)	37	5	0,13	+	37,57	8,19E-04
Interleukin-12 signaling (R-HSA-9020591)	46	5	0,17	+	30,22	2,21E-03
Interleukin-12 family signaling (R-HSA-447115)	56	6	0,2	+	29,79	1,87E-04
Apoptotic execution phase (R-HSA-75153)	51	5	0,18	+	27,26	3,54E-03
Innate Immune System (R-HSA-168249)	1105	15	3,97	+	3,77	1,76E-02
Immune System (R-HSA-168256)	2159	24	7,77	+	3,09	6,53E-04

Supplementary Table 2: PANTHER v.15.0 functional classification. Reactome pathways enrichment using Fisher's exact test with Bonferroni's adjustment in MS-based quantitative proteomic analysis from (A) STS-CMs and (B) UNT-CMs.

B

Reactome pathways	Homo sapiens - REFLIST (20851)	Client Text Box Input (83)	Client Text Box Input (expected)	Client Text Box Input (over/under)	Client Text Box Input (fold Enrichment)	Client Text Box Input (P-value)
Defective B4GALT1 causes B4GALT1-CDG (CDG-2d) (R-HSA-3656244)	8	3	0,03	+	94,21	2,00E-02
Defective ST3GAL3 causes MCT12 and EIEE15 (R-HSA-3656243)	8	3	0,03	+	94,21	2,00E-02
Defective CHST6 causes MCDC1 (R-HSA-3656225)	8	3	0,03	+	94,21	2,00E-02
Syndecan interactions (R-HSA-3000170)	27	9	0,11	+	83,74	2,76E-11
MET activates PTK2 signaling (R-HSA-8874081)	30	7	0,12	+	58,62	2,30E-07
Scavenging by Class A Receptors (R-HSA-3000480)	19	4	0,08	+	52,89	3,97E-03
Collagen chain trimerization (R-HSA-8948216)	44	9	0,18	+	51,39	1,23E-09
Non-integrin membrane-ECM interactions (R-HSA-3000171)	59	11	0,23	+	46,84	7,09E-12
MET promotes cell motility (R-HSA-8875878)	40	7	0,16	+	43,96	1,36E-06
Collagen degradation (R-HSA-1442490)	64	11	0,25	+	43,18	1,58E-11
Diseases associated with glycosaminoglycan metabolism (R-HSA-3560782)	41	7	0,16	+	42,89	1,59E-06
Assembly of collagen fibrils and other multimeric structures (R-HSA-2022090)	60	10	0,24	+	41,87	3,71E-10
ECM proteoglycans (R-HSA-3000178)	76	12	0,3	+	39,67	2,20E-12
Integrin cell surface interactions (R-HSA-216083)	84	12	0,33	+	35,89	6,52E-12
NCAM1 interactions (R-HSA-419037)	42	6	0,17	+	35,89	7,18E-05
Collagen biosynthesis and modifying enzymes (R-HSA-1650814)	67	9	0,27	+	33,75	3,68E-08
Signaling by PDGF (R-HSA-186797)	54	7	0,21	+	32,57	9,03E-06
Collagen formation (R-HSA-1474290)	89	11	0,35	+	31,05	4,22E-10
Defective B3GALTL causes Peters-plus syndrome (PpS) (R-HSA-5083635)	38	4	0,15	+	26,44	4,74E-02
NCAM signaling for neurite out-growth (R-HSA-375165)	59	6	0,23	+	25,55	4,58E-04
Degradation of the extracellular matrix (R-HSA-1474228)	140	13	0,56	+	23,33	7,13E-11
Signaling by MET (R-HSA-6806834)	76	7	0,3	+	23,14	8,02E-05
Post-translational protein phosphorylation (R-HSA-8957275)	107	9	0,43	+	21,13	1,73E-06
Extracellular matrix organization (R-HSA-1474244)	299	25	1,19	+	21	2,17E-22
Regulation of Insulin-like Growth Factor (IGF) transport and uptake by Insulin-like Growth Factor Binding Proteins (IGFBPs) (R-HSA-381426)	124	10	0,49	+	20,26	2,78E-07
Platelet degranulation (R-HSA-114608)	127	10	0,51	+	19,78	3,47E-07
Response to elevated platelet cytosolic Ca2+ (R-HSA-76005)	132	10	0,53	+	19,03	4,94E-07
Diseases of glycosylation (R-HSA-3781865)	146	11	0,58	+	18,93	6,22E-08
Binding and Uptake of Ligands by Scavenger Receptors (R-HSA-2173782)	104	7	0,41	+	16,91	6,00E-04
Glycosaminoglycan metabolism (R-HSA-1630316)	123	7	0,49	+	14,3	1,76E-03
Platelet activation, signaling and aggregation (R-HSA-76002)	259	11	1,03	+	10,67	1,97E-05
Cell surface interactions at the vascular wall (R-HSA-202733)	199	7	0,79	+	8,84	3,68E-02
Hemostasis (R-HSA-109582)	670	19	2,67	+	7,12	3,89E-08
Signaling by Receptor Tyrosine Kinases (R-HSA-9006934)	457	12	1,82	+	6,6	6,59E-04
Axon guidance (R-HSA-422475)	548	14	2,18	+	6,42	8,58E-05
Disease (R-HSA-1643685)	1127	17	4,49	+	3,79	4,21E-03

509 macrophages. *Biomaterials* **35**, 9660–9667 (2014).

510 11. Humbert, P. *et al.* Immune Modulation by Transplanted Calcium Phosphate
511 Biomaterials and Human Mesenchymal Stromal Cells in Bone Regeneration. *Front.*
512 *Immunol.* **10**, 1–15 (2019).

513 12. Giannoni, P. *et al.* Short-Time Survival and Engraftment of Bone Marrow Stromal Cells
514 in an Ectopic Model of Bone Regeneration. *Tissue Eng. Part A* **16**, 489–499 (2010).

515 13. Miron, R. J., Zohdi, H., Fujioka-Kobayashi, M. & Bosshardt, D. D. Giant cells around
516 bone biomaterials: Osteoclasts or multi-nucleated giant cells? *Acta Biomater.* **46**, 15–
517 28 (2016).

518 14. Sims, N. A. & Martin, T. J. Osteoclasts Provide Coupling Signals to Osteoblast Lineage
519 Cells Through Multiple Mechanisms. *Annu. Rev. Physiol.* **82**, annurev-physiol-021119-
520 034425 (2020).

521 15. Volarevic, V. *et al.* Mesenchymal stem cell-derived factors: Immuno-modulatory
522 effects and therapeutic potential. *BioFactors* **43**, 633–644 (2017).

523 16. Becquart, P. *et al.* Ischemia Is the Prime but Not the Only Cause of Human
524 Multipotent Stromal Cell Death in Tissue-Engineered Constructs In Vivo. *Tissue Eng.*
525 *Part A* **18**, 2084–2094 (2012).

526 17. Deschepper, M. *et al.* Proangiogenic and Prosurvival Functions of Glucose in Human
527 Mesenchymal Stem Cells upon Transplantation. *Stem Cells* **31**, 526–535 (2013).

528 18. Ferreira, J. R. *et al.* Mesenchymal Stromal Cell Secretome: Influencing Therapeutic
529 Potential by Cellular Pre-conditioning. *Front. Immunol.* **9**, 2837 (2018).

530 19. Goodman, S. B. & Lin, T. Modifying MSC Phenotype to Facilitate Bone Healing:
531 Biological Approaches. *Front. Bioeng. Biotechnol.* **8**, 1–16 (2020).

532 20. Weiss, A. R. R. & Dahlke, M. H. Immunomodulation by Mesenchymal Stem Cells
533 (MSCs): Mechanisms of Action of Living, Apoptotic, and Dead MSCs. *Front. Immunol.*
534 **10**, 1–10 (2019).

535 21. Mbalaviele, G. *et al.* Human mesenchymal stem cells promote human osteoclast
536 differentiation from CD34+ bone marrow hematopoietic progenitors. *Endocrinology*
537 **140**, 3736–3743 (1999).

538 22. Ogata, K., Katagiri, W. & Hibi, H. Secretomes from mesenchymal stem cells participate
539 in the regulation of osteoclastogenesis in vitro. *Clin. Oral Investig.* **21**, 1979–1988
540 (2017).

541 23. Oshita, K. *et al.* Human mesenchymal stem cells inhibit osteoclastogenesis through
542 osteoprotegerin production. *Arthritis Rheum.* **63**, 1658–1667 (2011).

543 24. Abe, T. *et al.* The effect of mesenchymal stem cells on osteoclast precursor cell
544 differentiation. *J. Oral Sci.* **61**, 30–35 (2019).

25. Chae, H. J. *et al.* Molecular mechanism of staurosporine-induced apoptosis in osteoblasts. *Pharmacol. Res.* **42**, 373–381 (2000).

26. Khan, U. A., Hashimi, S. M., Bakr, M. M., Forwood, M. R. & Morrison, N. A. Foreign body giant cells and osteoclasts are TRAP positive, have podosome-belts and both require OC-STAMP for cell fusion. *J. Cell. Biochem.* **114**, 1772–1778 (2013).

27. Blanchard, F., Duplomb, L., Baud'huin, M. & Brounais, B. The dual role of IL-6-type cytokines on bone remodeling and bone tumors. *Cytokine Growth Factor Rev.* **20**, 19–28 (2009).

28. Bendre, M. S. *et al.* Interleukin-8 stimulation of osteoclastogenesis and bone resorption is a mechanism for the increased osteolysis of metastatic bone disease. *Bone* **33**, 28–37 (2003).

29. Hardaway, A. L., Herroon, M. K., Rajagurubandara, E. & Podgorski, I. Marrow adipocyte-derived CXCL1 and CXCL2 contribute to osteolysis in metastatic prostate cancer. *Clin. Exp. Metastasis* **32**, 353–368 (2015).

30. Wang, X. *et al.* Increased expression of CXCL2 in ACPA-positive rheumatoid arthritis and its role in osteoclastogenesis. *Clin. Exp. Immunol.* **53**, cei.13527 (2020).

31. Kopesky, P. *et al.* Autocrine signaling is a key regulatory element during osteoclastogenesis. *Biol. Open* **3**, 767–776 (2014).

32. Yang, A. *et al.* IL-8 Enhances Therapeutic Effects of BMSCs on Bone Regeneration via CXCR2-Mediated PI3k/Akt Signaling Pathway. *Cell. Physiol. Biochem.* **48**, 361–370 (2018).

33. Pajarinen, J. *et al.* Mesenchymal stem cell-macrophage crosstalk and bone healing. *Biomaterials* **196**, 80–89 (2019).

34. Paquet, J. *et al.* Oxygen Tension Regulates Human Mesenchymal Stem Cell Paracrine Functions. *Stem Cells Transl. Med.* **4**, 809–821 (2015).

35. Abdeen, A. A., Weiss, J. B., Lee, J. & Kilian, K. A. Matrix composition and mechanics direct proangiogenic signaling from mesenchymal stem cells. *Tissue Eng. - Part A* **20**, 2737–2745 (2014).

36. Leuning, D. G. *et al.* The cytokine secretion profile of mesenchymal stromal cells is determined by surface structure of the microenvironment. *Sci. Rep.* **8**, 1–9 (2018).

37. Crisan, M. *et al.* A Perivascular Origin for Mesenchymal Stem Cells in Multiple Human Organs. *Cell Stem Cell* **3**, 301–313 (2008).

38. Bouacida, A. *et al.* Pericyte-Like Progenitors Show High Immaturity and Engraftment Potential as Compared with Mesenchymal Stem Cells. *PLoS One* **7**, (2012).

39. Bergmann, A. & Steller, H. Apoptosis, stem cells, and tissue regeneration. *Sci. Signal.* **3**, (2010).

581 40. Medina, C. B. *et al.* Metabolites released from apoptotic cells act as tissue
582 messengers. *Nature* **580**, 130–135 (2020).

583 41. Ma, Q. *et al.* Osteoclast-derived apoptotic bodies show extended biological effects of
584 parental cell in promoting bone defect healing. *Theranostics* **10**, 6825–6838 (2020).

585 42. Ma, Q. *et al.* Mature osteoclast–derived apoptotic bodies promote osteogenic
586 differentiation via RANKL-mediated reverse signaling. *J. Biol. Chem.* jbc.RA119.007625
587 (2019). doi:10.1074/jbc.RA119.007625

588 43. Galleu, A. *et al.* Apoptosis in mesenchymal stromal cells induces in vivo recipient-
589 mediated immunomodulation. *Sci. Transl. Med.* **9**, eaam7828 (2017).

590 44. Marolt Presen, D., Traweger, A., Gimona, M. & Redl, H. Mesenchymal Stromal Cell-
591 Based Bone Regeneration Therapies: From Cell Transplantation and Tissue
592 Engineering to Therapeutic Secretomes and Extracellular Vesicles. *Front. Bioeng.*
593 *Biotechnol.* **7**, 352 (2019).

594 45. Casabona, M. G., Vandenbrouck, Y., Attree, I. & Couté, Y. Proteomic characterization
595 of Pseudomonas aeruginosa PAO1 inner membrane. *Proteomics* **13**, 2419–2423
596 (2013).

597 46. Bouyssié, D. *et al.* Proline: An efficient and user-friendly software suite for large-scale
598 proteomics. *Bioinformatics* **36**, 3148–3155 (2020).

599 47. Wieczorek, S. *et al.* DAPAR & ProStaR: Software to perform statistical analyses in
600 quantitative discovery proteomics. *Bioinformatics* **33**, 135–136 (2017).

601 48. Mi, H. *et al.* Protocol Update for large-scale genome and gene function analysis with
602 the PANTHER classification system (v.14.0). *Nat. Protoc.* **14**, 703–721 (2019).

603

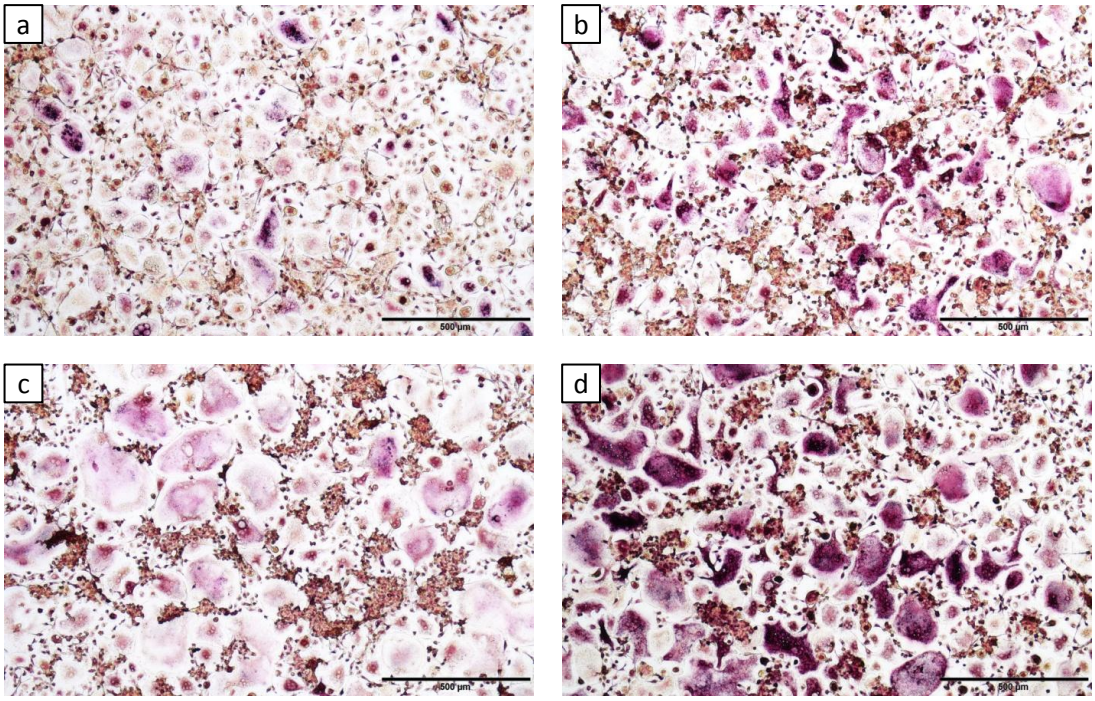

Figure I-1: Effect of heat shock and hypoxia on the osteoclastogenic effect of MSC-CM.

TRAP staining of osteoclasts at 8 days of differentiation by M-CSF and RANK-L stimulation; with 20% of (a) fresh serum-free media or CM from MSCs cultured 48h in serum-free media (b) untreated, (c) under 2% O_2 or (d) after a 1h at 50°C heat shock. Scale bar = 500 µm.

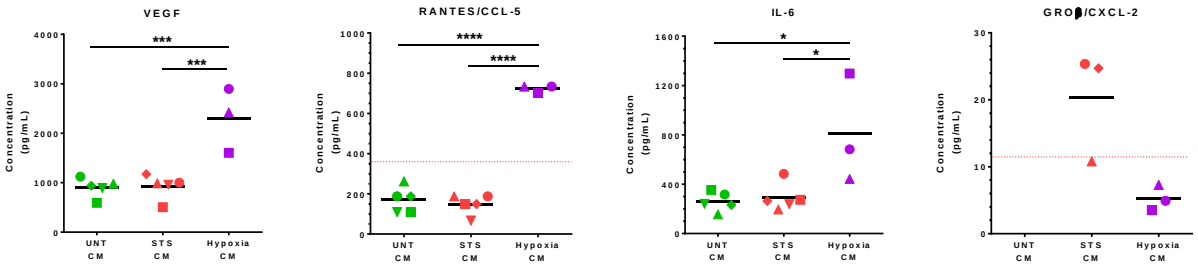

Figure I-2: Specific cytokines are secreted by MSCs under hypoxic conditions.

Quantification of cytokines concentration detected by multiplex immunoassay in CM collected after 48h in hypoxia (3 MSC donors) compared UNT and STS-CM from 5 MSC donors. Statistical analysis by ordinary one-way ANOVA with Tukey's multiple comparison test, * for p-value <0.05, *** = p-value <0.001, **** = p-value <0.0001

Additional Results

Hypoxia and other experiments with MSCs:

In addition to the presented results, various stresses and culture conditions were tested out to stimulate MSCs' pro-osteoclastogenic secretions. Heat and H_2O_2 treatments were experimented to induce cell death and collect apoptotic secretions. We did not experiment much with this these stimulations as they were not related to any biological event in bone regeneration. However, culture under hypoxic conditions was the most studied alternative to STS treatment as a main component of the implantation site (Becquart et al., 2012).

Figure I-1 presents an overview of osteoclasts differentiation with CM from various MSC cultures. The CM from untreated MSCs in serum-free media (Figure I-1, b) seemed to already enhance osteoclastogenesis compared to the control with only fresh media. CMs from culture under hypoxia (Figure I-1, c) or after a heat shock (Figure I-1, d) lead to even larger osteoclasts. While the effect seemed similarly favorable, the microscopic aspect of osteoclasts was different. They appeared rather flat and stained a light pink after differentiation with the hypoxic CM; stocky and darker with the CM after heat shock. A deeper phenotypic analysis would be required to really confirm this difference and understand its impact on the cell activity. The hypoxic CMs from 3 MSC donors were analyzed by multiplex immunoassay alongside UNT- and STS-CMs (Figure I-2). As previously reported in hypoxic conditions (Paquet et al., 2015) or with artificial overexpression of hypoxia-inducible factor 1 (Martinez et al., 2017), we observed an increase in the secretion of VEGF, RANTES/CCL5 and IL-6. As in STS-CM, GROβ/CXCL-2 could be detected in hypoxia CM but not in UNT-CM, suggesting a potential improved expression under low oxygen concentrations. Other factors presented in the article were unchanged compared to UNT-CM while the literature reported potential activation of IL-8/CXCL-8, SDF-1/CXCL-12 or MCP-1/CCL5 secretion.

Overall, the atmospheric oxygen pressure used in cell culture is largely superior to physiological values (Carreau et al., 2011), not to mention pathological ones. This has a significant influence on what are consider basal values *in vitro* and should be more widely taken into account. In bone development, hypoxia signaling is essential and tightly linked to vascularization, mainly through the expression of VEGF by bone cells (Stegen and Carmeliet, 2018). This may also be crucial in bone regeneration strategies. For example, the CM from hypoxic culture of MSCs enhanced angiogenesis and MSC migration in a collagen scaffold *in vitro* (Quade et al., 2020). Cultures under low oxygen percentages are among the increasingly studied techniques to improve MSCs' bone healing and immunomodulatory abilities (Goodman and Lin, 2020). Ina humanized mice model of graft-versus-host disease, umbilical cord blood MSCs primed with hypoxia and calcium ions had a higher potency through improved expression of numerous proteins of cell adhesion, proliferation and

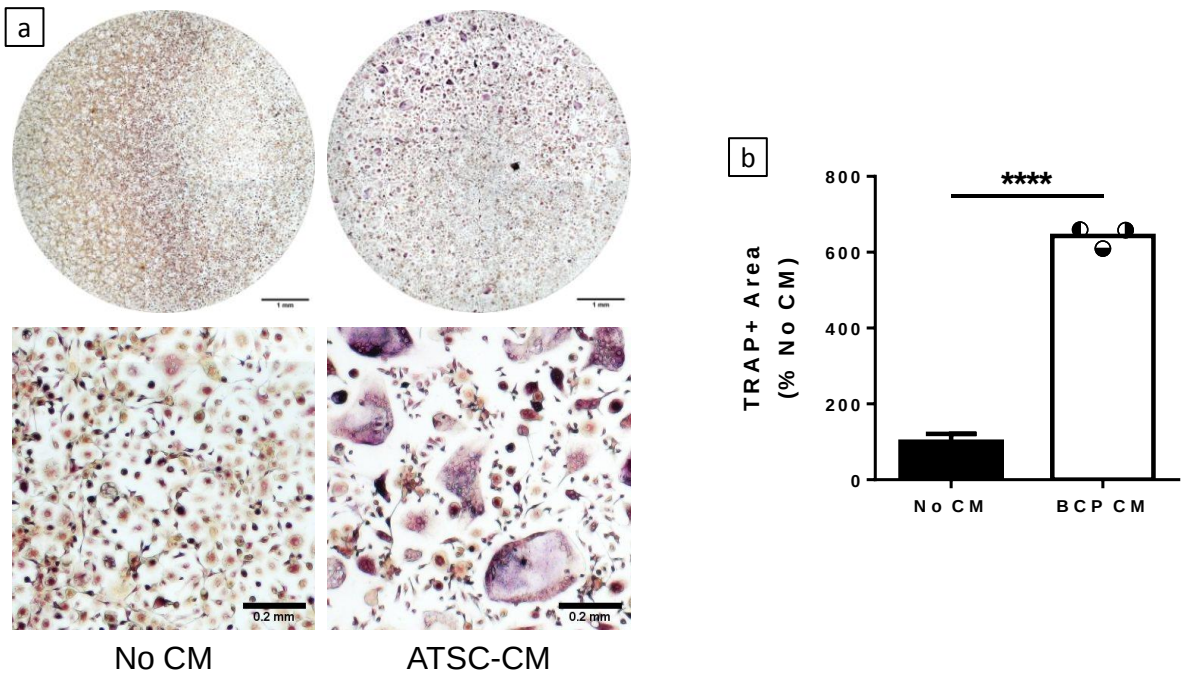

Figure I-3: Osteoclast differentiation with CM from ATSC seeded on MBCP+.

(a) Quantification by image analysis of TRAP+ surface between osteoclasts in control conditions (No CM) or with CM from ATSCs from three donors. Statistical analysis by unpaired t-test, **** for p-value < 0.0001. (b) Full well images (top, scale bar = 1 mm) and close-ups (bottom, scale bar = 0.2 mm) of the two conditions.

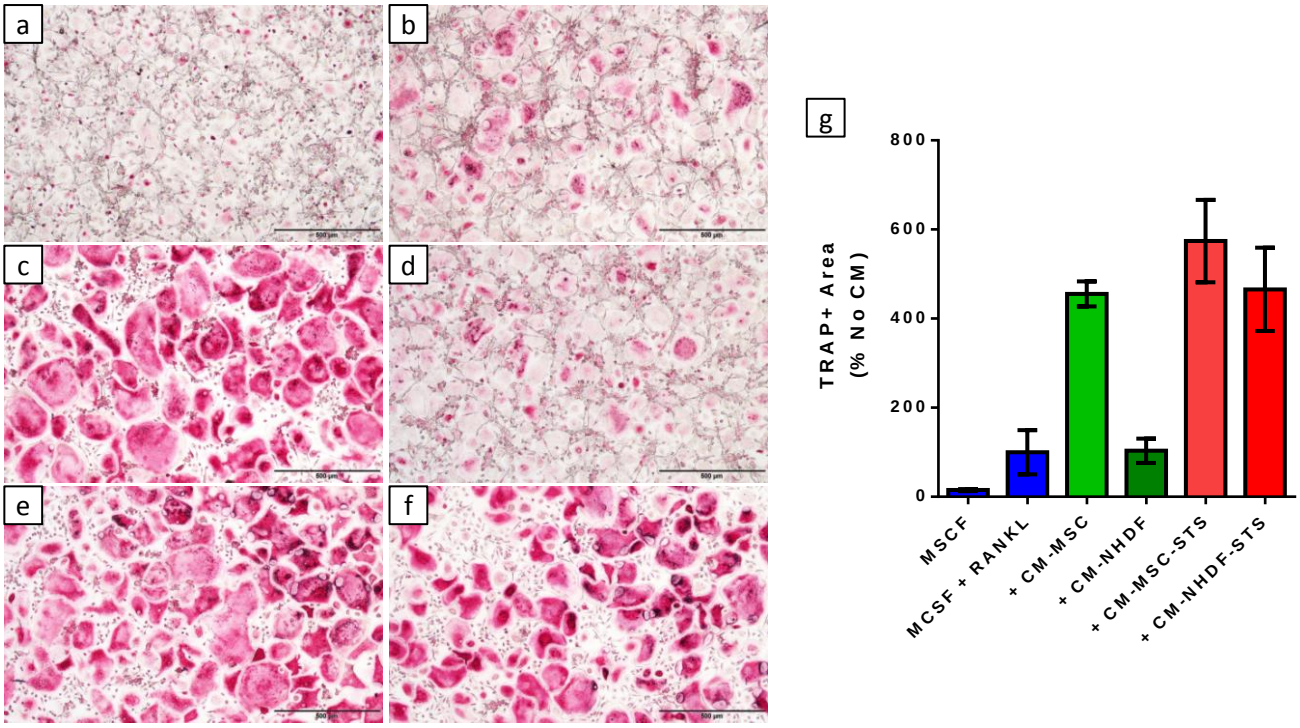

Figure I-4: CM from apoptotic fibroblasts has osteoclastogenic properties.

Osteoclasts differentiation assay with conditioned media (CM) from MSC and NHDF cultures, with or without 0.1µM STS treatment. Representative images of TRAP staining with (a) MCSF only, (b) MCSF + RANK-L, (c) + CM-MSC, (d) + CM-Fibro, (e) + CM-MSC-STS and (f) + CM-Fibro-STS. Scaled bar = 500 µm. (g) Image analysis of TRAP+ area, N=2.

immune modulation (Kim et al., 2018). Hypoxia priming also improved bone regeneration capacities of MSCs in a mandibular defect in aged rats (Zhang et al., 2018) and in a rabbit model of femoral head necrosis (Fan et al., 2015).

As mentioned in the introduction, ATSCs did not induce efficient bone formation *in vivo* in previous studies (Brennan et al., 2017; Xu et al., 2017). To assays if this was linked to their ability to interact with osteoclasts, we tested their secretions in the same condition as bone marrow MSC ones. ATSCs from three donors were seeded on the biomaterial in serum-free media and the supernatant was recovered after 48 hours. When added in the osteoclast differentiation test, these ATSC-CMs led to the formation of large and strongly stained osteoclasts (Figure I-3, a). The TRAP stained surface was very significantly higher with ATSC-CM than without (Figure I-3, b). Despite poor osteogenic properties, ATSCs convincingly improved osteoclastogenesis *in vitro*, very similarly to bone marrow-derived MSCs. This suggests that if osteoclast formation is important in the bone regenerative process, it is not the only critical parameter. ATSCs may have this property in common with bone marrow MSCs but lack other functions essential for osteoinduction. Interestingly, Ménard et al. (2020) recently reported that ATSCs and bone marrow-derived MSCs exhibited very different immune profiles, with a lower immunogenicity of ATSCs.

Fibroblasts in bone regeneration:

Additional experiments explored the use of normal human dermal fibroblasts (NHDF, PromoCell) as a control of MSCs' effect towards osteoclasts. Figure I-4 shows an osteoclast differentiation test with MSC- and NHDF-CM, with or without STS treatment. As previously described, MSCs have a basal pro-osteoclastogenic effect well visible here that an STS treatment may be enhancing. Using untreated NHDF-CM did not influence osteoclast differentiation while NHDF-CM after STS treatment greatly enhances osteoclastogenesis, to the same degree as MSC-CM. This effect was concomitant to drastic changes in the cytokine composition of the secretome (Figure I-5). Basal levels for most cytokines were lower in NHDF-CM than MSC-CM. That may be an indicator of MSCs' greater communication with immune cells. After STS treatment, levels of MCP-1/CCL2, MCP-3/CCL7 and IL-6 were unchanged or lowered in MSC-CM but increased in NHDF-CM. Concentrations of VEGF and IL-8 were augmented after STS treatment on both cell types but to a greater extent with NHDF. The IL-8 concentration of about 1.7 ng/mL in NHDF-STS-CM, more than 8-fold the concentration in MSC-STS-CM, may be the major activator of osteoclastogenesis. On the contrary, the level of OPG, already higher in NHDF-CM than MSC-CM, seems to stabilize or increase after STS treatment while it dropped for MSCs. Obviously, these data would need to be replicated to confirm these observations and perform statistical analysis.

These preliminary results tend to indicate that cell apoptosis, not necessarily MSC's, could activate osteoclastogenesis *in vitro* through intense IL-8 secretion. As this does not question the importance of osteoclasts in the bone healing mechanism, it challenges the particularities that make MSCs efficient in bone regeneration. As in numerous cell therapies

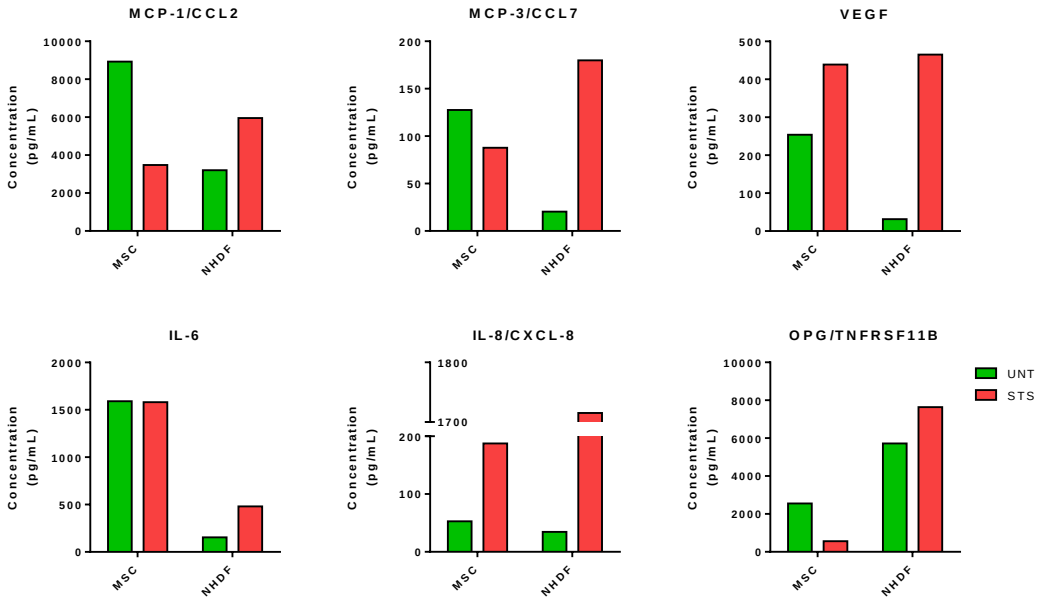

Figure I-5: Secretion from fibroblasts drastically changes after STS treatment.

Bio-Plex measurement of some cytokines in MSCs and fibroblasts conditioned media, with or without staurosporine treatment, N=1.

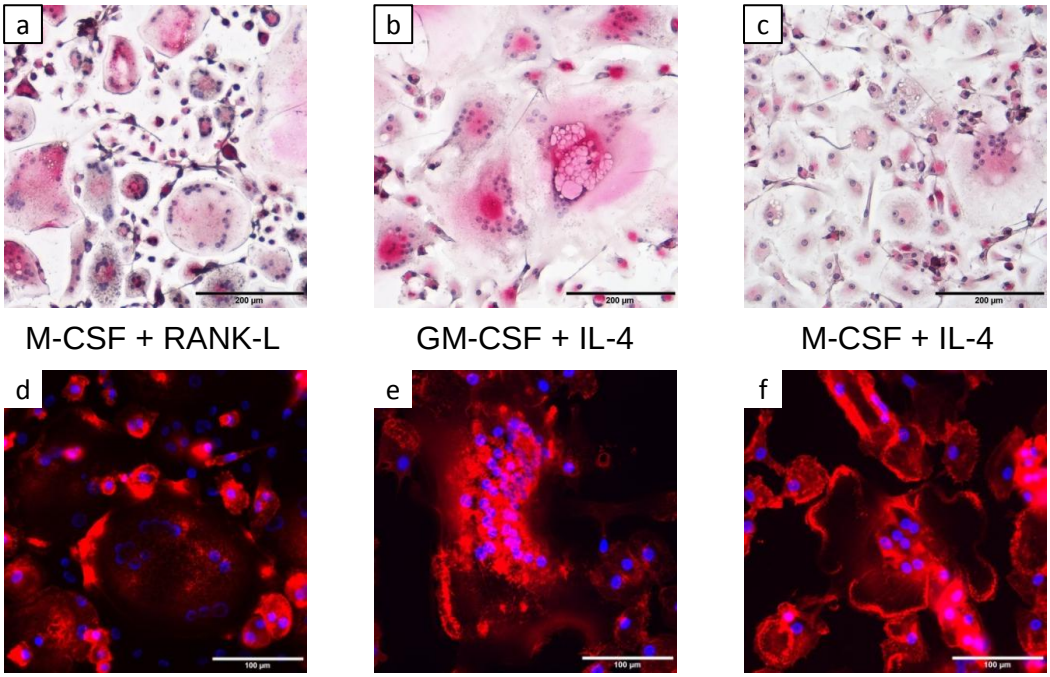

Figure I-6: Comparison of osteoclasts and MNGCs models *in vitro*.

TRAP (a-c, scale bar = 200 µm) and DAPI/Phalloidin (d-f, scale bar = 100 µm) staining after 8 days of differentiation of osteoclasts (a, d; M-CSF + RANK-L) and two types of IL-4 induced MNGCs co-stimulated with (b, e) GM-CSF or (c, f) M-CSF.

for other diseases, communication towards other players of the inflammation may be specific to MSCs. This immunomodulatory role could be slightly dissociated from this effect on osteoclastogenesis but most likely modulation of the inflammation, especially the alteration of macrophages polarization, is essential to effectively induce osteoclast formation *in vivo*. Ichim et al. (2018) reviewed fibroblasts properties compared to MSCs and encourage their study for clinical applications further than dermal regeneration. Both cell types share the same surface markers and the ability to differentiate into chondrocytes, adipocytes and osteoblasts. Based on the current international guidelines, Denu et al. (2016) could not distinguish MSCs, from bone marrow or adipose tissue, from foreskin, breast or lung fibroblasts. They also reported equivalent efficiency in suppressing T cell proliferation and modulating macrophages phenotype. Comparing NHDFs and MSCs, Blasi et al. (2011) also observed similarities in phenotypic characteristics but only MSCs exhibited high secretion of angiogenic factors (VEGF, HGF and Angiopoietin) and could inhibit the expression of RANTES and MCP-1/CCL2 in U937 cells.

MNGCs models in vitro:

MNGCs seem to act as polykarionic macrophages rather than differentiated cells of their own. They were described as “frustrated macrophages”, fusing with each other to phagocyte large particles that a single cell could not handle (Miron and Bosshardt, 2018). As proposed by Miron et al. (2016), two major phenotypes of MNGCs could exist following the macrophage polarization model; inflammatory MNGCs-1 and tissue-healing MNGCs-2. MNGCs-1, previously foreign body giant cells (FBGCs), could participate actively to the recruitment of other immune cells and prolonged the acute inflammation state into a chronic one as long as they cannot destroy the foreign body. Then, MNGCs-2 could be involved in the resolution of inflammation leading to fibrosis.

Interestingly, our models of MNGCs formed by IL-4 stimulation were somehow different after staining (Figure I-6) and had differential RNA expression when co-stimulated with M-CSF or GM-CSF (Figure I-7). GM-CSF stimulated MNGCs were overall larger, with more nuclei, than M-CSF stimulated ones. Osteoclasts had the fewest nuclei but a more regularly round shape than MNGCs. As expected, both MNGC types expressed low levels of the classical osteoclasts markers *NFATC1*, *CTSK*, *MMP9* or *CALCR*. As the staining suggested, *ACP5/TRAP* expression was rather similar in MNGCs and osteoclasts. Interestingly, *CSF1R*, the receptor for M-CSF, was more expressed in GM-CSF treated MNGCs than M-CSF treated ones. Integrin Subunit Alpha V (*ITGAV*) was less expressed in MNGCs than in osteoclasts. This could be explained by the affinity of the latter for physiological matrix while the former adhere to foreign surfaces. MNGCs had generally more nuclei, therefore fused from more cells, so it was not surprising to find higher *DCSTAMP* expression. In terms of cytokines, osteoclasts expressed more *TNF*, *TGFB1*, *OSM* and *CXCL-12/SDF-1* but less *IL6* and *IL10* at the mRNA level. BMP-2 seem also to be more expressed in MNGCs. Between MNGC subtypes, GM-CSF stimulated one’s had higher *OSM* and *IL6* while GM-CSF stimulated one’s

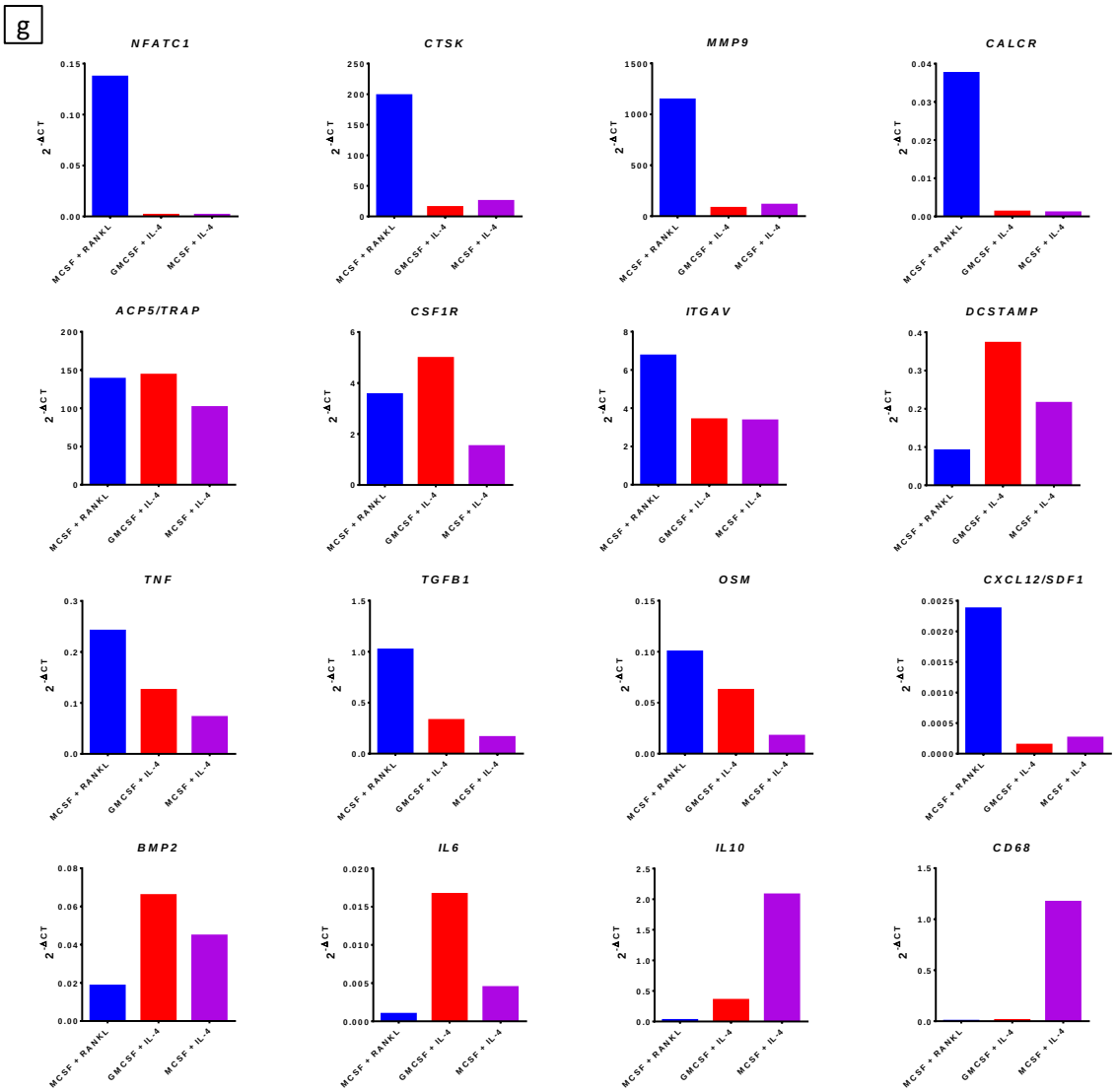

Figure I-7: M-CSF and GM-CSF induce different types of MNGCs.

Comparative gene expression analysis by RT-qPCR at 8 days of differentiation from osteoclasts (M-CSF + RANK-L) and MNGCs (GM-CSF + IL-4 or M-CSF + IL-4) cultures *in vitro*, N=1.

expressed more *IL10* and *CD68*. These results would need to be replicated and measuring cytokines levels in the media would be mandatory to draw any conclusion. Nevertheless, this could be a first approach for MNGC subtype models *in vitro*.

These results are consistent with the biological function of M-CSF and GM-CSF (Ushach and Zlotnik, 2016). Under homeostatic conditions, M-CSF is essential for DC and tissue macrophages development. It drives macrophages towards an anti-inflammatory M2 phenotype; in our case, tissue-healing MNGC-2 expressing *IL10*. On the contrary, GM-CSF peaks during inflammation in response to pro-inflammatory cytokines. It is associated to inflammatory M1 macrophages polarization and could lead to inflammatory MNGC-1. In tissue regeneration, the transition from early inflammation to wound healing should lead to lower GM-CSF to M-CSF ratio. As we detected *CSF1R* expression, MNGC-1 could still be responsive to M-CSF and transition towards a MNGC-2 phenotype.

Conclusion

In this study, we demonstrated that the secretome from apoptotic MSCs could stimulate osteoclastogenesis while restricting the formation of MNGCs. The effect on osteoclasts seemed associated with higher secretion of CXCR-1 and -2 ligands such as IL-8/CXCL-8. Additional results with ATSC or fibroblasts tend to indicate that this pro-osteoclastogenic effect is not restricted to bone-marrow MSCs and that their clinical efficacy also relies on other factors. Comparing in depth the secretions profile of these cell types, in both basal and apoptotic conditions, could better explain the specificities making bone marrow MSC suitable for bone regeneration.

We suggested a potential autocrine activation loop by osteoclast-secreted IL-8 but we did not explore completely the phenotypes of the osteoclasts formed after MSC-CM stimulation. It would be complementary to our experiments to analyze further the transcriptome of these osteoclasts and measure their secretions of chemotactic and osteogenic molecules. It would also be interesting to investigate their resorption ability, especially on a CaP coating. Conversely, the mediators inhibiting the formation of MNGCs could be identified with a similar approach using neutralizing antibodies. The phenotype of these cells at the transcriptional level and their secretion profile were also not studied.

In addition, the conclusions that can be drawn from an *in vitro* approach alone remain limited. Testing our CMs on osteoclast precursors from mice bone marrow would confirm the possibility of CXCR-1/-2 signaling between implanted human MSCs and mice cells in preclinical models. Then, the involvement of these mediators would need to be confirmed in the process of bone regeneration as a whole *in vivo*. If these proteins are essential in MSC-induced bone formation, neutralizing CXCR-1 or -2 would restrain osteoclastogenesis, thus bone formation, while local injection of IL-8-like cytokines could enhance it. Various methods effectively blocking CXCR-2 signaling *in vivo* were reviewed by Boppana et al. (2014). They include chemical antagonist, chemokine analogs, neutralizing antibodies and knock-out animal models. Overall, methods using CXCR-2 blockers seem prone to off-target and adverse effects given the broad range of immune cell types that could carry those receptors, especially neutrophils that are essential in the early stages of inflammation. CXCR-2 deficient mice seem rather unsuitable for bone formation as they exhibit delayed wound healing due to impaired neutrophil infiltration (Devalaraja et al., 2000), associated to a more intense acute inflammatory phase driven by macrophages (Dyer et al., 2017). To specifically study CXCR-2 in the communication between MSCs and osteoclasts precursors, a conditional knock-out of the receptors only in the monocytes/macrophage lineage would be ideal but could still impair the immune response. Implanting MSCs lacking the *CXCL8* gene in a nude mice model would be the easiest approach as it would not affect IL-8 produced by other cells at the implantation site.

Chapter II:
Influence of the biomaterial composition on osteoclasts formation

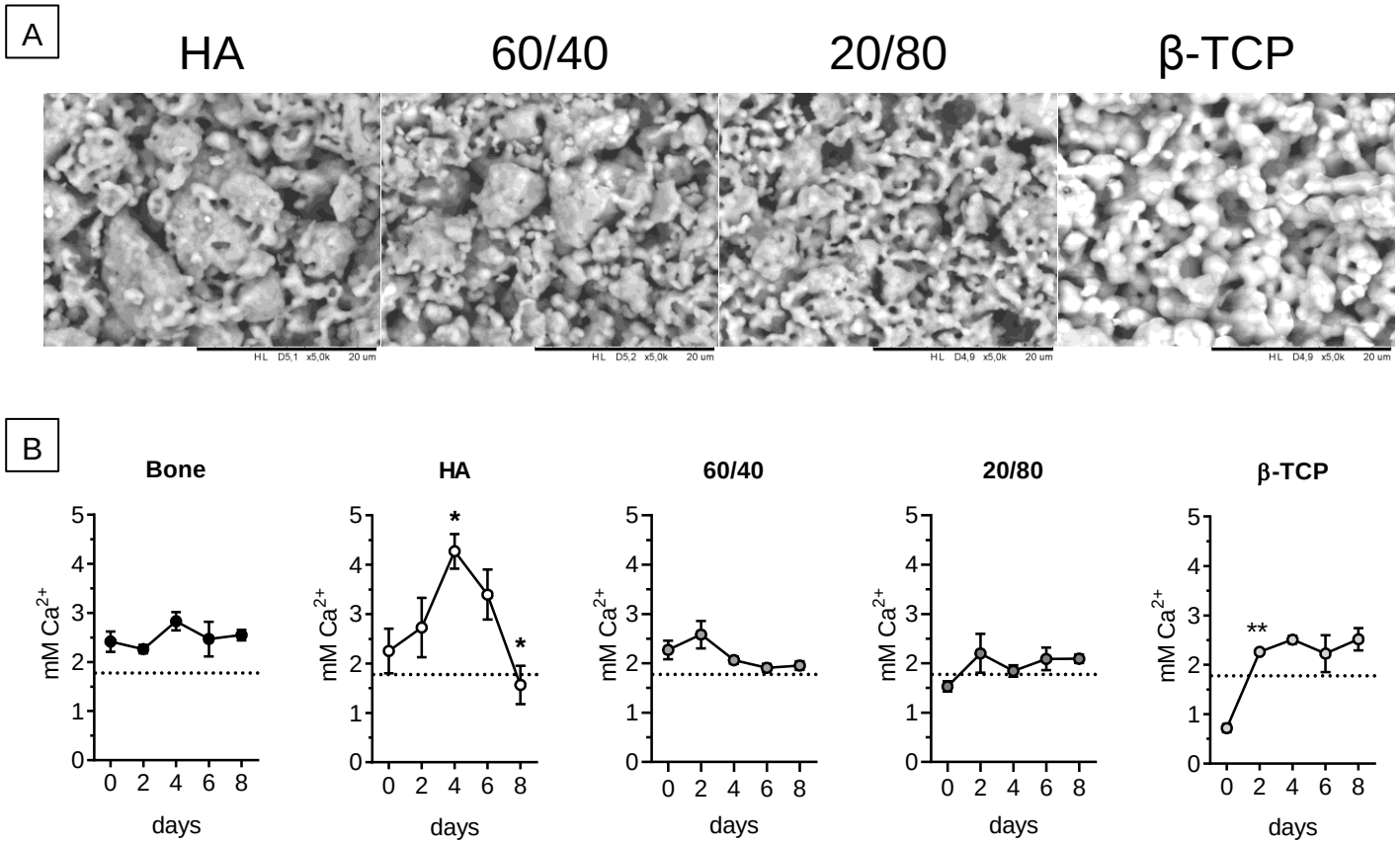

Figure II-1: Calcium phosphate biomaterials properties in media.

(A) Scanning electron microscopy images of the biomaterials surfaces. Scale bars = 20 µm. (B) Evolution of calcium ions (Ca^{2+}) content in the media when disks alone are incubated to mimic culture conditions with bone slices as controls. The first measure (D0) was performed in the pre-incubation media. Dashed line represent the measured value in basal media. Statistical analysis by repeated measure one-way ANOVA and Tukey's multiple comparisons test with each time points compared to the previous one, * p-value < 0.05, ** p-value < 0.01

Context & Acknowledgments

This project was initiated as part of a “Hubert Curien partnership” with the Bone Research group from the University of Vienna lead by Prof. Oskar Hoffmann and in collaboration with the Biomaterials, Biomechanics and Tissue Engineering Research Group from the Technical University of Catalonia in Barcelona lead by Prof. Maria-Pau Ginebra. Biomaterials were produced by Joanna Sadowska and Irene Lodoso in Barcelona. Carina Kampleitner performed all experiments involving mice cells in Vienna and participated in the *in vivo* experiment. In Nantes, human cell cultures were performed as well as the *in vivo* experiment and subsequent histological treatment of samples with the valuable help of Julien De Lima.

Unfortunately, the *in vivo* experiment was launched only on the 29th and 30th of September 2020. Hopefully, preliminary results will be available for presentation at this thesis defense. The final article will be written once these data collected, with an emphasis on the comparison between human and mice cells *in vitro*.

Introduction

CaP ceramics are among the most promising materials for bone regenerative therapies given their biomimetic composition resembling the mineral phase of bone (Ginebra et al., 2018). As previously mentioned, they have been extensively studied in combination with MSCs for ectopic bone formation and defect bridging in animal models, and for the treatment of non-union fractures in clinical trials. Their osteogenic properties have long been reported (Barradas et al., 2011b) but the exact mechanism linking their implantation to the formation of new bone remains elusive. We postulated that, when implanted with MSCs, the formation of osteoclasts is the first step for subsequent recruitment of new osteoprogenitors (Humbert et al., 2019). While MSCs seem essential in modulating the immune response, the material properties are key elements determining the fate of the first host cells interacting with it and, therefore, greatly influence the foreign body reaction.

Early on, CaP materials of different calcium to phosphate ratios were studied, namely hydroxyapatite (HA), beta tricalcium phosphate (β-TCP) and BCPs, combination of the two previous materials. When implanted in SCID mice in combination with MSCs, a 20/80 HA/β-TCP composite demonstrated the best osteoinductive properties compared to 60/40 HA/β-TCP or pure HA or β-TCP (Arinzeh et al., 2005). Jensen et al. (2008) also reported that the 20/80 HA/β-TCP material presented the most similarities with autografts in a mandibular defect in minipigs compared to other HA/β-TCP ratios. Interestingly, they found that this material had a higher resorption rate, also similar to autografts, suggesting that osteoclast formation could be associated to this favorable outcome. These experiments led to the extensive use of the 20/80 HA/β-TCP material in further research and clinical trials

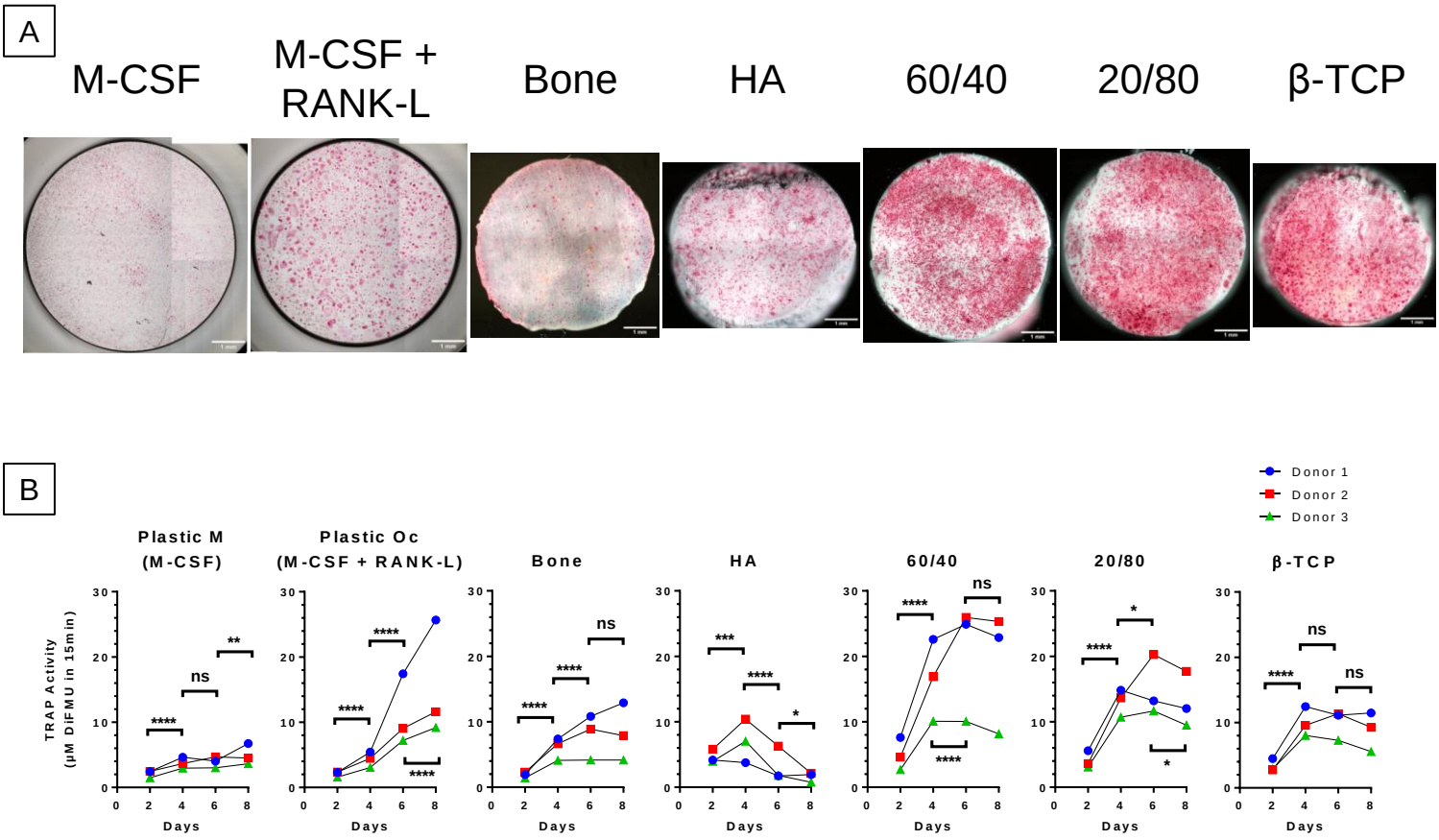

Figure II-2: Human osteoclasts differentiation on calcium phosphate materials.

Human osteoclasts differentiation (M-CSF + RANK-L) *in vitro* for 8 days on plastic, bovine bone or various CaP materials, Hydroxyapatite (HA), β-Tricalcium Phosphate (βTCP), composite of 20% of HA /80% of βTCP (20/80) and 60% of HA / 40% of βTCP (60/40). Negative control with M-CSF only on plastic. (A) Optical microscope images of the entire surface of wells or CaP disks after TRAP staining. Scale bars = 1 mm. (B) Acid phosphatase activity in the supernatant of CD14+ cultures from 3 donors, measured at every media change as the quantity of DiFMUP dephosphorylated in 15 minutes. Similar Y axis for each conditions. Statistical analysis by repeated measure two-way ANOVA with Tukey's multiple comparisons test. * p-value < 0.05, ** p-value < 0.01, *** p-value < 0.001, **** p-value <0.0001

such as ORTHOUNION. More recently, osteoclast formation was closely related to bone formation in a subcutaneous model in nude mice as a RANK-L antibody, preventing osteoclastogenesis, could also impede bone formation (Gamblin et al., 2014).

This naturally suggests that, among HA/β-TCP composites, the 20/80 ratio is the most favorable for osteoclast formation. Osteoclasts formed on this material could then participate in a bone remodeling cycle, leading to the efficient bone formation widely reported. The objectives of this study were (1) to confirm that some CaP materials better support osteoclastogenesis *in vitro*, with both human and mouse precursors, (2) to assess the osteogenic potential of osteoclasts, using the conditioned media (CM) of their culture on the biomaterials in osteoblast cultures, and (3) to correlate the *in vitro* results with *in vivo* outcomes, i.e. osteoclast and bone formation, after subcutaneous implantation of the materials in nude mice.

Results

HA and β-TCP composites are more stable in culture media:

Images from scanning electron microscopy (SEM) revealed microporous surfaces for all materials (Figure II-1, A). It seems that HA-heavy materials presented particles of different sizes associated with each other, while β-TCP ceramics seemed more homogeneous. However, the resolution was not sharp enough to precisely describe the surface architecture.

The pre-incubation media (Figure II-1, B, D0) presented slightly higher (HA, 60/40, bone) or lower (20/80) Ca^{2+} concentration compared to fresh media (1.8 mM Ca^{2+}) except with β-TCP where the Ca^{2+}concentration was divided by two. From day 2 onwards, the Ca^{2+} concentration roughly stabilized a little above the basal value; around 2 mM for the BCP materials and 2.5 mM for bone and β-TCP. Unexpectedly, the Ca2+ concentration in the media peaked above 4 mM at day 4 with the HA material before dropping down its initial value at the last measured point. While the pre-incubation period equilibrated efficiently the calcium content between most materials and the media, it was not sufficient with HA. The light variations from the basal concentration observed for the other ceramics could be attributed to a slow dissolution of the materials in liquid, potentially combined with superficial damage to the disks during media change.

BCP materials seem more favorable to the development of osteoclasts:

TRAP staining allowed visualizing of the overall development and distribution of osteoclasts on the various materials (Figure II-2, A). As expected, culture on plastic with M-CSF only for eight days gave very few TRAP stained cells, making it a viable negative control, while adjunction of RANK-L led to extensive osteoclasts formation. The thinness of bone slice made it difficult to properly acquire images but large TRAP positive cells are still visible. On the CaP materials, the staining was overall less defined, as large areas rather than

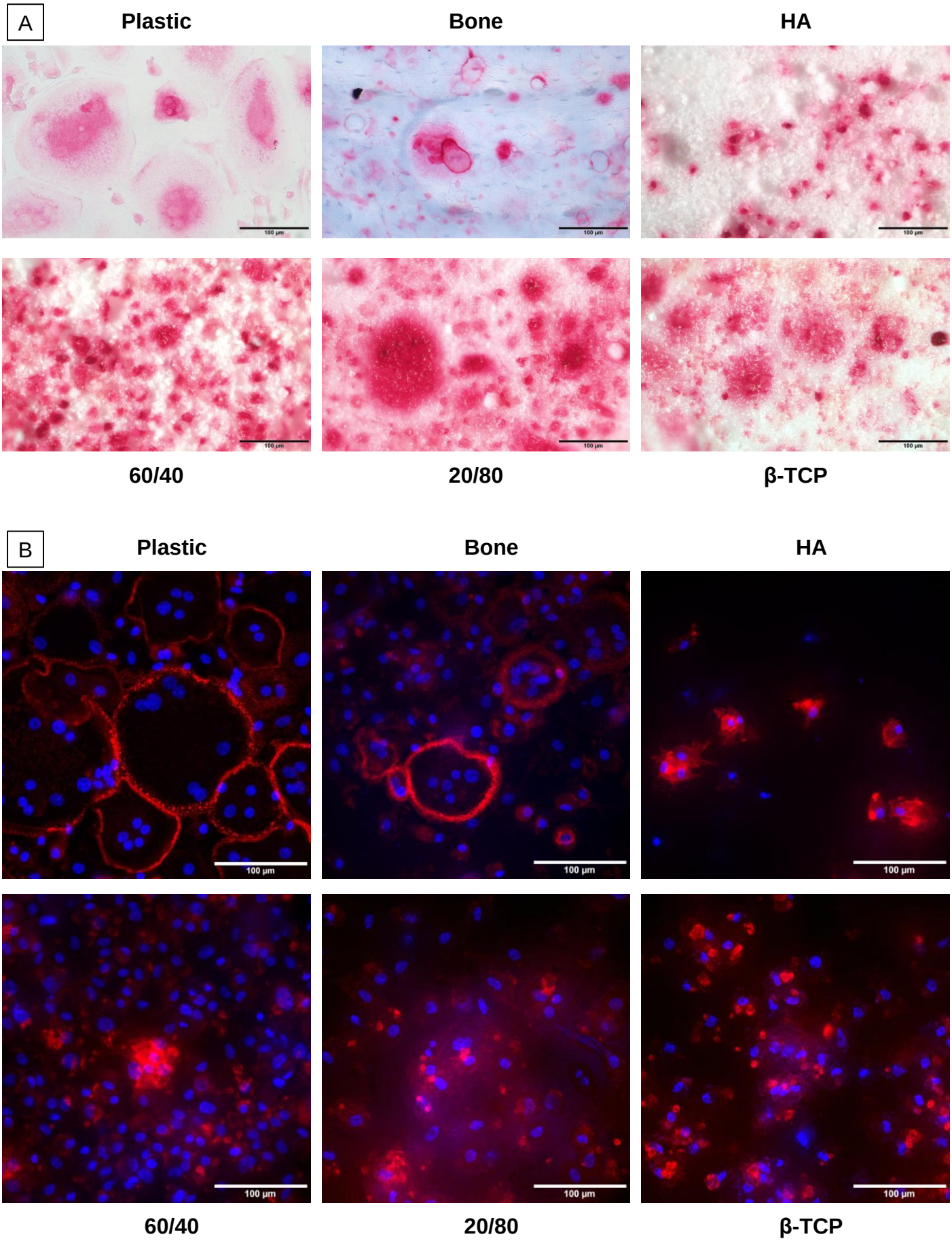

Figure II-3: Osteoclasts on CaP materials do not form actin rings.

Human osteoclasts differentiation *in vitro* on plastic, bovine bone or various CaP materials, β-Tricalcium Phosphate (βTCP), Hydroxyapatite (HA), composite of 20% of HA /80% of βTCP (20/80) and 60% of HA / 40% of βTCP (60/40). (A) Optical microscope images after TRAP staining (B) DAPI/Phalloidin fluorescent staining. All scale bars = 100 µm.

isolated cells appeared red. Notably less staining was observed on the HA material. Darker spots could be seen on 20/80 and β-TCP, potentially indicating larger or more mature cells.

Measuring the TRAP activity in the supernatant permitted to follow the differentiation over the course of the culture. As with TRAP staining, plastic cultures were reliable controls with 2 to 4 times more activity in RANK-L stimulated culture than in one's with only M-CSF at day 8. However, M-CSF only cultures also showed constant increase in TRAP activity, although lower than in M-CSF and RANK-L cultures. With bone slices cultures, the TRAP activity was increasing steadily after the first two media changes following RANK-L addition (D4 and D6) but stagnated at day 8. The activity was overall lower than osteoclasts on plastic, despite being on the most physiological material. On HA, the TRAP activity started increasing at day 4 but then dropped to finish lower than the M-CSF only culture. On the contrary, the TRAP activity increased sharply at day 4 on all β-TCP containing materials and then did not changed much. At the stabilization level, cultures on 60/40 resulted in the most activity followed by cultures on 20/80 while the lowest values were measured for β-TCP. Overall, these results matched the TRAP staining. Interestingly, a considerable variability was observed among the three donors despite similar patterns on each material. The first donor led to the highest TRAP activity measured, especially on plastic and bone, while the third systematically showed the lowest by far.

Looking in details at the TRAP staining (FigureII-3, A), multi-nucleation could easily be observed on plastic, even without hematoxylin counterstaining. On bone, the nuclei were more difficult to notice but the resorption pits left no doubt on the phenotypes of the TRAP positive cells. However, with all the CaP materials, nuclei could hardly be seen and counterstaining was not possible due to the material also absorbing the color. As seen from afar, cell density was lower on the HA material and larger spots were visible on 20/80 and β-TCP materials. These areas looked like they could be fused monocytes when compared to a dense layer of distinct mononuclear one's as seen on the 60/40 composite. However, these mononuclear cells are well stained for TRAP as it can also be observed on plastic, indicating that the expression of the enzyme is not restricted to osteoclasts. The bright staining of these cells on the biomaterials could either be just an optical effect with the underlying white material or be associated with higher TRAP production in these cells as suggested by the TRAP activity measurement.

To further analyze the potential multi-nucleation of the cells, DAPI/Phalloidin staining was use to clearly visualize the cytoskeleton and the nuclei (Figure II-3, B). It confirmed the first impression from TRAP staining of proper osteoclast formation on plastic and bone surfaces. Osteoclasts appeared mostly flat on plastic and bulkier on bone. As they were not resorbing on plastic, a podosome belt could be seen at the extreme limit of their cytoplasm in contact with adjacent cells. On bone, their cytoskeleton formed what resembled more to an appropriate actin ring, delimitating a resorptive area. On all CaP materials, only isolated podosome clusters could be seen. Crucially, as the limits of the

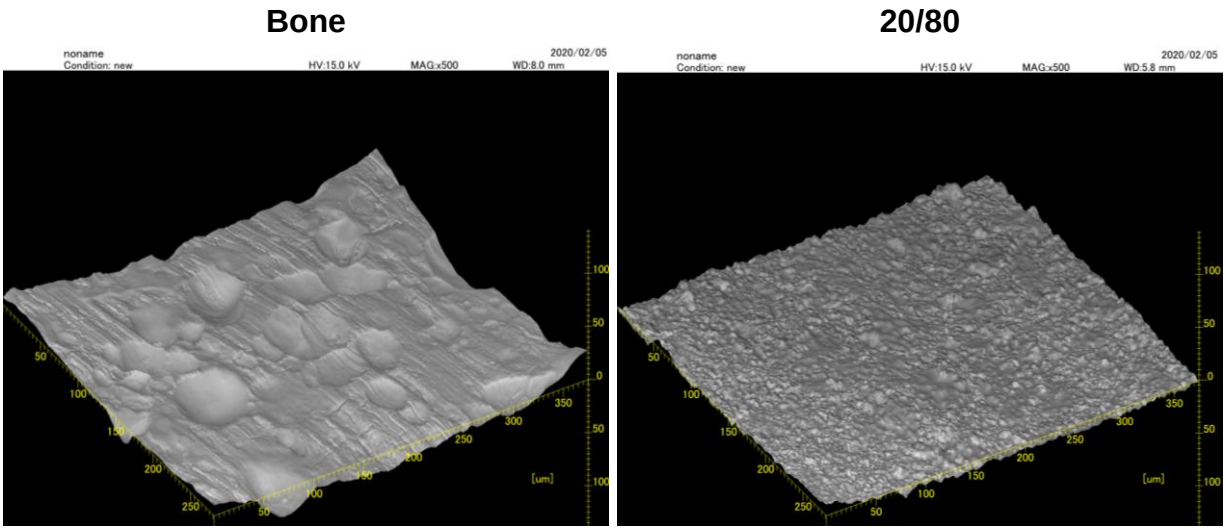

Figure II-4: Resorption pits can only be observed on bone slices.

Surface reconstruction from SEM images of bone slice and 20/80 material after 8 days of cultures with human CD14+ monocytes stimulated with M-CSF and RANK-L..

cytoplasm could not be clearly identified, it prevented the confirmation of multi-nucleated osteoclasts formation. Some nuclei seemed very close or even superimposed, especially on 20/80 BCP and β-TCP, but this could be easily linked with cell density. Also, the cytoskeletal arrangement of podosomes tends to indicate that if osteoclasts are well formed on these materials, they do not seem to be actively resorbing it as they do with bone surfaces. This was also supported by attempts of 3D reconstruction from SEM images presented in Figure II-4. Resorption pits could be undoubtedly seen on the surface of bovine bone slices, confirming the observation made with light microscopy. On the contrary, the surface of CaP materials, although uneven, did not present such deep holes. However, the microscope used had limited resolution and this technique was not explored further.

Overall, multiple clues indicate that osteoclast could fuse from human CD14+ precursors on CaP materials *in vitro* after RANK-L stimulation. However, they seem to prefer materials containing β-TCP. While the TRAP activity was at its highest with the 60/40 composite, possibly multinucleated cells were observed mostly on 20/80 and, to a lesser extent, pure β-TCP.

CaP properties have more effect on osteoblasts than osteoclasts secreted factors:

The osteogenic properties of the pre-incubation media and the CM from osteoclasts cultures were assessed on human MSCs cultures. Only one MSC donor was used against the three CD14+ donors. Alkaline phosphatase (ALP) staining was performed on the third and fifth days while alizarin red (AR) was realized on the tenth day. Overall, the first ALP staining exhibited high variability, probably due to a low cell density.

Using the pre-incubation (Figure II-5), no statistical difference could be seen by ALP staining after three days. However, some trends could be observed: staining seemed less spread on the negative control without osteogenic factors, as excepted, and with the HA pre-incubation media while appear slightly more intense with 60/40 and 20/80 pre-incubation media. After five days, only the lower ALP activity in the negative control and with the HA pre-incubation media were confirmed. The staining was similar to the control condition with all other media. AR staining after ten days confirmed the validity of the negative control and the lower differentiation with pre-incubation media from HA. Interestingly, mineralization was also significantly lower with pre-incubation from β-TCP, which had reduced Ca^{2+} content (Figure II-1, B). Most importantly, the staining was largely the most spread with the pre-incubation media from 60/40 and 20/80, potentially correlated to the trends observed in ALP at day three. These material themselves seems to indirectly improve the mineralization potential of MSCs without drastically changing the Ca^{2+} concentration in the media.

The CM from day four, six and eight were pooled to be used as “osteoclast CM” in the MSC osteoblastic differentiation test (Figure II-6). After three days, the ALP activity was significantly higher with any CM than in the control without CM, at the exception of the CM

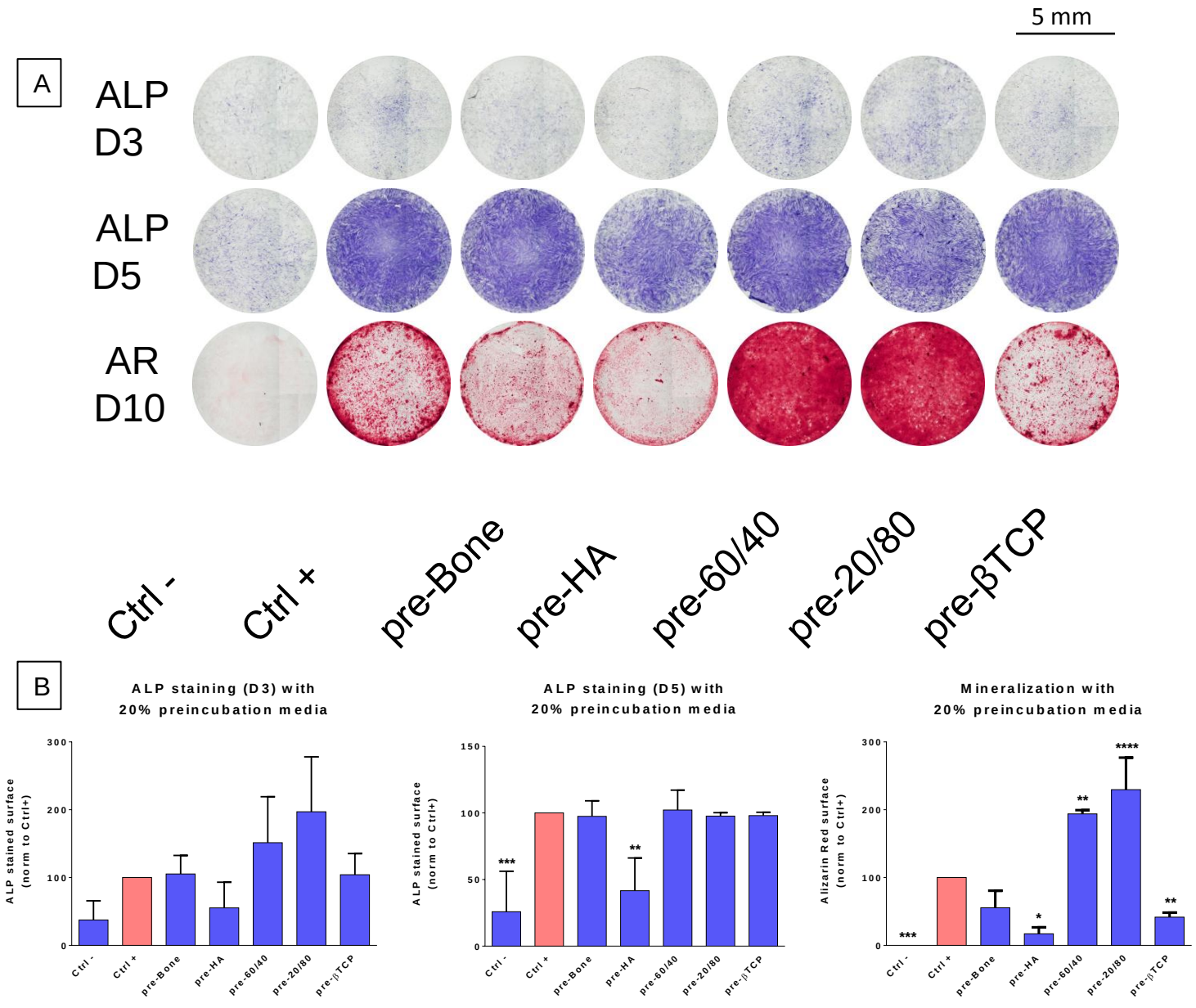

Figure II-5: Osteogenic differentiation of MSCs with pre-incubation media (pre-) from the different biomaterials.

Ctrl - = basal media, Ctrl + = osteogenic media. (A) Full well images of Alkaline Phosphatase (ALP) staining after 3 or 5 days, and Alizarin Red (AR) staining at 10 days of culture with 20% pre-incubation media. Scale bar = 1 mm. (B) Quantification of stained surface by image analysis. Statistical analysis by repeated measure one-way ANOVA and Dunnett's multiple comparisons test with differences to the Ctrl+ presented as ** = p-value < 0.01 and *** = p-value < 0.001.

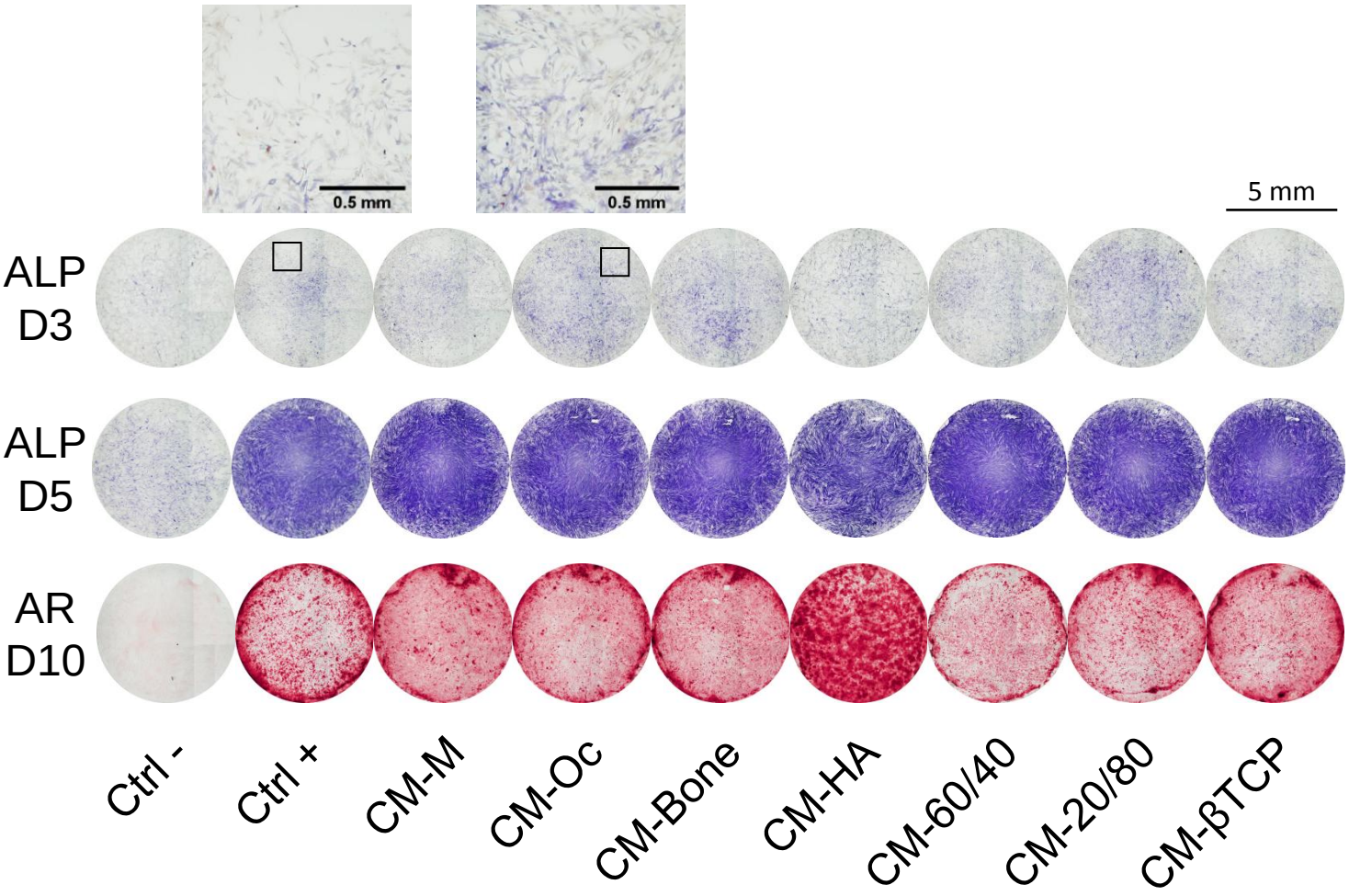

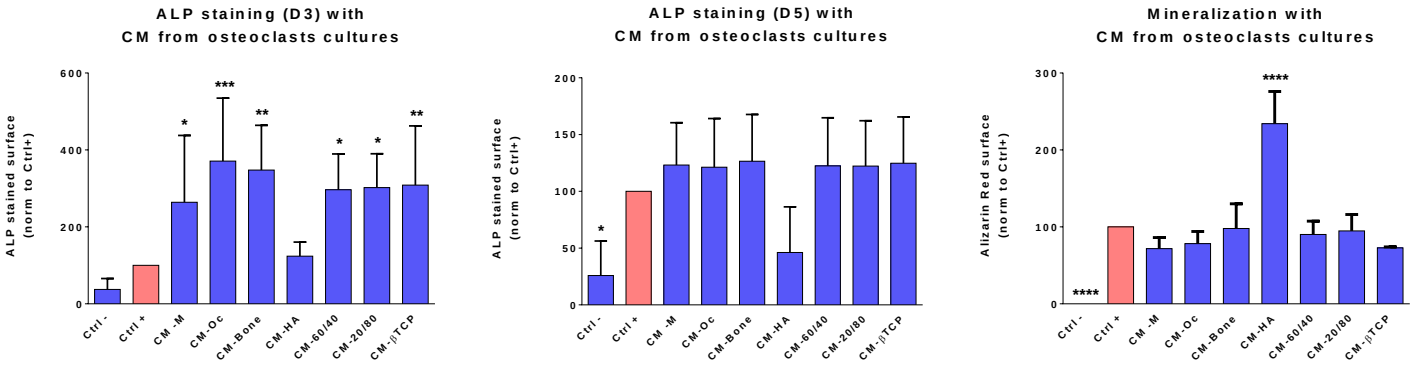

Figure II-6: Osteogenic differentiation of MSCs with condition media (CM) from CD14+ culture on the different biomaterials.

Ctrl - = basal media, Ctrl + = osteogenic media, M = Macrophage culture (M-CSF only) on plastic, Oc = Osteoclasts culture (M-CSF + RANK-L) on plastic. (A) Full well images of Alkaline Phosphatase (ALP) staining after 3 or 5 days, and Alizarin Red (AR) staining at 10 days of culture with 20% osteoclast culture media. Scale bar = 1 mm. Close up images of ALP staining "Ctrl+" and "CM-Oc" at day 3, scale bar = 0.5 mm. (B) Quantification of stained surface by image analysis. Statistical analysis by repeated measure one-way ANOVA and Dunnett's multiple comparisons test with differences to the control (Ctrl+) presented as * = p-value <0.05, ** = p-value < 0.01, *** = p-value < 0.001 and **** = p-value < 0.0001

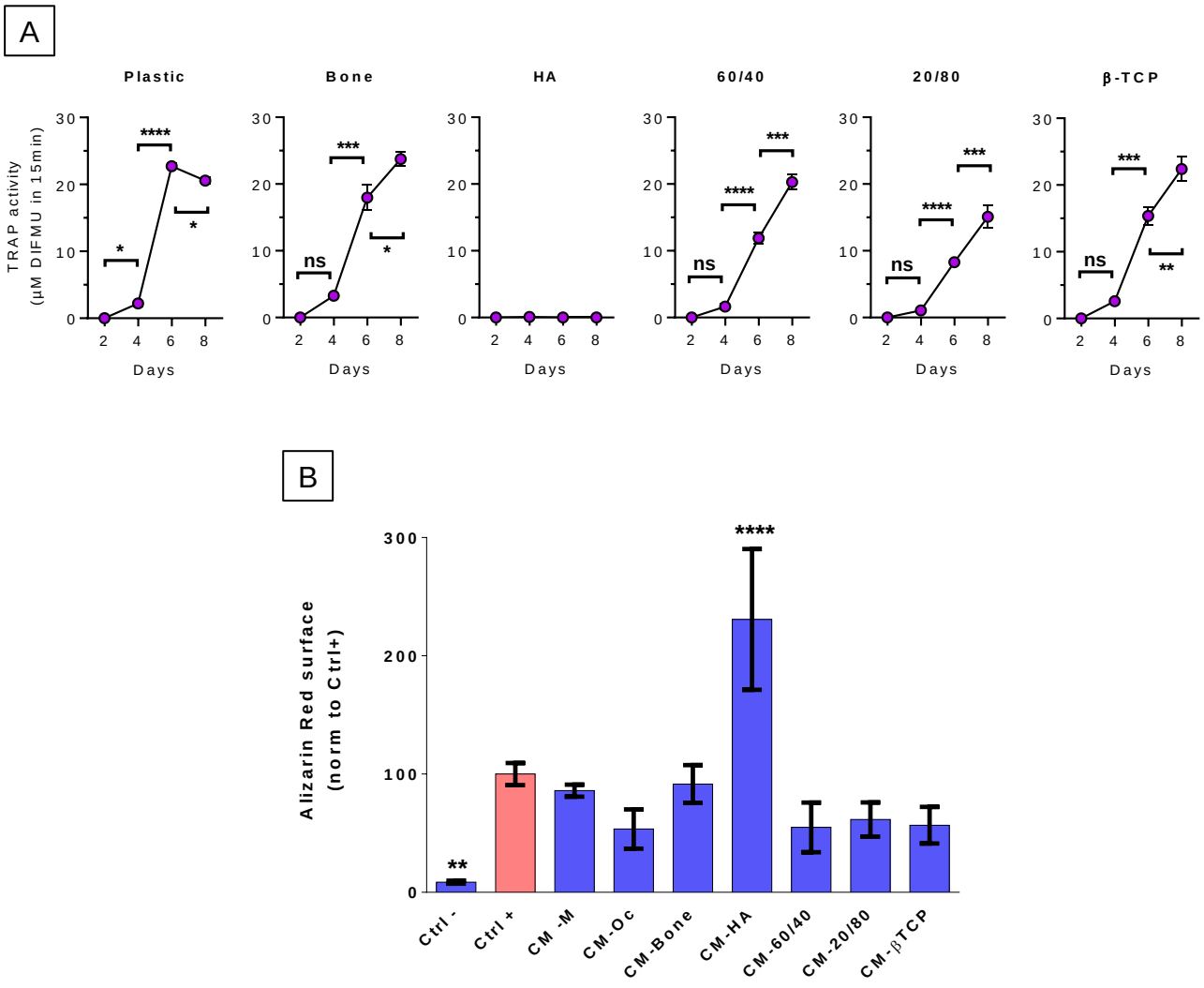

Figure II-7: Corresponding TRAP activity and Alizarin Red data from our collaborators using mice cells.

(A) Mice osteoclasts differentiation (M-CSF + RANK-L) *in vitro* for 8 days on plastic, bovine bone or various CaP materials, Hydroxyapatite (HA), β-Tricalcium Phosphate (β-TCP), composite of 20% of HA /80% of β-TCP (20/80) and 60% of HA / 40% of βTCP (60/40). Acid phosphatase activity in the supernatant at every media change, measured as the quantity of DiFMUP dephosphorylated in 15 minutes. Experiment representative of three. Similar Y axis for each conditions. Statistical analysis by repeated measure one-way ANOVA with Tukey's multiple comparisons test. * p-value < 0.05, ** p-value < 0.01, *** p-value < 0.001, **** p-value <0.0001 (B) Quantification of Alizarin Red staining from mice osteoblast mineralization assay with conditionned media from osteoclasts cultures. Statistical analysis by one-way ANOVA and Dunnett's multiple comparisons test with differences to the control (Ctrl+) presented as ** = p-value < 0.01 and *** = p-value < 0.001.

from HA cultures. The latter, as well as the negative control, were not different from the positive control at this point. These differences, as well as the overall variability of the ALP staining at day 3, seem due to differences in cell proliferation. Close up images in Figure II-6, A show this effect on the control condition compared to the condition with CM from osteoclasts on plastic. Large areas without cells could be observed on the former, while in the latter, the cell layer was almost covering the entire surface of the well. These differences at day three were not confirmed with the staining after five days as only the negative control was significantly lower than the other conditions. The addition of CM from HA culture also seemed to decrease ALP expression but this tendency was not statistically relevant. Overall, the replicates exhibited more variability than in the experiment with pre-incubation media, certainly due to the differences between CD14+ donors. Regarding mineralization, only the use of CM from HA cultures resulted in a drastically higher staining. All the other conditions with CMs seemed similar to the control or slightly lower but not statistically different. Given the low ALP activity with CM from HA cultures and the release of calcium measured with this material (Figure II-1, B), the AR staining may be a result of particle deposition from the CM rather than a biologic effect on osteogenic differentiation.

Overall, both osteoclast formation and osteoblast mineralization showed the same trends when mice cells (Figure II-7). The major difference was the absence of an initial spike in TRAP activity as observed at day 4 in human osteoclasts cultures the materials. With mice osteoclast precursors, the increase in TRAP activity was steadier during the eight days of culture. It peaked after six days on plastic while the maximums were reached at day 8 for all other materials. As with human MSCs, the differentiation assay with mice osteoblasts showed an improve mineralization only with CM from HA culture, despite no osteoclasts formation.

Discussion

Overall, our results indicate that the most favorable materials *in vitro* for the development of osteoclasts are BCPs, especially the 20/80 HA/ β-TCP composite. To go further, we tried to evaluate the osteogenic potential of osteoclasts secretions when cultured on these materials. Unfortunately, no clear differences could be observed between the conditions. On the contrary, pre-incubation media from BCP materials ameliorated the mineralization potential of MSCs, although this was not clearly associated with an improved ALP activity. Data produced by our collaborators using mice cells were very similar. The combination of these two models strengthens our conclusions and reinforces the pertinence of *in vivo* observation in mice for clinical applications but differences between them could be further explored.

Due to the absence of actin ring, we could not confirm multi-nucleation of cells observed on the biomaterial. However, it could also explain the TRAP activity measured in the supernatants, as the secreted enzymes would not be constrained to the cell's underlying

surface without a sealing zone. This effect could also be illustrated by the higher activity in supernatant from plastic compared to bone cultures. This interpretation would support the conclusion of osteoclasts formation on the biomaterials, to a similar extent than on plastic surfaces. Moreover, other authors have reported successful osteoclasts formation on CaP materials *in vitro*. Longer culture times even allowed the study of their resorption abilities. For example, Davison et al. (2014) showed that human osteoclasts could differentiate more efficiently and only resorb β-TCP with small grains (0.95 ± 0.27 µm) and micropores (0.63 ± 0.33 µm) compared to large ones (3.66 ± 1.05 and 1.78 ± 0.85 respectively). Chen et al. (2019) observed the opposite phenomenon on HA, where smaller grain size impaired RAW 264.7 cells differentiation. However, their range was lower, the material with the larger grain size averaging 0.48 µm, suggesting that ideal values for this parameter could be between 0.5 and 1 µm. Interestingly, Arbez et al. (2019) reported that human macrophages were able to resorb β-TCP while undifferentiated RAW 264.7 were not. This could imply differences between human and mouse models *in vitro*, or at least between primary cells and cell lines.

Once formed, osteoclasts are known to produce multiple coupling factors towards MSCs as part of the remodeling cycle (Sims and Martin, 2020b). On biomaterials, their resorption ability could also greatly participate in bone induction by releasing calcium and phosphate ions. In a coral-derived ceramic implantation model in baboons' muscle, the blockage of Ca^{2+} channels inhibited bone formation, suggesting that calcium sensing played a major role in osteoinduction (Klar et al., 2013). Additionally, González-Vázquez et al. (2014) showed *in vitro* that extracellular calcium, through the calcium sensing receptor, induced migration, proliferation and stimulated the expression of osteoblastic markers in rat bone marrow MSCs. In our experiments, the effect of the HA-CM on Alizarin Red staining seemed correlated to the peak in calcium release while the improved mineralization with the pre-incubation media from the 60/40 and 20/80 BCPs could not be explained. Surely those materials impact the media composition in other way such as phosphate content or pH. The only differences observed on MSCs that could be linked to osteoclasts activity were the increases in early ALP activity in presence of CM. This could be due to growth factor from osteoclasts improving MSC proliferation but not specifically enhancing differentiation.

Conclusion

Our observations *in vitro* tend to confirm the 20/80 BCP as the most relevant CaP material in bone regeneration. First, it supported osteoclasts formation, which could be essential to transition from foreign body reaction to bone remodeling. Also, its pre-incubation media improved mineralization in MSCs, possibly through ion exchange other than calcium, suggesting an important role of the biomaterial composition even later in the regeneration process. However, given the size of the materials, we could not seed large number of osteoclast precursors. This renders impossible to measure the levels of osteoclast-derived cytokines or the analysis from RNA or protein extraction. A new study design would be essential to investigate further the phenotypes of these cells on the different CaP surfaces *in vitro* and better evaluate potential differences between models with human or mouse cells.

Hopefully, the *in vivo* procedure will confirm that the 20/80 BCP also permit better osteoclasts formation in physiological conditions and engender the most bone formation. Other controversial topics in the field of bone regeneration will also be studied by immunohistochemistry. The labeling of osteoclasts and MNGCs markers (RANK, CD86, Cathepsin K, etc.) should allow us to refine our knowledge on the phenotypes of those cells. MSCs' engraftment on the different materials will be evaluated by using an antibody directed towards human vimentin. All together, this study could reinforce the use of the 20/80 BCP, the hypothesis of the implication of osteoclasts and the interest of *in vitro* models to evaluate new biomaterials for bone regeneration.

Material & Methods

Biomaterials

HA, β-TCP and the two BCP with HA to β-TCP ratio of 20/80 and 60/40 were studied. They were produced as dense disks (diameter 5 - 5.5mm, thickness 2mm) for *in vitro* experiments and granules (0.5 - 1mm) for *in vivo* implantation. Disks were sterilized 30 min in 70% ethanol and washed 3 times with PBS while granules were gamma-irradiated. The materials were compared to cultures on bovine bone slices and plastic. Bone slices were sterilized by autoclaving and carefully glued to the bottom of wells with silicone paste (Baysilone, Bayer). All materials were pre-incubated 24h before cell seeding. For disks, the pre-incubation media were collected and stored at -20° for analysis and use in osteoblast differentiation test.

SEM images were taken on a TM3000 Tabletop SEM (Hitachi) with the associated software. Three-dimensional (3D) reconstructions of the surface were made with the 3D-Image viewer software. Calcium ions (Ca^{2+}) release or uptake was evaluated in condition

mimicking cell culture with Calcium Colorimetric Assay (Sigma, MAK022). The disks were soaked in media for 24h as for preincuabtion (D0), the media was changed every 2 days afterwards (D2, 4, 6, 8) and the test was performed at each time point.

Osteoclasts Culture

Human osteoclast differentiation was performed on human CD14+ cells isolated from the peripheral blood of healthy donors, provided by the EFS (Etablissement Français du Sang). Human peripheral blood nuclear cells were isolated from whole blood by Ficoll®-Paque Premium (GE Healthcare) gradient and sorted with CD14 microbeads on LS MACS column (Miltenyi Biotec). Cell pools enriched in CD14+ monocytes were aliquoted and stored in liquid nitrogen until use, no longer than 6 months. Mouse osteoclasts were derived from bone marrow precursors from BALB/c mice. Mice were euthanized and dissected under sterile conditions to retrieve both femurs and tibia. Epiphyses were cut off, the medullary cavities were flushed to collect the marrow, and cells were used fresh for differentiation.

Osteoclasts precursors were seeded on the pre-incubated materials or on plastic in 96-well plates at a density of 100 000 cells/well in 200 µL αMEM, 10% FBS, 1% Penicillin/Streptomycin with 25 ng/mL rh/rmM-CSF. The media were changed every 2 days with the addition of rh/rmRANK-L at 100 ng/mL. All media were collected and stored at -20°C for TRAP activity assessment and use as CM on osteoblastic differentiation tests. After 8 days, cells were fixed in formalin for TRAP staining or in 4% PFA for DAPI/Phalloidin fluorescent staining. Fixed cells were washed 3 times with PBS, eventually stored in PBS at 4°C for up to a week.

TRAP Activity was evaluated in the culture media at every media change (D2, 4, 6 and 8) with EnzChek® Phosphatase Assay Kit (Invitrogen, E12020). After centrifugation (5min, 500g) of the uptaken media from osteoclast culture, 25 µL of supernatant were mixed with 25 µL of a 200 µM solution of the substrate 6,8-difluoro-4-methylumbelliferyl phosphate (DiFMUP) in the reaction buffer provided in the kit (0.1 M sodium acetate, pH 5.0). The dephosphorylation reaction was allowed to take place for 15 minutes at 37°C. Fluorescence was measured on a microplate reader (Berthold) and compared to a standard curve of the product DiFMU.

For TRAP staining, samples were incubated for 30 minutes at 37°C in a TRAP buffer (40 mM Sodium Acetate, 10mM Sodium Tartrate, pH=5). The buffer is removed and a 1:1 mixture of acetone and ethanol 100% is applied for 30 seconds. The samples are left to air dry for 2 minutes and incubated 30 minutes in a staining solution of TRAP buffer supplemented with 0.6 mg/mL Fast Red Violet LB salt (Sigma, 3381) and 100 µL/mL of a solution at 10 mg/mL Naphthol-AS-MX phosphate (Sigma, N4875) in N,N-dimethylformamide. The reaction is stopped with distilled water and the samples are dried for acquisition on an optical microscope Olympus IX73 with an Olympus DP74 color camera.

For fluorescent staining, cells were permeated with PBS/Triton X-100 for 1 minute and washed 3 times with PBS. F-actin proteins of the cytoskeletons were labeled by incubating the samples in a 1 U/mL solution of Alexa Fluor™ 546 Phalloidin (Life Technologies, A22283) in PBS for 30 minutes. After 3 PBS wash, nuclei were stained by incubation in a 0.2 µg/mL DAPI solution (Life Technologies, D21490) in PBS. The DAPI solution was removed and samples were directly stored in PBS/PFA 0.1%. Fluorescence images were acquired on an Olympus IX73 using a camera Hamamatsu ORCA Flash 4-0LT and processed with the cellSens software.

Mineralization and ALP Activity Assays

CM from osteoclast culture used in osteoblast differentiation tests were pooled from the 3 late collection times (4, 6, and 8 days). Mineralization tests and ALP activity assays were carried out either on human MSCs expanded from bone marrow aspiration or on neonatal mouse calvarial primary osteoblasts. MSCs were obtained from the Institut für Klinische Transfusionsmedizin und Immungenetik of Ulm, Germany. Cells from one 22 year old male donor were used for all experiments.

The culture medium for hMSCs consisted of αMEM (Gibco) containing 1% P/S (Eurobio), 1U/mL heparin, and 5% pooled human platelet lysate. The mineralization medium was obtained by supplementing with 250µM ascorbic acid, 10mM β-glycerophosphate, and 10nM dexamethasone. Cells were seeded in 96-well plates at a density of 4 000 cells/well in 100 µL of culture media. After 3 days, the medium was changed to mineralization media with 20% CM from osteoclast culture or disk preincubation media. The medium was changed every 3 to 4 days up to 3, 5 (ALP staining) or 10 days (Alizarin Red staining).

To assess mineralization, cells were fixed in PFA 4% for 20 minutes and stained 30 minutes with a 40 mM solution of Alizarin Red S (Sigma-Aldrich). ALP staining was performed with the Leukocyte Alkaline Phosphatase kit (Sigma, 85L2). Cells were fixed with a 2:3 mixture of 20 mM citrate solution and acetone for 30 secondes, washed in distilled water for 1 min and stained with a solution of Fast Blue RR and Naphtol AS-MX Phosphatase Alkaline Solution following the manufacturer's protocol.

Animal experiments

Animal experiments followed the European recommendations (2010/63/UE) and were authorized by the local ethical committee (project #6575). Six weeks old NMRI nude female mice were purchased from Janvier Labs. Animals received a buprenorphine (0.03 mg/kg) intramuscular injection 30 minutes before surgery. Anesthesia was obtained by inhalation of isoflurane, 3.5% at 1 L/min in the induction chamber, and 2.5% at 1 L/min in a mask during the procedure. Animal's temperature was maintained by a heating plate during surgery and waking. Two incisions were realized on the back of the animal, the skin was detached, the implants were placed and wounds were closed using non-resorbable sutures

(Filapeau 4/0, Peters Medical). Groups of five animals per material and per time point were created, each animal carrying one implant of the material alone and one with the material plus 2 million hMSCs. Additional analgesic injections could be performed during the 48h post-surgery if signs of pain were noticed. After 2, 4, or 8 weeks, animals were sacrificed and explants retrieved.

Histology (to come)

Explants will be fixed in a 4% formol solution. Decalcification will be performed in a microwave KOS Histostation (Milestone Med. Corp.) with samples in a pH 7.4 solution of 4.13% ethylenediaminetetraacetic acid (EDTA) and 0.2% paraformaldehyde in 1X PBS. Dehydration in increasing percentages of ethanol baths followed by a butanol bath will be carried out in an automated dehydration station (STP-120, Microm Microtech). Samples will be embedded in paraffin (Histowax; Histolab) in an embedding station (EC-350, Microm Microtech). Thin sections (3 µm) will be cut out on a microtome (RM2255, Leica).

Masson's Trichrome and TRAP staining will be realized on an automated staining station (HMS-740, Microm Microtech). For immunohistochemistry for human vimentin, mouse RANK and mouse CD86, slides will first be deparaffinised and incubated overnight at 60°C in Tris EDTA pH=9 buffer for antigen retrieval. Endogenous peroxidases will be blocked by incubating the slides in H_2O_2 3% for 15 min and aspecific sites will be saturated by a blocking solution (Goat Serum 2%, BSA 1% in TBS pH7.6, Tween 0.05%). Dilution and incubation time for primary and secondary antibodies will be optimized. Staining will be revealed by incubation with Streptavidin/Horseradish Peroxidase conjugate (Dako, P0397) followed by a 3,3' Diaminobenzidine solution (DAB Quanto, Thermo Scientific, TA-125-QHDX). Stained slides will be scanned using a NanoZoomer (Hamamatsu) and surface area for bone, osteoclasts and other staining will be measured with ImageJ software.

Statistical analysis

Statistical analyses were performed on GraphPad Prism software 6.0. Repeated measure one- or two-way ANOVA followed by Tukey's multiple comparison tests was used for comparing multiple groups with each other. When comparing multiple groups to a control group, Tukey's test was replaced by Dunnett's one.

Chapter III:
Exploratory *in vivo* experiments

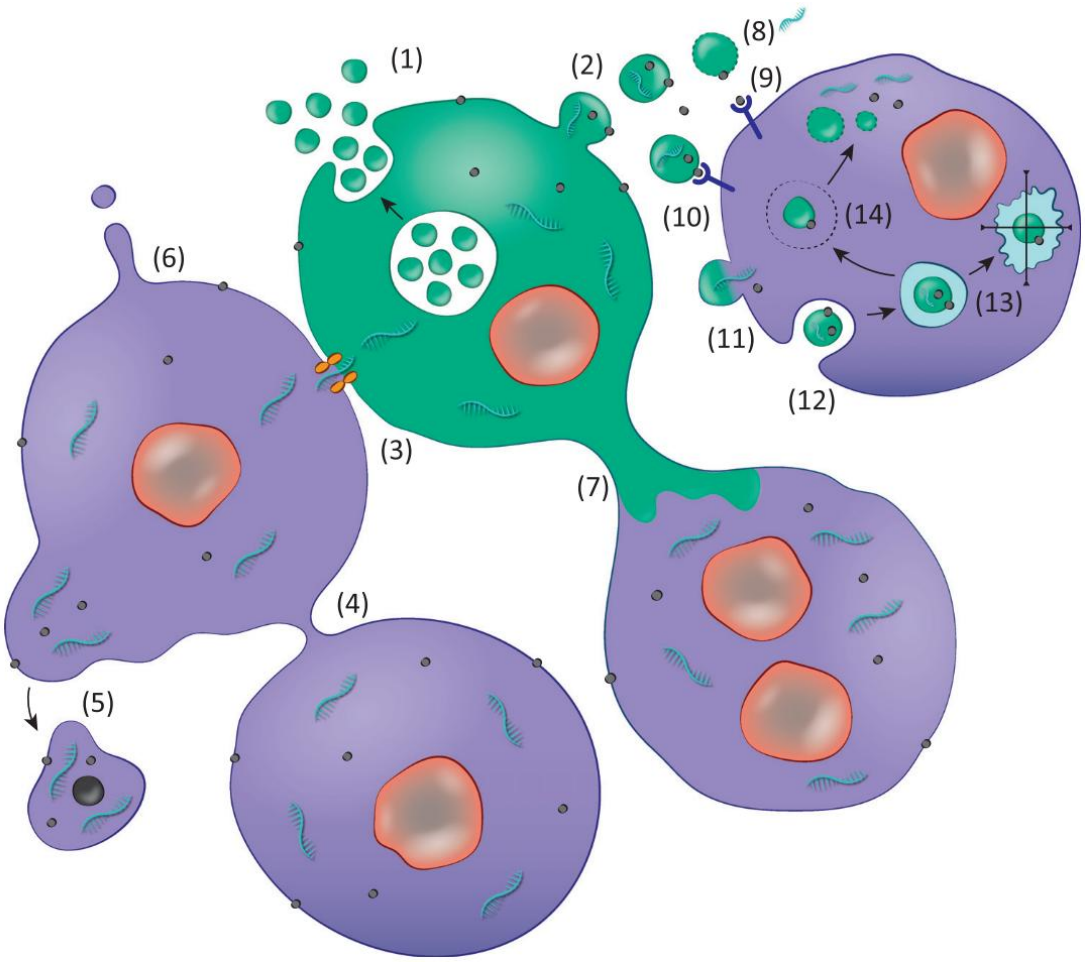

Figure III-1: Extracellular vesicles (EVs) are among the various means of cell communication.

They are mostly (1) exosomes released from multivesicular bodies (MVBs) or (2) microvesicles directly budding off the plasma membrane. Other ways of cell communications based on membrane boundaries include (3) exchange of molecules through gap junctions; (4) connections by nanotubes; (5) release of large vesicles from apoptotic cells (apoptotic bodies) or cancer cells (oncosomes); (6) release of vesicles from the tip of membrane protrusions and (7) connection by large microtubes. The delivery of EVs' signals can happen by (8) lysis in the extracellular space releasing the EVs' content; (9) free or (10) membrane-associated ligands binding to receptors on the target cell. The whole EV cargo can also be transferred to the recipient cell through (11) fusion with the membrane or (12) endocytosis where the EV is either (13) degraded via the lysosomal pathway or (14) escaping from the endosome and releasing its content in the cytoplasm. (from Maas et al., 2017)

The use of various materials and the addition of MSCs in bone regeneration strategies were led by intuition and basic knowledge of bone biology. Bone regeneration implies complex, multidimensional communications between a variety of cell types from blood and bone in an environment where ion levels (calcium & phosphate) and mechanical constrains are crucial, all of that evolving over time. Despite the development of multicellular and three-dimensional cultures, all those aspects can only be reunited in a living organism. As we try to better apprehend the successful mechanisms behind MSC-CaP implantation to rationally design future therapies, proceeding by trial and error *in vivo* is still valuable to bring out new therapeutic approaches and test hypothesis that cannot be tackled only *in vitro*.

Experiments in nude mice

As previously presented, most of the studies assessing material osteoinductivity were carried out at ectopic sites (Barradas et al., 2011a). The subcutaneous implantation seems more stringent and technically more reliable than intramuscular implantation. The nude mice model was chosen to allow the implantation of human MSCs as a positive control, without compatibility issues. In this model, the biomaterial alone does not exhibit osteoinductive properties after 8 weeks of implantation (Brennan et al., 2014).Our first *in vitro* results showing a possible pro-osteoclastogenic effect of MSCs' conditioned media comforted the possibility of osteoclast activation as the first step of bone regeneration. We tried to directly implant pre-differentiated osteoclasts from human CD14+ cells to see if they could set off bone remodeling on the biomaterial. Also, if enough of the immunomodulatory signal of MSCs is delivered by soluble factors, their secretome alone could be a therapeutic alternative to cell implantation.

Extracellular vesicles (EVs, Maas et al., 2017) are secreted elements participating in cell communication. EVs are cargos of proteins and nucleic acids of various types surrounded by a lipidic bilayer. Subtypes of EVs are defined by their size and means of formation. Exosomes are small EVs (diameter inferior to 150 nm) released from multivesicular bodies while microvesicles tend to be larger (200 to 500 nm) and directly bud form the plasma membrane. They were initially thought to be only debris discarded by cells or mistaken for apoptotic bodies. With the realization that they were actively produced by cells came an interest for their function. Alongside secreted or exposed proteins and junctions between adjacent cells, they are a part of the intercellular communication system (figure III-1) overlooked for a long time. They are involved in a variety of physiological or pathological processes and can be found in most tissues. Various stimuli and stresses can increase the production of EVs, hinting a central role in inflammation and response to tissue damage. In bone (Liu et al., 2018), they are involved in mineralization, osteoclast-osteoblast communication and more. EVs derived from MSCs are getting increasing interest in regenerative medicine for their immunomodulatory potential (Tsiapalis and O'Driscoll, 2020). Following many positive preclinical results, EVs are now being evaluated in clinical

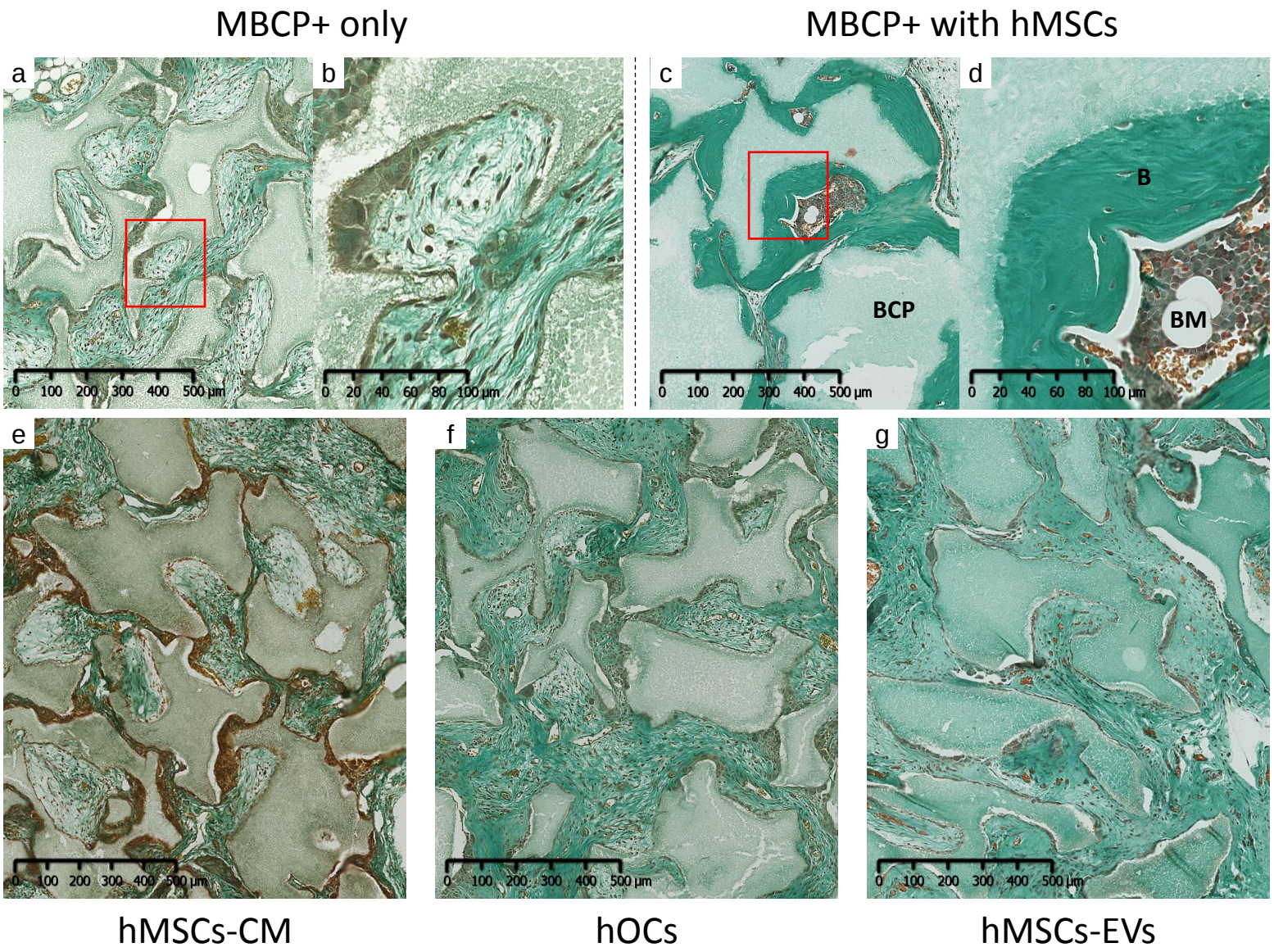

Figure III-2: Ectopic bone formation in nude mice with human osteoclasts and hMSC-CM or Evs.

Masson's trichome staining to evaluate ectopic bone formation in NMRI nude mice after 8 weeks of subcutaneous implantation of MBCP+ with various additives. Negative control with MBCP+ alone; x5 (a) and x20 (b). Positive control with MBCP+ and hMSCs; x5 (c) and x20 (d). Outcomes of implantation with the adjunction to the biomaterials of hMSCs conditioned media (hMSCs-CM, x5, e), human *in vitro* pre-differentiated osteoclasts (hOCs, x5, f) or hMSCs derived extracellular vesicles (hMSCs-EVs, x5, g). B = bone, BM = bone-marrow, BCP = MBCP+ biomaterial.

trials for the treatments of lung diseases, acute ischemic stroke, or chronic kidney damage. Based on those observations, we substituted MSCs in our subcutaneous model with their EVs to evaluate their potential of osteoinduction in the subcutaneous model. A hypoxic MSCs culture and a treatment with staurosporine were realized alongside the typical culture in an attempt to increase the EV content and/or their immunomodulatory properties.

Results

The negative and positive controls were consistent in the two sets of experiments. The subcutaneous implantation of MBCP+ alone never induced any bone formation (figure III-2 a,b). The material seemed even poorly integrated in the fibrous tissue making those samples difficult to process and resulting in heterogenous staining quality of the slides. On the contrary, the addition of hMSCs always led to abundant bone formation around the biomaterial granules and areas of bone-marrow embedded inside this new bone (figure III-2 c,d.). The positive controls only differ by their ratio of bone to bone-marrow and the sporadic areas of material not surrounded by new bone. Different timing of hMSCs seeding on the biomaterials were tested (data not shown). The hour of incubation before implantation used in the clinical protocol seemed to result in more homogeneous osteogenesis throughout the implant, maybe linked to a better distribution of the cells on the granules. All three experimental conditions (conditioned media, pre-differentiated osteoclasts and EVs) did not induce any bone formation. The addition of hMSCs culture supernatant (figure III-2 e) even lead to brown stains around the biomaterial, mixing the green color of collagen and the yellow/red associated with erythrocytes and muscle fibers. This could suggest prolonged and/or more intense inflammation. The implantation of pre-differentiated human osteoclasts (figure III-2 f) or EVs from hMSCs culture (figure III-2 g) resulted in outcomes closely resembling the implantation of the biomaterial alone. However, those explants seem slightly less inflammatory and the granules seemed better integrated in the tissue, but other analysis would be needed to confirm this impression. We choose to perform no further analysis or additional experiments as not a single condition seemed clearly superior to the implantation of the biomaterial alone.

Discussion

There are several issues regarding the implantation of pre-differentiated human osteoclasts. First, in our working hypothesis, the osteoclasts formed on the biomaterial are the results of a complex immune reaction modulated by implanted MSCs. Here, they were present from the beginning, with characteristics of *in vitro* grown cells, and without other anti-inflammatory agents. Secondly, proper osteoclast differentiation on the biomaterial could not be visually confirmed while survival of detached cells is also uncertain. Finally, these osteoclasts were from human origin. When implanting only MSCs, osteoclasts observed are inevitably from the host, and should therefore be able of efficient communications with other cells. In the case of human osteoclasts, there is no certainty in

their ability to properly initiate a bone remodeling cycle in mice. It was not surprising to have a disappointing result here.

The major limitation of all these experiments is the implantation site. Reaching subcutaneous bone formation has always been far more difficult than intramuscular osteogenesis or improving defect bridging. The subcutaneous environment lacks inherent osteogenic properties and is therefore prone to fibrous tissue formation (Scott et al., 2012). It was necessary to have stringent conditions when evaluating MSCs for bone regeneration, to ensure their efficacy in clinic and to compare their efficiency depending on the donor, the anatomical site of origin or the ratio of cells to biomaterial. However, the single implantation of MSC-derived components is unlikely to recreate the complex secretions and interactions of MSCs with host cells, and to compensate for the poor osteogenecity of the implantation site. While most MSCs are cleared from the implantation site within 2 weeks, proteins or EVs adsorbed on the biomaterial surface may not last longer than a few hours, especially in an inflammatory environment. Most studies reporting favorable effect of MSC-derived CM or EVs were focused on defect repair.

A systemic review by Benavides-Castellanos et al.(2020) concluded to an overall favorable effect of MSC-CM for bone regeneration. As these strategies only begin to emerge, they could include only nineteen animal studies and two clinical trials with limited patient numbers. All studies were applied to orthotopic bone regeneration such as calvarial defect or fracture healing, and the CM condition was almost never compared to a known positive protocol, including MSCs for example. Only Linero and Chaparro (2014) reported equivalent bone regeneration of a mandibular defect in rabbits by the combination of a human blood plasma hydrogel with either adipose-derived hMSCs or the CM from the same cells. This work solved two of the issues of our experiment; the study of a bone defect to have an osteogenic environment and the use of a hydrogel to limit immediate clearance of MSC secreted factors. As concluded by the authors of the meta-analysis, a lot remain to be done to consider the use of CMs or customized combinations of cytokines and growth factors in clinical procedures.

Specifically, exosomes and other extracellular vesicles play a major signaling role in natural fracture healing and are promising in bone regeneration strategies. $CD9^{-/-}$ C57BL/6 mice produce less exosomes and have a longer fracture healing period than WT mice. However, efficient callus formation can be restored by injection of hMSCs' exosomes (Furuta et al., 2016). In Wistar rats, regeneration of a calvarial bone defect could also be improved by implantation of atelocollagen sponges loaded with hMSCs' exosomes (Takeuchi et al., 2019). In our experiment, we stored EVs at -80°C and thawed them only once which seems to be the best storage method to preserve their integrity (Lorincz et al., 2014). However, freezing can still lead to vesicles aggregation and profound protein content changes that may alter their biological activity (Maroto et al., 2017). Other ways of storage such as lyophilization are being evaluated to allow easier transition into clinical application if

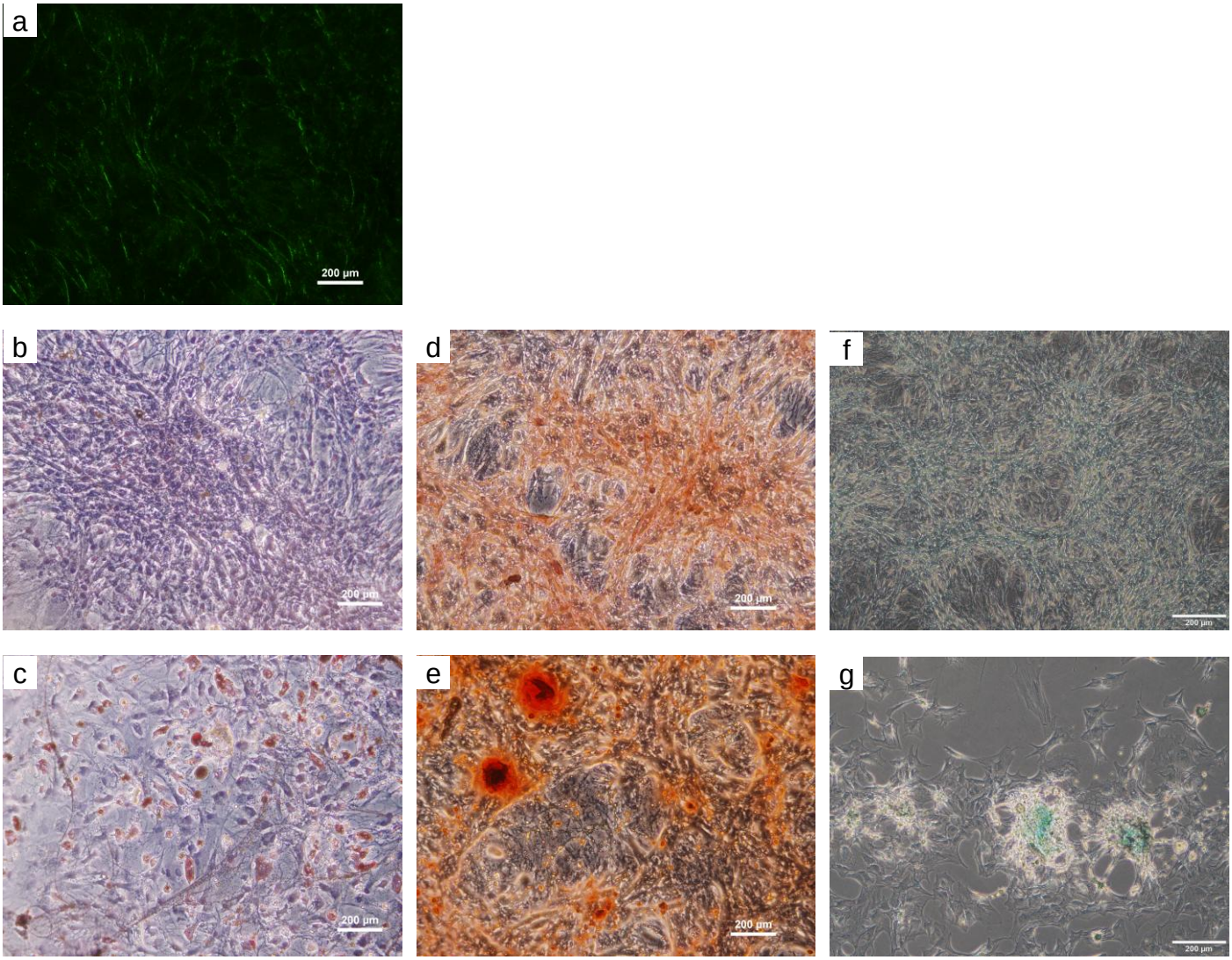

Figure III-3:Tri-lineage differentiation of GFP-expressing rat MSCs.

(a) Fluorescence imaging of GFP-rMSC in culture. Staining after tri-lineage differentiation : Oil Red O staining after culture in (b) proliferation medium and (c) adipogenic differentiation medium; Alizarin Red staining after culture in (d) proliferation medium and (e) osteogenic differentiation medium; Alcian Blue staining after culture in (f) proliferation medium and (g) chondrogenic differentiation medium.

the use of EVs confirm its potential as an alternative to cell therapy (Richter et al., 2019). Lyophilization, for example, could be an alternative to freezing as it seem to preserve EVs functionality and would allow easier transportation from the production facilities (Charoenviriyakul et al., 2018).

Experiments in rats

Autologous cell grafting faces major limitation to become a common practice for bone regeneration. The use of allogenic cells, if proven efficient, would remove the need for a bone-marrow aspiration before surgery, avoiding additional pain and complications. To go further, MSCs seem to disappear shortly after implantation (Gamblin et al., 2014), therefore allogenic ones may not be rejected as other types of long lasting tissue grafts. Even so, as "immunoprivileged" cells, they could avoid the allogenic reaction (Najar et al., 2016). If donor compatibility is no longer an issue, cell banks could provide a steady and reliable supply of MSCs, simplifying the quality control of the cells and reducing the amplification time.

The objective of this project was to study inflammation and immune reaction to allogenic cell implantation in an immunocompetent animal model. In rats, subcutaneous bone formation induced by bone marrow cells on CaP was obtain as early as 1990 by Ohgushi and colleagues. As a partnership with the Research Center in Transplantation and Immunology (UMR 1064, Nantes), green fluorescent protein (GFP)-transgenic Sprague-Dawley rats could be used for MSCs harvesting (Remy et al., 2010) allowing a follow-up of implanted cells' fate. Similarly to the experiment in mice, those cells were implanted subcutaneously on MBCP+ in non-GFP Sprague-Dawley or Lewis rats for 8 weeks and the explants were processed for histological analysis.

Results

The yield of MSCs retrieved from a rat was unpredictable but low overall. Consequently, implanted cells were generally at passage 4 or 5 with long culture time when implanted compared to human cells implanted in nude mice at passage 3. In culture, rMSCs isolated from GFP-transgenic Sprague-Dawley exhibited low fluorescence (figure III-3 a). Adipogenic (figure III-3 b,c) and osteogenic (figure III-3 d,e) differentiation with those cells were comparable to hMSCs differentiation. They formed proper adipocytes, with multiple lipid droplets appearing red in Oil Red O staining (figure Y.c), and mineralizing osteoblast, efficiently depositing calcium in the matrix stained with Alizarin Red S in figure Y.e. However, they failed to form a consistent spheroid necessary for chondrogenic differentiation with this kit (figure III-3 f,g). Cells tended to detach from the plastic with the differentiation medium, resulting in an incomplete cell layer (figure III-3 g) compared to the proliferating control (figure III-3 f). The Alcian Blue staining still revealed presence of secreted pools of proteoglycans, indicating at least partial differentiation.

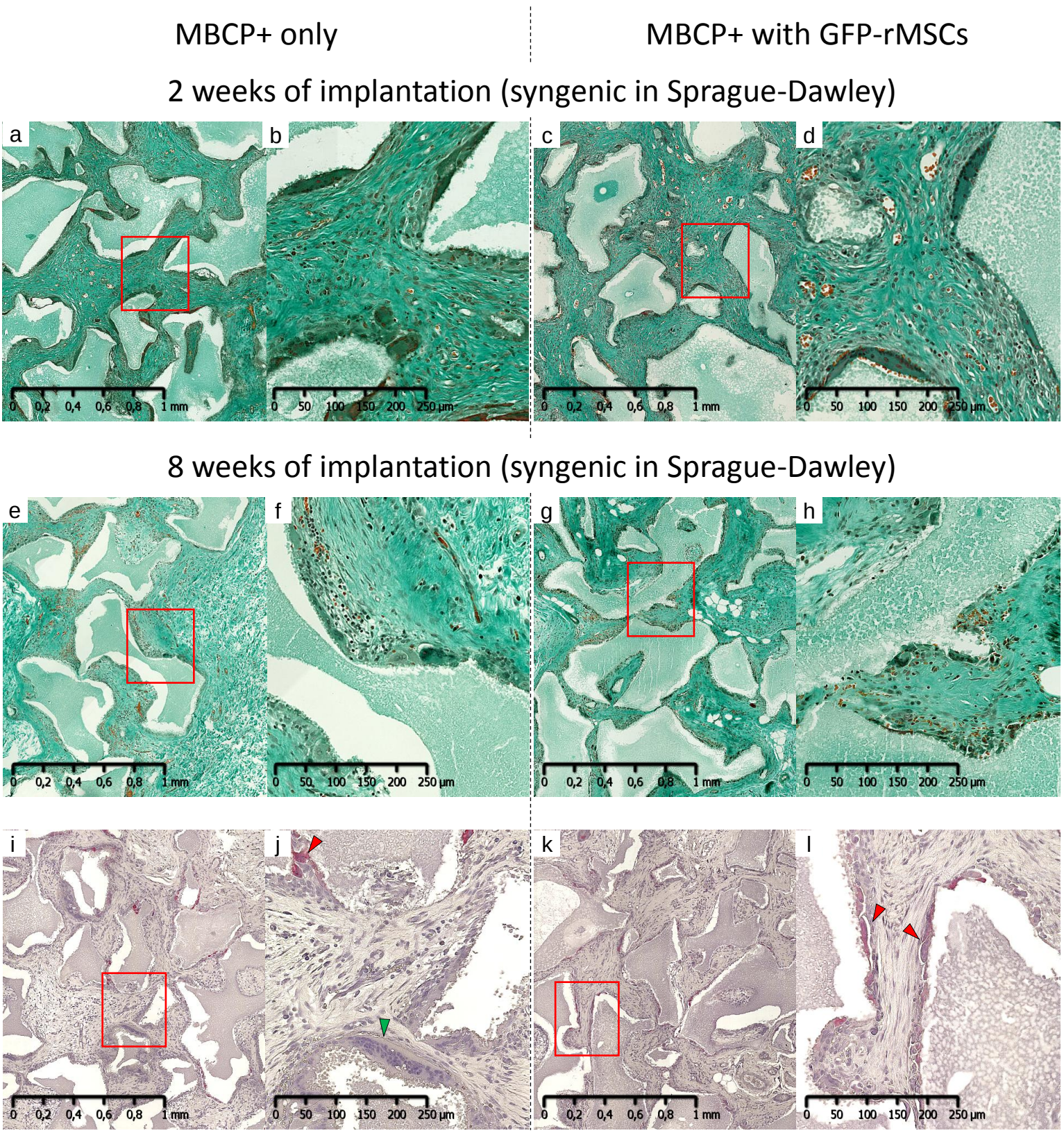

Figure III-4: Outcome of the first syngenic implantation experiment with rMSCs.

Histological analysis of subcutaneous MBCP+ implants with or without GFP-rMSCs in Sprague-Dawley rats (syngenic). Masson's trichrome staining after 2 weeks of implantation of MBCP+ alone (x2.5 (a) and x10 (b)) or with GFP-rMSCs (x2.5 (c) and x10 (d)). Masson's trichrome staining after 8 weeks of implantation of MBCP+ alone (x2.5 (e) and x10 (f)) or with GFP-rMSCs (x2.5 (g) and x10 (h)). TRAP staining for osteoclasts after 8 weeks of implantation of MBCP+ alone (x2.5 (i) and x10 (j)) or with GFP-rMSCs (x2.5 (k) and x10 (l)). ▼ = TRAP negative multinucleated giant cells; ▼ = TRAP positive osteoclasts.

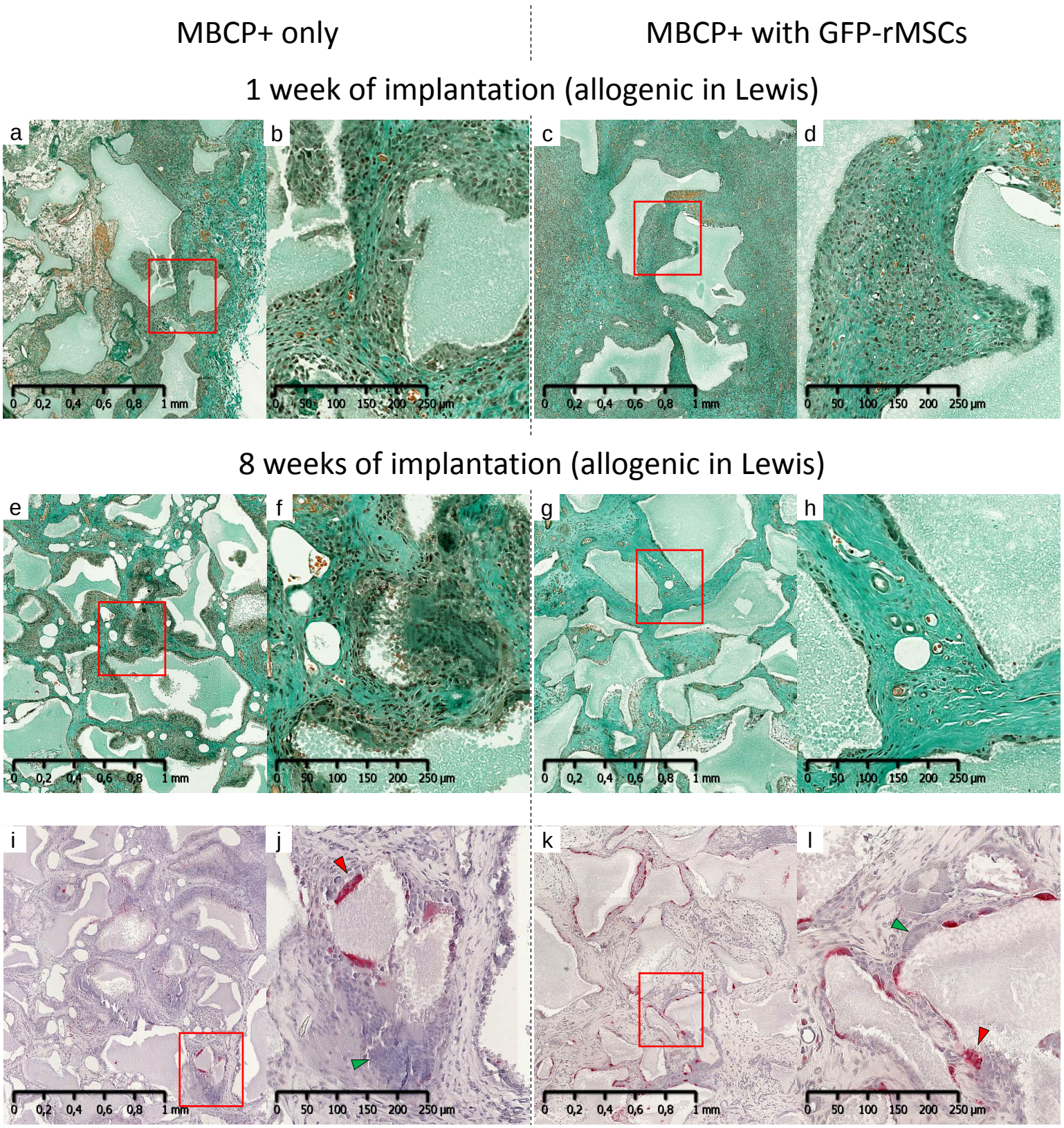

Figure III-5: Outcome of the first allogenic implantation experiment with rMSCs .

Histological analysis of subcutaneous MBCP+ implants with or without GFP-rMSCs in Lewis rats (allogenic). Masson's trichrome staining after 2 weeks of implantation of MBCP+ alone (x2.5 (a) and x10 (b)) or with GFP-rMSCs (x2.5 (c) and x10 (d)). Masson's trichrome staining after 8 weeks of implantation of MBCP+ alone (x2.5 (e) and x10 (f)) or with GFP-rMSCs (x2.5 (g) and x10 (h)). TRAP staining for osteoclasts after 8 weeks of implantation of MBCP+ alone (x2.5 (i) and x10 (j)) or with GFP-rMSCs (x2.5 (k) and x10 (l)). ▼ = TRAP negative multinucleated giant cells; ▼ = TRAP positive osteoclasts.

Cathepsin K TRAP

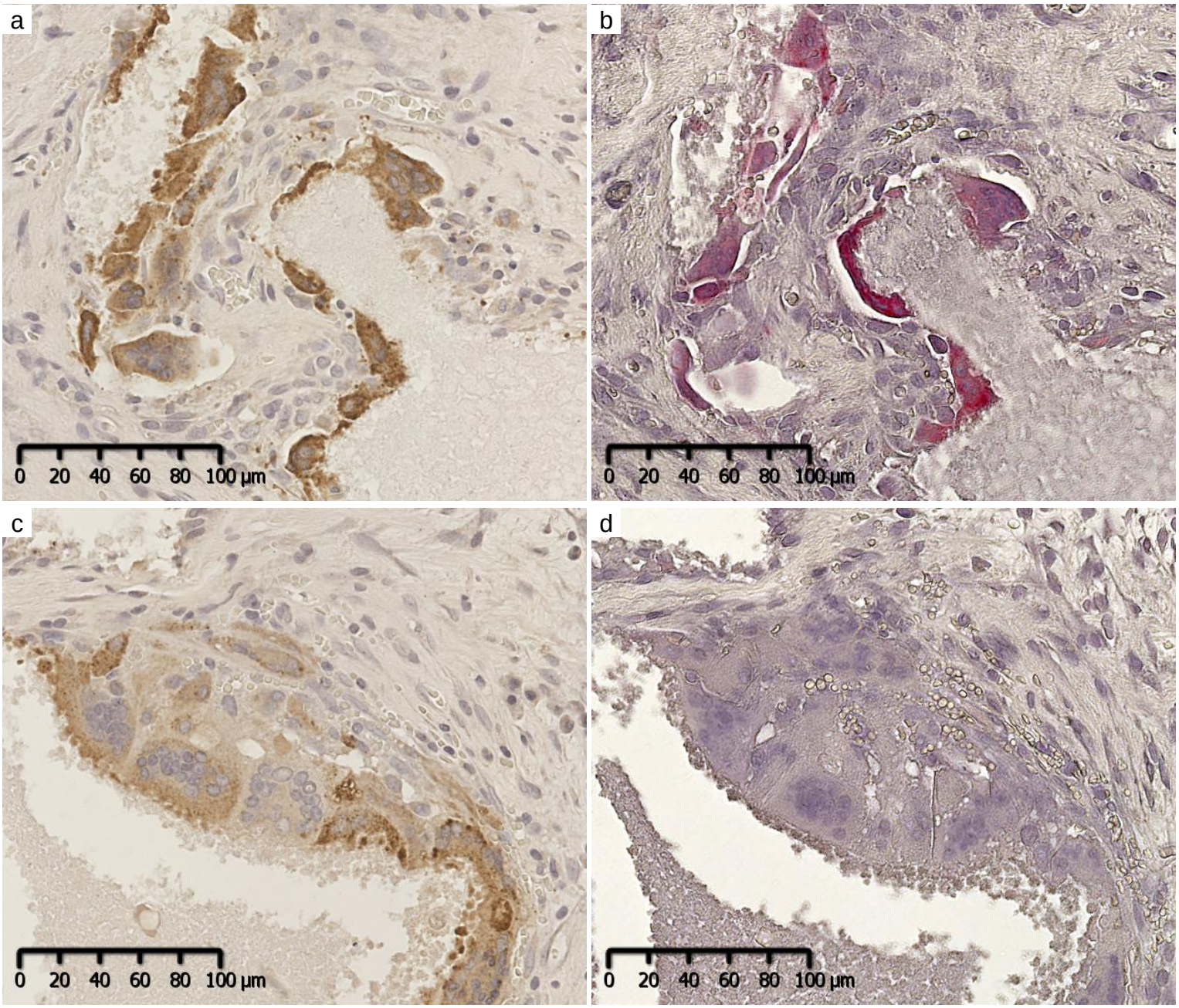

Figure III-6: Histological comparison of osteoclasts (a, b) and multinucleated giant cells (c, d) by Cathepsin K immunohistology (a, c) and TRAP staining (b, d).

The first experiment presents early (1 or 2 weeks) and late (8 weeks) outcomes of MBCP+ implantation with rMSCs isolated from GFP-transgenic female Sprague-Dawley rats either in a male non-transgenic Sprague Dawley (syngenic model, figure III-4) orin a male Lewis (allogenic model, figure III-5). Early explants were mostly used for optimization of immunohistochemistry protocols. The allogenic experiment was done first, and the early explants were collected after one week (figure III-5 a-d). The granules were not properly integrated in the tissue and processing was difficult. We choose to delay the first time point at two weeks for the syngenic experiment (figure III-4 a-d). In both cases, numerous cells surround the granules and some blood vessels are visible. In the allogenic explant, the first multinucleated cells can be observed (figure III-4 b,d), sign of host reaction against the granules of biomaterial. After 8 weeks of implantation, the implantation of MBCP+ alone, triggered a more intense inflammatory reaction in Lewis rats (figure III-5 e,f) revealed by the formation of larger and more numerous MNGCs. While the addition of rMSCs did not improved the already less inflammatory implantation in the Sprague-Dawley rat (figure III-4 g,h), it drastically reduced MNGCs aggregation on the granules in the Lewis. In both animals, implants with cells showed similar outcomes with no bone formation but reduced inflammation with dense collagen encapsulating the biomaterial. In addition, TRAP staining permit visualization of osteoclasts developing on the biomaterial. At 8 weeks, some could be observed in the conditions without rMSCs (figure III-4,5 i,j; red arrows) cohabiting with unstained MNGCs (green arrows). In both strains, the adjunction of rMSCs increased the number of TRAP-positive osteoclasts (figure III-4,5 k,l).

To go further in the characterization of the multinucleated cells forming on the biomaterial, Cathepsin K immunostaining was performed on slide series alongside TRAP staining (figure III-6). As expected, the Cathepsin K staining was intense on osteoclasts (figure III-6 a,b). Other multinucleated cells had various staining intensity, from none to almost comparable to TRAP-positive cells (figure III-6 c,d). While osteoclasts exhibited homogenous coloring, MNGCs mostly presented spots spread around their cytoplasm.

Following this first promising experiment, the number of implanted cells was double to 4 million and the implantation time was prolonged to 12 weeks to try to obtain bone formation in this model. Cells were harvested from both Lewis and Sprague-Dawley male rats previously used for implantation. This avoided implantation of cells from a female in a male animal, eliminated potential adverse effect of GFP-expression and allowed all possible combination of donor and receiver. As previously observed, implantation of MBCP+ alone triggered a way more inflammatory reaction in Lewis rat than in Sprague-Dawley (figure III-7 a, d). In Sprague-Dawley the tissue seemed mostly fibrous with limited formation of small multinucleated cells while in Lewis large MNGCs surrounded the granules of biomaterial with less organized matrix between cells. Implants containing rMSCs from a Sprague-Dawley did not change this outcome (figure III-7 b,e). As a syngenic graft, it led to somehow denser collagen matrix, but the conditions were not favorable enough to induce bone formation. As an allogenic graft, it did not reduce the inflammation and the apparition of MNGCs, in

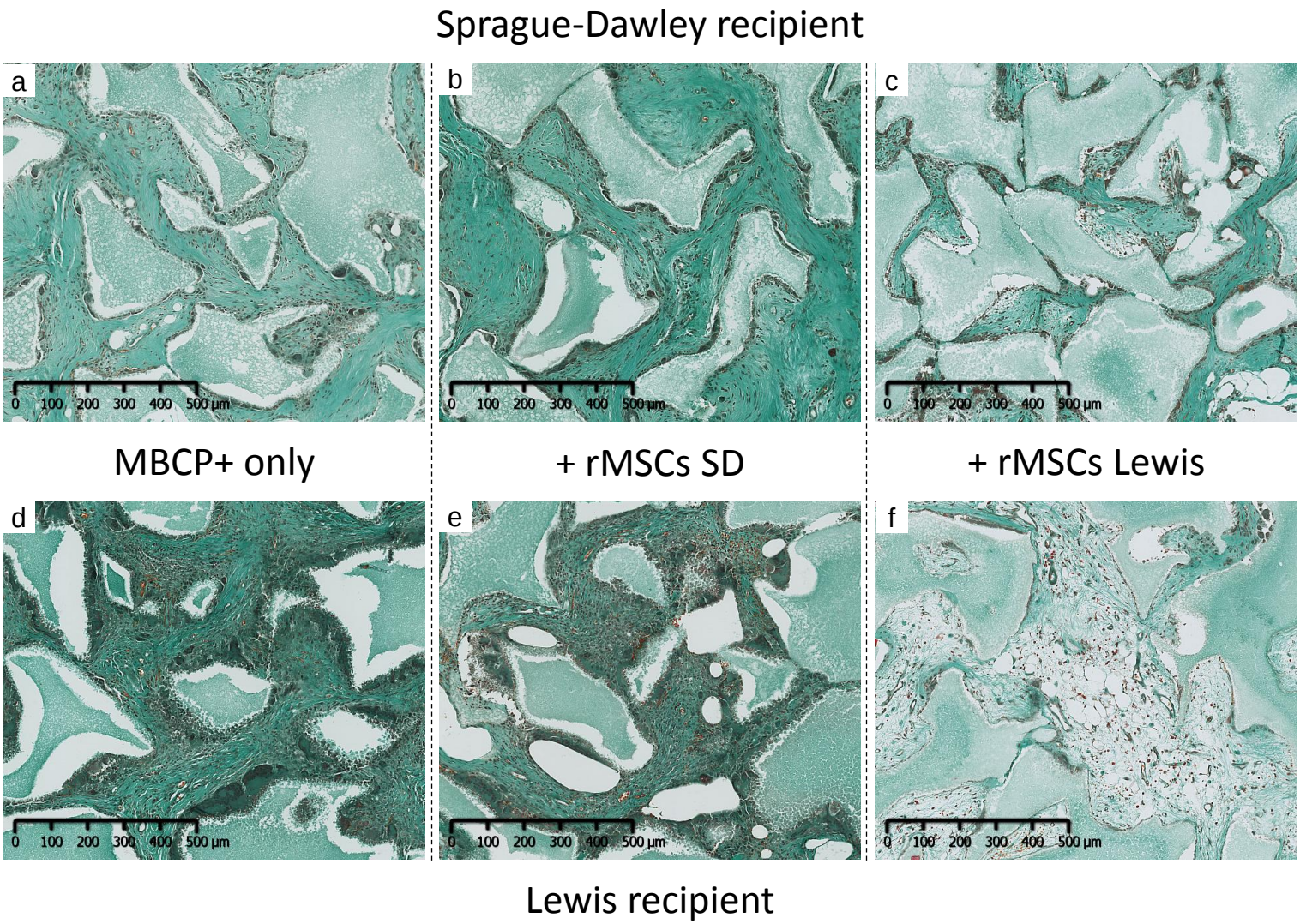

Figure III-7: Outcome of the second implantation experiment with rMSCs

Masson's trichrome after 12 weeks of subcutaneous MBCP+ implants with or without rMSCs from Lewis or Sprague-Dawely (SD) rats, in animals of both strains. Implants from Sprague-Dawley rats (a) without cells, (b) with rMSCs from Sprague-Dawley rats or (c) with rMSCs from Lewis rats. Implants from Lewis rats (d) without cells, (e) with rMSCs from Sprague-Dawley rats or (f) with rMSCs from Lewis rats.

contradiction with the observation from the first experiment. Regarding the implantation of rMSC from Lewis (figure III-7 c,f), it did not perform better than the biomaterial alone in a Sprague-Dawley rat but it clearly suppressed the intense inflammation normally observed in Lewis. However, it produced a looser tissue compared to the syngenic Sprague-Dawley implantation.

Discussion

In retrospect, the StemPro® kit being designed for human cells was suboptimal with rat bone-marrow cells but the differentiation obtained were sufficient to use the cells with confidence. Flow-cytometry for stem cell markers would be needed to fully characterize those cells, confirm their stemness and evaluate their homogeneity. However, the culture conditions, specifically the choice of serum and the addition of FGF2, should have been better evaluated to optimize the yield of isolation and the proliferation speed. Having cells at lower passages in faster exponential phase would have been optimal for implantation, as targeted in clinical protocols.

The histological observations drew our attention on MNGCs as potential inflammatory counterparts to osteoclasts, leading to the *in vitro* work in the first chapter. Their formation was systematically associated with implant failure to induce bone while our most promising conditions reduced their incidence and promoted osteoclasts. Obviously, given the limited number of animals and the absence of bone formation in those pilot experiments, little conclusion could be drawn for those results. The immune reaction to the biomaterial itself was different from one strain of rat to the other, complicating the interpretation of the results. However, this is not surprising given that genetic differences are known to influence the osteogenesis from CaP materials as showed in mice by Barradas et al. (2012). Our observations in Lewis rats from the first to the second experiment were drastically contradictory, suggesting differences even between individuals of the same strain.

Despite the immunological specificities of MSCs, allogenic cells are expected to provoke some immune response that could interfere with the regeneration process. Other groups also explored these questions in animal models. In Fischer 344 rats, Chatterjea et al. (2014) demonstrated a T and B immune reaction to cells from Wister but not from other Fischer 344, leading to ectopic bone formation on BCP only with syngenic cells. They could even restore osteogenic potential of allogenic cells by administrating an immunosuppressor (FK506). Also in rats, Longoni et al. (2020) compared the efficacy of syngenic, allogenic and xenogenic MSCs in a model of endochondral bone regeneration, where pre-differentiated chondrocytes are embedded in a collagen matrix and implanted in a critical size defect of the femur. Here again, syngenic cells performed better but allogenic ones triggered a milder immune reaction than xenogenic cells, resulting in defect bridging in 2 out of 8 animals. In humanized NSG mice, Rapp et al. (2018) reported better femoral defect repair with

autologous hMSCs than allogenic ones. This was also associated with a moderate immune reaction to allogenic cells while autologous cells did not trigger any inflammatory response. Overall, autologous cells remain the most efficient option for bone regeneration.

Material and Methods

Cells

All cell culture steps were performed under sterile conditions. Cells were incubated in a humid atmosphere at 37°C, 5% CO_2. MSCs from a single healthy 22-year-old male donor were used for of all implantation experiments and EVs isolation. The medium for hMSC culture consisted of αMEM (22571020, Gibco) containing 1% Penicillin/Streptomycin mixture (P/S, CABPES010U, Eurobio) and 5% heparinized pooled human platelet lysate. EVs isolation was performed on two T500 flasks of 80% confluent MSCs for each condition. Cells were either untreated, treated 4h with 0.1µM staurosporine or cultivated in 2% dioxygen. After 48h, the media was collected and concentrated on 3kD filters (Amicon Ultra-15, Millipore). Concentrated samples were run through exclusion chromatography columns (qEVoriginal, Izon) following the manufacturer protocol. All fractions theoretically containing EVs were pooled and concentrated down to 100µL on a 100 kD filter (Amicon Ultra-4, Millipore).

GFP-transgenic Sprague-Dawley rats provided by the UMR 1064 and non-GFP rats included in the implantation protocols were dissected after euthanasia. Femurs and tibias were cleaned from excess flesh and transported out of the animal facilities in 50mL falcon tubes of αMEM. Under sterile conditions, the bones were quickly dipped in 70% ethanol to minimize contamination. Epiphyses were cut and the medullary cavity was flushed with approximately 2 mL of αMEM, 1% P/S, 10% Fetal Bovine Serum (FBS, Eurobio). The medium was strained on a 70 µm filter to remove bone debris and diluted in the appropriate volume of the same medium to be cultivated in flasks. Adherent cells were amplified and considered rMSCs for those experiment. Isolated rMSCs were tested for osteogenesis, chondrogenesis and adipogenesis using StemPro® corresponding kits (Gibco) following the manufacturer's recommendation for culture and staining. Calcium deposits from osteoblasts were observed by Alizarin Red staining, glycosaminoglycans secreted by chondrocytes were visualized with Alcian Blue and lipid droplets in adipocytes were stained with Oil Red O.

Biomaterial

Granules (0.5-1 mm) of MBCP+ were provided by Biomatlante. Aliquots of 50 mg were isolated in 0.5 mL tubes and sterilized by autoclaving (121°C, 30 min). Preincubation in culture media was performed for 24h. One hour before implantation, the granules were washed twice in PBS and combined with cells, CM or EVs in 100µL media.

Animals

These experiments were performed under European recommendations (2010/63/UE), evaluated and authorized by the local ethical committee. All animals were purchased from Janvier Labs. Six weeks old NMRI nude female mice were used (project authorization #6575). Ten weeks old Lewis and Sprague-Dawley rats from both sexes were used (project authorization #14759). As analgesic, animals received 30 minutes before surgery an intramuscular injection of buprenorphine (0.03 mg/kg). The anesthesia was initiated in an induction chamber by inhalation of isoflurane 3.5% at 1 L/min and maintained at 2.5% in a mask during the procedure. During anesthesia, the temperature of the animal was maintained by a heating plate. Incisions were realized on the back of the animal, up to two for mice and four for rats. The skin was carefully detached from underlying tissue to create a pocket for the implant. After implantation, the skin was sutured with Filapeau® 4/0 (Péters Surgical). Animals were particularly looked after for 5 days after surgery to ensure proper healing of the incisions. Additional analgesic injection could be performed if any signs of pain were noticeable. After 1, 8 or 12 weeks of implantation, animal were anesthetized with isoflurane as previously described and sacrificed, by cervical dislocation for mice and decapitation for rats.

Histology

Explants were retrieved after euthanasia and immediately fixed in 4% formol solution for 5 days. Decalcification was performed in a pH 7.4 solution of 4.13% ethylenediaminetetraacetic acid (EDTA) and 0.2% paraformaldehyde in 1X PBS by a microwave apparatus (KOS Histostation, Milestone Med. Corp.). Samples were dehydrated in baths of increasing ethanol percentage followed by a butanol bath in an automated dehydration station (STP-120, Microm Microtech) and embedded in paraffin (Histowax; Histolab) in an embedding station (EC-350, Microm Microtech). Thin sections of 3 µm were cut on a microtome (RM2255, Leica). Masson's Trichrome and TRAP staining were performed on an automated staining station (HMS-740, Microm Microtech). For Cathepsin K detection, slides were deparaffinised and incubated overnight at 60°C in Tris EDTA pH=9 buffer for antigen retrieval. Endogenous peroxidases were blocked by incubating the slides in H_2O_2 3% for 15 min and aspecific sites were saturated by a blocking solution (Goat Serum 2%, BSA 1% in TBS pH7.6, Tween 0.05%). The primary antibody (rabbit polyclonal anti-Cathepsin K, Abcam, ab 19027) was diluted to 1/4000 in the blocking solution and applied on the slides for 2 hours at room temperature. The secondary antibody (biotinylated goat anti-rabbit, Dako, E0432) was diluted to 1/400 and applied for 1 hour at room temperature. Staining was revealed by incubation with Streptavidin/Horseradish Peroxidase conjugate (Dako, P0397) followed by a 3,3' Diaminobenzidine solution (DAB Quanto, Thermo Scientific, TA-125-QHDX). Slides were scanned using a NanoZoomer (Hamamatsu).

Chapter IV:
General Discussion

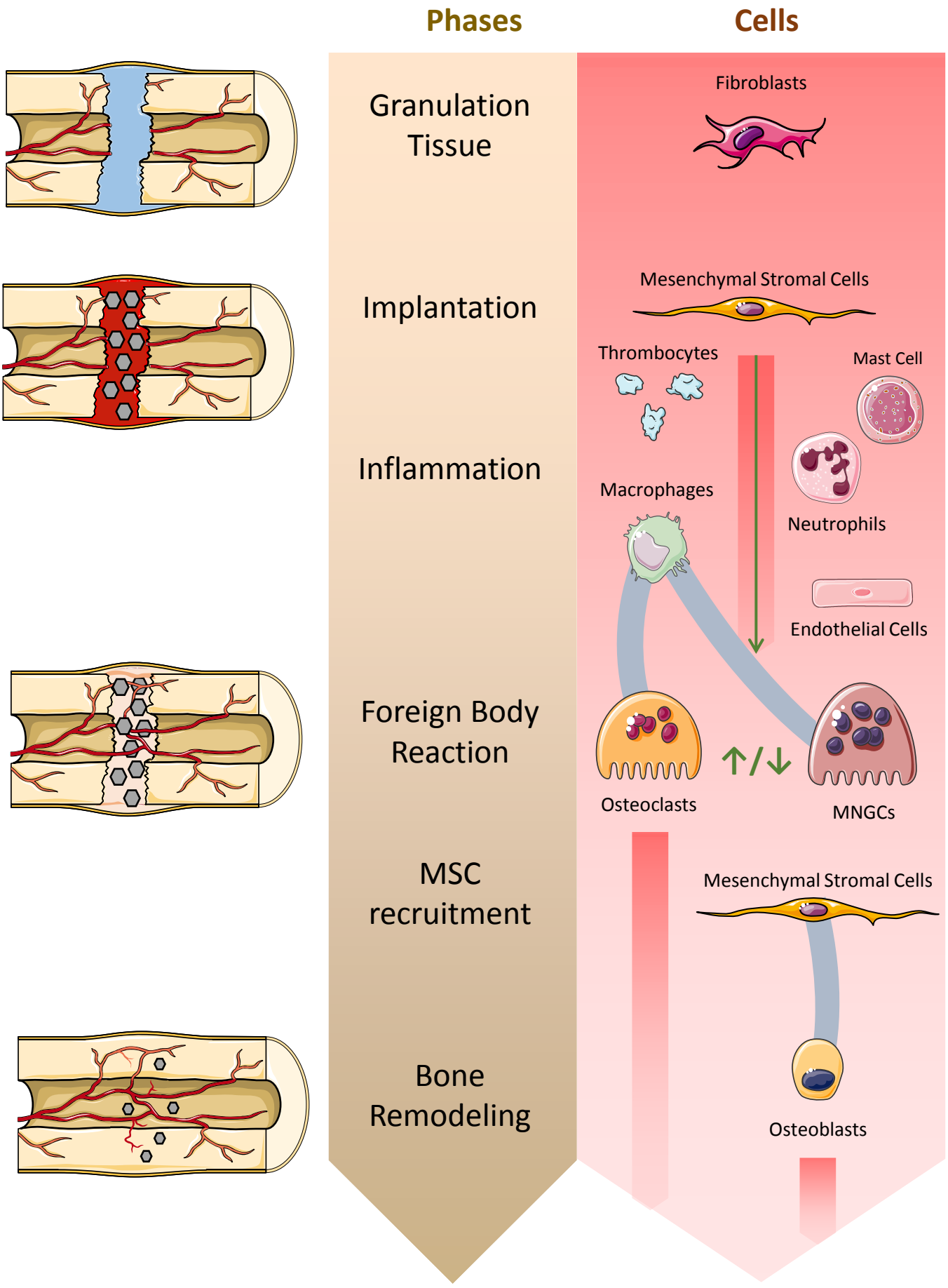

Figure IV-1: Hypothetical mechanism of bone regeneration by MSC-CaP implantation.

On the mechanism of bone regeneration by MSC-CaP

Just as in physiological fracture healing, the sequencing and timing of events are key elements to the success of bone regeneration following cell therapy (Figure IV-1). At the time of implantation, the fracture has not evolved for several months and remains at the state of a fibrocartilage callus. Surgeons remove the fibrous tissues before placing the biomaterial granules, disrupting newly formed vessels. This triggers an inflammatory reaction initiating wound healing combined with a foreign body reaction to the implanted materials. MSCs are known for their immunomodulatory capabilities and should help mitigate the inflammation and modulate the reaction to the material. Apoptosis of these cells while facing the hypoxic, nutrient-lacking and inflammatory environment of implantation participate in their unique regenerative ability.

Modulation of macrophages polarization seems essential (Horwood, 2016). M1 macrophages are often associated with osteoclast formation and bone resorption while M2 macrophages are linked to tissue regeneration. In our hypothetical model, both could be important at different times and MSCs could help transition smoothly and at the right moment from one to the other. Incidentally, Oya et al. (2018) associated osteoclasts with M1 macrophages stimulation and MNGCs with the M2 phenotype in a mice model with a conditional knockout of the TNF receptor associated factor 6. Early on after implantation, an intense inflammatory phase is essential to recruit immune cells to the site of implantation, particularly monocytes/macrophages, and initiate revascularization. Zhao et al. (2020) even showed that reducing the surgical trauma for CaP intramuscular implantation in mice was deleterious for subsequent bone formation. These observations coincide with the basics of physiological wound healing based on the interactions between factors released by damaged cells, immune cells and proteins from the blood.

In this acute inflammatory phase, recruited macrophages should first polarize mostly towards an M1 phenotype. This subtype is reportedly favoring osteoclast development by releasing known osteoclastogenic factors such as TNFα, IL-1β or IL-6 as demonstrated in inflammatory bone remodeling diseases such as orthodontic tooth movement (He et al., 2015) or bisphosphonate-related osteonecrosis of the jaw (Zhang et al., 2013). Here, our data suggest that MSCs could directly enhance the formation of osteoclasts, through CXCR-1 and -2 signaling, and inhibit fusion of MNGCs by an unknown mechanism. We also observed a potential upregulation of *RANKL* at the transcriptional level in apoptotic MSCs that did not play a role in our *in vitro* system but could be essential *in vivo*. RANK-L is also found soluble in the plasma and can be expressed by T lymphocytes. MSCs could also indirectly alter the osteoclast/MNGC balance by influencing other immune cells. For example, mast cells could be the main producers of IL-4 and IL-13 during acute inflammation, leading to the formation of MNGCs (Chu et al., 2020). However, MSCs from umbilical cord blood were shown to suppress mast cell degranulation through PGE_2 and TGFβ secretions (Kim et al., 2015), potentially limiting MNGC formation in our system.

Osteoclasts	Markers (Miron et al, 2016)	MNGCs
+++	Calcitonin Receptor	-
+++	TRAP	+
+++	RANK	-
+++	Cathepsin K	+/-
+	CD68	+++
-	CD86 (B7-2)	+++
+	CD98	+++
-	CD206	+
+++	MMP9	+
-	HLA-DR	+++

Table IV-1: Differentiating markers between osteoclasts and MNGCs (Miron et al., 2016). Key markers differentiating both cell types according to Miron et al. are in red.

In later stages, the transition from M1 to M2 macrophages is essential to prevent chronic inflammation and osteoclast over-activation, and permit bone formation (Pajarinen et al., 2019). Osteoclast formation to the detriment of MNGCs would in term push the balance towards bone remodeling signals rather than fibrous tissue healing. As previously mentioned, osteoclasts can indirectly, by partially dissolving the CaP material (González-Vázquez et al., 2014), or directly, through secretion of coupling signals (Sims and Martin, 2020b), recruit osteoprogenitors and promote their differentiation into bone forming osteoblasts. On the contrary, MNGCs would not be able to efficiently dissolve the material and therefore be detrimental to tissue healing by secreting reactive oxygen species and other degradation agents. The impact of MSCs' secretions on osteoclasts phenotype remains to be fully explored. We could postulate that osteoclasts with low resorbing abilities but highly communicating with immune and bone cells are favored. Macrophages themselves could participate in the recruitment and differentiation of skeletal stem cells, through secretions of factors such as OSM.

More than just a vehicle for the cells, the material can also greatly influence macrophage polarization (Li et al., 2020), their secretion profile (Wang et al., 2018c) and their potential to fuse into osteoclasts (Davison et al., 2014a). In our experiments, CaP materials that were previously reported osteogenic, and were selected as the most suitable for bone regeneration, were also better support for osteoclastogenesis *in vitro*. These results will hopefully be confirmed by a correlation between osteoclastogenesis and bone formation *in vivo*, in a model of subcutaneous implantation in nude mice. While this model is easy to perform and analyze, it is far from clinical applications in bone defects. As observed in the third chapter with this model, MSCs' secretions could not recapitulate the implantation of whole cells and we could not reach bone formation in immunocompetent rats.

On osteoclasts and MNGCs diversity

Osteoclasts are now viewed as way more than specialized cells resorbing bone matrix. They are highly involved in communications with other bone cells to regulate bone mass and participate in pathological bone loss in several diseases. Accumulating evidences point them out as the key link between inflammation and bone formation in MSC-CaP induced bone formation. In this work, we showed that (1) MSCs under apoptotic stress can release pro-osteoclastogenic factors, (2) osteoclasts affinity for various CaP materials *in vitro* seems correlated to the osteoinductivity of these materials *in vivo* and (3) MNGCs could be the inflammatory counterpart to osteoclasts, blocking the transition to bone formation. These findings reinforce our working hypothesis but question the phenotypic specificities of the osteoclasts formed on CaP materials and their connections with MNGCs.

MNGCs are globally understudied compared to osteoclasts and conflicting results emerge on their characteristics, especially when comparing *in vivo* observations and *in vitro*

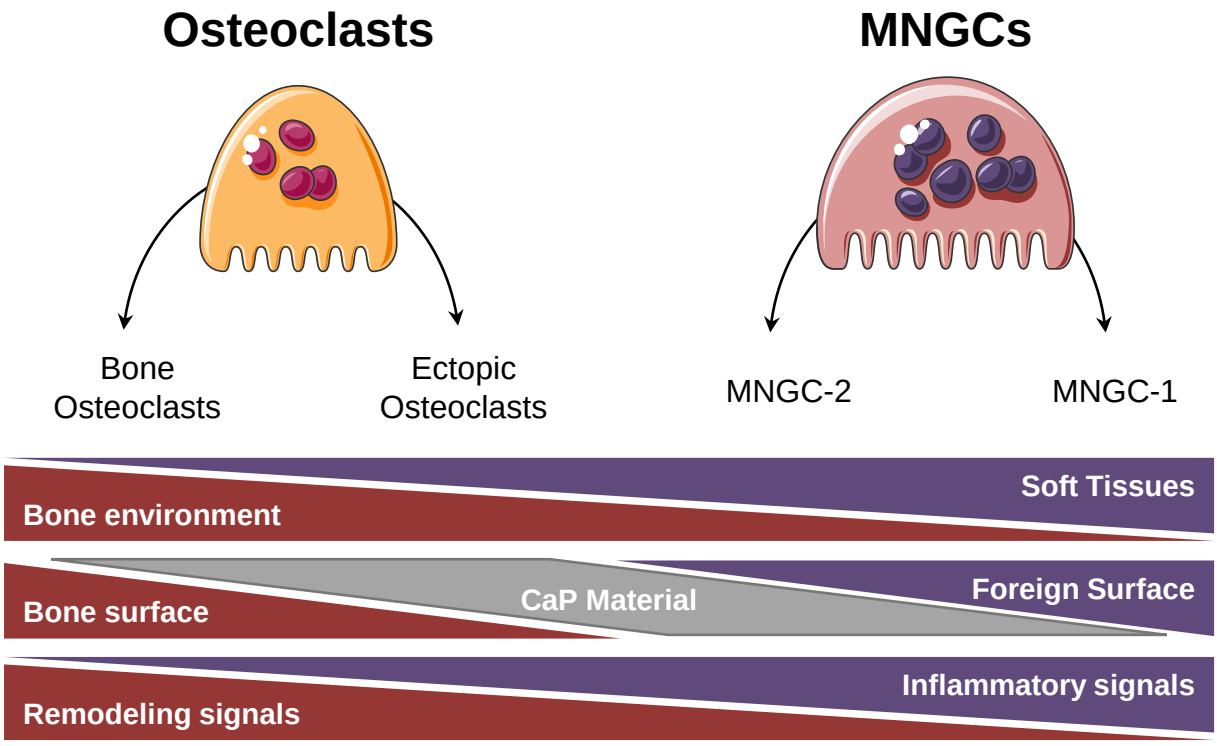

Figure IV-2: Possible continuum between osteoclasts and MNGCs.

models. Miron et al. (2016) previously reviewed the known differences between MNGCs and osteoclasts around biomaterials for bone regeneration (Table IV-1). They suggest the use of CALCR and RANK as markers of osteoclasts and CD86 and HLA-DR for MNGCs. In our *in vivo* observations on subcutaneous implants in rats, we associated all TRAP positive multinucleated cells with osteoclasts. This is based on previous work from the lab where the use of an anti-RANK-L (Gamblin et al., 2014) or clodronate (Davison et al., 2014b) reduced the occurrence of TRAP positive cells but also diminished the local expression of osteoclasts differentiation markers such as NFATC1 or CALCR. In contrast, we considered MNGCs as always TRAP negative. MNGCs were also Cathepsin K positive but with an uneven and less intense staining than osteoclasts. In previous reports, slightly TRAP positive MNGCs were described around implanted HA particles in a rat calvaria defect (Dersot et al., 1995). The authors differentiated these cells from osteoclasts by their unresponsiveness to salmon calcitonin, inducing the retraction of resorbing osteoclasts from the bone surface. In the future, multinucleated cells observed around biomaterials need to be better characterized by immunohistological labeling to confirm or deny the presence of osteoclasts. We could be mistaking these TRAP positive cells for another type of MNGCs. We also tried unsuccessfully to analyze osteoclasts and MNGCs population by flow-cytometry based on published protocols (Madel et al., 2018). As pointed out by the authors, large cells were difficult to detach and mostly lost in the process.

To reinforce this possibility and in line with previous studies (ten Harkel et al., 2015; Khan et al., 2013, 2014), our *in vitro* models of MNGCs were efficiently TRAP stained and RNA expression of the enzyme could be detected. Contrastingly, McNally and Anderson (2011) did not detect TRAP by Western-blotting in their very similar model. Regarding other markers, the expression patterns of Cathepsin K and MMP9 were very similar to what was already reported, with an average 10-fold lower RNA expression of both proteins in MNGCs. In contradiction with these articles, the expression of DC-Stamp was 2 to 4-fold higher in MNGCs than osteoclasts in our experiment. It is important to note that our results came from a rapid gene screening to give an idea of the phenotype of the cells, and therefore were not replicated to give a statistical analysis. The small differences observed with the literature could also result from the difference in species as Khan et al. used bone-marrow mononuclear cells from C57/BL6 mice. However, none of the studies with MNGCs derived from rat macrophages *in vitro* used TRAP staining.

Overall, the phenotypes and surface markers of multinucleated cells on the surface of implanted materials need to be better characterized to improve our understanding of the foreign body reaction and the differentiation potential of myeloid cells. *In vitro* models can also help predicting the characteristics of stereotypical cells by intense, one-sided cytokine stimulation but cannot render the complexity of possible phenotypes *in vivo* where multiple signals coexist. As previously discussed, MNGCs could have various phenotypes and role in different stages of the foreign body reaction. Given their common origin and the difficulties to distinguish one from the other, MNGCs and osteoclasts could be more related than

previously thought (Figure IV-2). Their specialization could depend on a number of environmental factors including stimulatory molecules and growth surface. Similarly to the continuum of monocyte phenotypes and the macrophage polarization model that keeps getting more complex as our knowledge grows, multinucleated cells could have a range of linked and interconnected possible phenotypes rather than distinct and irreversible ones. However, *in vitro* differentiated MNGCs seem unresponsive to RANK-L stimulation (ten Harkel et al., 2015). Conversely, IL-4 inhibits osteoclastogenesis (Wei et al., 2002) but only partially impairs bone resorption capacities and does not inhibit osteoclasts-specific gene expression in mature osteoclasts (Cheng et al., 2011). Even if the cells cannot transition from one to the other, MNGCs and osteoclasts could still cohabitate in the environment of implantation. Their ratio of formation could then determine the fate of the procedure.

On *in vitro* models and clinical predictions

Overall, *in vitro* studies on MNGCs suffer from the same limitations as other cell culture experiments. As for osteoclasts, the surface is highly influencing MNGCs formation *in vivo*. While plastic dishes are a foreign surface for the cells, they are not representative of every implanted material, definitely not the ones used in bone regeneration. Also, these cells appear in an intense inflammatory environment, simplified to only a couple of cytokines *in vitro*. The development of 3-dimentional and multi-cellular culture systems would greatly improve our understanding of MNGC formation and their interactions with other immune cells. In the case of osteoclasts, cultures on dentin or bone slides can be used and co-cultures with osteoblast progenitors are possible but we are still far from a reliable model of bone remodeling (Kohli et al., 2018). Our collaborators in Vienna previously suggested using a multitude of complementary approaches *in vitro* and *in vivo* to evaluate the suitability of new materials for bone regeneration therapies (Kampleitner et al., 2018). Notably, they routinely use co-cultures of osteoclasts precursors from the bone marrow and primary osteoblasts from the calvaria of BALB/c mice. Addition in the culture media of 1α,25-Dihydroxyvitamin D3 and prostaglandin E2 is sufficient for osteoblast to express osteoclastogenic factors and obtain mature resorbing cells. To match their experiments for this project, we tried to performed co-cultures of human cells based on previous protocols (Heinemann et al., 2011). Our few attempts were promising but osteoclasts formed were very difficult to visualize with classical staining techniques, as they fused below the MSC layer. Optimization of specific microscopy techniques would be required to further analysis such systems.

A major parameter of *in vitro* approaches using human cells is the specificities associated to individual donors and cell subtypes. Using multiple donors strengthened the conclusion of our experiments when a strong trend emerged. However, it also diminished the reproducibility and thus did not improve the statistical power, as we could have expected with a higher number of replicates. We experienced variability in both MSCs (proliferation, mineralization, secretion and resistance to stresses) and CD14+ monocytes

(survival to freezing, differentiation potential). The latter were isolated in-house from whole blood samples and could have been subjected to changes from one batch to the other. The purity of isolated cells is obviously critical for reproducibility. While we usually got over 95 % CD14+ cells with our protocol, as detected by flow cytometry; one manipulation resulted in some lymphocyte contamination that correlated with fewer osteoclast formation and we could not exploit the data produced with these cells. In addition, the subsets of monocytes are known to have different secretion profiles and differentiation potential *in vitro* (Boyette et al., 2017). The impact of CD16 expression on the osteoclast differentiation potential seems controversial. While Bolzoni et al. (2017) reported that $CD16^{+}$ monocytes from myeloma patients had a higher osteoclastogenic potential, other studied showed the opposite (Xue et al., 2020). Additionally, intermediate monocytes ($CD14^{high}$, $CD16^{low}$) formed larger concanavalin A-induced MNGCs compared to classical ($CD16^{-}$) or non-classical ($CD16^{high}$) ones (Champion et al., 2018). In our experiments, all CD14-positive cells were collected without secondary selection based on CD16. From one patient to the other, or from one isolation procedure to the other, the ratio of each subtype could have been different, probably biased towards classical monocytes expressing more CD14. A precise sorting would be interesting to identify if a subset is more responsive to biomaterial surfaces or secretion from MSCs. Leaning in that direction, Boersema et al. (2016) compared the response to biomaterials of monocytes from healthy and obese individuals. Overall, the obese subjects tended to have less classical monocytes, even though the differences were not statistically significant, and these cells exhibited a more inflammatory response to biomaterials. These results suggest the importance of monocytes subsets in the response to implanted materials but this may not be the unique parameter associated to monocytes directing the implantation outcome.

On the other hand, MSC characteristics were controlled by the supplier and met the minimal criteria. We checked the batches again for tri-lineage differentiation capacity before use and still observed disparities. In addition to the differences between MSCs from various tissues, donor variability is often observed. Despite matching the minimal criteria for the major surface markers, MSCs prepared from the bone marrow are often composed of several subpopulations of heterogenic phenotypes that can be distinguished by flow cytometry (Rostovskaya and Anastassiadis, 2012). As each subtype seem to have lineage specificities, their ratio could influence what we observed on the pooled population. In ATSC (Liu et al., 2017) and in bone marrow MSCs (Siegel et al., 2013), the age of the donor seem to impact negatively the proliferation and differentiation abilities of the cells. Siegel et al. (2013) also noted significant differences in growth and surface markers between MSCs from male and female donors. Additionally, Kowal et al. (2020) found correlations between features of cell morphology and expression of membrane markers, suggesting new tools to predict MSCs' phenotype. As our knowledge on MSC subtype grows, new criteria will be needed to identify precisely the most efficient cell for clinical applications. In addition to the complexity of MSC biology, Stroncek et al. (2020) showed that MSCs isolated in different

laboratories from the same bone marrow exhibited significant differences, highlighting the necessity to homogenized culture conditions.

In the first part, we had to focus on the MSC donor that gave the most drastic effects for the experiment with neutralizing antibodies. This choice was based on a general trend from five donors but one could consider that we singled-out an outlier that matched our hypothesis. This was the same donor used in the second and third chapters, for both *in vitro* and *in vivo* experiments, as it induced extensive bone formation in pilot studies. As donor variability in inducing bone formation was previously reported in pre-clinical studies (Brennan et al., 2014), it would be interesting to see if *in vivo* potency could correlate with osteoclastogenic properties *in vitro*. Janicki et al. (2011) previously reported that mineralization *in vitro* did not correlate with bone formation *in vivo*. However, the doubling time of MSC at the time of implantation seemed to be critical, suggesting that cells with a high anabolism are needed. Finding good prediction tools for bone formation would be of primary importance for clinical applications. Other markers of healing from blood samples are evaluated by our colleagues from the ORTHOUNION project (Granchi et al., 2019). They notably reported C-Propeptide of Type I Procollagen and C-terminal telopeptide of type-I collagen as discriminating between healed and unresponsive patients. Future predictions will most likely rely on a range of measured parameters before surgery and throughout the healing phase. These analyses could implicate characteristics of expanded MSCs (markers, differentiation, doubling time etc.), monocytes subtypes and other immune cells from the blood for early predictions, and levels of specific circulating proteins associated to CT scans to follow the healing progress.

Conclusion & Perspectives

Hopefully, this work reinforces the hypothesis that osteoclasts are the pivotal players in bone regeneration induced by the combination of CaP materials and MSCs. Previously, TRAP positive cells were observed around implanted biomaterials, their number correlated with bone formation. Conversely, their differentiation as well as subsequent bone formation were inhibited by an anti-RANK-L antibody (Gamblin et al., 2014). Here in Chapter I, we showed that secretion from MSCs seeded on the biomaterial favored osteoclastogenesis *in vitro*. As for *in vivo* observations, the cells were rapidly undergoing apoptosis. This phenomenon of apoptosis, modeled by a staurosporine treatment, participated in the pro-osteoclastogenic effect of MSCs' CM by increasing secretions of IL-8/CXCL-8, GROα/CXCL-1 and potentially GROβ/CXCL-2 and GROγ/CXCL-3. Concurrently, CM from apoptotic MSCs inhibited the formation of IL-4-stimulated MNGCs. Commonly associated with prolonged inflammation and fibrosis, these cells could be osteoclasts' counterpart in unsuccessful implantation as observed in our experiment with rats. In Chapter II, we observed better osteoclasts differentiation on 20/80 HA/β-TCP biomaterial *in vitro* compare to other CaPs. Also, pre-incubation media from BCPs (20/80 and 60/40) seemed to enhance MSC mineralization potential. These results were quite similar in our

collaborators' experiments with mice cells. An ongoing experiment will evaluate osteoclastogenesis and bone formation produce by the various CaP tested in subcutaneous implantation in nude mice. In Chapter III, the different approaches we used in vivo were not producing bone, highlighting the limitation of the subcutaneous model and the difficulties to outperform MSCs' implantation.

Identifying mediators of MSCs communication towards host cells is the first step towards rationally designed cell-free therapies. This knowledge of biological mechanism has to be combined with improved understanding of the chemistry of material integration and degradation. A complex biomaterial would be ideal, most likely a composite of CaP, for its mineral composition and osteoconductive properties, and a polymer to ensure cohesion of the implant and carry osteogenic factors. Mimicking the dual organization of bone, with a mineral phase of hydroxyapatite and an organic phase based on collagens, is one of the promising approach for composite materials (Kołodziejska et al., 2020). In the case of large and complex defect, this material could be supported by, or coated on, a more stable metallic structure. The use of 3D printing could be both an opportunity to personalize the shape of the implant and a constrain to use materials with specific physical properties (Chen et al., 2020). The osteogenic factors carried by the polymer should contain pro-osteoclasts and/or anti-MNGCs cytokines but in combination with others, such as pro-angiogenic molecules or BMPs. Ideally, the factors would be gradually released by the polymer as it is degraded or would be supplemented by local injections, to match the state of healing. To that end, Spiller et al. (2015) demonstrated efficient M1 to M2 transition on decellularized bone by attaching IFNγ and IL-4 with two methods of different strength (adsorption and biotin-streptavidin binding). Here again, 3D printing could be a valuable tool to design layered implants containing gradients of growth factors (Freeman et al., 2020). Finally, despite our poor results *in vivo*, exosomes and other extracellular vesicles from MSCs have promising characteristics for tissue regeneration, in bone and beyond (Brennan et al., 2020). They convey complex messages without the need of whole cells and could potentially be produced in large quantities with allogenic or genetically engineered cells.

References

Albrektsson, T., and Johansson, C. (2001). Osteoinduction, osteoconduction and osseointegration. Eur. Spine J. *10*, S96–S101.

Alford, A.I., Kozloff, K.M., and Hankenson, K.D. (2015). Extracellular matrix networks in bone remodeling. Int. J. Biochem. Cell Biol. *65*, 20–31.

Amarasekara, D.S., Yun, H., Kim, S., Lee, N., Kim, H., and Rho, J. (2018). Regulation of Osteoclast Differentiation by Cytokine Networks. Immune Netw. *18*, 1–18.

Anderson, J.M., Rodriguez, A., and Chang, D.T. (2008). Foreign body reaction to biomaterials. Semin. Immunol. *20*, 86–100.

Angel, N.Z., Walsh, N., Forwood, M.R., Ostrowski, M.C., Cassady, A.I., and Hume, D.A. (2000). Transgenic Mice Overexpressing Tartrate-Resistant Acid Phosphatase Exhibit an Increased Rate of Bone Turnover. J. Bone Miner. Res. *15*, 103–110.

Arbez, B., Manero, F., Mabilleau, G., Libouban, H., and Chappard, D. (2019). Human macrophages and osteoclasts resorb β-tricalcium phosphate in vitro but not mouse macrophages. Micron *125*, 102730.

Arinzeh, T.L., Tran, T., Mcalary, J., and Daculsi, G. (2005). A comparative study of biphasic calcium phosphate ceramics for human mesenchymal stem-cell-induced bone formation. Biomaterials *26*, 3631–3638.

Arron, J.R., and Choi, Y. (2000). Osteoimmunology: Bone versus immune system. Nature *408*, 535–536.

Ascenzi, M.-G. (2012). The osteon: the micromechanical unit of compact bone. Front. Biosci. *17*, 1551.

Atkins, G.J., and Findlay, D.M. (2012). Osteocyte regulation of bone mineral: A little give and take. Osteoporos. Int. *23*, 2067–2079.

Azi, M.L., Aprato, A., Santi, I., Junior, M.K., Masse, A., and Joeris, A. (2016). Autologous bone graft in the treatment of post-traumatic bone defects: a systematic review and meta-analysis. BMC Musculoskelet. Disord. *17*, 1–10.

Barba, M., Di Taranto, G., and Lattanzi, W. (2017). Adipose-derived stem cell therapies for bone regeneration. Expert Opin. Biol. Ther. *17*, 677–689.

Barradas, A., Yuan, H., van Blitterswijk, C., and Habibovic, P. (2011a). Osteoinductive biomaterials: current knowledge of properties, experimental models and biological mechanisms. Eur. Cells Mater. *21*, 407–429.

Barradas, A.A.M.C.A.A.M.C., Yuan, H., van Blitterswijk, C.C.A.C.C.A.C., and Habibovic, P. (2011b). Osteoinductive biomaterials: current knowledge of properties, experimental models and biological mechanisms. Eur. Cell. Mater. *21*, 407–429.

Barradas, A.M.C., Yuan, H., van der Stok, J., Le Quang, B., Fernandes, H., Chaterjea, A., Hogenes, M.C.H., Shultz, K., Donahue, L.R., van Blitterswijk, C., et al. (2012). The influence of genetic factors on the osteoinductive potential of calcium phosphate ceramics in mice. Biomaterials *33*, 5696–5705.

Bastian, O.W., Croes, M., Alblas, J., Koenderman, L., Leenen, L.P.H., and Blokhuis, T.J. (2018). Neutrophils inhibit synthesis of mineralized extracellular matrix by human bone marrow-derived stromal cells in vitro. Front. Immunol. *9*, 1–13.

Batoon, L., Millard, S.M., Raggatt, L.J., and Pettit, A.R. (2017). Osteomacs and Bone Regeneration. Curr. Osteoporos. Rep. *15*, 385–395.

Becquart, P., Cambon-Binder, A., Monfoulet, L.-E.E., Bourguignon, M., Vandamme, K., Bensidhoum, M., Petite, H., and Logeart-Avramoglou, D. (2012). Ischemia Is the Prime but Not the Only Cause of Human Multipotent Stromal Cell Death in Tissue-Engineered Constructs In Vivo. Tissue Eng. Part A *18*, 2084–2094.

Beeton, C.A., Bord, S., Ireland, D., and Compston, J.E. (2006). Osteoclast formation and bone resorption are inhibited by megakaryocytes. Bone *39*, 985–990.

Benavides-Castellanos, M.P., Garzón-Orjuela, N., and Linero, I. (2020). Effectiveness of mesenchymal stem cell-conditioned medium in bone regeneration in animal and human models: a systematic review and meta-analysis. Cell Regen. (London, England) *9*, 5.

Berendsen, A.D., and Olsen, B.R. (2015). Bone development. Bone *80*, 14–18.

Bergdolt, S., Kovtun, A., Hägele, Y., Liedert, A., Schinke, T., Amling, M., Huber-Lang, M., and Ignatius, A. (2017). Osteoblast-specific overexpression of complement receptor C5aR1 impairs fracture healing. PLoS One *12*, 1–17.

Bethel, M., Barnes, C.L.T., Taylor, A.F., Cheng, Y.-H., Chitteti, B.R., Horowitz, M.C., Bruzzaniti, A., Srour, E.F., and Kacena, M.A. (2015). A Novel Role for Thrombopoietin in Regulating Osteoclast Development in Humans and Mice. J. Cell. Physiol. *230*, 2142–2151.

Blair, H.C., Larrouture, Q.C., Li, Y., Lin, H., Beer-Stoltz, D., Liu, L., Tuan, R.S., Robinson, L.J., Schlesinger, P.H., and Nelson, D.J. (2017). Osteoblast differentiation and bone matrix formation in vivo and in vitro. Tissue Eng. - Part B Rev. *23*, 268–280.

Blasi, A., Martino, C., Balducci, L., Saldarelli, M., Soleti, A., Navone, S.E., Canzi, L., Cristini, S., Invernici, G., Parati, E.A., et al. (2011). Dermal fibroblasts display similar phenotypic and differentiation capacity to fat-derived mesenchymal stem cells, but differ in anti-inflammatory and angiogenic potential. Vasc. Cell *3*, 5.

Boersema, G.S.A., Utomo, L., Bayon, Y., Kops, N., van der Harst, E., Lange, J.F., and Bastiaansen-Jenniskens, Y.M. (2016). Monocyte subsets in blood correlate with obesity related response of macrophages to biomaterials in vitro. Biomaterials *109*, 32–39.

Bolzoni, M., Ronchetti, D., Storti, P., Donofrio, G., Marchica, V., Costa, F., Agnelli, L., Toscani, D., Vescovini, R., Todoerti, K., et al. (2017). IL21R expressing CD14+CD16+ monocytes expand in multiple myeloma patients leading to increased osteoclasts. Haematologica *102*, 773–784.

Bonanni, V., Sciumè, G., Santoni, A., and Bernardini, G. (2019). Bone Marrow NK Cells: Origin, Distinctive Features, and Requirements for Tissue Localization. Front. Immunol. *10*, 1569.

Boppana, N.B., Devarajan, A., Gopal, K., Barathan, M., Bakar, S.A., Shankar, E.M., Ebrahim, A.S., and Farooq, S.M. (2014). Blockade of CXCR2 signalling: A potential therapeutic target for preventing neutrophil-mediated inflammatory diseases. Exp. Biol. Med. *239*, 509–518.

Bord, S., Frith, E., Ireland, D.C., Scott, M.A., Craig, J.I.O., and Compston, J.E. (2005). Megakaryocytes modulate osteoblast synthesis of type-I collagen, osteoprotegerin, and RANKL. Bone *36*, 812–819.

Boskey, A.L. (2013). Bone composition: relationship to bone fragility and antiosteoporotic drug effects. Bonekey Rep. *2*, 1–11.

Boyette, L.B., Macedo, C., Hadi, K., Elinoff, B.D., Walters, J.T., Ramaswami, B., Chalasani, G., Taboas, J.M., Lakkis, F.G., and Metes, D.M. (2017). Phenotype, function, and differentiation potential of human monocyte subsets.

Boyle, W.J., Simonet, W.S., and Lacey, D.L. (2003). Osteoclast differentiation and activation. Nature *423*, 337–342.

Brennan, M., Layrolle, P., and Mooney, D.J. (2020). Biomaterials Functionalized with MSC Secreted Extracellular Vesicles and Soluble Factors for Tissue Regeneration. Adv. Funct. Mater. *30*.

Brennan, M.A., Renaud, A., Guilloton, F., Mebarki, M., Trichet, V., Sensebé, L., Deschaseaux, F., Chevallier, N., and Layrolle, P. (2017). Inferior In Vivo Osteogenesis and Superior Angiogeneis of Human Adipose-Derived Stem Cells Compared with Bone Marrow-Derived Stem Cells Cultured in Xeno-Free Conditions. Stem Cells Transl. Med. *6*, 2160–2172.

Brennan, M.Á., Renaud, A., Amiaud, J., Rojewski, M.T., Schrezenmeier, H., Heymann, D., Trichet, V., and Layrolle, P. (2014). Pre-clinical studies of bone regeneration with human bone marrow stromal cells and biphasic calcium phosphate. Stem Cell Res. Ther. *5*, 114.

Brylka, L.J., and Schinke, T. (2019). Chemokines in Physiological and Pathological Bone Remodeling. Front. Immunol. *10*, 2182.

Canè, S., Ugel, S., Trovato, R., Marigo, I., De Sanctis, F., Sartoris, S., and Bronte, V. (2019). The endless saga of monocyte diversity. Front. Immunol. *10*, 1786.

Carreau, A., Hafny-Rahbi, B. El, Matejuk, A., Grillon, C., and Kieda, C. (2011). Why is the partial oxygen pressure of human tissues a crucial parameter? Small molecules and hypoxia. J. Cell. Mol. Med. *15*, 1239–1253.

Carvalho, P.P., Leonor, I.B., Smith, B.J., Dias, I.R., Reis, R.L., Gimble, J.M., and Gomes, M.E. (2014).

Undifferentiated human adipose-derived stromal/stem cells loaded onto wet-spun starch-polycaprolactone scaffolds enhance bone regeneration: Nude mice calvarial defect in vivo study. J. Biomed. Mater. Res. - Part A *102*, 3102–3111.

Chagin, A.S., and Newton, P.T. (2019). Postnatal skeletal growth is driven by the epiphyseal stem cell niche: potential implications to pediatrics. Pediatr. Res.

Champion, T.C., Partridge, L.J., Ong, S.-M., Malleret, B., Wong, S.-C., and Monk, P.N. (2018). Monocyte Subsets Have Distinct Patterns of Tetraspanin Expression and Different Capacities to Form Multinucleate Giant Cells. Front. Immunol. *9*, 1247.

Chan, C.K.F., Gulati, G.S., Sinha, R., Tompkins, J.V., Lopez, M., Carter, A.C., Ransom, R.C., Reinisch, A., Wearda, T., Murphy, M., et al. (2018). Identification of the Human Skeletal Stem Cell. Cell *175*, 43-56.e21.

Chang, M.K., Raggatt, L.-J., Alexander, K.A., Kuliwaba, J.S., Fazzalari, N.L., Schroder, K., Maylin, E.R., Ripoll, V.M., Hume, D.A., and Pettit, A.R. (2008). Osteal Tissue Macrophages Are Intercalated throughout Human and Mouse Bone Lining Tissues and Regulate Osteoblast Function In Vitro and In Vivo. J. Immunol. *181*, 1232–1244.

Charoenviriyakul, C., Takahashi, Y., Nishikawa, M., and Takakura, Y. (2018). Preservation of exosomes at room temperature using lyophilization. Int. J. Pharm. *553*, 1–7.

Chatterjea, A., Lapointe, V.L.S., Alblas, J., Chatterjea, S., van Blitterswijk, C.A., and De Boer, J. (2014). Suppression of the immune system as a critical step for bone formation from allogeneic osteoprogenitors implanted in rats. J. Cell. Mol. Med. *18*, 134–142.

Chen, F., Wang, M., Wang, J., Chen, X., Li, X., Xiao, Y., and Zhang, X. (2019). Effects of hydroxyapatite surface nano/micro-structure on osteoclast formation and activity. J. Mater. Chem. B *7*, 7574–7587.

Chen, Y., Li, W., Zhang, C., Wu, Z., and Liu, J. (2020). Recent Developments of Biomaterials for Additive Manufacturing of Bone Scaffolds. Adv. Healthc. Mater. *2000724*, 1–28.

Cheng, J., Liu, J., Shi, Z., Xu, D., Luo, S., Siegal, G.P., Feng, X., and Wei, S. (2011). Interleukin-4 inhibits RANKL-induced NFATc1 expression via STAT6: A novel mechanism mediating its blockade of osteoclastogenesis. J. Cell. Biochem. *112*, 3385–3392.

Chu, C., Liu, L., Rung, S., Wang, Y., Ma, Y., Hu, C., Zhao, X., Man, Y., and Qu, Y. (2020). Modulation of foreign body reaction and macrophage phenotypes concerning microenvironment. J. Biomed. Mater. Res. - Part A *108*, 127–135.

Claes, L., Recknagel, S., and Ignatius, A. (2012). Fracture healing under healthy and inflammatory conditions. Nat. Rev. Rheumatol. *8*, 133–143.

Collin, M., and Bigley, V. (2018). Human dendritic cell subsets: an update. Immunology *154*, 3–20.

Colonna, M. (2018). Innate Lymphoid Cells: Diversity, Plasticity, and Unique Functions in Immunity. Immunity *48*, 1104–1117.

Costello, L.C., Chellaiah, M., Zou, J., Franklin, R.B., and Reynolds, M.A. (2014). The status of citrate in the hydroxyapatite/collagen complex of bone; and Its role in bone formation. J. Regen. Med. Tissue Eng. *3*, 4.

Croes, M., Öner, F.C., van Neerven, D., Sabir, E., Kruyt, M.C., Blokhuis, T.J., Dhert, W.J.A., and Alblas, J. (2016). Proinflammatory T cells and IL-17 stimulate osteoblast differentiation. Bone *84*, 262–270.

Darnell, M., Gu, L., and Mooney, D. (2018). RNA-seq reveals diverse effects of substrate stiffness on mesenchymal stem cells. Biomaterials *181*, 182–188.

Davison, N.L., ten Harkel, B., Schoenmaker, T., Luo, X., Yuan, H., Everts, V., Barrère-de Groot, F., and de Bruijn, J.D. (2014a). Osteoclast resorption of beta-tricalcium phosphate controlled by surface architecture. Biomaterials *35*, 7441–7451.

Davison, N.L., Gamblin, A.-L., Layrolle, P., Yuan, H., de Bruijn, J.D., and Barrère-de Groot, F. (2014b). Liposomal clodronate inhibition of osteoclastogenesis and osteoinduction by submicrostructured beta-tricalcium phosphate. Biomaterials *35*, 5088–5097.

Denu, R.A., Nemcek, S., Bloom, D.D., Goodrich, A.D., Kim, J., Mosher, D.F., and Hematti, P. (2016). Fibroblasts and Mesenchymal Stromal/Stem Cells Are Phenotypically Indistinguishable. Acta Haematol. *136*, 85–97.

Dersot, J.M., Colombier, M.L., Lafont, J., Baroukh, B., Septier, D., and Saffar, J.L. (1995). Multinucleated giant

cells elicited around hydroxyapatite particles implanted in craniotomy defects are not osteoclasts. Anat. Rec. *242*, 166–176.

Deshet-Unger, N., Kolomansky, A., Ben-Califa, N., Hiram-Bab, S., Gilboa, D., Liron, T., Ibrahim, M., Awida, Z., Gorodov, A., Oster, H.S., et al. (2020). Erythropoietin receptor in B cells plays a role in bone remodeling in mice. Theranostics *10*, 8744–8756.

Devalaraja, R.M., Nanney, L.B., Qian, Q., Du, J., Yu, Y., Devalaraja, M.N., and Richmond, A. (2000). Delayed Wound Healing in CXCR2 Knockout Mice. J. Invest. Dermatol. *115*, 234–244.

Dominici, M., Le Blanc, K., Mueller, I., Slaper-Cortenbach, I., Marini, F.., Krause, D.S., Deans, R.J., Keating, A., Prockop, D.J., and Horwitz, E.M. (2006). Minimal criteria for defining multipotent mesenchymal stromal cells. The International Society for Cellular Therapy position statement. Cytotherapy *8*, 315–317.

Dumic-Cule, I., Peric, M., Kucko, L., Grgurevic, L., Pecina, M., and Vukicevic, S. (2018). Bone morphogenetic proteins in fracture repair. Int. Orthop.

Dyer, D.P., Pallas, K., Ruiz, L.M., Schuette, F., Wilson, G.J., and Graham, G.J. (2017). CXCR2 deficient mice display macrophage-dependent exaggerated acute inflammatory responses. Sci. Rep. *7*, 1–11.

Ehrnthaller, C., Huber-Lang, M., Nilsson, P., Bindl, R., Redeker, S., Recknagel, S., Rapp, A., Mollnes, T., Amling, M., Gebhard, F., et al. (2013). Complement C3 and C5 deficiency affects fracture healing. PLoS One *8*, 1–15.

Einhorn, T.A., and Gerstenfeld, L.C. (2014). Fracture healing: mechanisms and interventions. Nat. Rev. Rheumatol. *11*, 45–54.

Ercal, P., Pekozer, G.G., and Kose, G.T. (2018). Dental Stem Cells in Bone Tissue Engineering: Current Overview and Challenges. In Advs Exp. Medicine, Biology-Neuroscience and Respiration., pp. 113–127.

Everts, V., Delaissé, J.M., Korper, W., Jansen, D.C., Tigchelaar-Gutter, W., Saftig, P., and Beertsen, W. (2002). The Bone Lining Cell: Its Role in Cleaning Howship's Lacunae and Initiating Bone Formation. J. Bone Miner. Res. *17*, 77–90.

Fan, L., Zhang, C., Yu, Z., Shi, Z., Dang, X., and Wang, K. (2015). Transplantation of hypoxia preconditioned bone marrow mesenchymal stem cells enhances angiogenesis and osteogenesis in rabbit femoral head osteonecrosis. Bone *81*, 544–553.

Feng, W., Guo, J., and Li, M. (2019). RANKL-independent modulation of osteoclastogenesis. J. Oral Biosci. *61*, 16–21.

Fillingham, Y., and Jacobs, J. (2016). Bone Grafts and Bone Substitutes. Bone Jt. J. 6–9.

Franco, C.B., Chen, C.-C., Drukker, M., Weissman, I.L., and Galli, S.J. (2010). Distinguishing Mast Cell and Granulocyte Differentiation at the Single-Cell Level. Cell Stem Cell *6*, 361–368.

Freeman, F.E., Pitacco, P., van Dommelen, L.H.A., Nulty, J., Browe, D.C., Shin, J.Y., Alsberg, E., and Kelly, D.J. (2020). 3D bioprinting spatiotemporally defined patterns of growth factors to tightly control tissue regeneration. Sci. Adv. *6*, 1–16.

Freitas, J., Santos, S.G., Gonçalves, R.M., Teixeira, J.H., Barbosa, M.A., and Almeida, M.I. (2019). Genetically Engineered-MSC Therapies for Non-unions, Delayed Unions and Critical-size Bone Defects. Int. J. Mol. Sci. *20*, 3430.

Furuta, T., Miyaki, S., Ishitobi, H., Ogura, T., Kato, Y., Kamei, N., Miyado, K., Higashi, Y., and Ochi, M. (2016). Mesenchymal Stem Cell-Derived Exosomes Promote Fracture Healing in a Mouse Model. Stem Cells Transl. Med. *5*, 1620–1630.

Gamblin, A.-L., Brennan, M.A., Renaud, A., Yagita, H., Lézot, F., Heymann, D., Trichet, V., and Layrolle, P. (2014). Bone tissue formation with human mesenchymal stem cells and biphasic calcium phosphate ceramics: The local implication of osteoclasts and macrophages. Biomaterials *35*, 9660–9667.

García-García, A., de Castillejo, C.L.F., and Méndez-Ferrer, S. (2015). BMSCs and hematopoiesis. Immunol. Lett. *168*, 129–135.

García-Gareta, E., Coathup, M.J., and Blunn, G.W. (2015). Osteoinduction of bone grafting materials for bone repair and regeneration. Bone *81*, 112–121.

Geering, B., Stoeckle, C., Conus, S., and Simon, H.U. (2013). Living and dying for inflammation: Neutrophils,

eosinophils, basophils. Trends Immunol. *34*, 398–409.

Giannoudis, P. V., Einhorn, T.A., and Marsh, D. (2007). Fracture healing: The diamond concept. Injury *38*, S3–S6.

Gilbert, W., Bragg, R., Elmansi, A.M., McGee-Lawrence, M.E., Isales, C.M., Hamrick, M.W., Hill, W.D., and Fulzele, S. (2019). Stromal cell-derived factor-1 (CXCL12) and its role in bone and muscle biology. Cytokine *123*, 154783.

Ginebra, M.-P., Espanol, M., Maazouz, Y., Bergez, V., and Pastorino, D. (2018). Bioceramics and bone healing. EFORT Open Rev. *3*, 173–183.

Gómez-Barrena, E., Padilla-Eguiluz, N.G., Avendaño-Solá, C., Payares-Herrera, C.C.C.C., Velasco-Iglesias, A., Torres, F., Rosset, P., Gebhard, F., Baldini, N., Rubio-Suarez, J.C., et al. (2018). A Multicentric, Open-Label, Randomized, Comparative Clinical Trial of Two Different Doses of Expanded hBM-MSCs Plus Biomaterial versus Iliac Crest Autograft, for Bone Healing in Nonunions after Long Bone Fractures: Study Protocol. Stem Cells Int. *2018*, 1–13.

Gómez-Barrena, E., Rosset, P., Gebhard, F., Hernigou, P., Baldini, N., Rouard, H., Sensebé, L., Gonzalo-Daganzo, R.M., Giordano, R., Padilla-Eguiluz, N., et al. (2019). Feasibility and safety of treating non-unions in tibia, femur and humerus with autologous, expanded, bone marrow-derived mesenchymal stromal cells associated with biphasic calcium phosphate biomaterials in a multicentric, non-comparative trial. Biomaterials *196*, 100–108.

González-Vázquez, A., Planell, J.A., and Engel, E. (2014). Extracellular calcium and CaSR drive osteoinduction in mesenchymal stromal cells. Acta Biomater. *10*, 2824–2833.

Goodman, S.B., and Lin, T. (2020). Modifying MSC Phenotype to Facilitate Bone Healing: Biological Approaches. Front. Bioeng. Biotechnol. *8*, 1–16.

Granchi, D., CIAPETTI, G., GÓMEZ-BARRENA, E., ROJEWSKI, M., ROSSET, P., LAYROLLE, P., SPAZZOLI, B., DONATI, D.M., and BALDINI, N. (2019). Biomarkers of bone healing induced by a regenerative approach based on expanded bone marrow–derived mesenchymal stromal cells. Cytotherapy *21*, 870–885.

Guihard, P., Danger, Y., Brounais, B., David, E., Brion, R., Delecrin, J., Richards, C.D., Chevalier, S., Rédini, F., Heymann, D., et al. (2012). Induction of Osteogenesis in Mesenchymal Stem Cells by Activated Monocytes/Macrophages Depends on Oncostatin M Signaling. Stem Cells *30*, 762–772.

Guihard, P., Boutet, M.-A., Brounais-Le Royer, B., Gamblin, A.-L., Amiaud, J., Renaud, A., Berreur, M., Rédini, F., Heymann, D., Layrolle, P., et al. (2015). Oncostatin M, an Inflammatory Cytokine Produced by Macrophages, Supports Intramembranous Bone Healing in a Mouse Model of Tibia Injury. Am. J. Pathol. *185*, 765–775.

Guilliams, M., Mildner, A., and Yona, S. (2018). Developmental and Functional Heterogeneity of Monocytes. Immunity.

Habraken, W., Habibovic, P., Epple, M., and Bohner, M. (2016). Calcium phosphates in biomedical applications: Materials for the future? Mater. Today *19*, 69–87.

Han, Y., Li, X., Zhang, Y., Han, Y., Chang, F., and Ding, J. (2019). Mesenchymal Stem Cells for Regenerative Medicine. Cells *8*, 886.

ten Harkel, B., Schoenmaker, T., Picavet, D.I., Davison, N.L., de Vries, T.J., and Everts, V. (2015). The Foreign Body Giant Cell Cannot Resorb Bone, But Dissolves Hydroxyapatite Like Osteoclasts. PLoS One *10*, e0139564.

Hasegawa, T., Kikuta, J., Sudo, T., Matsuura, Y., Matsui, T., Simmons, S., Ebina, K., Hirao, M., Okuzaki, D., Yoshida, Y., et al. (2019). Identification of a novel arthritis-associated osteoclast precursor macrophage regulated by FoxM1. Nat. Immunol. *20*, 1631–1643.

Hayman, A.R., Jones, S.J., Boyde, A., Foster, D., Colledge, W.H., Carlton, M.B., Evans, M.J., and Cox, T.M. (1996). Mice lacking tartrate-resistant acid phosphatase (Acp 5) have disrupted endochondral ossification and mild osteopetrosis. Development *122*, 3151–3162.

He, D., Kou, X., Yang, R., Liu, D., Wang, X., Luo, Q., Song, Y., Liu, F., Yan, Y., Gan, Y., et al. (2015). M1-like Macrophage Polarization Promotes Orthodontic Tooth Movement. J. Dent. Res. *94*, 1286–1294.

Heinemann, C., Heinemann, S., Worch, H., and Hanke, T. (2011). Development of an osteoblast/osteoclast co-culture derived by human bone marrow stromal cells and human monocytes for biomaterials testing. Eur. Cells Mater. *21*, 80–93.

Henkel, J., Woodruff, M.A., Epari, D.R., Steck, R., Glatt, V., Dickinson, I.C., Choong, P.F.M., Schuetz, M.A., and Hutmacher, D.W. (2013). Bone Regeneration Based on Tissue Engineering Conceptions — A 21st Century Perspective. Nat. Publ. Gr. *3*, 216–248.

Ho-Shui-Ling, A., Bolander, J., Rustom, L.E., Johnson, A.W., Luyten, F.P., and Picart, C. (2018). Bone regeneration strategies: Engineered scaffolds, bioactive molecules and stem cells current stage and future perspectives. Biomaterials *180*, 143–162.

Horwood, N.J. (2016). Macrophage Polarization and Bone Formation: A review. Clin. Rev. Allergy Immunol. *51*, 79–86.

Horwood, N.J., Kartsogiannis, V., Quinn, J.M.W., Romas, E., Martin, T.J., and Gillespie, M.T. (1999). Activated T Lymphocytes Support Osteoclast Formation in Vitro. Biochem. Biophys. Res. Commun. *265*, 144–150.

Hu, K., and Olsen, B.R. (2016). The roles of vascular endothelial growth factor in bone repair and regeneration. Bone *91*, 30–38.

Humbert, P., Brennan, M.Á., Davison, N., Rosset, P., Trichet, V., Blanchard, F., and Layrolle, P. (2019). Immune Modulation by Transplanted Calcium Phosphate Biomaterials and Human Mesenchymal Stromal Cells in Bone Regeneration. Front. Immunol. *10*, 1–15.

Ichim, T.E., O'Heeron, P., and Kesari, S. (2018). Fibroblasts as a practical alternative to mesenchymal stem cells. J. Transl. Med. *16*, 212.

Ignatius, A., Ehrnthaller, C., Brenner, R.E., Kreja, L., Schoengraf, P., Lisson, P., Blakytny, R., Recknagel, S., Claes, L., Gebhard, F., et al. (2011). The anaphylatoxin receptor C5aR is present during fracture healing in rats and mediates osteoblast migration in vitro. J. Trauma - Inj. Infect. Crit. Care *71*, 952–960.

Ikebuchi, Y., Aoki, S., Honma, M., Hayashi, M., Sugamori, Y., Khan, M., Kariya, Y., Kato, G., Tabata, Y., Penninger, J.M., et al. (2018). Coupling of bone resorption and formation by RANKL reverse signalling. Nature *561*, 195–200.

Italiani, P., and Boraschi, D. (2014). From monocytes to M1/M2 macrophages: Phenotypical vs. functional differentiation. Front. Immunol. *5*, 1–22.

Izu, Y., Sun, M., Zwolanek, D., Veit, G., Williams, V., Cha, B., Jepsen, K.J., Koch, M., and Birk, D.E. (2011). Type XII collagen regulates osteoblast polarity and communication during bone formation. J. Cell Biol. *193*, 1115–1130.

Jacome-Galarza, C.E., Percin, G.I., Muller, J.T., Mass, E., Lazarov, T., Eitler, J., Rauner, M., Yadav, V.K., Crozet, L., Bohm, M., et al. (2019). Developmental origin, functional maintenance and genetic rescue of osteoclasts. Nature *568*, 541–545.

Jakoi, A.M., Iorio, J.A., and Cahill, P.J. (2015). Autologous bone graft harvesting: a review of grafts and surgical techniques. Musculoskelet. Surg. *99*, 171–178.

Janicki, P., Boeuf, S., Steck, E., Egermann, M., Kasten, P., and Richter, W. (2011). Prediction of in vivo bone forming potency of bone marrowderived human mesenchymal stem cells. Eur. Cells Mater. *21*, 488–507.

Jensen, S.S., Bornstein, M.M., Dard, M., Bosshardt, D.D., and Buser, D. (2008). Comparative study of biphasic calcium phosphates with different HA/TCP ratios in mandibular bone defects. A long-term histomorphometric study in minipigs. J. Biomed. Mater. Res. Part B Appl. Biomater. *90B*, 171–181.

Jones, H.R., Robb, C.T., Perretti, M., and Rossi, A.G. (2016). The role of neutrophils in inflammation resolution. Semin. Immunol. *28*, 137–145.

Kampleitner, C., Obi, J., Vassilev, N., Epstein, M.M., and Hoffmann, O. (2018). Biological Compatibility Profile on Biomaterials for Bone Regeneration. J. Vis. Exp. e58077.

Kanagasabapathy, D., Blosser, R.J., Maupin, K.A., Hong, J.M., Alvarez, M., Ghosh, J., Mohamad, S.F., Aguilar-perez, A., Srour, E.F., Melissa, A., et al. (2020). Megakaryocytes promote osteoclastogenesis in aging. *12*, 16–20.

Kawamoto, H., Wada, H., and Katsura, Y. (2010). A revised scheme for developmental pathways of hematopoietic cells: The myeloid-based model. Int. Immunol. *22*, 65–70.

Kenkre, J.S., and Bassett, J.H.D. (2018). The bone remodelling cycle (SAGE Publications Ltd).

Keselowsky, B.G., and Lewis, J.S. (2017). Dendritic cells in the host response to implanted materials. Semin. Immunol. *29*, 33–40.

Khan, N.M., Clifton, K.B., Lorenzo, J., Hansen, M.F., and Drissi, H. (2020). Comparative transcriptomic analysis identifies distinct molecular signatures and regulatory networks of chondroclasts and osteoclasts. Arthritis Res. Ther. *22*, 168.

Khan, U.A., Hashimi, S.M., Bakr, M.M., Forwood, M.R., and Morrison, N.A. (2013). Foreign body giant cells and osteoclasts are TRAP positive, have podosome-belts and both require OC-STAMP for cell fusion. J. Cell. Biochem. *114*, 1772–1778.

Khan, U.A., Hashimi, S.M., Khan, S., Quan, J., Bakr, M.M., Forwood, M.R., and Morrison, N.M. (2014). Differential Expression of Chemokines, Chemokine Receptors and Proteinases by Foreign Body Giant Cells (FBGCs) and Osteoclasts. J. Cell. Biochem. *115*, 1290–1298.

Khassawna, T. El, Serra, A., Bucher, C.H., Petersen, A., Schlundt, C., Könnecke, I., Malhan, D., Wendler, S., Schell, H., Volk, H.D., et al. (2017). T lymphocytes influence the mineralization process of bone. Front. Immunol. *8*.

Kim, S.Y., and Nair, M.G. (2019). Macrophages in wound healing: activation and plasticity. Immunol. Cell Biol. *97*, 258–267.

Kim, A.R., Hye, J., Yun, K., Choi, H., Jeong, Y.J., Cha, H., Jung, E., Yun, B., and Yoo, J. (2020). The presence of neutrophils causes RANKL expression in periodontal tissue , giving rise to osteoclast formation. 1–9.

Kim, H.S., Yun, J.W., Shin, T.H., Lee, S.H., Lee, B.C., Yu, K.R., Seo, Y., Lee, S., Kang, T.W., Choi, S.W., et al. (2015). Human umbilical cord blood mesenchymal stem cell-derived PGE2 and TGF-β1 alleviate atopic dermatitis by reducing mast cell degranulation. Stem Cells *33*, 1254–1266.

Kim, Y., Jin, H.J., Heo, J., Ju, H., Lee, H.-Y., Kim, S., Lee, S., Lim, J., Jeong, S.Y., Kwon, J., et al. (2018). Small hypoxia-primed mesenchymal stem cells attenuate graft-versus-host disease. Leukemia 1–13.

Klar, R.M., Duarte, R., Dix-Peek, T., Dickens, C., Ferretti, C., and Ripamonti, U. (2013). Calcium ions and osteoclastogenesis initiate the induction of bone formation by coral-derived macroporous constructs. J. Cell. Mol. Med. *17*, 1444–1457.

Klopfleisch, R., and Jung, F. (2017). The pathology of the foreign body reaction against biomaterials. J. Biomed. Mater. Res. Part A *105*, 927–940.

Kohli, N., Ho, S., Brown, S.J., Sawadkar, P., Sharma, V., Snow, M., and García-Gareta, E. (2018). Bone remodelling in vitro: Where are we headed?: -A review on the current understanding of physiological bone remodelling and inflammation and the strategies for testing biomaterials in vitro. Bone.

Kołodziejska, B., Kaflak, A., and Kolmas, J. (2020). Biologically inspired collagen/apatite composite biomaterials for potential use in bone tissue regeneration-A review. Materials (Basel). *13*.

Komori, T. (2019). Regulation of proliferation, differentiation and functions of osteoblasts by runx2. Int. J. Mol. Sci. *20*.

Kowal, J.M., Schmal, H., Halekoh, U., Hjelmborg, J.B., and Kassem, M. (2020). Single-cell high-content imaging parameters predict functional phenotype of cultured human bone marrow stromal stem cells. Stem Cells Transl. Med. *9*, 189–202.

Kroner, J., Kovtun, A., Kemmler, J., Messmann, J.J., Strauss, G., Seitz, S., Schinke, T., Amling, M., Kotrba, J., Froebel, J., et al. (2017). Mast Cells Are Critical Regulators of Bone Fracture–Induced Inflammation and Osteoclast Formation and Activity. J. Bone Miner. Res. *32*, 2431–2444.

Lee, E.R., Lamplugh, L., Shepard, N.L., and Mort, J.S. (1995). The septoclast, a cathepsin B-rich cell involved in the resorption of growth plate cartilage. J. Histochem. Cytochem. *43*, 525–536.

Lewinson, D., and Silbermann, M. (1992). Chondroclasts and endothelial cells collaborate in the process of cartilage resorption. Anat. Rec. *233*, 504–514.

Li, M., Guo, X., Qi, W., Wu, Z., de Bruijn, J.D., Xiao, Y., Bao, C., and Yuan, H. (2020). Macrophage polarization plays roles in bone formation instructed by calcium phosphate ceramics. J. Mater. Chem. B *8*, 1863–1877.

Li, Z., Hardij, J., Bagchi, D.P., Scheller, E.L., and MacDougald, O.A. (2018). Development, regulation, metabolism and function of bone marrow adipose tissues. Bone *110*, 134–140.

Lin, A., and Loré, K. (2017). Granulocytes: New members of the antigen-presenting cell family. Front. Immunol. *8*, 1–8.

Lin, Z., Fateh, A., Salem, D.M., and Intini, G. (2014). Periosteum: Biology and applications in craniofacial bone regeneration. J. Dent. Res. *93*, 109–116.

Linero, I., and Chaparro, O. (2014). Paracrine effect of mesenchymal stem cells derived from human adipose tissue in bone regeneration. PLoS One *9*, 1–12.

Liu, M., Lei, H., Dong, P., Fu, X., Yang, Z., Yang, Y., Ma, J., Liu, X., Cao, Y., and Xiao, R. (2017). Adipose-Derived Mesenchymal Stem Cells from the Elderly Exhibit Decreased Migration and Differentiation Abilities with Senescent Properties. Cell Transplant. *26*, 1505–1519.

Liu, M., Sun, Y., and Zhang, Q. (2018). Emerging Role of Extracellular Vesicles in Bone Remodeling. J. Dent. Res. *97*, 859–868.

Loi, F., Córdova, L.A., Pajarinen, J., Lin, T., Yao, Z., and Goodman, S.B. (2016). Inflammation, fracture and bone repair. Bone *86*, 119–130.

Longoni, A., Pennings, I., Cuenca Lopera, M., van Rijen, M.H.P., Peperzak, V., Rosenberg, A.J.W.P., Levato, R., and Gawlitta, D. (2020). Endochondral Bone Regeneration by Non-autologous Mesenchymal Stem Cells. Front. Bioeng. Biotechnol. *8*, 1–14.

Lopes, D., Martins-Cruz, C., Oliveira, M.B., and Mano, J.F. (2018). Bone physiology as inspiration for tissue regenerative therapies. Biomaterials *185*, 240–275.

Lorenzo, J. (2020). Cytokines and Bone: Osteoimmunology. In Cytokines, pp. 385–402.

Lorincz, Á.M., Timár, C.I., Marosvári, K.A., Veres, D.S., Otrokocsi, L., Kittel, Á., and Ligeti, E. (2014). Effect of storage on physical and functional properties of extracellular vesicles derived from neutrophilic granulocytes. J. Extracell. Vesicles *3*.

Maas, S.L.N., Breakefield, X.O., and Weaver, A.M. (2017). Extracellular Vesicles: Unique Intercellular Delivery Vehicles. Trends Cell Biol. *27*, 172–188.

Madel, M.-B., Ibáñez, L., Wakkach, A., de Vries, T.J., Teti, A., Apparailly, F., and Blin-Wakkach, C. (2019). Immune Function and Diversity of Osteoclasts in Normal and Pathological Conditions. Front. Immunol. *10*, 1–18.

Madel, M.B., Ibáñez, L., Rouleau, M., Wakkach, A., and Blin-Wakkach, C. (2018). A novel reliable and efficient procedure for purification of mature osteoclasts allowing functional assays in mouse cells. Front. Immunol. *9*, 1–12.

Maroto, R., Zhao, Y., Jamaluddin, M., Popov, V.L., Wang, H., Kalubowilage, M., Zhang, Y., Luisi, J., Sun, H., Culbertson, C.T., et al. (2017). Effects of storage temperature on airway exosome integrity for diagnostic and functional analyses. J. Extracell. Vesicles *6*.

Martinez, V.G., Ontoria-Oviedo, I., Ricardo, C.P., Harding, S.E., Sacedon, R., Varas, A., Zapata, A., Sepulveda, P., and Vicente, A. (2017). Overexpression of hypoxia-inducible factor 1 alpha improves immunomodulation by dental mesenchymal stem cells. Stem Cell Res. Ther. *8*, 208.

Matic, I., Matthews, B.G., Wang, X., Dyment, N.A., Worthley, D.L., Rowe, D.W., Grcevic, D., and Kalajzic, I. (2016). Quiescent Bone Lining Cells Are a Major Source of Osteoblasts During Adulthood. Stem Cells *34*, 2930–2942.

McLeod, J.J.A., Baker, B., and Ryan, J.J. (2015). Mast cell production and response to IL-4 and IL-13. Cytokine *75*, 57–61.

McNally, A.K., and Anderson, J.M. (2011). Foreign body-type multinucleated giant cells induced by interleukin-4 express select lymphocyte co-stimulatory molecules and are phenotypically distinct from osteoclasts and dendritic cells. Exp. Mol. Pathol. *91*, 673–681.

Ménard, C., Dulong, J., Roulois, D., Hébraud, B., Verdière, L., Pangault, C., Sibut, V., Bezier, I., Bescher, N., Monvoisin, C., et al. (2020). Integrated transcriptomic, phenotypic, and functional study reveals tissue-specific immune properties of mesenchymal stromal cells. Stem Cells *38*, 146–159.

Miron, R.J., and Bosshardt, D.D. (2016). OsteoMacs: Key players around bone biomaterials. Biomaterials *82*, 1–19.

Miron, R.J., and Bosshardt, D.D. (2018). Multinucleated Giant Cells: Good Guys or Bad Guys? Tissue Eng. - Part B Rev. *24*, 53–65.

Miron, R.J., Zohdi, H., Fujioka-Kobayashi, M., and Bosshardt, D.D. (2016). Giant cells around bone biomaterials: Osteoclasts or multi-nucleated giant cells? Acta Biomater. *46*, 15–28.

Mödinger, Y., Löffler, B., Huber-Lang, M., and Ignatius, A. (2018a). Complement involvement in bone homeostasis and bone disorders. Semin. Immunol. *37*, 53–65.

Mödinger, Y., Teixeira, G.Q., Neidlinger-Wilke, C., and Ignatius, A. (2018b). Role of the complement system in the response to orthopedic biomaterials. Int. J. Mol. Sci. *19*.

Morrison, S.J., and Scadden, D.T. (2014). The bone marrow niche for haematopoietic stem cells. Nature *505*, 327–334.

Mougiakakos, D., Jitschin, R., Johansson, C.C., Okita, R., Kiessling, R., and Le Blanc, K. (2011). The impact of inflammatory licensing on heme oxygenase-1-mediated induction of regulatory T cells by human mesenchymal stem cells. Blood *117*, 4826–4835.

Mulari, M.T.K., Zhao, H., Lakkakorpi, P.T., and Väänänen, H.K. (2003). Osteoclast Ruffled Border Has Distinct Subdomains for Secretion and Degraded Matrix Uptake. Traffic *4*, 113–125.

Murphy, P.M. (2018). Chemokines and Chemokine Receptors (Elsevier Ltd).

Murray, P.J. (2017). Macrophage Polarization. Annu. Rev. Physiol. *79*.

Mushahary, D., Spittler, A., Kasper, C., Weber, V., and Charwat, V. (2018). Isolation, cultivation, and characterization of human mesenchymal stem cells. Cytom. Part A *93*, 19–31.

Najar, M., Raicevic, G., Crompot, E., Fayyad-Kazan, H., Bron, D., Toungouz, M., and Lagneaux, L. (2016). The Immunomodulatory Potential of Mesenchymal Stromal Cells. J. Immunother. *39*, 45–59.

Narisawa, M., Kubo, S., Okada, Y., Yamagata, K., Nakayamada, S., Sakata, K., Yamaoka, K., and Tanaka, Y. (2020). Human dendritic cell-derived osteoclasts with high bone resorption capacity and T cell stimulation ability. Bone 115616.

Ng, P.Y., Brigitte Patricia Ribet, A., and Pavlos, N.J. (2019). Membrane trafficking in osteoclasts and implications for osteoporosis. Biochem. Soc. Trans. *47*, 639–650.

Nurden, A.T. (2011). Platelets, inflammation and tissue regeneration. Thromb. Haemost. *105*, 13–33.

Ohgushi, H., Okumura, M., Tamai, S., Shors, E.C., and Caplan, A.I. (1990). Marrow cell induced osteogenesis in porous hydroxyapatite and tricalcium phosphate: A comparative histomorphometric study of ectopic bone formation. J. Biomed. Mater. Res. *24*, 1563–1570.

Ono, T., Hayashi, M., Sasaki, F., and Nakashima, T. (2020). RANKL biology : bone metabolism , the immune system , and beyond. *3*, 1–16.

OpenStax College (2016). Anatomy & Physiology (OpenStax).

Orimo, H. (2010). The Mechanism of Mineralization and the Role of Alkaline Phosphatase in Health and Disease. J. Nippon Med. Sch. *77*, 4–12.

Ota, N., Takaishi, H., Kosaki, N., Takito, J., Yoda, M., Tohmonda, T., Kimura, T., Okada, Y., Yasuda, H., Kawaguchi, H., et al. (2009). Accelerated cartilage resorption by chondroclasts during bone fracture healing in osteoprotegerin-deficient mice. Endocrinology *150*, 4823–4834.

Owen, M., and Friedenstein, A.J. (1988). Stromal stem cells: marrow-derived osteogenic precursors. Ciba Found. Symp. *136*, 42–60.

Oya, A., Katsuyama, E., Morita, M., Sato, Y., Kobayashi, T., Miyamoto, K., Nishiwaki, T., Funayama, A., Fujita, Y., Kobayashi, T., et al. (2018). Tumor necrosis factor receptor-associated factor 6 is required to inhibit foreign body giant cell formation and activate osteoclasts under inflammatory and infectious conditions. J. Bone Miner. Metab. *36*, 679–690.

Pajarinen, J., Lin, T., Gibon, E., Kohno, Y., Maruyama, M., Nathan, K., Lu, L., Yao, Z., and Goodman, S.B. (2019). Mesenchymal stem cell-macrophage crosstalk and bone healing. Biomaterials *196*, 80–89.

Palis, J. (2014). Primitive and definitive erythropoiesis in mammals. Front. Physiol. *5 JAN*, 3.

Paquet, J., Deschepper, M., Moya, A., Logeart-Avramoglou, D., Boisson-Vidal, C., and Petite, H. (2015). Oxygen Tension Regulates Human Mesenchymal Stem Cell Paracrine Functions. Stem Cells Transl. Med. *4*, 809–821.

Periayah, M.H., Halim, A.S., and Saad, A.Z.M. (2017). Mechanism action of platelets and crucial blood coagulation pathways in Hemostasis. Int. J. Hematol. Stem Cell Res. *11*, 319–327.

Petri, R.M., Hackel, A., Hahnel, K., Dumitru, C.A., Bruderek, K., Flohe, S.B., Paschen, A., Lang, S., and Brandau, S. (2017). Activated Tissue-Resident Mesenchymal Stromal Cells Regulate Natural Killer Cell Immune and Tissue-Regenerative Function. Stem Cell Reports *9*, 985–998.

Pettit, A.R., Chang, M.K., Hume, D.A., and Raggatt, L.J. (2008). Osteal macrophages: A new twist on coupling during bone dynamics. Bone *43*, 976–982.

Pinho, S., and Frenette, P.S. (2019). Haematopoietic stem cell activity and interactions with the niche. Nat. Rev. Mol. Cell Biol. *20*, 303–320.

Quade, M., Münch, P., Lode, A., Duin, S., Vater, C., Gabrielyan, A., Rösen-Wolff, A., and Gelinsky, M. (2020). The Secretome of Hypoxia Conditioned hMSC Loaded in a Central Depot Induces Chemotaxis and Angiogenesis in a Biomimetic Mineralized Collagen Bone Replacement Material. Adv. Healthc. Mater. *9*.

Ragipoglu, D., Dudeck, A., Haffner-Luntzer, M., Voss, M., Kroner, J., Ignatius, A., and Fischer, V. (2020). The Role of Mast Cells in Bone Metabolism and Bone Disorders. Front. Immunol. *11*.

Rapp, A., Bindl, R., Erbacher, A., Kruchen, A., Rojewski, M., Schrezenmeier, H., Müller, I., and Ignatius, A. (2018). Autologous Mesenchymal Stroma Cells Are Superior to Allogeneic Ones in Bone Defect Regeneration. Int. J. Mol. Sci. *19*, 2526.

Reis, M., Mavin, E., Nicholson, L., Green, K., Dickinson, A.M., and Wang, X.N. (2018). Mesenchymal stromal cell-derived extracellular vesicles attenuate dendritic cell maturation and function. Front. Immunol. *9*, 1–14.

Remy, S., Tesson, L., Usal, C., Menoret, S., Bonnamain, V., Nerriere-Daguin, V., Rossignol, J., Boyer, C., Nguyen, T.H., Naveilhan, P., et al. (2010). New lines of GFP transgenic rats relevant for regenerative medicine and gene therapy. Transgenic Res. *19*, 745–763.

Richter, M., Fuhrmann, K., and Fuhrmann, G. (2019). Evaluation of the storage stability of extracellular vesicles. J. Vis. Exp. *2019*, 1–9.

Rieger, M.A., and Schroeder, T. (2012). Hematopoiesis. Cold Spring Harb. Perspect. Biol. *4*, a008250–a008250.

Riffel, P., Schwaab, J., Lutz, C., Naumann, N., Metzgeroth, G., Fabarius, A., Schoenberg, S.O., Hofmann, W.K., Valent, P., Reiter, A., et al. (2020). An increased bone mineral density is an adverse prognostic factor in patients with systemic mastocytosis. J. Cancer Res. Clin. Oncol. *146*, 945–951.

Riley, R.S., Williams, D., Ross, M., Zhao, S., Chesney, A., Clark, B.D., and Ben-Ezra, J.M. (2009). Bone marrow aspirate and biopsy: a pathologist's perspective. II. interpretation of the bone marrow aspirate and biopsy. J. Clin. Lab. Anal. *23*, 259–307.

Robey, P.G. (2008). Noncollagenous Bone Matrix Proteins. Princ. Bone Biol. Two-Volume Set *1*, 335–349.

Rodriguez, A., MacEwan, S.R., Meyerson, H., Kirk, J.T., and Anderson, J.M. (2009). The foreign body reaction in T-cell-deficient mice. J. Biomed. Mater. Res. Part A *90A*, 106–113.

Romeo, S.G., Alawi, K.M., Rodrigues, J., Singh, A., Kusumbe, A.P., and Ramasamy, S.K. (2019). Endothelial proteolytic activity and interaction with non-resorbing osteoclasts mediate bone elongation. Nat. Cell Biol. *21*, 430–441.

Roschger, A., Wagermaier, W., Gamsjaeger, S., Hassler, N., Schmidt, I., Blouin, S., Berzlanovich, A., Gruber, G.M., Weinkamer, R., Roschger, P., et al. (2020). Newly formed and remodeled human bone exhibits differences in the mineralization process. Acta Biomater.

Rostovskaya, M., and Anastassiadis, K. (2012). Differential Expression of Surface Markers in Mouse Bone Marrow Mesenchymal Stromal Cell Subpopulations with Distinct Lineage Commitment. PLoS One *7*.

Salazar, V.S., Gamer, L.W., and Rosen, V. (2016). BMP signalling in skeletal development, disease and repair. Nat. Rev. Endocrinol. *12*, 203–221.

Schmidt-Bleek, K., Willie, B.M., Schwabe, P., Seemann, P., and Duda, G.N. (2016). BMPs in bone regeneration: Less is more effective, a paradigm-shift. Cytokine Growth Factor Rev. *27*, 141–148.

Scott, M.A., Levi, B., Askarinam, A., Nguyen, A., Rackohn, T., Ting, K., Soo, C., and James, A.W. (2012). Brief Review of Models of Ectopic Bone Formation. Stem Cells Dev. *21*, 655–667.

Sheikh, Z., Brooks, P.J., Barzilay, O., Fine, N., and Glogauer, M. (2015). Macrophages, foreign body giant cells and their response to implantable biomaterials. Materials (Basel). *8*, 5671–5701.

Siegel, G., Kluba, T., Hermanutz-Klein, U., Bieback, K., Northoff, H., and Schäfer, R. (2013). Phenotype, donor age and gender affect function of human bone marrow-derived mesenchymal stromal cells. BMC Med. *11*.

Sims, N.A., and Martin, T.J. (2020a). Coupling of bone formation and resorption (Elsevier Inc.).

Sims, N.A., and Martin, T.J. (2020b). Osteoclasts Provide Coupling Signals to Osteoblast Lineage Cells Through Multiple Mechanisms. Annu. Rev. Physiol. *82*, annurev-physiol-021119-034425.

Søe, K., and Delaissé, J.M. (2017). Time-lapse reveals that osteoclasts can move across the bone surface while resorbing. J. Cell Sci. *130*, 2026–2035.

Spiller, K.L., Nassiri, S., Witherel, C.E., Anfang, R.R., Ng, J., Nakazawa, K.R., Yu, T., and Vunjak-Novakovic, G. (2015). Sequential delivery of immunomodulatory cytokines to facilitate the M1-to-M2 transition of macrophages and enhance vascularization of bone scaffolds. Biomaterials *37*, 194–207.

Stegen, S., and Carmeliet, G. (2018). The skeletal vascular system – Breathing life into bone tissue. Bone *115*, 50–58.

Stellos, K., Kopf, S., Paul, A., Marquardt, J.U., Gawaz, M., Huard, J., and Langer, H.F. (2010). Platelets in regeneration. Semin. Thromb. Hemost. *36*, 175–184.

Stock, S.R. (2015). The Mineral–Collagen Interface in Bone. Calcif. Tissue Int. *97*, 262–280.

Stroncek, D.F., Jin, P., McKenna, D.H., Takanashi, M., Fontaine, M.J., Pati, S., Schäfer, R., Peterson, E., Benedetti, E., and Reems, J.A. (2020). Human Mesenchymal Stromal Cell (MSC) Characteristics Vary Among Laboratories When Manufactured From the Same Source Material: A Report by the Cellular Therapy Team of the Biomedical Excellence for Safer Transfusion (BEST) Collaborative. Front. Cell Dev. Biol. *8*, 1–13.

Su, Y., Cockerill, I., Zheng, Y., Tang, L., Qin, Y.X., and Zhu, D. (2019). Biofunctionalization of metallic implants by calcium phosphate coatings. Bioact. Mater. *4*, 196–206.

Suresh, S., Lee, J., and Noguchi, C.T. (2020). Erythropoietin signaling in osteoblasts is required for normal bone formation and for bone loss during erythropoietin-stimulated erythropoiesis. FASEB J. 1–13.

Takeuchi, R., Katagiri, W., Endo, S., and Kobayashi, T. (2019). Exosomes from conditioned media of bone marrow-derived mesenchymal stem cells promote bone regeneration by enhancing angiogenesis. PLoS One *14*, e0225472.

Terajima, M., Perdivara, I., Sricholpech, M., Deguchi, Y., Pleshko, N., Tomer, K.B., and Yamauchi, M. (2014). Glycosylation and cross-linking in bone type I collagen. J. Biol. Chem. *289*, 22636–22647.

Theoharides, T.C., Valent, P., and Akin, C. (2015). Mast cells, mastocytosis, and related disorders. N. Engl. J. Med. *373*, 163–172.

Thon, J.N., and Italiano, J.E. (2012). Platelets: Production, Morphology and Ultrastructure. P. Gresele, G.V.R. Born, C. Patrono, and C.P. Page, eds. (Berlin, Heidelberg: Springer Berlin Heidelberg), pp. 3–22.

Tsiapalis, D., and O'Driscoll, L. (2020). Mesenchymal Stem Cell Derived Extracellular Vesicles for Tissue Engineering and Regenerative Medicine Applications. Cells *9*.

Tzelepi, V., Tsamandas, A.C., Zolota, V., and Scopa, C.D. (2009). Bone Anatomy, Physiology and Function. 3–30.

Ushach, I., and Zlotnik, A. (2016). Biological role of granulocyte macrophage colony-stimulating factor (GM-CSF) and macrophage colony-stimulating factor (M-CSF) on cells of the myeloid lineage. J. Leukoc. Biol. *100*, 481–489.

Vidal, L., Kampleitner, C., Brennan, M.Á., Hoornaert, A., and Layrolle, P. (2020). Reconstruction of Large Skeletal Defects: Current Clinical Therapeutic Strategies and Future Directions Using 3D Printing. Front. Bioeng. Biotechnol. *8*, 61.

Villani, A.-C.C., Satija, R., Reynolds, G., Sarkizova, S., Shekhar, K., Fletcher, J., Griesbeck, M., Butler, A., Zheng, S., Lazo, S., et al. (2017). Single-cell RNA-seq reveals new types of human blood dendritic cells, monocytes, and progenitors. Science (80-.). *356*, eaah4573.

Volk, S.W., Shah, S.R., Cohen, A.J., Wang, Y., Brisson, B.K., Vogel, L.K., Hankenson, K.D., and Adams, S.L. (2014). Type III collagen regulates osteoblastogenesis and the quantity of trabecular bone. Calcif. Tissue Int. *94*, 621–631.

Wakkach, A., Mansour, A., Dacquin, R., Coste, E., Jurdic, P., Carle, G.F., and Blin-Wakkach, C. (2008). Bone marrow microenvironment controls the in vivo differentiation of murine dendritic cells into osteoclasts. Blood *112*, 5074–5083.

Wang, H., Leng, Y., and Gong, Y. (2018a). Bone Marrow Fat and Hematopoiesis. Front. Endocrinol. (Lausanne). *9*, 694.

Wang, M., Yuan, Q., and Xie, L. (2018b). Mesenchymal Stem Cell-Based Immunomodulation: Properties and Clinical Application. Stem Cells Int. *2018*, 1–12.

Wang, M., Chen, F., Wang, J., Chen, X., Liang, J., Yang, X., Zhu, X., Fan, Y., and Zhang, X. (2018c). Calcium phosphate altered the cytokine secretion of macrophages and influenced the homing of mesenchymal stem cells. J. Mater. Chem. B *6*, 4765–4774.

Wang, P., Liu, X., Zhao, L., Weir, M.D., Sun, J., Chen, W., Man, Y., and Xu, H.H.K. (2015). Bone tissue engineering via human induced pluripotent, umbilical cord and bone marrow mesenchymal stem cells in rat cranium. Acta Biomater. *18*, 236–248.

Wang, Y.Y., Zhang, H.Q., Fan, S., Zhang, D.M., Huang, Z.Q., Chen, W.L., Ye, J.T., and Li, J.S. (2016). Mandibular reconstruction with the vascularized fibula flap: comparison of virtual planning surgery and conventional surgery. Int. J. Oral Maxillofac. Surg. *45*, 1400–1405.

Wei, S., Wang, M.W.H., Teitelbaum, S.L., and Patrick Ross, F. (2002). Interleukin-4 reversibly inhibits osteoclastogenesis via inhibition of NF-κB and mitogen-activated protein kinase signaling. J. Biol. Chem. *277*, 6622–6630.

Wein, M.N. (2017). Bone Lining Cells: Normal Physiology and Role in Response to Anabolic Osteoporosis Treatments. Curr. Mol. Biol. Reports *3*, 79–84.

De Witte, T.M., Fratila-Apachitei, L.E., Zadpoor, A.A., and Peppas, N.A. (2018). Bone tissue engineering via growth factor delivery: From scaffolds to complex matrices. Regen. Biomater. *5*, 197–211.

Witzler, M., Büchner, D., Shoushrah, S.H., Babczyk, P., Baranova, J., Witzleben, S., Tobiasch, E., and Schulze, M. (2019). Polysaccharide-based systems for targeted stem cell differentiation and bone regeneration. Biomolecules *9*.

Xu, L., Liu, Y., Sun, Y., Wang, B., Xiong, Y., Lin, W., Wei, Q., Wang, H., He, W., Wang, B., et al. (2017). Tissue source determines the differentiation potentials of mesenchymal stem cells: A comparative study of human mesenchymal stem cells from bone marrow and adipose tissue. Stem Cell Res. Ther. *8*, 1–11.

Xue, J., Xu, L., Zhu, H., Bai, M., Li, X., Zhao, Z., Zhong, H., Cheng, G., Li, X., Hu, F., et al. (2020). CD14+CD16- monocytes are the main precursors of osteoclasts in rheumatoid arthritis via expressing Tyro3TK. Arthritis Res. Ther. *22*, 221.

Yamaguchi, F.S.M., Shams, S., Silva, E.A., and Stilhano, R.S. (2019). PRP and BMAC for musculoskeletal conditions via biomaterial carriers. Int. J. Mol. Sci. *20*.

Yunus Basha, R., Sampath, S.K., and Doble, M. (2015). Design of biocomposite materials for bone tissue regeneration. Mater. Sci. Eng. C *57*, 452–463.

Zamborsky, R., Svec, A., Bohac, M., Kilian, M., and Kokavec, M. (2016). Infection in bone allograft transplants. Exp. Clin. Transplant. *14*, 484–490.

Zhang, J., Feng, Z., Wei, J., Yu, Y., Luo, J., Zhou, J., Li, Y., Zheng, X., Tang, W., Liu, L., et al. (2018). Repair of critical-sized mandible defects in aged rat using hypoxia preconditioned BMSCs with Up-regulation of Hif-1α. Int. J. Biol. Sci. *14*, 449–460.

Zhang, Q., Atsuta, I., Liu, S., Chen, C., Shi, S., Shi, S., and Le, A.D. (2013). IL-17-Mediated M1/M2 Macrophage Alteration Contributes to Pathogenesis of Bisphosphonate-Related Osteonecrosis of the Jaws. Clin. Cancer Res. *19*, 3176–3188.

Zhao, Z., Zhao, Q., Gu, B., Yin, C., Shen, K., Tang, H., Xia, H., Zhang, X., Zhao, Y., Yang, X., et al. (2020). Minimally invasive implantation and decreased inflammation reduce osteoinduction of biomaterial. Theranostics *10*,

3533–3545.

Zhou, J., Tian, Z., and Peng, H. (2020). Tissue-resident NK cells and other innate lymphoid cells (Elsevier Inc.).

Zura, R., Xiong, Z., Einhorn, T., Watson, J.T., Ostrum, R.F., Prayson, M.J., Della Rocca, G.J., Mehta, S., McKinley, T., Wang, Z., et al. (2016). Epidemiology of fracture nonunion in 18 human bones. JAMA Surg. *151*, e162775–e162775.

DOCTORAT BIOLOGIE BRETAGNE SANTE LOIRE

UNIVERSITÉ DE NANTES

Titre : Rôle de l'ostéoclaste dans la régénération osseuse induite par des cellules souches mésenchymateuses et des biomatériaux phosphocalciques

Mots clés :

Résumé : L'os est le tissu le plus fréquemment greffé au monde mais de nombreuses complications accompagnent ces interventions. De nouvelles stratégies thérapeutiques, basées sur la combinaison de biomatériaux et de cellules souches dérivées de la moelle osseuse, sont prometteuses. L'essai clinique européen ORTHOUNION vise à comparer l'efficacité de ce traitement avec la greffe osseuse autologue dans la consolidation des fractures des os longs. Malgré les précédents succès précliniques et cliniques de ces thérapies cellulaires, le mécanisme exact de la formation osseuse n'est pas complètement compris à ce jour. Plusieurs équipes ont démontré l'importance de la formation précoce d'ostéoclastes sur le biomatériau, alors que les cellules implantées disparaissaient rapidement. L'hypothèse à l'origine de ce travail est que les cellules souches secrètent de nombreux médiateurs de l'inflammation, d'autant plus dans les conditions extrêmes qu'elles rencontrent après implantation, favorisant le développement des ostéoclastes. Ces derniers pourraient alors recruter de nouveaux précurseurs ostéoblastiques de l'hôte, déclenchant localement un cycle de remodelage osseux. Dans ce travail, l'effet pro-ostéoclastique du sécrétome des cellules souches sur le biomatériau et en conditions d'apoptose a été démontré in vitro. Les principales protéines sécrétées ont été détectées par protéomique et dosage immunologique en multiplex. L'utilisation d'anticorps neutralisants a permis d'identifier les chimiokines interagissant avec les récepteurs CXCR1 et CXCR2 (GROα/CXCL1, GROβ/CXCL2, IL-8/CXCL8) comme étant les signaux majeurs de cette stimulation. Dans un second projet collaboratif, le développement in vitro d'ostéoclastes humains et murins sur des matériaux de différentes compositions a été évalué et mis en parallèle de l'efficacité in vivo de ces biomatériaux. Enfin, deux études préliminaires in vivo sont présentés, explorant l'utilisation à la place des cellules souches autologues (1) de milieu de culture conditionné ou de vésicules extracellulaires et (2) de cellules souches d'origines allogéniques.

Title : Role of the osteoclast in bone regeneration induced by mesenchymal stem cells and calcium phosphate biomaterials

Keywords :

Abstract : Bone is the most frequently grafted tissue in the world but multiple complications go with those operations. New therapeutic strategies, based on the combination of biomaterials and mesenchymal stem cells derived from the bone marrow, are promising. The European clinical trial ORTHOUNION aims at comparing the efficacy of this treatment to autologous bone grafting in the consolidation of long bone fractures. Despite the previous preclinical and clinical successes of these cell therapies, the exact mechanism of bone formation is not completely understood so far. Several teams have demonstrated the importance of early osteoclast formation on the biomaterial, while implanted cells rapidly disappear. The hypothesis initiating this work is that stem cells secrete numerous inflammatory mediators, even more in the extreme conditions they face after implantation, favoring the development of osteoclasts. The latter could then recruit new osteoblast progenitors from the host, locally triggering a bone remodeling cycle. In this work, the pro-osteoclastic effect of the secretome from mesenchymal stem cells on the biomaterial or in apoptotic conditions was demonstrated in vitro. The major secreted proteins were detected by proteomic and multiplex immunoassay. The use of neutralizing antibodies allowed the identification of the chemokines interacting with CXCR1 and CXCR2 receptors (GROα/CXCL1, GROβ/CXCL2, IL-8/CXCL8) as the main signals of this stimulation. In a second collaborative project, the development in vitro of human and mouse osteoclasts on biomaterials of various composition was evaluated and compared to the in vivo efficiency of those biomaterials. Finally, two in vivo preliminary studies are presented; exploring, in lieu of autologous stem cells, the use of (1) conditioned culture media or extracellular vesicles and (2) allogenic stem cells.